

**Fig. 20.2** Flow diagram for uptake and distribution of inhaled anesthetics. Major compartments for anesthetic flow are depicted, including the breathing circuit, alveolar gas space, and three major tissue compartments: vessel-rich group (VRG), muscle, and fat. The physiological volumes of the tissue compartments are approximately in proportion to the labeled face of the compartment, while the blood-tissue partition coefficients are depicted as the depth of the compartment. Thus the effective volume of the VRG is much smaller than that of muscle, which in turn is much smaller than that of fat. Carrier flows and exchange in different parts of the model are depicted by arrows: Fresh gas flow (FGF) moves anesthetic from the vaporizer to the circuit; ventilation drives exchange of anesthetic between the circuit and alveoli; pulmonary blood flow transfers anesthetic from alveoli into the circulation, which then distributes drug to different compartments depending on blood flow to various tissues. Relative blood flow is approximately proportional to the width of the arrows into and out of tissue compartments, as well as for shunts. The diagram depicts an early phase of anesthetic uptake when organs of the VRG, including the brain, are approaching equilibrium with alveolar and arterial anesthetic partial pressure, while anesthetic partial pressures in muscle and fat remain relatively low. Quantitative modeling of anesthetic gas movement in this system was performed using numerical integration of equations describing anesthetic flow into and out of each compartment (Eqs. 20.5, 20.8–20.11). Figs. 20.4–20.7, 26.9, 20.10, and 20.12 were all generated using this model. Standardized parameters used in the model are summarized in Table 20.2.

and diffusive equilibration across capillary membranes. Note that when anesthetic transfer occurs between gas and blood or between blood and tissue, the effective volume of the downstream compartment must be adjusted with the appropriate partition coefficient (see Table 20.2).

### Rate of Wash-In of the Circuit: Equilibration Between Vaporizer and Circuit

Equipment for controlled delivery of inhaled anesthetic drugs are described elsewhere in this text (see Chapter 22). Wash-in of the ventilator breathing circuit represents an example of bulk transfer exchange, wherein the gas in circuit components is replaced by fresh gases emerging from the gas outlet of the anesthesia machine.

**Anesthetic Delivery from the Vaporizer:** VA delivery (in liters per minute of gaseous drug) from a vaporizer is closely approximated as the product of the delivered anesthetic

concentration (fraction =  $F_{del}$  or partial pressure at 1 atm =  $P_{del}$ ) of the anesthetic in a gas mixture and the fresh gas flow (FGF):

$$dVA_{del}/dt = P_{del} \times FGF. \quad (20.1)$$

Thus we can readily calculate the volume of delivered gas-phase anesthetic by simply integrating this function over time. In the simplest case where  $P_{del}$  and FGF remain constant,

$$VA_{del}(t) = P_{del} \times FGF \times t. \quad (20.2)$$

**Fresh Gas Wash-In to the Breathing Circuit:** The factors that affect the speed at which the gas mixture delivered from the anesthesia machine replaces gases in the breathing circuit (wash-in) are FGF and the breathing circuit volume ( $V_{circ}$ ). Consider a typical situation where FGF at the beginning of an anesthetic is 6 L/min, and the gas volume

inside the components of a breathing circuit is 6 L. If FGF is doubled to 12 L/min, then wash-in will proceed at twice the rate (halving the time). Conversely, if the  $V_{circ}$  doubles to 12 L, then wash-in will proceed at half the rate (doubling the time).

The gas exchange process is independent of the concentration of anesthetic in the circuit, because the exchange is simply through bulk flow and mixing. However, the *difference between the delivered concentration and that in the circuit determines the magnitude and direction of net anesthetic gas flow*. When the delivered anesthetic partial pressure ( $P_{del}$ ) is greater than that in the circuit ( $P_{circ}$ ), net anesthetic flow is into the circuit (and subsequently the patient). To remove anesthetic from the circuit,  $P_{del}$  must be less than  $P_{circ}$ . When there is no concentration gradient (i.e., equal partial pressures), bulk flow exchange may replace all the old anesthetic molecules with new ones, but there is no net flow and anesthetic concentrations in the circuit remain unchanged.

Mathematically, we can describe the breathing circuit exchange process as a differential equation that incorporates all of the above factors:

$$\frac{dP_{circ}}{dt} = \frac{FGF}{V_{circ}} \times (P_{del} - P_{circ}). \quad (20.3)$$

If  $P_{del}$  is constant, integrating this equation results in a single exponential function that defines  $P_{circ}$  at any given time following a change in  $P_{del}$  at  $t = 0$ :

$$P_{circ}(t) = P_{circ}(0) + (P_{del} - P_{circ}(0)) \times \left(1 - e^{-t/[V_{circ}/FGF]}\right) \quad (20.4)$$

$P_{circ}$  approaches  $P_{del}$  following an exponential time course with a time constant of  $\tau = V_{circ}/FGF$ . Thus if  $V_{circ} = 6$  L and  $FGF = 6$  L/min, the exponential time constant will be 1 minute (Fig. 20.3). Each minute results in the fraction of old gas in the breathing circuit dropping by 63.1%, and after 4 minutes, less than 2% old gas remains. The half-life for the process (time for halving the vaporizer-circuit concentration difference) is  $0.693 \times \tau$ .

Breathing circuit components, such as  $\text{CO}_2$  absorbents and the plastic or rubber of the circuit tubing and connectors, influence the rate of equilibration between vaporizer and circuit, because they absorb VAs, increasing the effective circuit volume.<sup>19</sup> The more hydrophobic VAs absorb more into circuit components, whereas absorption negligibly affects wash-in and wash-out of low-solubility anesthetics.

The clinical relevance of the wash-in process is readily appreciated. An example of the importance of FGF is “priming” the anesthetic circuit for a single-breath induction technique. The FGF setting and the circuit volume influence the required duration of priming. More generally, whenever the vaporizer settings are altered, the speed at which the new settings influence the wash-in or wash-out of the circuit (and subsequently the patient) will depend on FGF. Open (nonrebreathing) anesthetic breathing circuits are designed to have low exchange volumes and to be used with high fresh-gas flows. These features allow rapid changes in the delivered anesthetic concentration, while minimizing rebreathing of exhaled gases. The choice of an open versus

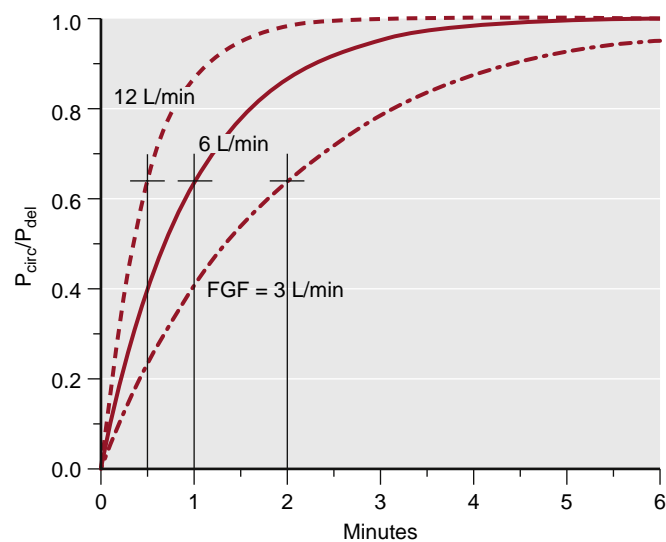


**Fig. 20.3** Wash-in of the breathing circuit depends on fresh gas flow (FGF). The curves depict the rate of rise of anesthetic concentration (partial pressure) in a breathing circuit with 6 L gas volume, depending on FGF. Higher FGF results in more rapid exchange of circuit gases with fresh gas. The exponential time constant for the wash-in process is the circuit volume in liters divided by FGF flow in liters per minute (see Eq. 20.4). Cross marks overlaying the curves indicate time constants under different gas flow rates. Each time constant correlates with a 63.1% exchange.

rebreathing system influences the impact of various other factors that can affect uptake and distribution of inhaled anesthetics downstream from the breathing circuit. Some of the subsequent figures show models for both conditions.

### Equilibration Between Circuit and Pulmonary Airspace

Transfer of anesthetic gases from the breathing circuit to the pulmonary airspace is another bulk exchange process similar to that from vaporizer to breathing circuit. In this case, gas flow via ventilation is cyclical and bidirectional, and the factors that determine the rate of anesthetic exchange are minute ventilation (MV) and total pulmonary airspace volume ( $V_{pulm}$ ).<sup>20</sup> Because transfer from the circuit to the lungs represents anesthetic flow out of the circuit, we alter Eq. (20.3) to include both inflow to the circuit and outflow from the circuit,

$$\frac{dP_{circ}}{dt} = \frac{FGF}{V_{circ}} \times (P_{del} - P_{circ}) - \frac{MV}{V_{pulm}} \times (P_{circ} - P_{pulm}), \quad (20.5)$$

where  $P_{pulm}$  is a weighted average of the anesthetic partial pressure in dead space and alveolar space.

Eq. (20.5) describes how rebreathing affects the inhaled (breathing circuit) anesthetic concentration. Most inhaled anesthetics are delivered using a rebreathing circuit, which includes one-way flow valves and adsorbent material to chemically remove exhaled  $\text{CO}_2$ . Rebreathing depends primarily on the balance between fresh gas flow and MV. The anesthetic gas in the breathing circuit represents a mixture of fresh gas and exhaled gases. Increased fresh gas flow reduces rebreathing, whereas increased MV increases rebreathing.

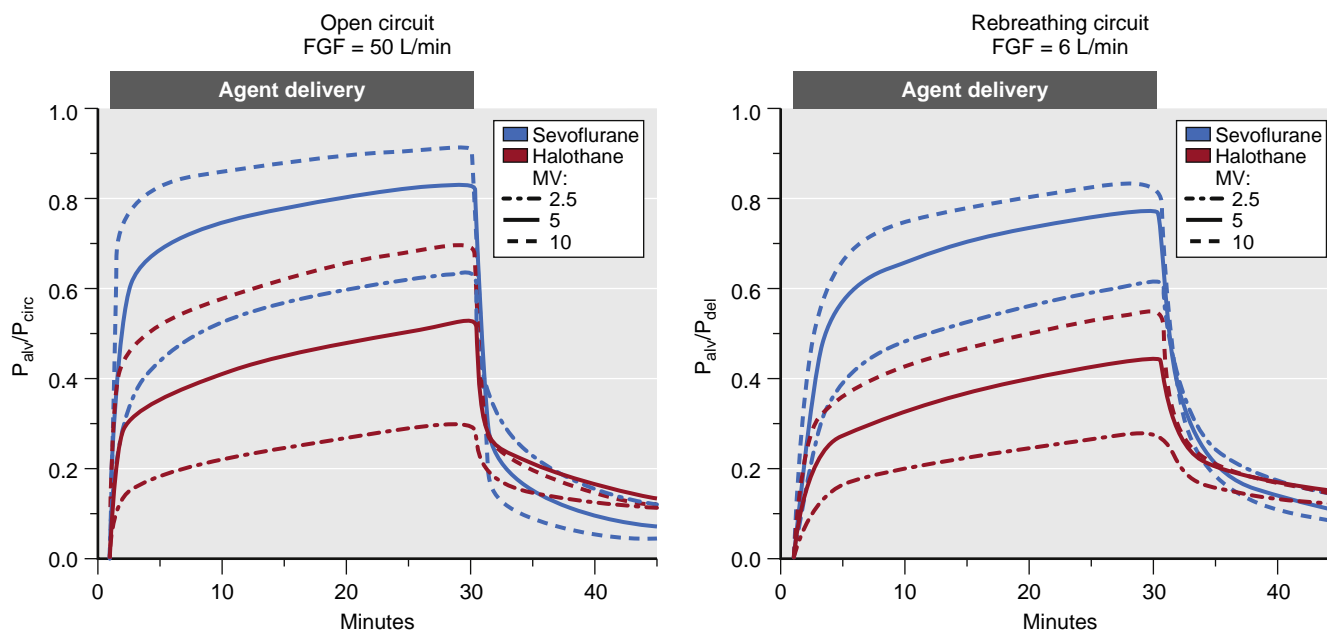


**Fig. 20.4** Effect of ventilation on the rise of alveolar anesthetic partial pressure ( $P_{\text{alv}}$ ). Left, A traditional open-circuit model with very high fresh gas flow (FGF) and therefore constant  $P_{\text{del}} = P_{\text{circ}}$ . Right, A more common clinical situation with constant vaporized output ( $P_{\text{del}}$ ) and partial rebreathing at a 6 L/min fresh gas flow rate. Raising minute ventilation accelerates the rise of  $P_{\text{alv}}$  by delivering more anesthetic to the lungs. The effect is seen whether anesthetic is highly soluble in blood (e.g., halothane) or relatively insoluble (e.g., sevoflurane). However, the relative size of the ventilation effect is greater for soluble agents. Increased ventilation also accelerates clearance of anesthetic agents after delivery ceases. MV, Minute ventilation;  $P_{\text{circ}}$ , Anesthetic partial pressure in the breathing circuit;  $P_{\text{del}}$ , delivered anesthetic partial pressure from the anesthesia machine gas outlet.

### The Alveolar Anesthetic Concentration

The alveolar anesthetic concentration ( $P_{\text{alv}}$  or  $F_A$ ) is a critically important factor in anesthetic uptake and distribution because (1) it is in rapid equilibrium with circulating blood and highly perfused tissues, including target tissues in the CNS, and (2)  $P_{\text{alv}}$  can be measured in exhaled end-tidal gases. Thus, except during periods of rapid change,  $P_{\text{alv}}$  in exhaled breath represents a useful estimate of the anesthetic concentration in the patient's CNS and other highly perfused organs.

Because only alveolar gas is relevant to transpulmonary exchange of anesthetic into and out of the body, *alveolar ventilation* ( $\dot{V}_{\text{alv}}$ ) is the proper gas flow to calculate anesthetic exchange into this part of the pulmonary airspace,

$$\frac{dP_{\text{alv}}}{dt} = \frac{\dot{V}_{\text{alv}}}{V_{\text{alv}}} \times (P_{\text{circ}} - P_{\text{alv}}), \quad (20.6)$$

where  $\dot{V}_{\text{alv}}$  is MV corrected for dead space ventilation.

### Alveolar Uptake of Anesthetic into Pulmonary Blood

During inhaled anesthetic induction, anesthetic flows from alveolar gas to pulmonary blood across the alveolar/capillary interface separating these compartments and is driven by the partial pressure gradient between alveolar gas ( $P_{\text{alv}}$ ) and mixed venous blood ( $P_{\text{MV}}$ ) entering the pulmonary arteries. The net flow of anesthetic reverses during anesthetic wash-out when  $P_{\text{alv}}$  drops below  $P_{\text{MV}}$ . Anesthetic uptake into blood also depends on the pulmonary blood flow (which is typically close to cardiac output,  $\dot{Q}$ ) and the blood's capacity to solvate anesthetic from the gas state (the blood/gas partition coefficient,  $\lambda_{\text{b/g}}$ ):

$$\text{uptake} = \dot{Q} \times \lambda_{\text{b/g}} \times (P_{\text{alv}} - P_{\text{MV}}). \quad (20.7)$$

We therefore correct Eq. (20.6) to reflect both anesthetic inflow into alveolar airspace and its uptake into blood:

$$\frac{dP_{\text{alv}}}{dt} = \frac{\dot{V}_{\text{alv}}}{V_{\text{alv}}} \times (P_{\text{circ}} - P_{\text{alv}}) - \frac{\dot{Q} \times \lambda_{\text{b/g}}}{V_{\text{alv}}} \times (P_{\text{alv}} - P_{\text{MV}}). \quad (20.8)$$

Thus, during an inhaled anesthetic induction, the rate of increase of  $P_{\text{alv}}$  relative to  $P_{\text{circ}}$  is governed by (1) alveolar ventilation, (2) cardiac output, and (3) anesthetic solubility in blood. Increased ventilation delivers more anesthetic from circuit to alveoli and increases  $P_{\text{alv}}/P_{\text{circ}}$  (Fig. 20.4). Importantly, increased pulmonary blood flow removes more anesthetic from alveoli, thereby decreasing the rate of increase in alveolar concentration of anesthetic ( $P_{\text{alv}}/P_{\text{circ}}$ ) (Fig. 20.5). Indeed, significant decreases in cardiac output are suspected when end-tidal  $\text{CO}_2$  (ETCO<sub>2</sub>) decreases and end-tidal concentration of VA increases.<sup>21</sup> The more soluble an anesthetic is in blood (i.e., the higher its  $\lambda_{\text{b/g}}$ ), the greater is the capacity for each volume of blood to take up anesthetic from alveolar gases (i.e., the larger the effective blood flow). Thus as  $\lambda_{\text{b/g}}$  increases,  $P_{\text{alv}}/P_{\text{circ}}$  increases more slowly (Fig. 20.6).

### Other Factors That Affect the Rate of Rise of $P_{\text{alv}}$

Other factors affecting alveolar uptake of anesthetic include ventilation-perfusion matching and the absolute concentration of anesthetic in alveolar gases.

**Pulmonary Dead Space.** Dead space (ventilated but not perfused pulmonary regions) reduces effective alveolar ventilation (see Eqs. 20.7 and 20.8), and thus slows anesthetic

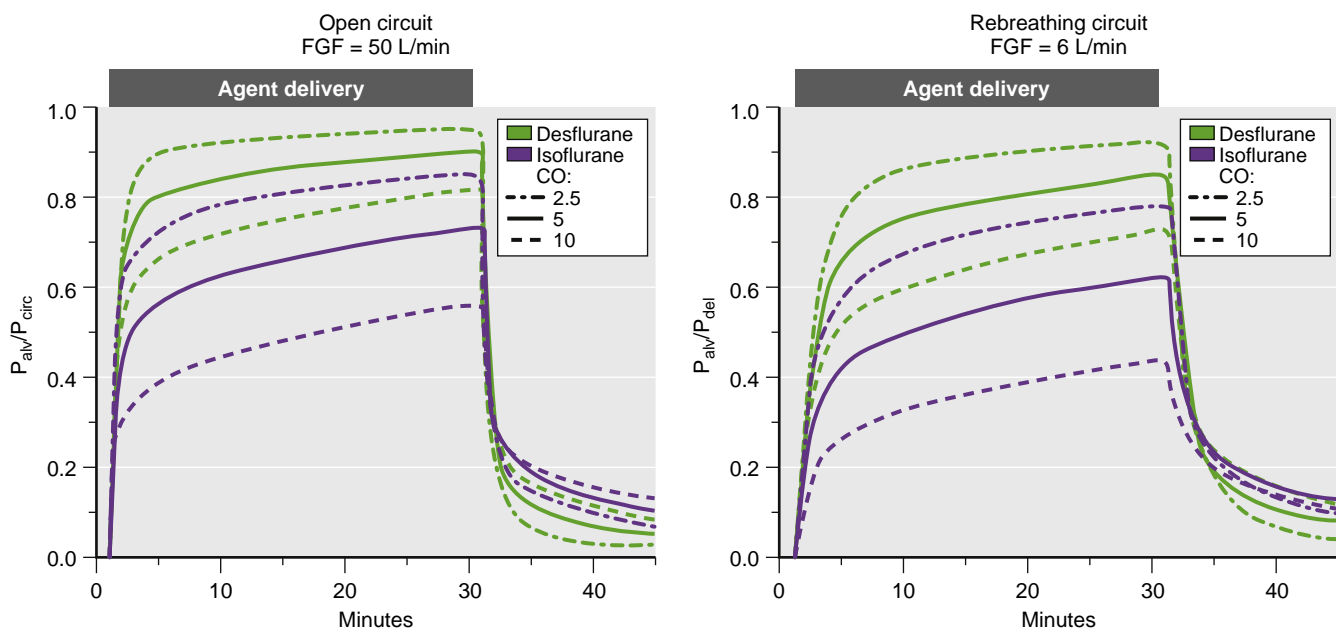


**Fig. 20.5** Effect of cardiac output on the rise of alveolar anesthetic partial pressure ( $P_{\text{alv}}$ ). Left, A traditional open-circuit model with very high fresh gas flows and therefore constant  $P_{\text{del}} = P_{\text{circ}}$ . Right, A more common clinical situation with constant vaporizer output ( $P_{\text{del}}$ ) and partial rebreathing at a 6 L/min FGF. Increasing cardiac output slows the rise of  $P_{\text{alv}}$  by increasing anesthetic uptake into blood (removing anesthetic from alveolar gases). This effect is observed for both soluble (e.g., isoflurane) and relatively insoluble (e.g., desflurane) anesthetics, but the relative effect is greater for soluble agents. Cardiac output also affects clearance of anesthetics from the lungs in the same way it affects uptake (i.e., increased cardiac output slows anesthetic clearance rate). CO, Cardiac output;  $P_{\text{circ}}$ , anesthetic partial pressure in the breathing circuit;  $P_{\text{del}}$ , delivered anesthetic partial pressure from the anesthesia machine gas outlet.

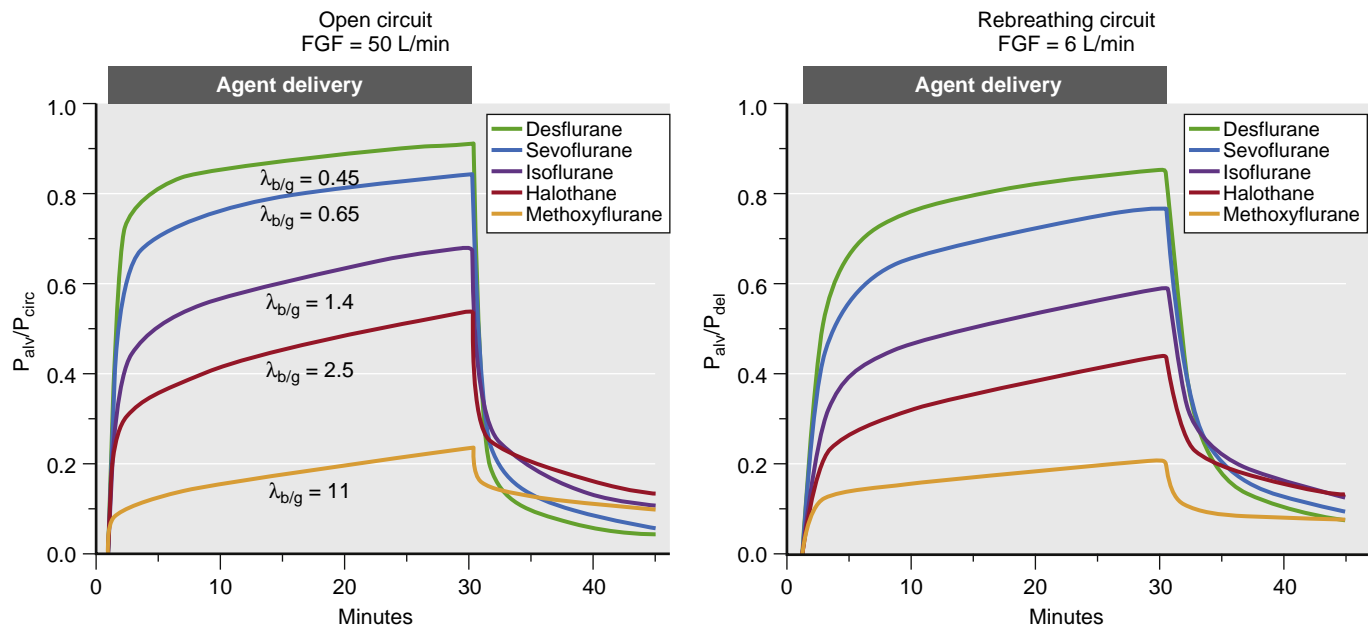


**Fig. 20.6** Effect of blood solubility on the rise of alveolar anesthetic partial pressure ( $P_{\text{alv}}$ ). Left, A traditional open-circuit model with very high fresh gas flow (FGF) and therefore constant  $P_{\text{del}} = P_{\text{circ}}$ . Right, A more common clinical situation with constant vaporizer output ( $P_{\text{del}}$ ) and partial rebreathing at a 6 L/min FGF rate. As blood solubility ( $\lambda_{\text{b/g}}$ ) increases, the rate of rise in  $P_{\text{alv}}$  slows, because uptake into blood is greater for high solubility agents. The major impact of blood solubility is the magnitude of the rapid initial rise in  $P_{\text{alv}}$ , which represents a balance between anesthetic delivery and uptake into pulmonary blood. Blood solubility similarly affects clearance from alveoli after anesthetic delivery ceases (i.e., increased blood solubility results in slower clearance from alveolar gas).  $P_{\text{circ}}$ , Anesthetic partial pressure in the breathing circuit;  $P_{\text{del}}$ , delivered anesthetic partial pressure from the anesthesia machine gas outlet.

uptake. This effect is strongest under conditions of high FGF and low blood-solubility agents, where alveolar ventilation is the limiting factor in uptake. Under conditions of low FGF and a highly blood-soluble agent, increased dead space, by reducing initial uptake, serves to maintain the inhaled

anesthetic concentration ( $P_{\text{circ}}$ ), which creates a compensatory increase in  $P_{\text{alv}}$  and subsequent uptake.

**Pulmonary (Right to Left) Shunting.** Pulmonary right to left shunting can be physiologic, pathologic, or iatrogenic, such as during one-lung ventilation. Right-to-left

shunting results in a difference between  $P_{\text{alv}}$  and the partial pressure of anesthetic in arterial blood ( $P_{\text{art}}$ ). This is because arterial blood represents a mixture of shunted mixed venous blood combined with blood that has equilibrated with alveolar gases (Eq. 20.9). Because such shunts also reduce transcapillary gas exchange in the lung and slow anesthetic uptake (Eqs. 20.7 and 20.8, after correcting pulmonary blood flow for shunt), right-to-left shunting sustains  $P_{\text{circ}}$ , an effect that is more pronounced for highly soluble drugs compared with insoluble anesthetics. Thus shunt reduces the ratio of  $P_{\text{art}}:P_{\text{alv}}$  more for insoluble anesthetics, such as  $\text{N}_2\text{O}$  (Fig. 20.7).<sup>22,23</sup>

$$P_{\text{art}} = P_{\text{MV}} \times \dot{q}_{\text{RLshunt}} + P_{\text{alv}} \times (\dot{Q} - \dot{q}_{\text{RLshunt}}). \quad (20.9)$$

**Concentration and Second Gas Effects.** The absolute concentration of anesthetic influences its uptake and that of other gases. In the previous discussion and illustrations, it was presumed that an inhaled anesthetic represents a small fraction of the inhaled gas mixture and that transalveolar uptake of the anesthetic results in a decrease in  $P_{\text{alv}}$  and negligible changes in alveolar gas volume. However, when the anesthetic represents a large fraction of the inhaled gas mixture, its rapid uptake results in a smaller relative alveolar anesthetic concentration drop, because the volume of alveolar gas also decreases. This is known as the **concentration effect**.<sup>24</sup> In an imaginary situation where a patient is breathing 100% anesthetic, uptake into pulmonary blood reduces the volume of anesthetic gas in the alveoli without altering its concentration or partial pressure (oxygen-induced atelectasis occurs through a similar mechanism). A typical situation, illustrated in Fig. 20.8, is delivery of 66%  $\text{N}_2\text{O}$  with 33%  $\text{O}_2$  and 1% isoflurane. Assuming cardiac output equals 5 L/min, the initial rate of  $\text{N}_2\text{O}$  uptake is given by Eq. (20.7) as  $5000 \text{ mL/min} \times 0.47 \times 0.66 \text{ atm} = 1550 \text{ mL/min}$ , indicating that a large fraction of  $\text{N}_2\text{O}$  is taken up into blood during the first few breaths. If we assume that half the  $\text{N}_2\text{O}$  and half the isoflurane are rapidly taken up following the first breath of this gas mixture, then alveolar volume drops by 33.5% and the remaining alveolar gas contains 33 parts  $\text{N}_2\text{O}$ , 33 parts  $\text{O}_2$ , and 0.5 parts isoflurane (49.6%  $\text{N}_2\text{O}$ , 49.6%  $\text{O}_2$ , and 0.8% isoflurane). Despite 50% uptake of  $\text{N}_2\text{O}$ , the significant reduction

in alveolar gas volume results in a concentration of remaining alveolar  $\text{N}_2\text{O}$  that is only 24% less than its initial value.

The **second gas effect** is also evident in this example: the rapid uptake of  $\text{N}_2\text{O}$  and reduced alveolar gas volume sustains  $P_{\text{iso}}$  near its original inspired value and increases alveolar  $P_{\text{O}_2}$ , thereby augmenting uptake of these gases.<sup>25</sup> The rapid uptake of  $\text{N}_2\text{O}$  into blood also results in an effective increase in MV, because more gas from the breathing circuit is passively drawn into lung as alveolar gas is rapidly absorbed. These effects have been demonstrated in

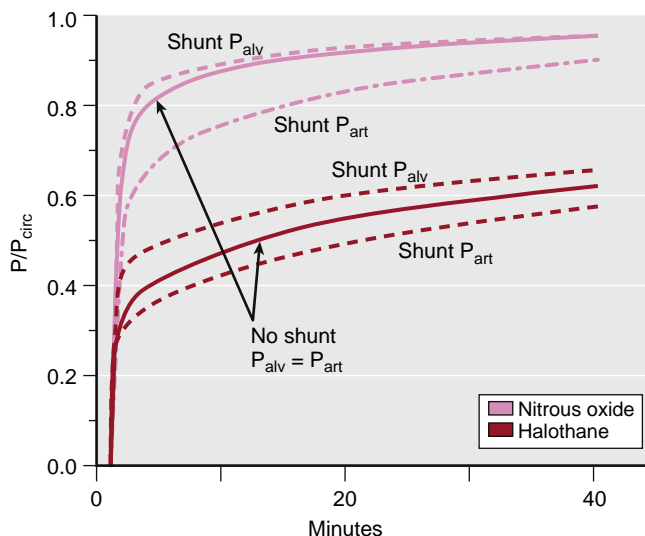


**Fig. 20.7** Effect of right-to-left pulmonary shunt on the anesthetic partial pressure in alveolar gas and arterial blood. The curves represent anesthetic partial pressures in alveolar gases (dashed lines) and arterial blood (dash-dot lines) under conditions of 40% right-to-left shunt and no shunt (solid lines). Pulmonary right-to-left shunting bypasses alveolar uptake, so less anesthetic is removed from pulmonary gases; this accelerates the rise in  $P_{\text{alv}}$ . In addition, the anesthetic partial pressure in arterial blood ( $P_{\text{art}}$ ) is a mixture of pulmonary venous blood at  $P_{\text{alv}}$  and shunted mixed venous blood at  $P_{\text{MV}}$ . Thus  $P_{\text{art}}$ , which determines the rate of anesthetic uptake into tissues, rises more slowly than  $P_{\text{alv}}$  when R-to-L shunting is present. The shunt effect on  $P_{\text{art}}$  versus  $P_{\text{alv}}$  is larger for insoluble anesthetics (e.g.,  $\text{N}_2\text{O}$ ) than for soluble anesthetics (e.g., halothane). Other model parameters were set for open circuit delivery (constant  $P_{\text{circ}}$ ) with  $MV = 6 \text{ L/min}$  and  $CO = 5 \text{ L/min}$ .  $CO$ , Cardiac output;  $MV$ , minute ventilation;  $P_{\text{MV}}$ , anesthetic partial pressure in mixed venous blood;  $P/P_{\text{circ}}$ .

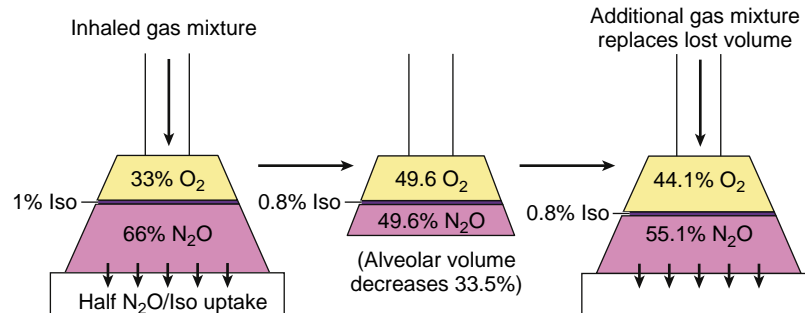


**Fig. 20.8** Concentration and second gas effects. The figure depicts alveolar gases at the beginning of an anesthetic. After an initial inspiratory breath, alveoli are filled with the gas mixture in the circuit (66%  $\text{N}_2\text{O}$ , 33%  $\text{O}_2$ , 1% isoflurane) at their normal end-inspiratory volume (left panel). After half of the  $\text{N}_2\text{O}$  and isoflurane are absorbed into pulmonary blood, the alveolar gas volume is reduced by 33.5%. At this point, the volume of  $\text{N}_2\text{O}$  equals the volume of  $\text{O}_2$  and the gas mixture is 49.6%  $\text{N}_2\text{O}$ , 49.6%  $\text{O}_2$ , 0.8% isoflurane. Inflow of additional inspired gas mixture returns alveolar volume to its original value, resulting in a gas mixture of 55.1%  $\text{N}_2\text{O}$ , 44.1%  $\text{O}_2$ , 0.8% isoflurane. The alveolar partial pressure of  $\text{N}_2\text{O}$  falls much less than the fractional uptake (the concentration effect). In addition, the partial pressure of  $\text{O}_2$  increases relative to the inspired gas  $\text{O}_2$  content, and the partial pressure of isoflurane is sustained close to the inspired value, increasing its rate of uptake (the second gas effect).  $\text{Iso}$ , Isoflurane;  $\text{N}_2\text{O}$ , nitrous oxide;  $\text{O}_2$ , oxygen.

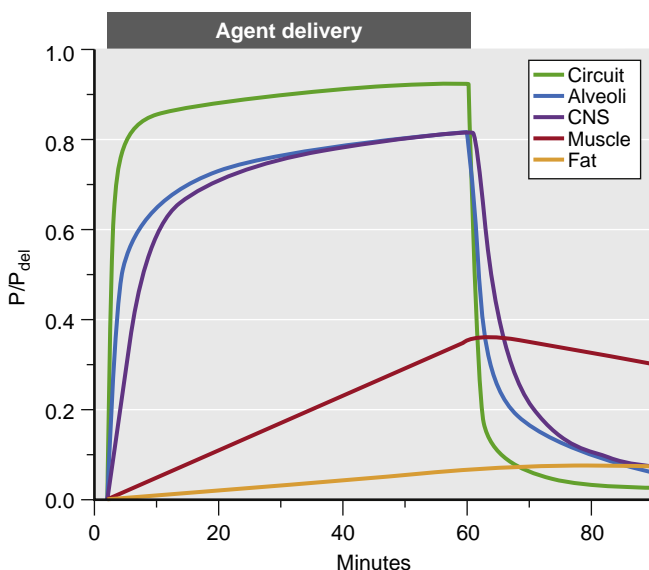


**Fig. 20.9** The rate of anesthetic partial pressure rise in different tissue compartments. The curves represent model calculations for sevoflurane delivered at 6 L/min fresh gas flow, with 5 L/min ventilation and 5 L/min cardiac output. The anesthetic partial pressure in the central nervous system (CNS; purple line), part of the vessel rich group, equilibrates rapidly with  $P_{alv}$  (blue line), although a lag-time of several minutes is evident when  $P_{alv}$  is rapidly rising or falling. The anesthetic partial pressures in both muscle (red line) and fat (orange line) rise and fall much more slowly, because muscle and fat compartments represent much larger effective volumes (see Fig. 20.2) and have lower blood flow than the vessel-rich group. Note that anesthetic partial pressure in fat continues to rise after anesthetic delivery stops, as long as partial pressure in alveolar gas (and arterial blood) is greater than that in the fat compartment.<sup>30</sup>

humans<sup>26</sup> and lab animals.<sup>25</sup> Recent clinical studies and mathematical modeling indicate that, because of ventilation-perfusion heterogeneity, the second gas effect is greater in arterial blood than in expired gas, influenced by the blood solubility of VAs, and significantly affects anesthetic onset at relatively low rates of  $N_2O$  uptake.<sup>27-29</sup>

### Distribution of Anesthetic into Tissues

Blood exiting the pulmonary capillaries enters the pulmonary vein and the left heart. Inhaled anesthetics are then distributed via arterial blood to various body tissues. The rate of increase of anesthetic partial pressure within each tissue is determined by tissue-specific arterial blood flow ( $q$ ), effective volume (the product of anatomic volume and tissue/blood partition coefficient,  $\lambda_{t/b}$ ), and the anesthetic partial pressure gradient between arterial blood and the tissue,

$$\frac{dP_i}{dt} = \frac{\dot{q}_i}{V_i \times \lambda_{i/b}} \times (P_{art} - P_i), \quad (20.10)$$

where  $i$  designates a particular organ or type of tissue. Values used in model calculations are summarized in Table 20.2. The time required for anesthetic partial pressure equilibration between arterial blood ( $P_{art} = P_{alv}$ ) and a specified tissue is shorter if its blood flow is high, and longer if that tissue has a large effective volume (Figs. 20.2 and 20.9).

Traditionally, anesthetic distribution has been described for four distinct tissue groups. The **vessel-rich group**

(VRG) includes the heart, brain, lungs, spinal cord, liver, and kidney. Together, these organs compose approximately 10% of the adult human body mass; however, they receive approximately 70% of cardiac output under normal resting conditions. As a result, time constants for anesthetic equilibration between blood and these organs are typically only a few minutes (see Table 20.2). Of particular interest is the equilibration time for the CNS, where anesthetic effects are mediated. After the highly perfused VRG tissues, **skeletal muscle** is the next compartment to equilibrate with inhaled anesthetics. Muscle composes approximately 40% of body mass in a healthy adult, making muscle the largest single compartment based on weight. Moreover, most inhaled anesthetics partition into muscle more than into brain, resulting in an increased effective volume for anesthetic uptake into this compartment. At rest, muscle receives about 10% to 15% of cardiac output (20 mL/kg/min), but this value can increase dramatically during exercise, stress, fever, or other states associated with high cardiac output.<sup>30</sup> Taken together, these factors generally result in slow equilibration between anesthetic in blood and muscle, with typical time constants of hours (see Table 20.2). The third tissue group is **fat**, which in a healthy adult composes less than 25% of body mass and receives approximately 10% of cardiac output.<sup>31</sup> Potent VAs partition avidly into fat; therefore, fat represents the largest effective volume for uptake of these drugs (see Fig. 20.2, Table 20.2). The extremely large effective volume coupled with low blood flow results in very slow equilibration of anesthetics between blood and fat, with time constants approaching days. A fourth group, including skin, cortical bone, and connective tissue, is referred to as **vessel poor tissues**. These tissues compose 10% to 15% of an average adult body while receiving less than 5% of cardiac output at rest. Induction of general anesthesia impairs normal sympathetic nervous function, resulting in increased blood flow to normally cool skin in the extremities.<sup>32</sup> The blood volume represents approximately 7% of body mass and may be considered another compartment for anesthetic uptake, while also conveying drug to other tissue compartments.

As stated previously, increased cardiac output results in increased anesthetic uptake and a slower rate of rise of  $P_{alv}$ . Clinical studies confirm that, other factors being equal, increasing cardiac output slows the induction of general anesthesia with inhaled anesthetics.<sup>21,33</sup> This result can seem counterintuitive when increasing cardiac output increases uptake of anesthetic into the patient's body and hastens its delivery to the tissues. However, during induction, the anesthetic partial pressure in blood and downstream tissue compartments cannot be higher than that in the upstream alveolar compartment. Increased cardiac output slows the rise of  $P_{alv}$  and thus also slows the rate of increase of the anesthetic partial pressure in blood ( $P_{art}$ ), the CNS ( $P_{CNS}$ ), and other highly perfused tissues. The extra anesthetic uptake is primarily into muscle, which is a large tissue compartment with a high capacity for anesthetic and is where much of the excess cardiac output flows. For example, a 50% increase in cardiac output can more than double muscle blood flow, diverting the majority of anesthetic to muscle, lowering  $P_{alv}$ , and thus slowing anesthetic uptake into target tissues in the CNS. If one could manipulate inhaled anesthetic delivery to maintain constant  $P_{alv}$ ,

which may be achievable with automated feedback control of vaporizer output and FGF,<sup>34</sup> then increased cardiac output might have a different effect. Model simulations where  $P_{alv}$  is maintained at a constant level show that uptake into VRG tissues, including brain tissue, increases more rapidly as cardiac output increases.<sup>35</sup>

In pediatric patients, the balance of cardiac output to various tissue beds differs from that in adults. Thus, although cardiac output per kilogram body weight is larger in children than in adults, anesthetic induction in young children is more rapid than in adults, because a disproportionate amount of perfusion goes to the vessel rich organs, such as the brain.<sup>36</sup>

The equilibrium distribution volumes for most inhaled anesthetics are extremely large, with the largest compartment by far being fat. However, equilibration with fat is so slow that this compartment usually plays a relatively minor role in the pharmacokinetics of inhaled anesthetics. During a typical general anesthetic lasting from 30 minutes to several hours, the blood, VRG organs, and muscle are the compartments into which inhaled anesthetics mostly distribute.

Although the model in Fig. 20.2 illustrates anesthetic distribution only via arterial blood flow, **intertissue diffusion** takes place between abutting tissues that have large interfacial surface areas. In particular, direct diffusion from organs with high anesthetic partial pressures to abutting tissues with low partial pressure and high capacity for anesthetic uptake may also contribute to drug distribution. Examples of this process include anesthetic diffusion from the heart, liver, and kidneys to surrounding fat in the pericardium and abdomen.<sup>37,38</sup>

### The Mixed Venous Anesthetic Partial Pressure

The anesthetic partial pressure in mixed venous blood entering the pulmonary circulation is a weighted average of the venous outflows from all tissues and organs, which converge in the right ventricle:

$$P_{MV} = \sum_{i=1}^n \frac{Q_i}{Q} \times P_i. \quad (20.11)$$

As  $P_{MV}$  rises, the gradient driving uptake of inhaled anesthetics from alveoli weakens. The difference between the delivered (inspired) and the alveolar (end-expiratory) anesthetic concentrations also shrinks, causing transpulmonary uptake to slow (Eq. 20.7). *Systemic (left to right) shunting* causes  $P_{MV}$  to increase more rapidly than it would in the absence of such shunts. When blood flow to other tissues remains normal and the left-to-right shunt simply represents excess cardiac output, the resulting increase in anesthetic uptake (Eq. 20.7) is offset by the increase in  $P_{MV}$ , resulting in a slight increase in the rate of anesthetic delivery or uptake into the brain, muscle, and other tissues. In cases where large left-to-right shunts result in reduced blood flow to other tissues, anesthetic equilibration in those tissues will be relatively slow.

## Synthesis of the Model and Inhaled Anesthetic Induction: PK/PD

The earlier discussion emphasized the rate of equilibration (pharmacokinetics) of inhaled anesthetics among the

various compartments involved in delivery to a patient: vaporizer, circuit, lung, blood, and various tissues. However, in a clinical setting, the goal of the anesthesia provider is the reversible production of certain desired effects (amnesia, unconsciousness, and immobility) in the patient within a reasonable period of time. To achieve this goal, pharmacokinetics must be combined with knowledge of the effects produced at different anesthetic partial pressures in target tissues (i.e., dose-response or pharmacodynamics).<sup>39</sup> The most relevant pharmacodynamic guidelines are minimum alveolar concentration (MAC)-immobility,<sup>40</sup> the alveolar anesthetic concentration preventing movement response to surgical stimulus in 50% of subjects, and MAC-awake,<sup>7</sup> the alveolar anesthetic concentration preventing perceptive awareness in 50% of subjects, both measured under conditions where  $P_{alv}$  is in equilibrium with anesthetic partial pressure in the CNS ( $P_{CNS}$ ). MAC-awake for potent VAs is typically  $0.34 \times$  MAC-immobility,<sup>41</sup> whereas MAC-awake for  $N_2O$  is approximately  $0.7 \times$  MAC-immobility (see Table 20.1). During induction of anesthesia, the goal may be achieving a high probability of immobility following incision ( $P_{CNS} \approx 1.2 \times$  MAC-immobility) within 15 minutes, while avoiding the deleterious effects of overly deep anesthesia. At the end of an anesthetic, return of consciousness is likely to occur when  $P_{CNS}$  decreases to less than MAC-awake. The targets used for this illustrative model patient are estimates. In clinical practice, the target for depth of general anesthesia should always minimize the risk of awareness (consciousness), but may vary, depending on patient factors, the presence of noxious stimuli, and other drugs that may be administered.

There are a variety of strategies to deliver inhaled anesthetics and to achieve the desired and reversible effects of anesthesia within a reasonable timeframe. The first important consideration is that  $P_{del}$  from the vaporizer must be higher than our target  $P_{alv}$  or  $P_{CNS}$  (**overpressure**). The more overpressure used, the more rapidly anesthetic is delivered. High fresh gas flows, large MV, and a low-solubility drug will also increase the rate of anesthetic delivery and the rate of rise of  $P_{alv}$  and  $P_{CNS}$ . These factors, and particularly overpressure, also increase the risk of delivering an overdose of anesthetic drug. A common strategy is to initiate inhaled anesthetic delivery with moderate to high fresh gas flows ( $\geq 6$  L/min) and moderate overpressure ( $P_{del} = 2 \times$  MAC-immobility), and reduce  $P_{del}$  after  $P_{alv}$  reaches or slightly exceeds the target level (Fig. 20.10, left). The need to maintain overpressure and slightly overshoot  $P_{alv}$  derives from the fact that distribution of drug to muscle maintains a high delivery requirement after the initial rapid phase of uptake. If  $P_{del}$  is decreased too quickly, then  $P_{alv}$  can decrease below the target.  $P_{del}$  or FGF is slowly adjusted downward as the anesthetic inspired-to-expired difference in anesthetic partial pressures ( $P_{del} - P_{alv}$ ) decreases.

### Closed-Circuit or Low-Flow Delivery of Anesthesia

The use of high or moderate fresh gas flows, while enabling use of less overpressure, results in far more anesthetic drug being delivered than being taken up into tissues. As illustrated in Fig. 20.10C, the amount of isoflurane delivered is 4.5-fold greater than that taken up, and delivered sevoflurane is 7.2-fold greater than absorbed drug. Thus more than 80% of delivered VA is waste using the moderately

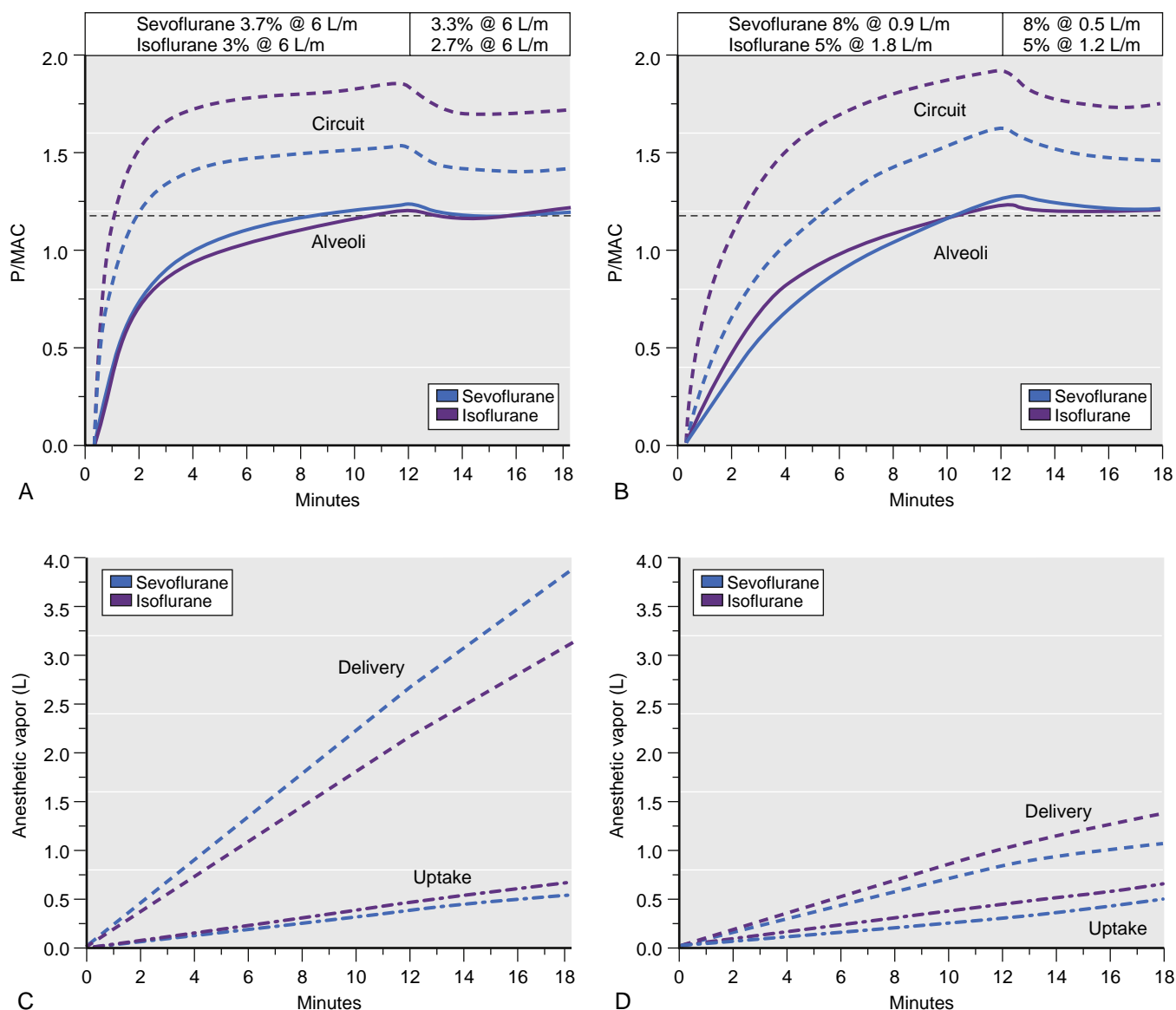


**Fig. 20.10** Effect of induction technique on uptake and delivery of inhaled anesthetics. (A) Anesthetic partial pressures in both the circuit (dashed lines) and alveoli (solid lines) during inhalation induction with moderate (6 L/min) fresh gas flows and modest (twofold to threefold) overpressure for sevoflurane (blue) and isoflurane (purple).  $P_{\text{alv}}$  reaches  $1.2 \times \text{MAC}$  in about 12 minutes, and approximately 10% downward adjustment of vaporizer settings results in maintenance of  $P_{\text{alv}}$  near this target level. Additional downward adjustments in vaporizer setting or fresh gas flows, or both, would be needed to further maintain this  $P_{\text{alv}}$  level. (B) Anesthetic partial pressures in both the circuit and alveoli during inhalation induction with low (<2 L/min) fresh gas flows and maximal (fourfold) overpressure for sevoflurane (blue) and isoflurane (purple).  $P_{\text{alv}}$  reaches  $1.2 \times \text{MAC}$  in approximately 12 minutes, and a downward adjustment of fresh gas flow results in maintenance of  $P_{\text{alv}}$  near this target level. (C) The total anesthetic vapor delivered and taken up into the model patient from panel A. Note that delivery far exceeds uptake, more so for the low solubility anesthetic (sevoflurane). (D) The total amount of anesthetic vapor delivered and taken up into the model patient from panel B. Note that uptake is very similar to that in panel C, whereas delivery is much lower. The low fresh gas flow technique (panels B and D) reduces waste more so for anesthetics with low blood solubility (e.g., sevoflurane) than for soluble drugs (e.g., isoflurane). MAC, Minimum alveolar concentration;  $P_{\text{alv}}$ , alveolar anesthetic partial pressure.

high FGF approach illustrated in this example (settings are shown in Fig. 20.10A). Rebreathing circuits allow the use of fresh gas flows well below MV, which results in reduced anesthetic discharge into the waste-scavenging system. Less waste discharge translates into both reduced costs and reduced global environmental impact of anesthetic gases in the atmosphere, where they contribute to climate change (discussed later in this chapter). Additional benefits of low FGF and rebreathing include retention of expired heat and water vapor in rebreathed gas, improving airway epithelial health, and reducing accumulation of dried airway secretions.<sup>42</sup>

**Closed-circuit anesthesia** represents the ultimate limit of low gas flows, where fresh gases are delivered only in quantities sufficient to replace those taken up into tissues, metabolized (especially  $O_2$ ), or otherwise lost to the environment, and the vast majority of gas in the breathing circuit undergoes rebreathing.<sup>43</sup> Achieving this goal requires a leak-free breathing circuit, complete removal of  $CO_2$ , and careful attention to the inspired-to-expired values of oxygen and anesthetic gases, and even to expired nitrogen that may slowly accumulate in the breathing circuit. Under these conditions, oxygen consumption in an anesthetized patient may be lower than 3 mL/kg/min, translating to

$P_{\text{O}_2}$  replacement of approximately 200 mL/min in a 70 kg patient. There are several significant limitations to this technique. Because all exhaled  $CO_2$  must be removed by absorbents, closed-circuit anesthesia increases the risk of rebreathing  $CO_2$  as absorbent capacity diminishes. Anesthetic breakdown products, carbon monoxide (CO), and slowly degassing nitrogen from blood can accumulate in the breathing circuit.<sup>44</sup> Clinicians must be aware that patient metabolism may deplete oxygen from the breathing circuit and result in delivery of a hypoxic gas mixture during use of closed circuit anesthesia. When using very low FGF values, changes in the vaporizer output ( $P_{\text{del}}$ ) result in extremely slow changes in  $P_{\text{circ}}$  and the subsequent depth of anesthesia. Closed circuit anesthetic administration is often guided by the “square root of time rule,” proposed by Severinghaus<sup>45</sup> and detailed in now classic descriptions.<sup>46</sup> This rule states that the rate of anesthetic uptake decreases approximately as the square root of delivery time. We can estimate the uptake of 1.2 MAC isoflurane during the first minute of anesthesia using Eq. (20.7). Thus cardiac output  $\times \lambda_{b/g} \times 1.2 \text{ MAC} = \text{Initial uptake of isoflurane vapor}$  ( $5000 \text{ mL/min} \times 1.4 \times 0.0128 \text{ atm} = 90 \text{ mL/min}$ ). Using the square-root of time rule, uptake at 4 minutes would be half of the initial rate (45 mL/min), and at 9 minutes, uptake would be one-third of the initial rate (30 mL/min). It should be noted that to deliver 90 mL/min of isoflurane vapor at a maximal vaporizer setting of 5% requires 1800 mL/min of FGF, far greater than the target FGF for closed circuit anesthesia. Anesthetists can overcome this limitation by directly injecting small volumes of liquid anesthetic into the expiratory limb of the breathing circuit;<sup>47</sup> however, this technique requires vigilant attention to the clock along with many other factors. In inexperienced hands, miscalculation or mistiming of anesthetic injection runs the risk of overdose.

Because of the challenges of closed-circuit administration, a more common practice is to use moderate to high fresh gas flows to achieve rapid changes during induction of anesthesia, reserving closed circuit anesthesia to periods where the  $P_{\text{circ}} - P_{\text{alv}}$  difference is small. Even so, changes in a patient’s metabolism because of temperature variation, degree of muscle relaxation, or surgical stimulation can result in the need for frequent adjustments to oxygen flow and anesthetic depth, making anesthesia delivery in a closed circuit system relatively unstable and difficult.

**Low-flow anesthetic delivery**, typically with fresh gas flows of 0.5 to 1.0 L/min during the maintenance phase of an anesthetic, is a compromise between closed-circuit conditions and the use of high fresh gas flows. Much of the waste and other problems associated with high fresh gas flows are avoided, while the instability associated with a strict closed-circuit technique is also moderated. As noted earlier (see section on “Equilibration Between Circuit and Pulmonary Airspace”), the inspired anesthetic concentration ( $P_{\text{circ}}$ ) depends on both  $P_{\text{del}}$  and  $P_{\text{pulm}}$  when rebreathing occurs. Thus, as FGF diminishes,  $P_{\text{del}}$  must be adjusted upward to compensate for diminished delivery. Given that the maximal output setting on most vaporizers is about  $4 \times \text{MAC-immobility}$ , anesthetic delivery at 1 L/min and maximal  $P_{\text{del}}$  is still far less than the previous example with 6 L/min and  $P_{\text{del}} = 2 \times \text{MAC isoflurane}$ . Higher FGF or a less soluble anesthetic drug, or both, is needed to achieve target

$P_{\text{CNS}}$  in less than 15 minutes, but as uptake diminishes, FGF can be gradually reduced (Fig. 20.10, right panels). With soluble anesthetics like isoflurane, maximal vaporizer settings and FGF near 2 L/min is required for reasonably rapid induction. FGF can be incrementally decreased as  $P_{\text{alv}}$  reaches the target level, and eventually vaporizer output setting is decreased as well. With low solubility anesthetics like desflurane or sevoflurane, initial FGF values near 1.0 L/min can be used in combination with maximal vaporizer settings and a similar strategy of reducing FGF. These conditions result in reasonably rapid induction while minimizing waste of VAs. Low FGF can be maintained until high FGF is again needed to achieve emergence at the end of the anesthetic administration.

When using high vaporizer output settings, diligence must be maintained to avoid overdosing the patient by reducing FGF and the vaporizer setting in a timely and deliberate manner. Use of significant overpressure should be avoided in situations when other clinical issues require the attention of the anesthesia provider.

## PHARMACODYNAMIC EFFECTS OF ANESTHETICS ON UPTAKE AND DISTRIBUTION

The pharmacodynamic effects of most inhaled anesthetics also include changes in ventilatory and cardiac function that thereby introduce dynamic changes in the drug pharmacokinetics. **Spontaneous ventilation** is reduced by inhalation of potent VAs in a dose-dependent manner.<sup>48</sup> As a result, spontaneously breathing patients will autoregulate to some degree by reducing their uptake of anesthetic agent as depth of anesthesia increases. This autoregulation provides a degree of safety that is absent in ventilated patients, who may be subjected to excessive delivery of inhaled anesthetics if a vaporizer is inadvertently set to deliver overpressure.<sup>49</sup> Inhaled anesthetics also reduce **cardiac output**, a pharmacodynamic effect that leads to a more rapid increase in  $P_{\text{alv}}/P_{\text{circ}}$  and consequently a more rapid increase in the anesthetic partial pressure in heart, brain, and other highly perfused tissues.<sup>50</sup> Halothane is the anesthetic associated with the greatest reduction in cardiac output. If anesthetic delivery continues in the face of a falling cardiac output, this can lead to a positive feedback loop of worsening cardiac depression and a rapid descent toward hemodynamic collapse. More details on the effects of inhaled anesthetics on respiratory and circulatory systems are provided in Chapter 21.

## THE EFFECT OF NITROUS OXIDE ON GAS-FILLED SPACES

Because  $N_2O$  is often used at high partial pressures, it diffuses into and accumulates in spaces containing air or other immobile gases, with potentially deleterious physiologic consequences. Clinically relevant examples include intravascular air emboli,<sup>51</sup> pneumothorax,<sup>52</sup> air in the inner chamber of the ear,<sup>53</sup> intravitreal gas bubbles,<sup>54</sup> intrathecal air, pneumoencephalus,<sup>55</sup> and air in the gastrointestinal tract.<sup>52</sup> Air-filled spaces contain mostly nitrogen, a gas that composes 78% of air but is 30-fold less soluble in blood than  $N_2O$  ( $\lambda_{b/g}$  for  $N_2$  is 0.015). Thus  $N_2O$  diffuses down its pressure gradient from blood and surrounding tissues into

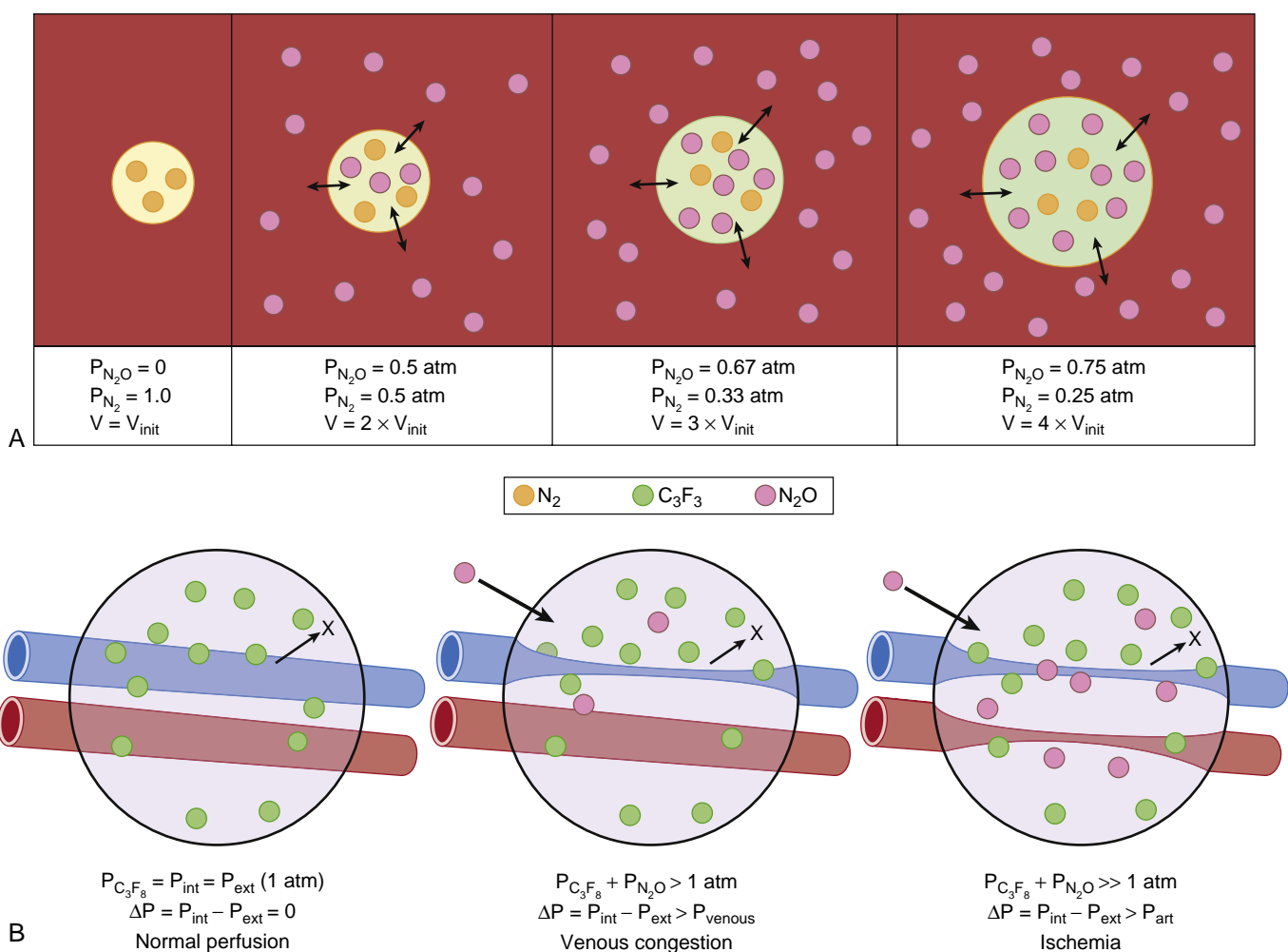


**Fig. 20.11** Nitrous oxide accumulation in gas-filled spaces. **A**, Expansion of a compliant air-filled space (a small vascular air embolus) occurs as the partial pressure of nitrous oxide in surrounding blood increases. Each panel depicts the equilibrium condition with  $P_{N_2O}$  inside the bubble equal to that in blood. Labels below each panel summarize the partial pressures of  $N_2O$  and  $N_2$  in the bubble as well as the bubble volume relative to its initial value ( $V_{init}$ ). **B**, The increase in pressure inside a noncompliant, gas-filled compartment (e.g., an eye following perfluoropropene [ $C_3F_8$ ] injection) with blood vessels passing through it. As  $N_2O$  accumulates, the pressure in the compartment increases, which can result in venous congestion (middle panel) or ischemia (right panel) in tissues that are perfused by the vessels in this compartment (e.g., the retina). *Atm*, Atmosphere;  $\Delta P$ , difference between internal and external pressure;  $N_2$ , nitrogen;  $N_2O$ , nitrous oxide;  $P_{art}$ , arterial blood pressure;  $P_{C_3F_8}$ , partial pressure of perfluoropropene;  $P_{ext}$ , pressure outside the compartment;  $P_{int}$ , internal compartment pressure;  $PN_2$ , partial pressure of nitrogen;  $PN_2O$ , partial pressure of  $N_2O$ ;  $P_{venous}$ , venous blood pressure.

air-filled spaces, whereas  $N_2$  elimination from these spaces is far slower, even with inspired  $P_{N_2} = 0$ . As  $N_2O$  enters and the total number of gas molecules in an air space increases, it will expand in volume, increase in pressure, or both, depending on the compliance of the tissues surrounding the air-filled space.

In **highly compliant air-filled spaces**, such as intravascular air bubbles or small pneumothoraces,  $N_2O$  accumulation increases the total volume of gas (Fig. 20.11A) with minimal changes in pressure. Air spaces expand as  $N_2O$  enters until the  $P_{N_2O}$  within the air space matches that in surrounding blood, establishing equilibrium. The maximum potential gas volume expansion in a highly compliant space is

$$\frac{V}{V_{init}} = \frac{1}{1 - P_{N_2O}}. \quad (20.12)$$

Thus administration of 50%  $N_2O$  can double air-space volume, whereas 67% can potentially triple air-space

volume.  $N_2O$  can significantly worsen the cardiovascular or tissue consequences of intravascular air emboli, potentially making a nonlethal volume of venous air embolus become lethal.<sup>51</sup> Expansion of gastrointestinal gas volume by  $N_2O$  may impede surgical exposure or abdominal wound closure. Gas-space compartment compliance eventually decreases as volume expands, resulting in increased pressure. For example,  $N_2O$  may expand a small pneumothorax to a point where intrathoracic pressure rises, compressing lung, displacing the mediastinum, and reducing venous return (tension pneumothorax).  $N_2O$  is contraindicated in patients with intracranial air until after dural opening, in order to avoid intracranial hypertension.<sup>56</sup> The endotracheal tube cuff filled with air is also susceptible to expansion by  $N_2O$ . Increased tracheal cuff pressure may impair perfusion of surrounding mucosa.<sup>57</sup> Air-filled laryngeal mask airway cuffs<sup>58</sup> and the air-filled balloon of a Swan-Ganz catheter<sup>59</sup> may similarly expand during  $N_2O$  administration.

In **noncompliant gas-filled spaces**, gas pressure rises as  $N_2O$  enters, until  $P_{N_2O}$  within the air space matches that

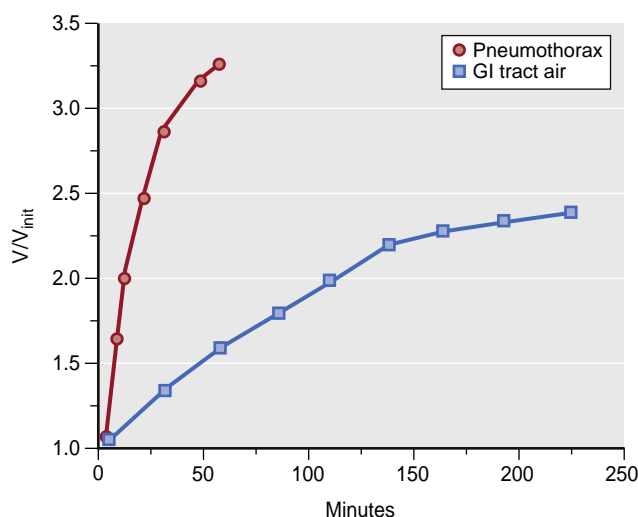


**Fig. 20.12** The rate of air-space expansion during nitrous oxide administration. The rate and extent of expansion of air pockets injected into either the pleural space (red circles) or the gastrointestinal tract (blue squares) of dogs during the inhalation of a 25% oxygen/75% nitrous oxide gas mixture is shown. Air pockets in the stomach, small intestine, and colon expand more slowly than do those in a pneumothorax. GI, Gastrointestinal. (Data are approximations from the results reported in Eger EI II, Saidman LJ. Hazards of nitrous oxide anesthesia in bowel obstruction and pneumothorax. *Anesthesiology*. 1965;26:61–66.)

in blood. The maximal potential pressure in such a space, relative to surrounding ambient pressure, is therefore  $P_{N2O}$ . Thus, in a patient inhaling 50%  $N_2O$ , pressure in such a gas-filled compartment could approach 380 mm Hg, far greater than typical arterial perfusion pressures. A clinically important example is that of intravitreal sulfur hexafluoride ( $SF_6$ ) or perfluoropropane ( $C_3F_8$ ) bubbles, which are injected as the sclera is closed at the end of intraocular or retinal surgery (see Fig. 20.11B).<sup>54</sup> These gases persist even longer than  $N_2$  does, because of their low blood solubility. If  $N_2O$  is administered to these patients at the time of intravitreal bubble injection, its diffusion into the bubble can rapidly increase intraocular pressure above that in retinal veins, producing retinal congestion. If the pressure in the eye further increases above systolic arterial pressure, retinal ischemia resulting in blindness may ensue.

The **rate of  $N_2O$  diffusion into gas-filled spaces** in the body depends on local blood flow and the surface to volume ratio of the space. Thus small air emboli expand within seconds, because they have high surface/volume ratios and are surrounded by a very high relative flow of blood containing dissolved  $N_2O$ . Larger air emboli expand more slowly, because their surface/volume ratios are smaller (spherical surface/volume is inversely proportional to radius). Small pneumothoraces typically have large surface/volume ratios and high local blood flow. Animal experiments show that inhalation of 75%  $N_2O$  approximately doubles pneumothorax volume in 10 minutes and triples it in 30 minutes (Fig. 20.12). Compared with a pneumothorax, gastrointestinal air pockets have lower surface/volume ratios and lower blood flow. Thus expansion of gas in the gastrointestinal tract is much slower than that in a pneumothorax. In animal studies (see Fig. 20.12), inhalation of 70% to 80%  $N_2O$  doubled intestinal gas volume after approximately 2 hours.<sup>52</sup>

$N_2O$  use is contraindicated in patients with pneumothorax, pneumocephalus, and closed dura, or in those at high risk for vascular air embolus. Air-space expansion may impede surgery when substantial gastrointestinal air is present and  $N_2O$  exposure is prolonged, or it can be of little consequence when the initial volume of gas in the gut is small or when the surgery is brief.

## RECOVERY FROM ANESTHESIA

### Similarities and Differences to Induction

Clearance of inhaled anesthetics from target tissues (brain and spinal cord) is primarily via the same pathways used for anesthetic induction: anesthetic gases flow from tissue into venous blood and then to the lungs. If  $P_{alv}$  is less than  $P_{MV}$ , then the net flow of anesthetic will be out of the blood and into alveoli, where it is subsequently exhaled. To achieve the fastest clearance possible,  $P_{circ}$  must therefore be as low as possible, and this is achieved using high flows of nonanesthetic carrier gases (oxygen and air) after discontinuing delivery of anesthetic. The same factors that affect transalveolar anesthetic exchange during induction will also affect clearance via this route. Increasing ventilation will accelerate clearance (see Fig. 20.4), whereas increased cardiac output slows clearance, because more gas-exchange volumes are required to remove anesthetic from the larger blood flow (see Fig. 20.5). Highly blood-soluble anesthetics, which increase the *effective* blood flow, clear more slowly than insoluble anesthetics (see Fig. 20.6). Return-to-consciousness, which usually occurs after  $P_{CNS}$  decreases below MAC-awake, is faster following desflurane or sevoflurane anesthesia than after isoflurane anesthesia.  $N_2O$ , which is characterized by blood solubility similar to that of desflurane, provides an even faster return to consciousness, because of two additional advantages. First, the concentration effect works in reverse during clearance of  $N_2O$ , increasing effective alveolar ventilation and maintaining the gradient for flow from pulmonary blood to alveoli. Second, MAC-awake for  $N_2O$  (0.71 atm at 40 years old) is near typical inhaled concentrations during general anesthesia; therefore, elimination of only a small fraction of this drug is associated with return to consciousness. This is also why  $N_2O$  as the sole hypnotic drug is associated with a high risk of intraoperative awareness, which can be prevented by using a balanced gas mixture of  $N_2O$  together with end-tidal concentrations of about  $1 \times$  MAC-awake of a second potent inhaled anesthetic.

Body composition has an increasing impact as the length of anesthetic exposure increases, especially for highly soluble anesthetics. Compared with standard models, patients with increased muscle or fat will have larger volumes of anesthetic drug distribution over time, resulting in slower clearance rates.<sup>60</sup> One important difference between anesthetic uptake and clearance is that although overpressure can be utilized to hasten uptake and induction of anesthesia, the vaporizer setting cannot be set to less than zero. As a consequence, the most readily modifiable factors to affect the rate of anesthetic clearance are fresh gas flow and MV. Indeed, after prolonged (>4 hours) exposure to  $1 \times$  MAC inhaled anesthesia, maintenance of adequate ventilation should be a high priority, even after end-tidal anesthetic concentrations reach MAC-awake. Hypoventilation in this

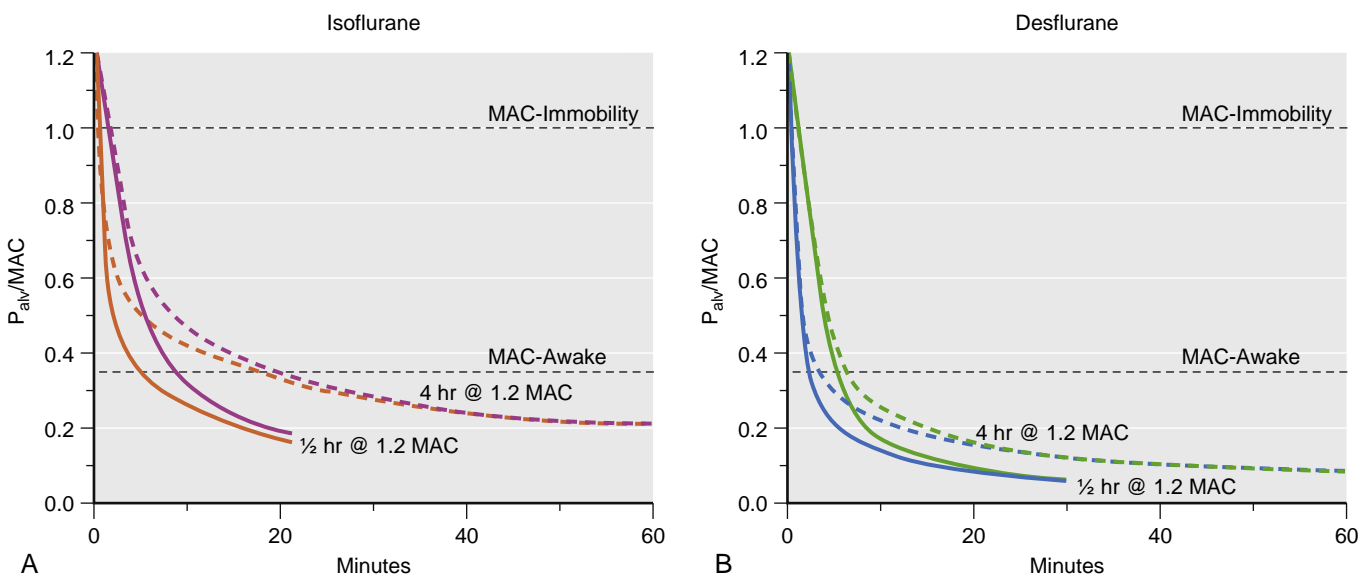


**Fig. 20.13** Inhaled anesthetic wash-out and time to awakening depends on duration of anesthesia. The panels depict model calculations of  $P_{\text{alv}}$  and  $P_{\text{CNS}}$  normalized to MAC during wash-out at 10 L/min FGF and 5 L/min MV following anesthesia at approximately  $1.2 \times \text{MAC}$ -immobility for 30 minutes (solid lines) or 4 hours (dashed lines). The MAC-awake (approximately  $0.34 \times \text{MAC}$ -immobility) is shown to indicate the threshold below which typical patients regain perceptive awareness after general anesthesia. Although  $P_{\text{alv}}$  drops earlier than  $P_{\text{CNS}}$ , the clinically relevant endpoint (return of consciousness) is predicted when  $P_{\text{CNS}}$  falls below MAC-awake. (A) Wash-out using a pharmacokinetic model for isoflurane (orange is  $P_{\text{alv}}$ , purple is  $P_{\text{CNS}}$ ). The 30-minute isoflurane uptake was 990 mL of vapor, and the 4-hour isoflurane uptake was 3420 mL of vapor. Prolonged anesthesia with isoflurane dramatically increases the time required to wash-out sufficient drug to achieve awakening. After a 30-minute anesthetic,  $P_{\text{CNS}}$  (solid purple line) drops to MAC-awake in 9 minutes, whereas it takes more than 20 minutes of wash-out to reach the same  $P_{\text{CNS}}$  following a 4-hour anesthetic (dashed purple line). (B) Wash-out using a desflurane model (blue is  $P_{\text{alv}}$ , green is  $P_{\text{CNS}}$ ). The 30-minute desflurane uptake was 1530 mL of vapor, and the 4-hour desflurane uptake was 4600 mL of vapor. The predicted times to awakening (solid versus dashed green lines) reach MAC-awake at 5.2 and 6.3 minutes, respectively) are much closer following different durations of desflurane anesthesia, because of its low blood solubility. Clinical studies demonstrate that emergence and recovery (time to extubation) following isoflurane anesthesia nearly doubles when exposure increases from 20 to 75 minutes, whereas extubation is achieved in less than 10 minutes following desflurane anesthesia from 20 to 100 minutes' duration.<sup>63</sup> FGF, Fresh gas flow; MAC, minimum alveolar concentration; MV, minute ventilation;  $P_{\text{alv}}$ , Alveolar anesthetic partial pressure;  $P_{\text{CNS}}$ , anesthetic partial pressure in the central nervous system.

situation can result in reanesthetization caused by redistribution of anesthetic drug from muscle into blood and highly perfused tissues.<sup>61</sup>

### Context Sensitive Recovery from Anesthesia

Although the concept of context sensitive half-time is typically applied to continuously infused anesthetics that distribute among multiple pharmacokinetic compartments, it also applies to inhaled anesthetics.<sup>62</sup> After a short period of inhalation and uptake, anesthetic clearance from blood is rapid through both exhalation and distribution to muscle and other tissues. As a result,  $P_{\text{alv}}$  decreases rapidly to a low value after discontinuing anesthetic delivery. After prolonged periods of inhalation and uptake, the anesthetic partial pressures in muscle and other compartments increase closer to that in blood, reducing the contribution of distributive clearance. Instead, clearance from the central blood compartment is slowed by the reverse flow of anesthetic from the high-capacity tissues. Thus, in comparison with a short period of inhalation, prolonged inhaled anesthesia is followed by a smaller initial decrease in  $P_{\text{alv}}$  and a more pronounced slow clearance phase, resulting in slower recovery from anesthesia (Fig. 20.13).<sup>63</sup> As with other factors, context sensitivity is exaggerated in highly soluble anesthetics, and it has less impact with anesthetics that display low blood and tissue solubilities.<sup>63</sup> The relative advantage of low blood solubility anesthetics increases with the duration of anesthesia. There is only a small (2.5 minutes) difference

between predicted times to awakening after a short anesthetic with isoflurane versus desflurane, but significantly faster awakening can be achieved using the low-solubility drug for long cases.

### Percutaneous and Visceral Anesthetic Loss

Aside from pulmonary exchange, some portion of inhaled anesthetics is lost by diffusion through other large area interfaces between the body and surrounding air. The skin surface area of an average human is about  $2 \text{ m}^2$ , and blood flow through skin during general anesthesia may be substantial because of inhibition of normal thermoregulatory vasoconstriction.<sup>32</sup> Nonetheless, transcutaneous losses of general anesthetics probably contribute negligibly to their clearance.<sup>64,65</sup> During open abdominal or thoracic surgery, visceral surfaces are also directly exposed to air, and under these circumstances, anesthetic losses via direct transfer and air movements are larger than those via skin, but still a small fraction of total clearance.<sup>66</sup>

### Effect of the Anesthetic Circuit

As mentioned earlier, circuit components, including tubing, connectors, manual ventilation bag, and  $\text{CO}_2$  absorbent material, absorb inhaled anesthetics, effectively creating another compartment that fills while anesthetic is flowing, and needs to be emptied during wash-out.<sup>19</sup> Low-level release of anesthetic gases from these components can continue for a considerable time.

## Clearance via Metabolism of Anesthetics

Metabolism of inhaled anesthetics in tissues, particularly liver, contributes a variable degree to drug clearance. Metabolism of inhaled anesthetics is reviewed in detail in the second part of this chapter (see section on “Metabolism and Toxicity of Inhaled Anesthetics”). Methoxyflurane, a drug that is no longer in clinical use, and halothane, an older drug that is rarely used in the United States, are highly metabolized inhaled anesthetics. Methoxyflurane undergoes extensive metabolism in humans, with only 19% of an inhaled dose recovered in exhaled gases.<sup>67</sup> Approximately 20% to 25% of inhaled halothane is metabolized through biotransformation in the liver. A high rate of metabolism will reduce the anesthetic partial pressure in tissues, resulting in reduced  $P_{MV}$  and increased rates of overall anesthetic clearance. Tissue-dependent breakdown contributes less to clearance of newer inhaled anesthetics.

## Additional Considerations and Possibilities

Modern inhaled anesthetics like sevoflurane and desflurane have low blood solubility, and therefore provide a distinct advantage for both anesthetic induction and recovery from anesthesia. However, they present no advantage over older drugs like isoflurane for maintenance of anesthesia during long cases and are far more expensive. What if anesthesia is induced with one drug, followed by a switch to isoflurane during the maintenance period, and then switched back to the more soluble drug, such as desflurane, for a period preceding emergence? This might allow for more rapid induction and wakeup than with isoflurane alone. Although a fast wakeup can be achieved by allowing sufficient time for near total washout of isoflurane and its replacement with desflurane, this type of crossover requires significant lead time and high fresh gas flows. As an illustration, Neumann and colleagues<sup>68</sup> compared 2-hour anesthetics at  $1.25 \times \text{MAC}$  (2 L/min FGF) with isoflurane alone, desflurane alone, or isoflurane with a crossover to desflurane during the last half hour. Although subjects awoke faster with desflurane alone, the crossover strategy did not result in acceleration of wakeup compared to isoflurane alone.

## Diffusion Hypoxia

Diffusion hypoxia is another sequelae of rapid outgassing from the tissues of patients anesthetized with  $\text{N}_2\text{O}$ . During the initial 5 to 10 minutes after discontinuation of anesthesia, the flow of  $\text{N}_2\text{O}$  from blood into the alveoli can be several liters per minute, resulting in dilution of alveolar oxygen.<sup>69</sup> Another effect of rapid outgassing is reduction of alveolar  $P_{\text{CO}_2}$ , which may also reduce respiratory drive.<sup>70</sup> If the patient does not receive supplemental oxygen during this period, then the combined effects of respiratory depression from anesthesia, reduced alveolar  $P_{\text{CO}_2}$ , and reduced alveolar  $P_{\text{O}_2}$  can result in hypoventilation and oxyhemoglobin desaturation. This outcome is avoided by routinely providing supplemental  $\text{O}_2$  for the first 5 to 10 minutes of recovery, together with vigilant attention to respiration and oxygenation.

## Metabolism and Toxicity of Inhaled Anesthetics

This portion of the chapter focuses on adverse effects that are attributable to inhaled anesthetics, excluding most of

the acutely reversible pharmacodynamic effects of inhaled anesthetics on various physiologic systems (see [Chapters 11, 14, and 21](#)).

The inhaled anesthetics are a unique group of drugs that can both enter and leave the body unchanged through the lungs. Thus chemical transformation of inhaled anesthetics is unrelated to their therapeutic activities such as amnesia, hypnosis, and immobilization. Nonetheless, the carbon-halogen and other bonds of volatile alkanes and ethers can break down under certain conditions: biotransformation by enzymes in various tissues, reactions with strong bases in  $\text{CO}_2$  absorbents, and exposure to ultraviolet radiation in the environment. Anesthetic breakdown resulting from decomposition in tissues or the breathing circuit can produce toxic reactive intermediates, which in sufficient amounts can harm patients directly or indirectly.  $\text{N}_2\text{O}$  gas is not biotransformed, but selectively reacts with and inactivates vitamin  $\text{B}_{12}$  and perturbs  $\text{B}_{12}$ -dependent biochemical pathways. The breakdown of waste anesthetics in the atmosphere also has potential environmental and health consequences. There are potential long-term neurotoxic effects of anesthetic exposure in patients that are not associated with chemical breakdown. Potential neurotoxic properties of inhaled anesthetics are further described in [Chapters 78 and 84](#).

## BIOTRANSFORMATION OF INHALED ANESTHETICS

The extent and location of inhaled anesthetic metabolism depends on multiple chemical factors. Inhaled anesthetics undergo varying degrees of biotransformation ([Table 20.3](#))<sup>71</sup> in various tissues. Methoxyflurane undergoes by far the greatest metabolism, estimated at 70%, and experiments indicate that only a small fraction of drug taken up into body tissues is exhaled.<sup>67</sup> Given the remarkable lipophilicity of methoxyflurane, respiratory clearance of this drug from muscle and fat extends over a period of days (see [Tables 20.1 and 20.2](#)). Halothane is the next most lipophilic drug and ranks second in metabolic clearance (see [Table 20.3](#)).<sup>72-96</sup> Thus prolonged residence in body tissues is an important factor in biotransformation of inhaled anesthetics. Chemical stability is another important factor. Isoflurane is an isomer of enflurane, and the two drugs display comparable respiratory uptake, distribution, and respiratory clearance. Nonetheless, isoflurane is metabolized only one tenth as much as enflurane. Although sevoflurane and desflurane represent another pair of anesthetics, both are characterized by rapid uptake, distribution, and respiratory clearance with 5% of sevoflurane biotransformed versus 0.02% of desflurane.

Of the major organs involved in anesthetic biotransformation, the liver and kidneys are exposed to the highest metabolite concentrations and thus are also most susceptible to damage from toxic metabolites. Clinically significant hepatotoxicity is primarily associated with exposure to halothane, and nephrotoxicity is associated with methoxyflurane.<sup>71</sup> Investigations into the mechanisms of these toxicities have influenced drug development and also provided important insights into human toxicology.<sup>97</sup>

**TABLE 20.3** Metabolism of Halogenated Volatile Anesthetics

Anesthetic	Halothane	Methoxyflurane	Enflurane	Isoflurane	Desflurane	Sevoflurane
Extent of tissue metabolism (%)	25	70	2.5	0.2	0.02	5
Oxidizing enzymes	CYP2E1 CYP2A6	CYP2E1 CYP1A2, 2C9/10, 2D6	CYP2E1	CYP2E1	CYP2E1	CYP2E1
Oxidative metabolites	F <sub>3</sub> C-COOH HBr, HCl	H <sub>3</sub> C-O-CF <sub>2</sub> -COOH HCl <sub>2</sub> C-COOH HOOC-COOH HF, HCl	HF <sub>2</sub> C-O-CF <sub>2</sub> -COOH HCl, HF	HF <sub>2</sub> C-O-CO-CF <sub>3</sub> F <sub>3</sub> C-COOH CF <sub>2</sub> HOH HCl	HF <sub>2</sub> C-O-CO-CF <sub>3</sub> F <sub>3</sub> C-COOH CF <sub>2</sub> HOH HF	HO-CH(CF <sub>3</sub> ) <sub>2</sub> HF
Trifluoroacetylated hepatocellular proteins	+++++	n/a	++	+	+	none
Reducing enzymes	CYP2A6 CYP3A4	n/a	n/a	n/a	n/a	
Reductive metabolites	F <sup>-</sup> , Br <sup>-</sup> F <sub>2</sub> C=CHCl F <sub>3</sub> C-CH <sub>2</sub> Cl					
Tissue toxicities	Hepatic	Renal Hepatic	Renal Hepatic	Hepatic	Hepatic	Hepatic
Fulminant hepatitis incidence	1:20,000	Reported, incidence unknown	1:300,000	rare	rare	Few case reports
References	72-76	77-80	81-85	84,86-88	89-92	78,93-96

The plus signs indicate relative degree of protein modification. n/a, the specific enzymes are not identified in these cases. Kharasch ED. Adverse drug reactions with halogenated anesthetics. *Clin Pharmacol Ther*. 2008;84:158–162.

### Biotransformation in the Liver

The liver is the major site of metabolism for most drugs, particularly lipophilic drugs, which typically are transformed into hydrophilic metabolites that are more readily excreted. The liver is large and contains high concentrations of many drug-metabolizing enzymes. Other organs that contribute to drug metabolism and clearance include the gastrointestinal tract, kidneys, and lungs.<sup>98,99</sup> Drug biotransformation reactions include oxidation, hydrolysis, and conjugation. A single drug may be transformed into several metabolites, depending on the relative rates of various enzyme reactions, the drug concentration in different tissues expressing relevant enzymes, competition at enzyme sites with other drugs or endogenous substances, and other factors. Oxidation and hydrolysis are also known as *phase 1 reactions*, and they result in the introduction or exposure of a polar group on the drug. The phase 1 enzymes that metabolize inhaled anesthetics in the liver are various cytochrome P450 (CYP) isoforms in the endoplasmic reticulum of hepatocytes. These catalyze oxidation reactions such as dehalogenation, N- and O-dealkylation, N- and S-oxidation, and deamination. These reactions require oxygen and NADPH-dependent cytochrome P450 reductase as cofactors. Under hypoxic conditions, some P450 enzymes can also catalyze reductive reactions. More than 50 CYP isoforms are active in humans, and CYP3A4 and CYP3A5 are the most abundant. Conjugations are also known as *phase 2 reactions*, and they often append highly polar groups such as glucuronic acid, sulfate, or glycine to polar groups on phase 1 metabolites. The resulting hydrophilic products are readily excreted in urine via the kidneys or in bile via the gastrointestinal tract. N-Acetylation reactions are an exception that result in metabolites that are less water-soluble than the parent drug.

Many factors affect hepatic drug metabolism, including concomitant drugs, disease, age, and genetics.<sup>100</sup> Induction and inhibition of enzymes are associated with exposure to certain drugs or other exogenous substances. Induction of specific CYP isoforms is a gene-mediated response to chronic exposure to substances that often are substrates of the enzyme, resulting in accelerated enzyme production or slowed turnover. For example, phenobarbital use results in increased production of CYP3A4 as well as NADPH-cytochrome P450 reductase, leading to dramatically increased metabolism of all CYP3A4 substrates. Enhanced metabolism can reduce drug efficacy (and therefore is one mechanism of drug tolerance) or, in cases of prodrug transformation to active metabolites, increased efficacy. If metabolites are toxic, as is the case with VAs, enhanced metabolism may increase toxicity. Conversely, CYP inhibition leads to enhanced activity of parent drugs and reduced metabolite effects. CYP enzyme inhibition is associated with hepatic disease and exposure to certain substances. An important example is CYP3A4 inhibition by grapefruit juice.<sup>100</sup> Regarding VAs, the major oxidative enzyme CYP2E1 is inducible by ethanol and isoniazid and is inhibited by disulfiram.<sup>101</sup> Diseases such as hepatitis, various cirrhotic diseases, and hepatocarcinoma can also reduce enzymatic activity, as can cardiac failure with reduced hepatic perfusion.

Neonates have different dominant CYP isoforms than adults. Impaired hepatic metabolism is common in premature and full-term infants, notably in bilirubin glucuronidation, leading to hyperbilirubinemia of the newborn.<sup>102,103</sup> Pharmacogenomics is a growing area of pharmacologic research that has linked variable drug metabolism to genetic variability. A well-established example in anesthesiology is homozygous inheritance of atypical butyrylcholinesterase,

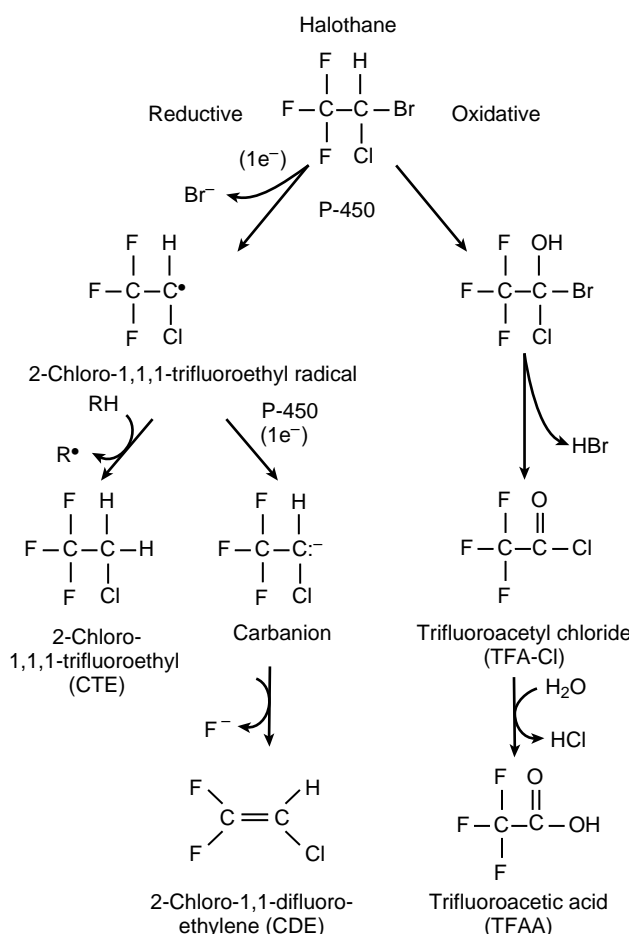


**Fig. 20.14** Oxidative and reductive metabolism of halothane. Major products of hepatic CYP2E1 catalyzed halothane metabolism are shown. Under normal conditions, 24% of halothane undergoes oxidative metabolism, and 1% undergoes reductive metabolism.

resulting in slow hydrolysis of succinylcholine.<sup>104</sup> Genetic variations in CYP2D6 have clarified the basis for widely varying efficacies and toxicities of codeine (a prodrug), metoprolol, nortriptyline, dextromethorphan, and other substrate drugs.<sup>105</sup>

Hepatic CYP2E1 is particularly important in the oxidative metabolism of halogenated inhaled anesthetics (see Table 20.3). Under conditions of systemic hypoxia or decreased blood flow, or in liver regions of low  $P_{O_2}$ , CYP2A6 and CYP3A4 catalyze breakdown of VAs via reductive pathways. Halothane metabolism is primarily oxidative, and under normal conditions, about 1% of halothane undergoes reductive metabolism. Oxidative metabolism of halothane releases chloride and bromide ions, resulting in trifluoroacetyl chloride, which reacts with water to form trifluoroacetic acid (Fig. 20.14). Reductive metabolism of halothane results initially in loss of bromide, and the intermediate either reacts with a hydrogen donor to form 2-chloro-1,1,1-trifluoroethane or captures an electron, further reducing the carbon-carbon bond to form 2-chloro-1,1-difluoroethylene (see Fig. 20.14). Halothane reduces hepatic blood flow and can cause hepatocellular hypoxia in some regions in the liver, potentially leading to an increase in its reductive metabolism.<sup>71</sup> All of the ether anesthetics undergo similar oxidative metabolism catalyzed by CYP2E1

(see Table 20.3, Fig. 20.15). Oxidative metabolism of these drugs results in the release of fluoride ( $F^-$ ) and chloride ( $Cl^-$ ) ions and the formation of reactive intermediates that react with water to form carboxylic acids. Isoflurane and desflurane both produce trifluoroacetic acid, whereas enflurane forms 2-difluoromethoxy-2,2-difluoroacetic acid. Oxidative metabolism of methoxyflurane may follow several paths, releasing either  $Cl^-$  or  $F^-$  in sequential steps and producing methoxy-difluoroacetic acid, dichloroacetic acid, and acetic acid (see Table 20.3).

### Halothane Hepatotoxicity

The first modern halogenated VA, halothane, was introduced in 1955. Clinical exposure to halothane is associated with two distinct types of hepatic injury.<sup>76,106,107</sup> Subclinical hepatotoxicity occurs in 20% of adults who receive halothane. It is characterized by mild postoperative elevations in alanine aminotransferase (ALT) and aspartate aminotransferase (AST), but is reversible and innocuous. Anaerobic halothane reduction by CYP2A6 to a 2-chloro-1,1,1-trifluoroethyl radical (see Fig. 20.14) is thought to mediate this mild hepatic injury.<sup>72</sup> The fulminant form of hepatotoxicity, commonly known as halothane hepatitis, is characterized by elevated ALT, AST, bilirubin, and alkaline phosphatase levels, and massive hepatic necrosis following the administration of halothane. Halothane hepatitis is rare (1 in 5000-35,000 administrations in adults) but is fatal in between 50% to 75% of cases. Because of the potential for fatal hepatitis, halothane is no longer used in adult patients in most countries.

Halothane hepatitis is caused by a hypersensitivity reaction associated with oxidative metabolism of halothane. The highly reactive trifluoroacetyl chloride metabolite of halothane oxidation can react with nearby liver proteins (see Table 20.3). In most patients who developed hepatic necrosis after halothane anesthesia, antibodies against trifluoroacetyl-modified proteins were detected, suggesting that the hepatic damage is linked to an immune response against the modified protein, which acts as a neoantigen (Fig. 20.16). Accordingly, patients who develop halothane hepatitis often have a history of prior exposures to halothane or other VAs, together with symptoms suggestive of immune reactivity, such as fever, rash, arthralgia, and eosinophilia.<sup>75</sup> It is hypothesized that trifluoroacetyl-protein adducts induce a cytotoxic T-cell reaction in sensitized individuals, which leads to liver damage.<sup>76</sup> However, definitive evidence that liver injury is immune-mediated in halothane hepatitis is lacking.

Hepatotoxicity and massive hepatic necrosis after halothane anesthesia also occurs in children. However, two large retrospective studies have demonstrated that the clinical syndrome of halothane hepatitis is even more rare in pediatric patients (1 in 80,000-200,000) than in adults.<sup>108-110</sup> Halothane is metabolized to a similar degree in adults and children, and children are immune competent from birth. Pediatric cases of halothane hepatitis are also associated with multiple anesthetic exposures, suggesting a mechanism similar to that in adults. Why the incidence of halothane hepatitis is significantly higher in the adult population remains unknown.

Other VAs including enflurane, isoflurane, and desflurane have also been associated with fulminant hepatic necrosis,<sup>92,111-115</sup> but compared with halothane, the incidence of

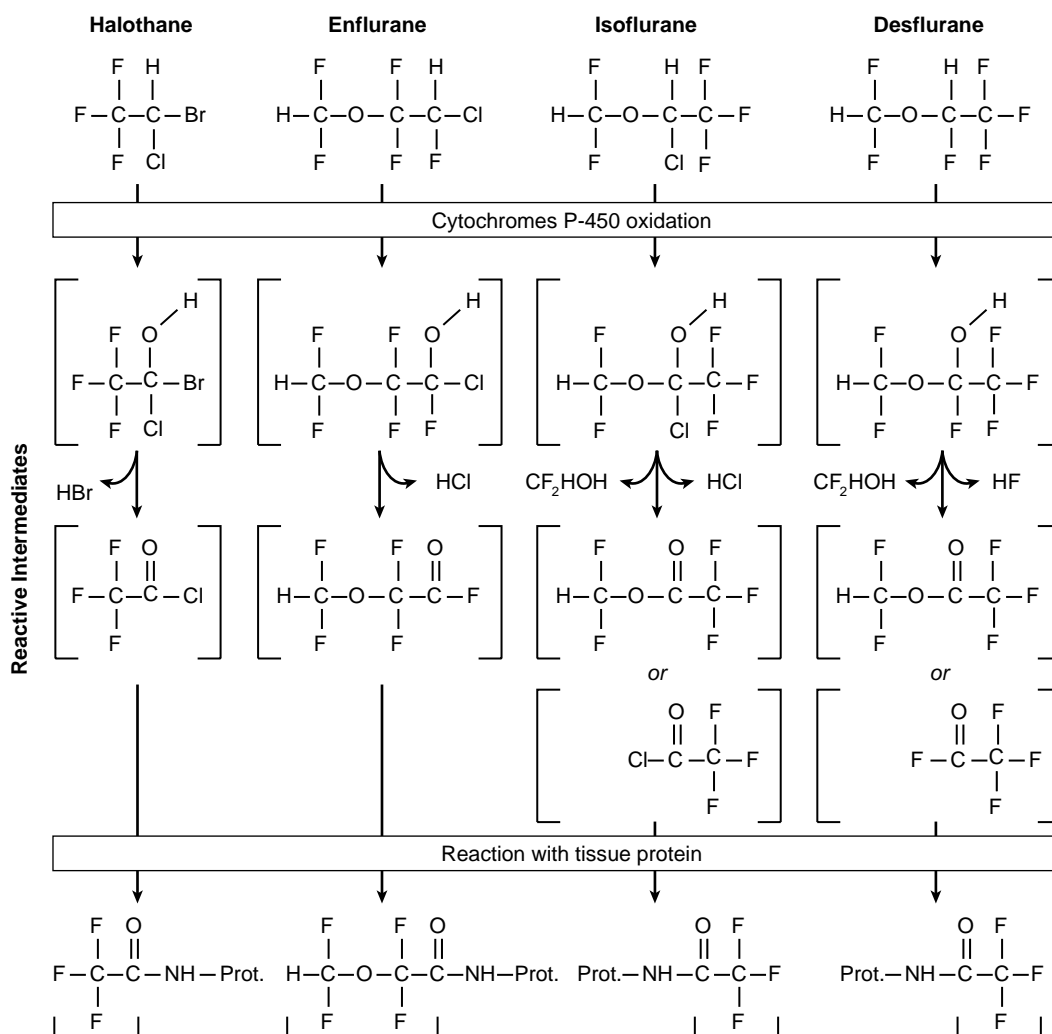


**Fig. 20.15** Proposed pathways for inhaled anesthetic metabolism to reactive intermediates. CYP2E1 catalyzes oxidative metabolism of halothane, enflurane, isoflurane, and desflurane to a variety of reactive intermediates that can form adducts with hepatocellular proteins. Trifluoroacetylated proteins are identical after halothane, isoflurane, and desflurane, whereas adducts following enflurane are immunologically similar.

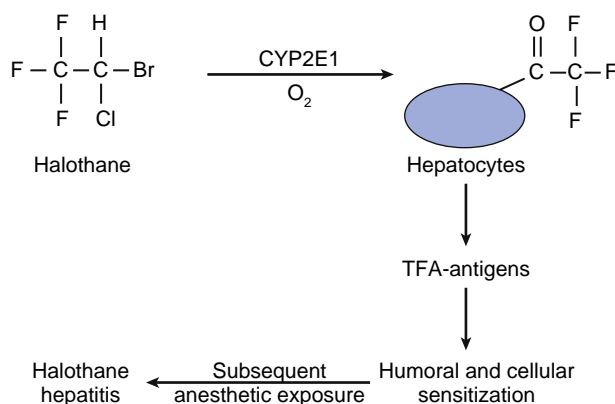


**Fig. 20.16** Pathways generating the immune response after exposure to inhaled anesthetics. Halothane is metabolized to a reactive trifluoroacetyl intermediate that forms an amide bond with hepatocellular proteins. The altered protein triggers an immune response, which on subsequent exposure to anesthetic results in hepatocellular damage and necrosis. A similar process may ensue after exposure to other fluorinated drugs metabolized to similar halo-acyl intermediates. TFA, Trifluoroacetic acid. (Modified from Njoku D, Laster MJ, Gong DH, et al. Biotransformation of halothane, enflurane, isoflurane and desflurane to trifluoroacetylated liver proteins: association between protein acylation and liver injury. *Anesth Analg*. 1997;84:173–178.)

this potentially fatal toxicity is very rare after administration of these newer VAs. The mechanism of severe hepatitis following enflurane, isoflurane, and desflurane may be the same as for halothane, because all of these drugs are oxidatively metabolized to highly reactive intermediates that can covalently modify hepatic proteins (see Fig. 20.15). As with halothane, case investigations usually reveal that patients have had prior exposure to VAs, and antibodies to modified hepatic proteins can be detected. The extremely infrequent incidence of severe hepatitis for modern VAs is likely because of their lower degree of oxidative metabolism and subsequent immune sensitization. In fact, hepatitis was also commonly reported soon after introduction of methoxyflurane, another anesthetic that is mostly metabolized to highly reactive acidic intermediates.<sup>77,116</sup> Unlike all other VAs, sevoflurane is oxidized at the fluoromethoxy C-H bond and forms hexafluoroisopropanol and inorganic F<sup>-</sup> (see Table 20.3; Fig. 20.17).<sup>117,118</sup> Hexafluoroisopropanol is relatively stable, and modified liver proteins are not formed after sevoflurane anesthesia. Cases of hepatitis and rapid death after sevoflurane anesthesia have been reported, but there was no evidence of an immune-mediated mechanism.<sup>96</sup>

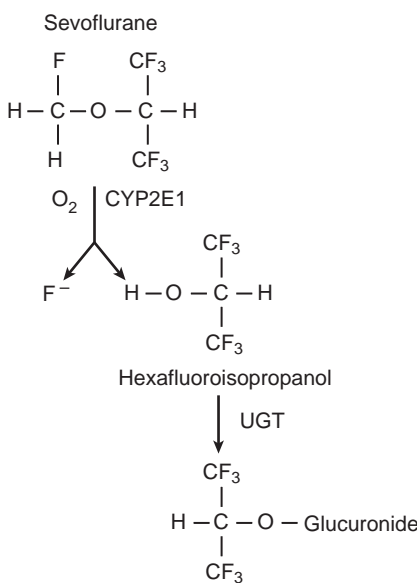


**Fig. 20.17** Metabolic oxidation of Sevoflurane. CYP2E1 catalyzes phase 1 defluorination of sevoflurane, forming hexafluoroisopropanol. Phase 2 glucuronidation is catalyzed by uridine 5'-diphosphate glucuronosyltransferase (UGT).

### Biotransformation in Kidneys

The kidneys are large organs that receive high blood flow. Renal physiologic activities include glomerular filtration of water-soluble metabolites, reabsorption of water and essential metabolites, urinary excretion of waste, and regulation of hormones involved in vascular tone (renin) and water balance (aldosterone). The kidneys clear most of the water-soluble metabolites resulting from biotransformation of inhaled anesthetics. Kidneys also contain CYP enzymes, including CYP2E1, that catalyze both phase 1 and phase 2 reactions and are therefore additional sites where inhaled anesthetic metabolism occurs. As in the liver, various CYPs in renal parenchyma may undergo induction or inhibition by exogenous substances.<sup>119-122</sup>

### Fluoride-Associated Nephrotoxicity

The first modern halogenated ether anesthetic, methoxyflurane was introduced in 1959. Methoxyflurane causes polyuric renal insufficiency and is no longer used in clinical practice.<sup>123</sup> The nephrotoxic effect of methoxyflurane is attributed to inorganic fluoride ( $\text{F}^-$ ) released during its metabolism. Investigations have provided significant insights into potential nephrotoxic mechanisms by fluorinated VAs and have influenced the development of subsequent halogenated anesthetic agents.

Absorbed methoxyflurane undergoes extensive biotransformation,<sup>67</sup> including cytochrome-catalyzed oxidation that releases inorganic fluoride ions ( $\text{F}^-$ ) into blood. Animal studies provide clear evidence of the nephrotoxicity of methoxyflurane, which includes a strong relationship between methoxyflurane dose and renal injury,<sup>124</sup> increased nephrotoxicity with induction of CYP enzymes,<sup>125,126</sup> and decreased nephrotoxicity with inhibition of methoxyflurane metabolism.<sup>84,127</sup> Clinical data further indicate that severity of nephrotoxicity and mortality are associated with high plasma fluoride concentrations after methoxyflurane anesthesia.<sup>128,129</sup> Patients with serum inorganic fluoride

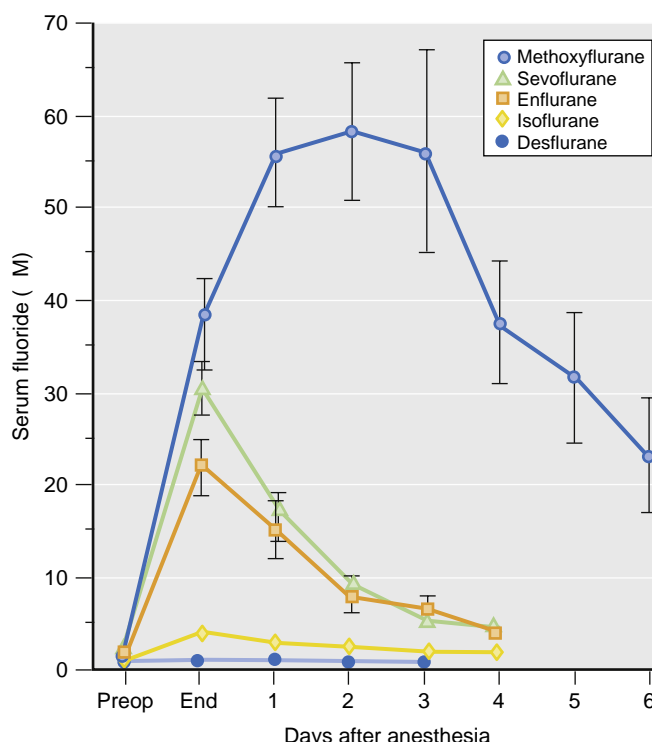


**Fig. 20.18** Serum inorganic fluoride ( $\text{F}^-$ ) exposure during and after methoxyflurane anesthesia is much greater than with other anesthetics. Points represent serum  $\text{F}^-$  measurements (mean  $\pm$  SD) from multiple subjects. After 2 to 3 MAC-hours of methoxyflurane anesthesia,  $\text{F}^-$  rises during and after drug administration ends, peaks above 60  $\mu\text{mol/L}$  on postanesthesia days 2 and 3, then declines slowly, remaining elevated for more than 1 week. Sevoflurane anesthesia (3.7 MAC-hours) produces an early peak  $\text{F}^-$  concentration averaging 31  $\mu\text{mol/L}$ , which declines over 3 to 4 days. Enflurane anesthesia (2.7 MAC-hours) results in an early average peak of 22  $\mu\text{mol/L}$  that declines in 3 to 4 days. Isoflurane and desflurane result in small and negligible rises in serum  $\text{F}^-$  concentrations. Only methoxyflurane is associated with fluoride-associated renal toxicity. MAC, Minimum alveolar concentration (immobility).

levels below 50  $\mu\text{M}$  had no evidence of renal injury, whereas patients with postmethoxyflurane serum  $\text{F}^-$  greater than 50  $\mu\text{M}$  suffered high rates of renal dysfunction and increased mortality.<sup>79,130</sup> Moreover, serum  $\text{F}^-$  concentrations were significantly higher after the administration of methoxyflurane than with other halogenated VAs, which are not associated with nephrotoxicity (Fig. 20.18). Inorganic fluoride released during methoxyflurane metabolism probably causes renal injury, and the nephrotoxic threshold for plasma  $\text{F}^-$  is approximately 50  $\mu\text{M}$ . Individual variability among patients in the degree of apparent renal injury after methoxyflurane exposure was observed. Genetic heterogeneity, drug interactions, and preexisting renal disease likely account for these differences.

Since the introduction of methoxyflurane, all prospective halogenated anesthetic agents have been extensively tested experimentally and clinically for their degree of defluorination and the resulting serum  $\text{F}^-$  concentrations. However, experience with newer drugs, particularly with sevoflurane, has caused investigators to reexamine the classical fluoride-induced nephrotoxicity hypothesis. Sevoflurane was initially synthesized in the 1970s, but because of its relatively large defluorination rate (2%-5%), its introduction into clinical practice was delayed. It was first widely used

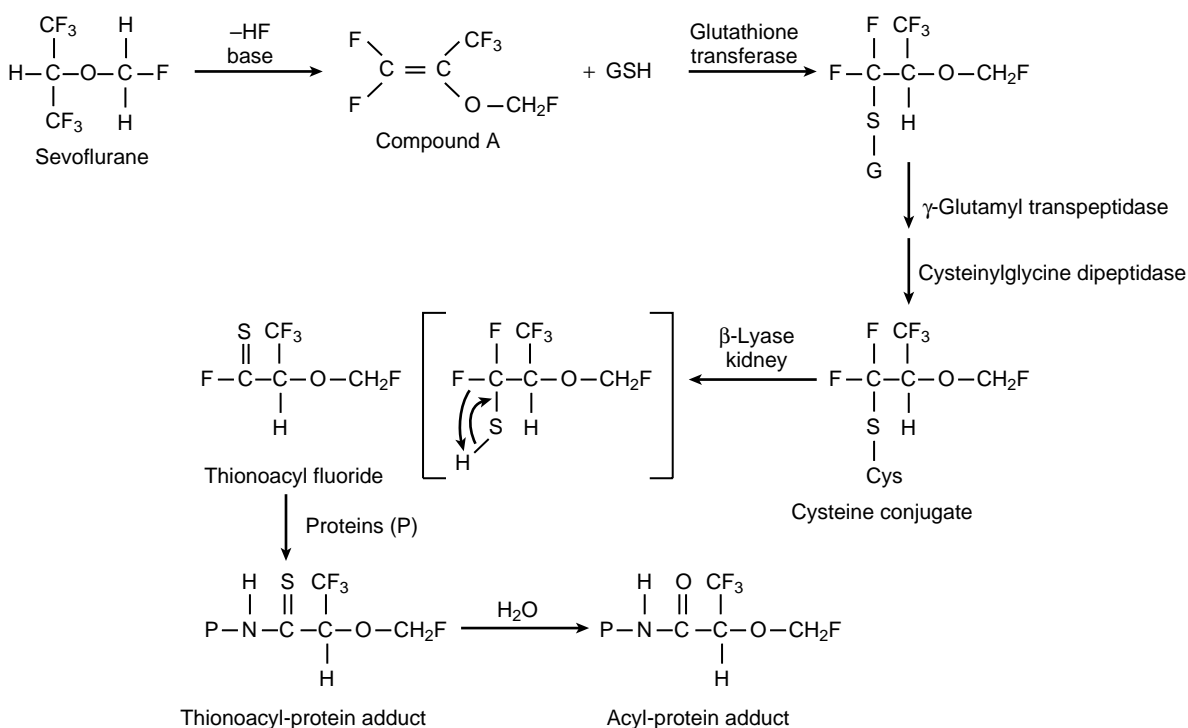


**Fig. 20.19** Proposed pathway mediating nephrotoxic effects of compound A in rodents. Sevoflurane degrades to compound A in the presence of strong base in some  $\text{CO}_2$  absorbent materials. Compound A itself is not nephrotoxic but undergoes hepatic S-conjugation with glutathione. In the kidney, additional metabolic steps produce a S-cysteine compound A conjugate, which is metabolized by  $\beta$ -lyase to a reactive thionoacyl fluoride that is proposed to damage proteins essential for kidney function. Humans have very low  $\beta$ -lyase activity, which is hypothetically the basis for the lack of reported nephrotoxicity in patients.  $\text{CO}_2$ , Carbon dioxide; GSH, glutathione; HF, hydrofluoric acid. (Adapted from Martin JL, Kandel L, Laster MJ, et al. Studies of the mechanism of nephrotoxicity of compound A in rats. *J Anesth*. 1997;11:32-37.)

in Japan in 1990. Subsequent clinical studies demonstrated no clinically significant nephrotoxicity after the administration of sevoflurane, even when the high peak blood  $\text{F}^-$  concentrations greater than 50  $\mu\text{M}$  were confirmed.<sup>117</sup> Typical peak fluoride concentrations after 2 to 3 MAC-hours of sevoflurane anesthesia are 20 to 30  $\mu\text{M}$ , and less than 5  $\mu\text{M}$  after isoflurane and desflurane (see Fig. 20.18). Enflurane metabolism also often results in peak blood  $\text{F}^-$  concentrations greater than 20  $\mu\text{M}$ . Isoflurane and desflurane are minimally metabolized and produce lower plasma fluoride concentrations. However, none of these anesthetics is associated with clinically significant renal toxicity, suggesting that methoxyflurane is unique in its ability to harm kidneys. One important difference between methoxyflurane and current VAs is its extreme lipophilicity and extremely long residence time in tissues. This results in prolonged elevated  $\text{F}^-$  concentrations in blood (see Fig. 20.18), suggesting that the length of  $\text{F}^-$  exposure is a key risk factor. However, prolonged moderate elevations of plasma fluoride (25-38  $\mu\text{M}$ ) during several days of isoflurane anesthesia without adverse renal effects have been documented.<sup>131,132</sup> Thus neither the peak level nor the duration of high plasma fluoride concentration entirely explains the nephrotoxic effects by the halogenated anesthetics. It is also not clear whether the integrated concentration multiplied by time exposure to inorganic  $\text{F}^-$  represents the key risk factor. However, methoxyflurane is metabolized to a large extent within kidney parenchyma, producing high intrarenal inorganic fluoride concentrations (likely much higher than those measured in blood), which are proposed to cause renal injury.<sup>78,80</sup> Thus, compared with methoxyflurane,

the absence of renal toxicity with newer volatile halogenated agents likely derives from a combination of factors: (1) their lower tissue solubilities, particularly in kidney (see Table 20.2), resulting in lower intrarenal fluoride production; (2) lower overall degrees of biotransformation; and (3) more rapid respiratory clearance from the body.

## ANESTHETIC DEGRADATION IN CARBON DIOXIDE ABSORBENTS

### Sevoflurane, Compound A, and Renal Toxicity

Halogenated anesthetics can undergo chemical breakdown while interacting with carbon dioxide ( $\text{CO}_2$ ) absorbents that contain strong bases such as sodium hydroxide (NaOH) and potassium hydroxide (KOH), which are present in soda lime and Baralyme.<sup>133</sup> Strong bases extract a proton from the isopropyl group of sevoflurane, primarily forming a haloalkene [fluoromethyl-2,2-difluoro-1-(trifluoromethyl) vinyl ether], known as compound A (Fig. 20.19). Compound A is volatile and can be absorbed via alveolar gas exchange. Compound A exposure is nephrotoxic in laboratory animals, causing proximal tubular necrosis and, with sufficient exposure, death. In rats, renal injury is observed with cumulative exposure to compound A above 150 parts per million (ppm)-hours (e.g., 50 ppm inhalation for 3 hours).<sup>134,135</sup> Moderately severe but reversible histopathologic damage was found in rats after 200 ppm-hour exposure, associated with increased blood and urea nitrogen (BUN), creatinine, and other measures of renal damage. Compound A exposure over 1000 ppm-hours is lethal in half of exposed rats.

Patients receiving sevoflurane anesthesia are routinely exposed to compound A in rebreathing circuits, and the inhaled concentration is dependent on the fresh gas flow rate and the type of  $\text{CO}_2$  absorbent present. Fresh gas flows of 1 L/min result in maximal compound A concentrations around 20 ppm with soda lime and 30 ppm with Baralyme.<sup>136</sup> Higher FGF rates result in less compound A accumulation in the breathing circuit. However, compound A exposure is not associated with clinically significant nephrotoxicity in humans. There is no threshold exposure level known to cause more than subclinical renal damage. Numerous studies in which human subjects or patients were exposed to more than 200 ppm-hours of compound A have reported that clinical measures of renal function (BUN, creatinine, urinary protein or glucose, and urine concentrating ability) and laboratory tests for subtle renal damage (N-acetyl- $\beta$ -glucosaminidase, alanine aminopeptidase,  $\gamma$ -GTP, and  $\beta$ 2-microglobulin) remain unchanged.<sup>81,86,137-139</sup> Kharasch and colleagues<sup>140</sup> compared the effects of low-flow sevoflurane and isoflurane anesthesia in patients with stable renal insufficiency, and found no significant difference in post-operative renal function tests. Other studies have reported normal BUN and creatinine, but transient reversible abnormalities in other renal function test values following prolonged sevoflurane anesthesia at low FGF (>330 ppm-hour compound A exposure in one study).<sup>141-144</sup>

The evidence of nephrotoxicity in rats compared with the remarkably benign results in humans suggests that mechanisms of sevoflurane metabolism and toxicity differ between these species. The difference in the nephrotoxic effects of compound A between humans and rats may be attributed to the doses of compound A, interspecies differences in metabolic toxicification, and sensitivity of the proximal tubular cells to compound A cytotoxicity.<sup>71</sup> Detailed studies show that in rats, compound A undergoes S-conjugation to cysteine, and that the resulting cysteine conjugate is metabolized by renal  $\beta$ -lyase to form a reactive thionoacyl fluoride intermediate that acylates proteins and has been proposed to mediate the nephrotoxic effect (see Fig. 20.19).<sup>133,145</sup> Human kidneys have far lower  $\beta$ -lyase activity than rat kidneys, accounting for the differential toxicity of compound A in the two species. Experiments testing whether inhibition of  $\beta$ -lyase with aminoxy-acetic acid (AOAA) protects rats from compound A nephrotoxicity have had mixed results.<sup>146,147</sup> Alternative mechanisms underlying compound A toxicity have been proposed, including formation of reactive sulfoxides catalyzed by CYP3A isozymes,<sup>148</sup> which are also more active in rat than human kidneys.

Although the mechanism underlying compound A toxicity in laboratory animals remains uncertain, the lack of significant sevoflurane nephrotoxicity in human clinical data is reassuring. Compound A exposure can be limited by careful selection of fresh gas flows, vaporizer output, and  $\text{CO}_2$  absorbent materials. The use of 2 L/min fresh gas flows assures that for the vast majority of patients, exposure to compound A will be below the most conservative threshold for nephrotoxicity. Although clinical studies indicate that sevoflurane is most likely safe, even in patients with preexisting renal dysfunction, the drug should be administered in accordance with the approved package labeling guidelines.

Like sevoflurane, halothane degrades in the presence of  $\text{CO}_2$  absorbents to form a reactive intermediate,

**TABLE 20.4** Composition of Base Chemicals and Water Content of Carbon Dioxide Absorbents

$\text{CO}_2$ absorbent	$\text{Ca}(\text{OH})_2$ (%)	$\text{Ba}(\text{OH})_2$ (%)	KOH (%)	NaOH (%)	LiOH (%)	$\text{H}_2\text{O}$ (%)
Baralyme*	70	10	4.6	—	—	14
Soda lime I	80	—	2.6	1.3	—	15
Sodasorb	90	—	0.0005	3.8	—	16
Drägersorb 800 plus	82	—	0.003	2	—	16
Soda lime II/ Medisorb	81	—	0.003	2.6	—	16
Spherisorb	84.5	—	0.003	1.5	—	14
Amsorb	83.2	—	—	—	—	14.4
LofloSorb	84	—	—	—	—	16
Superia	79.5	—	—	—	—	17.5
Lithium hydroxide	—	—	—	—	99	1

\*Baralyme was withdrawn from the market in 2004.

Various absorbents also contain other components, such as polyvinylpyrrolidine, calcium chloride, calcium sulfate, magnesium chloride, and aluminosilicate.

Data from Keijzer C, Perez RS, de Lange JJ. Compound A and carbon monoxide production from sevoflurane and seven different types of carbon dioxide absorbent in a patient model. *Acta Anaesthesiol Scand*. 2007;51:31-37, and Kharasch ED, Powers KM, Artru AA. Comparison of Amsorb, sodalime, and Baralyme degradation of volatile anesthetics and formation of carbon monoxide and compound A in swine in vivo. *Anesthesiology*. 2002;96:173-182.

bromochlorodifluoroethylene (BCDFE),<sup>133</sup> which has also been investigated as a possible nephrotoxin. Eger and colleagues<sup>149</sup> found that in comparison to compound A, BCDFE accumulates 20- to 40-fold less in breathing circuits and is 4-fold less reactive. Thus the risk of BCDFE nephrotoxicity is negligible.

### Carbon Monoxide and Heat

In the presence of strong bases in dry  $\text{CO}_2$  absorbents (water content <5%), some halogenated VAs undergo degradation, resulting in the formation of CO, trifluoromethane ( $\text{CF}_3\text{H}$ ), and hydrogen fluoride (HF).<sup>133</sup> The factors that determine the amount of CO produced include the chemical makeup of  $\text{CO}_2$  absorbent (KOH > NaOH >>  $\text{Ba}(\text{OH})_2$ ,  $\text{Ca}(\text{OH})_2$ ), dryness of the absorbent material, the concentration of volatile agent, and its chemical structure.<sup>150</sup> Baralyme contains 4.6% KOH, whereas soda lime contains 2.5% KOH and 1.3% NaOH, and reacts less vigorously with halogenated anesthetics. The relatively weak bases  $\text{Ba}(\text{OH})_2$  and  $\text{Ca}(\text{OH})_2$  are other major constituents in  $\text{CO}_2$  absorbents, and do not catalyze CO formation (Table 20.4).<sup>136,151</sup> The anesthetics that contain a difluoromethyl group (difluoromethyl-ethyl ethers) are most susceptible to this degradation, and for these drugs CO production correlates with anesthetic concentration in the breathing circuit (desflurane > enflurane > isoflurane)<sup>152</sup> (Fig. 20.20).<sup>152</sup> Sevoflurane, methoxyflurane, and halothane also degrade in the presence of strong bases, but do not produce CO. Production of CO appears to require nearly complete desiccation (i.e., removal of moisture) of the  $\text{CO}_2$  absorbent, and typically occurs after high-flow “flushing” of the breathing circuit for 1 to 2 days. Soda

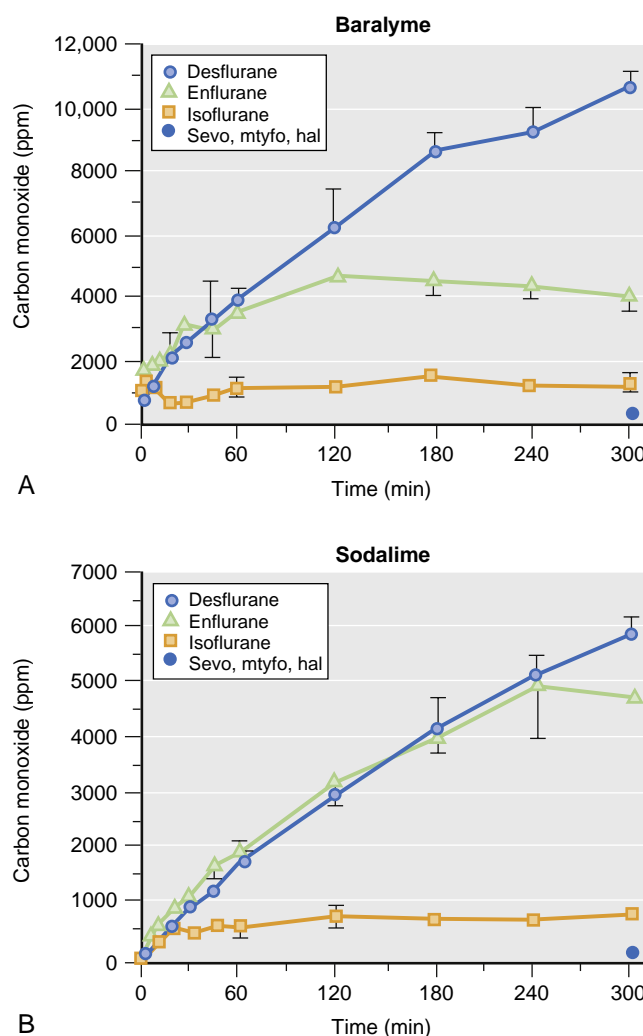


**Fig. 20.20** Inhaled anesthetic degradation and carbon monoxide production. Points represent mean  $\pm$  SD of three measurements with equivalent anesthetic doses ( $1.5 \times \text{MAC}$ ) in the presence of dry  $\text{CO}_2$  absorbents at identical fresh gas flows. (A) Degradation and CO production with Baralyme. (B) Degradation and CO production with soda lime. Degradation and CO production was observed with anesthetics containing difluoromethoxy groups (desflurane, enflurane, and isoflurane), but not halothane (hal) or those with monofluoromethoxy groups such as sevoflurane (sevo) and methoxyflurane (mtyfo). CO, Carbon monoxide; MAC, minimum alveolar concentration. (Adapted from Baxter PJ, Garton K, Kharasch ED. Mechanistic aspects of carbon monoxide formation from volatile anesthetics. *Anesthesiology*. 1998;89:929–941.)

lime contains 15% water by weight, and Baralyme contains 13% water by weight (see Table 20.4). CO production is observed when the water content of soda lime or Baralyme falls below 1.4% and 5%, respectively.<sup>153</sup> High ambient temperatures also accelerate desiccation of  $\text{CO}_2$  absorbent materials and may increase the rate of CO producing reactions. As noted with compound A, CO accumulation in the breathing circuit is inversely related to the fresh gas flow.

Anesthetic degradation in the breathing circuit has resulted in CO poisoning during clinical anesthesia.<sup>154,155</sup> CO has 250-fold greater affinity for hemoglobin than  $\text{O}_2$  does; therefore, the formation of carboxyhemoglobin reduces blood oxygen carrying capacity and tissue oxygen delivery, and is difficult to reverse. The detrimental effects and signs of CO toxicity are well known. However, during

general anesthesia, signs of patient exposure to CO are masked and hypoxia may be difficult to detect because most pulse oximetry equipment cannot distinguish between carboxyhemoglobin and oxyhemoglobin.

The degradation of VAs by bases in  $\text{CO}_2$  absorbents is an exothermic reaction that results in the production of heat. Sevoflurane produces the most heat when it is used with desiccated  $\text{CO}_2$  absorbent. The absorbent canister and anesthetic circuit can reach extremely high temperatures, which can lead to explosion or fire, or both.<sup>156,157</sup>

Current recommendations to minimize anesthetic degradation to CO and heat include machine maintenance measures to avoid desiccation of  $\text{CO}_2$  absorbents and the use of absorbents that contain less KOH and NaOH. Newer  $\text{CO}_2$  absorbents (see Table 20.4) contain little or no strong base and do not degrade VAs, regardless of hydration status.<sup>136,158,159</sup> The use of the newer  $\text{CO}_2$  absorbents also reduces the production of compound A during sevoflurane anesthesia.<sup>160–162</sup>

## NITROUS OXIDE, VITAMIN B12, AND HOMOCYSTEINE

$\text{N}_2\text{O}$  is unique among anesthetics in irreversibly inhibiting cobalamins (vitamin B12) by oxidizing the Co (I) ligand. Cobalamins are ingested or produced by bacteria in the gut and are critical cofactors together with 5-methyltetrahydrofolate in the activity of methionine synthase (Fig. 20.21). Methionine synthase catalyzes methylation of homocysteine to methionine, while demethylating 5-methyltetrahydrofolate to tetrahydrofolate. Methionine, converted to S-adenosylmethionine, is the major substrate for methylation in biochemical pathways involved in the synthesis of DNA, RNA, myelin, and catecholamines.<sup>163</sup> Chronic vitamin B12 deficiency (as in pernicious anemia) results in hematologic and neurologic dysfunction. Long-term  $\text{N}_2\text{O}$  exposure, typically among individuals who frequently inhale it as a recreational drug, can also cause megaloblastic anemia, myelopathy (subacute combined degeneration), neuropathy, and encephalopathy, sometimes presenting as psychosis.<sup>164–167</sup>  $\text{N}_2\text{O}$  is the eighth most commonly used recreational substance in the United Kingdom.<sup>168</sup> Risk factors that increase susceptibility to  $\text{N}_2\text{O}$  toxicity include pernicious anemia or other gastrointestinal malabsorption syndromes, extremes of age, alcoholism, malnutrition, a strict vegetarian diet, and inborn deficiencies in cobalamin or tetrahydrofolate metabolism.<sup>164</sup> Inhibitors of folate metabolism, such as methotrexate, may also enhance sensitivity to  $\text{N}_2\text{O}$  toxicity.<sup>169</sup>

In healthy surgical patients, megaloblastic changes in the bone marrow are rare, and reported only after a prolonged period of exposure ( $>12$  hours) to  $\text{N}_2\text{O}$ . Healthy pediatric patients exposed to  $\text{N}_2\text{O}$  for up to 8 hours during spine surgery do not develop evidence of megaloblastic anemia.<sup>170</sup> However, in seriously ill patients or those with risk factors noted earlier, shorter (or repetitive) periods of  $\text{N}_2\text{O}$  exposure may lead to significant subacute pathology. Megaloblastic bone marrow changes can be induced after a short period (2–6 hours) of  $\text{N}_2\text{O}$  exposure.<sup>171</sup> Vitamin B12 deficiency or reduced methionine synthase activity can also lead to subacute myelopathy and neuropathy.<sup>172–175</sup> A case highlighting the potential importance of inborn

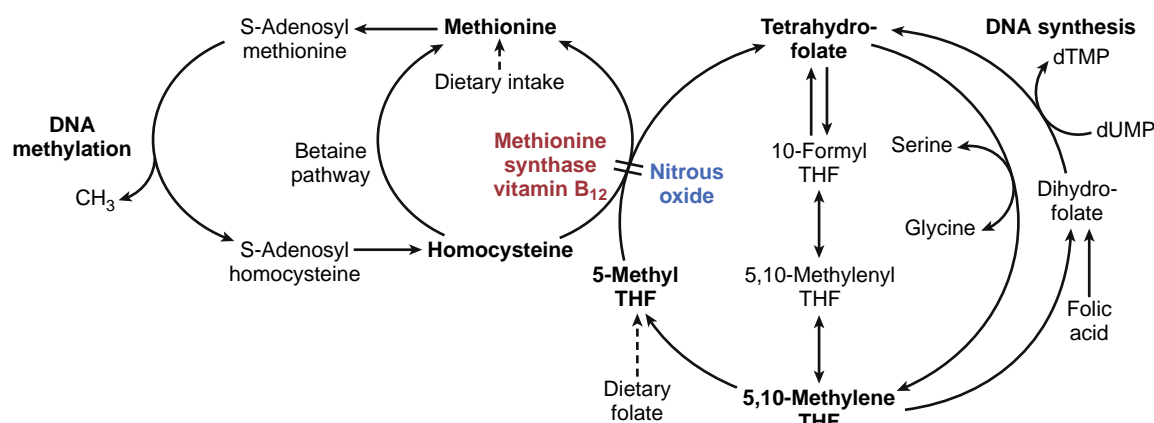


**Fig. 20.21** Nitrous oxide inhibition of methionine synthase. Biochemical cycles involved in methylation reactions are shown. Methionine synthase (red) catalyzes methylation of homocysteine with 5-methyl tetrahydrofolate as the donor, producing methionine and tetrahydrofolate (THF). Both vitamin B12 and folate are essential cofactors for methionine synthase. Nitrous oxide (blue) inhibits methionine synthase by oxidizing the cobalt of cobalamin (vitamin B12). Methyl transfer pathways are important in synthesis of protein and DNA. dTMP, Deoxythymidine; dUMP, 2'-Deoxyuridine 5'-Monophosphate.

metabolism was reported by Selzer and colleagues.<sup>176</sup> In this case, a 4-month-old child developed an irreversibly and ultimately fatal seizure disorder several weeks after receiving N<sub>2</sub>O during anesthesia. Autopsy revealed widespread brain atrophy and demyelination, and biochemical investigations revealed reduced methyltetrahydrofolate reductase (MTHFR) activity, which eventually were linked to several mutations in the gene encoding MTHFR.

Another consequence of reduced methionine synthase activity is accumulation of its substrate: homocysteine (see Fig. 20.21). Homocystinuria caused by severe inborn deficiency of methionine synthase activity is associated with extremely elevated blood homocysteine levels, early atherosclerosis of coronary and cerebral arteries, and premature death.<sup>177</sup> These observations led to the “homocysteine hypothesis,” which postulates that homocysteine stimulates inflammation and atherosclerosis, and is a key modifiable factor in vascular morbidity and mortality. Despite some evidence that increased homocysteine levels are an independent risk factor for cardiac and cerebrovascular morbidity,<sup>178,179</sup> the association between homocysteine levels and atherothrombotic disease is weak, as some large prospective studies have found.<sup>180</sup> Moreover, studies in which diet and vitamin supplementation was used to reduce homocysteine levels demonstrate improvement in some markers of vascular risk, but do not reduce the rate of myocardial infarction and atherosclerotic stroke.<sup>180,181</sup> Thus it appears that the importance of chronic *moderate* elevation in homocysteine to cardiovascular outcomes is tenuous, or perhaps only pertinent to limited patient populations.

Does the rapid increase of homocysteine levels during N<sub>2</sub>O anesthesia influence the risk of cardiovascular and neurovascular morbidity following surgery and anesthesia? Badner and colleagues<sup>182</sup> reported that N<sub>2</sub>O administration significantly increased homocysteine levels and increased myocardial risk in carotid endarterectomy patients. The Evaluation of Nitrous Oxide in a Gas Mixture for Anesthesia (ENIGMA) trial in more than 2000 patients reported that avoidance of N<sub>2</sub>O combined with increased inspired oxygen concentration during anesthesia decreased the incidence of a variety of complications after major surgery, but found no reduction in death, myocardial infarction, stroke,

or hospital length of stay.<sup>183</sup> In a follow-up study of the ENIGMA trial, patients reported that those exposed to N<sub>2</sub>O for more than 2 hours were at increased risk (odds ratio 1.6; 95% confidence interval, 1.01–2.5) of myocardial infarction up to 5.7 years after enrollment.<sup>184</sup> No difference in rates of death or stroke were found. Unfortunately, diagnosis of myocardial infarction in ENIGMA was often based on data obtained in telephone interviews, rather than established diagnostic criteria. However, a follow-up randomized trial in 7112 patients (ENIGMA-II) reported no difference in myocardial infarction, stroke, pulmonary embolism, or cardiac arrest risk within 30 days of surgery.<sup>185</sup> A recent post hoc study of 5133 enrollees in the Perioperative Ischemic Evaluation (POISE) trial<sup>186</sup> also found no increase in rates of death, myocardial infarction, or stroke in approximately 1500 patients who received N<sub>2</sub>O.

Anecdotally, N<sub>2</sub>O use is thought to contribute to myocardial infarction in patients with elevated homocysteine levels at baseline.<sup>187</sup> Homocysteine elevation following N<sub>2</sub>O inhalation is a useful marker for assessing the sensitivity of methionine synthase and related biochemical pathways to N<sub>2</sub>O inhibition. Nagele and colleagues<sup>188</sup> studied a small group of surgical patients with common mutations in the gene encoding MTHFR, and found that those with 667C→T and 1298A→C mutations were at risk of developing abnormally high homocysteine levels after N<sub>2</sub>O exposures of at least 2 hours. However, a common gene variant (66A→G) associated with reduced methionine synthase reductase activity did not result in abnormally high homocysteine levels after anesthesia with N<sub>2</sub>O.<sup>189</sup> Preoperative infusions of vitamin B12 and folate do not prevent the normal elevation in homocysteine observed following anesthesia with N<sub>2</sub>O.<sup>190</sup>

The continued value of N<sub>2</sub>O, first used as an anesthetic in the early 19th century, has been questioned by some who view its known and potential toxicities as outweighing benefits such as rapid onset and offset and relative cardiovascular stability during anesthesia.<sup>191,192</sup> Currently available data indicate that N<sub>2</sub>O does not alter the risk of cardiovascular morbidity in the vast majority of patients. The authors recommend careful screening of patients to identify the few most likely to suffer N<sub>2</sub>O toxicity, and to avoid the drug in these cases.

**TABLE 20.5** Atmospheric Lifetimes and Environmental Effects of Inhaled Anesthetics

Compound		Lifetime (years)	Ozone-Depleting Potential	Global Warming Potential (20 years)	Global Warming Potential (100 years)
CFC-12	CCl <sub>2</sub> F <sub>2</sub>	100	1	11,000	10,900
Carbon dioxide	CO <sub>2</sub>	5-200	— <sup>§</sup>	1	1
Nitrous oxide	N <sub>2</sub> O	114	0.017 <sup>212</sup>	289	298
Halothane	CF <sub>3</sub> CHBrCl	7 <sup>213</sup>	0.36	—	218
Isoflurane	CHF <sub>2</sub> OCHClCF <sub>3</sub>	2.6-3.6 <sup>214</sup>	0.01	1230-1401 <sup>214</sup>	350
Sevoflurane	CH <sub>2</sub> FOCH(CF <sub>3</sub> ) <sub>2</sub>	1.2-5.2 <sup>214</sup>	0	349-1980 <sup>214</sup>	575
Desflurane	CHF <sub>2</sub> OCHFCF <sub>3</sub>	10 <sup>214</sup>	0	3714 <sup>214</sup>	—

Ozone depleting potential (ODP) is the ratio of integrated perturbations to total ozone relative to an equal emission of CFC-12. Global warming potential (GWP) is defined as the cumulative radiative retention integrated over a period of time from the emission of gas relative to reference gas (Carbon Dioxide). The data are based on the Intergovernmental Panel on Climate Change (IPCC) Fourth Assessment Report<sup>215</sup> unless otherwise indicated. <sup>§</sup> CO<sub>2</sub> unlikely reacts and depletes ozone. However, CO<sub>2</sub> producing the greenhouse effect in the troposphere is predicted to reduce stratospheric temperatures and cause further ozone depletion.<sup>216</sup> Computed value for halothane relative to GWP for CFC-12.

## INHALED ANESTHETICS AND NEUROTOXICITY

For a comprehensive description of potential neurotoxic properties of inhaled anesthetics, see [Chapter 78](#).

The ability of general anesthetics to reversibly ablate consciousness has benefitted millions of patients and enabled dramatic advances in health care. While inhaled agents were the first class of anesthetics and continue to be used in the vast majority of cases, accumulating evidence suggests potential long-lasting neurotoxic effects of inhaled and other general anesthetics in patients of extreme ages (see [Chapter 78](#)).<sup>193,194</sup> The greatest concern surrounds the impact of general anesthetics in the youngest patients during periods of rapid brain development. In a seminal study, Jevtovic-Todorovic and coworkers<sup>195</sup> demonstrated widespread neuronal death (apoptosis) in the brains of 7-day-old rats after exposure to midazolam, isoflurane, and N<sub>2</sub>O, associated with long-lasting (up to 4.5 months) changes in neurophysiological correlates of learning and memory, and performance deficits in spatial learning tests. Other animal studies in various species, including nonhuman primates, demonstrate that during sensitive periods of early brain development, exposure to most general anesthetics is associated with accelerated neuronal apoptosis and degeneration.<sup>196-200</sup> Neonatal primate studies suggest that exposure to anesthetics for as little as 3 hours leads to neuro-apoptosis and neurocognitive problems.<sup>197,199,201</sup> Other studies suggest that low nonapoptotic concentrations of general anesthetics may inhibit normal synapse formation and damage developing neuronal networks.<sup>202</sup> Mechanisms underlying neurodevelopmental toxicity are potentially linked to the same ion channels hypothesized to mediate general anesthesia. General anesthetic actions are attributed in part to both antagonism of N-methyl-D-aspartate (NMDA) receptor and potentiation of GABA<sub>A</sub> receptor signal transduction, and drugs with either or both of these activities damage developing brains.<sup>194,203,204</sup>

Based on preclinical studies showing that anesthetic exposure consistently impairs neurodevelopment, the US Food and Drug Administration (FDA) issued a safety announcement that repeated or lengthy exposures to general anesthetics and sedative drugs before the age of three have the potential to harm the development of children's brains

(<http://www.fda.gov/drugs/drugsafety/ucm532356.htm>). Emerging clinical data, however, indicate either no or very modest associations between exposure to surgical procedures requiring general anesthesia and neurodevelopmental outcomes.<sup>205-208</sup> The Pediatric Anesthesia NeuroDevelopment Assessment (PANDA) trial compared a cohort of children who received general anesthesia for hernia repair before age 3 with siblings.<sup>209</sup> The neuropsychological outcomes showed no difference between groups. A randomized clinical study, the General Anesthesia Compared to Spinal Anesthesia (GAS) trial, compared infants who underwent hernia repair with awake-spinal versus inhaled general anesthesia. At age 2, cognitive scores in the two groups were equivalent,<sup>210</sup> whereas the primary outcome at age 5 has not been reported. Related clinical studies exploring a variety of long-term outcomes in children are underway, adding uncertainty to clinical decision making. A comprehensive examination of this topic is provided elsewhere in this textbook ("Pediatric Anesthesia," [Chapter 78](#)). For updated recommendations to healthcare providers and parents regarding exposure to anesthesia and surgery in early life, please consult <https://smarittots.org/about/consensus-statement/>. For a comprehensive description of long-term cognitive effects of surgery and anesthesia in adults, see [Chapter 84](#).

## INHALED ANESTHETICS AND ENVIRONMENTAL EFFECTS

Anesthetic gases in the workplace and in the outdoor environment have the potential to cause harm. An American Society of Anesthesiologists (ASA) Task Force released a comprehensive document on environmentally sustainable anesthesia practice, including the choice of anesthetic gases and reduction of waste: <https://www.asahq.org/resources/resources-from-asa-committees/environmental-sustainability/greening-the-operating-room>.<sup>211</sup> Three potential sequelae have been investigated: global warming, ozone depletion, and health effects from workplace exposure ([Table 20.5](#)).<sup>212-216</sup>

### Global Warming Effects

Atmospheric trapping of thermal radiation from the Earth's surface is known as the *greenhouse effect*, which the

Intergovernmental Panel on Climate Change<sup>217</sup> deems a major contributor to global warming. Inhaled anesthetics are recognized greenhouse gases.<sup>218,219</sup> Isoflurane, sevoflurane, and desflurane, the most widely used current inhaled anesthetics, are minimally metabolized in the body and are substantially eliminated through exhalation. Most anesthesia waste scavenging systems transfer these gases directly and unchanged into the atmosphere, which has drawn attention to the ecotoxicologic properties of inhaled anesthetics. The global warming potential (GWP) takes into account the heat-trapping efficiency and life-span of atmospheric gases (i.e., the time for removal by chemical reaction with radicals, photolysis, and deposition). The GWP of halogenated anesthetics is reported to range from 1230-fold (isoflurane) to 3714-fold (desflurane)—that of an equal mass of CO<sub>2</sub>. Ryan and Nielsen<sup>214</sup> suggested that the most common VAs can significantly influence global warming, with the greatest impact produced by atmospheric desflurane.<sup>214</sup>

The GWP of N<sub>2</sub>O is approximately 300-fold greater than that of an equal mass of CO<sub>2</sub>.<sup>220,221</sup> N<sub>2</sub>O is administered to patients in much larger quantities relative to VA gases and is remarkably stable, with an atmospheric life-span of approximately 120 years.<sup>222</sup> Atmospheric N<sub>2</sub>O is produced by natural sources in soil and water, as well as human sources, including agriculture (nitrogen-based fertilizers) and combustion of fossil fuels. Sherman and Cullen<sup>223</sup> first reported that N<sub>2</sub>O could contribute to global warming and estimated that approximately 1% of man-made N<sub>2</sub>O production was for anesthesia. Anesthetic use may contribute 3.0% of total N<sub>2</sub>O emissions in the United States.<sup>219</sup> Although the use of N<sub>2</sub>O is declining in many countries, data on the worldwide medical use of N<sub>2</sub>O are not available.

### Ozone Depletion

The ozone layer of the Earth's atmosphere, which has been declining 4% per decade since the 1970s, absorbs damaging ultraviolet B light (UVB; wavelengths 280-315 nm). The biologic consequences of increasing UVB radiation include increases in skin cancer, cataracts, damage to plants, and reduction of oceanic plankton populations. Halogenated VAs are similar to chlorofluorocarbons (CFCs), which are major ozone depleting pollutants. Ozone depletion by halocarbons depends on molecular weight, number and type of halogen atoms, and atmospheric life-span.<sup>224</sup> The atmospheric life-span of halogenated anesthetics is much shorter (4.0-21.4 years)<sup>225</sup> than that of many CFCs (up to 100 years). Fluorination is associated with longer atmospheric life-span because of the stability of carbon-fluorine (C-F) bonds. Chemicals with a lifetime of more than 2 years are believed to reach the stratosphere in significant quantities. There they are exposed to intense ultraviolet radiation that can break carbon-halogen bonds, creating halogen radicals that catalytically destroy ozone. Chlorine-containing anesthetics such as halothane, isoflurane, and enflurane may be more destructive to the ozone layer than sevoflurane and desflurane, which contain only C-F bonds. Carbon-hydrogen bonds are susceptible to attack by hydroxyl radicals (OH) in the troposphere,<sup>226</sup> making them less likely to reach the stratosphere. However, even compounds with a lifetime of a few months may potentially contribute to ozone destruction.<sup>227</sup> Contributions to total stratospheric ozone

depletion were estimated as 1% for halothane and 0.02% for enflurane and isoflurane.<sup>225</sup>

N<sub>2</sub>O is the primary source of stratospheric nitrogen oxides, NO and NO<sub>2</sub>, and both destroy ozone. Because only 10% of N<sub>2</sub>O is converted to NO<sub>x</sub>, its ozone depleting potential is lower than that of an equal mass of CFCs. However, N<sub>2</sub>O emission is reported to be the single largest ozone depleting human emission, and is expected to remain so for the rest of this century.<sup>212</sup> The use of N<sub>2</sub>O could actually contribute additional environmental harm when used with halogenated anesthetics.

The environmental impact of all inhaled anesthetics could be reduced by 80% to 90% if closed circuit anesthesia is widely employed, and to a lesser degree if low carrier gas flow rates are routinely used (see Fig. 20.13). Technologies that trap anesthetics in waste gas flows have the potential to reduce emissions into the environment, and can reduce drug costs by reusing (after redistillation) the trapped drugs.<sup>228</sup> Physician education warning that the medical use of N<sub>2</sub>O can significantly contribute to both the greenhouse effect and ozone depletion should be maintained. Avoiding N<sub>2</sub>O when it provides no clinical advantage is suggested for a more environmentally sound anesthetic practice.<sup>218</sup>

### Exposure to Waste Anesthetic Gases

Healthcare personnel can be exposed to waste anesthetic gases both in and out of the operating room environment. Possible adverse health effects by chronic exposure to trace concentrations of inhaled anesthetics has concerned healthcare professionals for many years.<sup>229,230</sup> Laboratory studies suggest reproductive abnormalities in animals exposed to high concentrations of N<sub>2</sub>O (1000 ppm or greater).<sup>231,232</sup> Long-term occupational exposure to anesthetic gases may be associated with genomic alterations.<sup>233</sup> However, a long-term prospective study found no causal relationship between adverse health effects and exposure to waste anesthetic gases with or without a scavenging system.<sup>234</sup>

All inhaled anesthetics cross the placental-fetal exchange barrier. Teratogenicity, which has been demonstrated in animal fetuses chronically exposed to N<sub>2</sub>O,<sup>235,236</sup> is of particular concern in pregnant healthcare workers, but there is no evidence of harm in humans. Furthermore, there is no definitive evidence of harm to fetuses of women anesthetized while pregnant,<sup>237</sup> although studies are underway addressing the possibility that anesthetics cause harm during critical phases of fetal brain development (see earlier section, "Inhaled Anesthetics and Neurotoxicity," and Chapter 78).<sup>238</sup> The US Occupational Safety and Health Administration (OSHA) recommends that no worker should be exposed to concentrations of halogenated anesthetic greater than 2 ppm for a period exceeding 1 hour during anesthesia administration (<http://www.osha.gov/dts/osta/anestheticgases/index.html>). OSHA also recommends that no worker should be exposed to 8-hour time-weighted average concentrations of N<sub>2</sub>O greater than 25 ppm.

Potential postoperative exposure of healthcare workers to exhaled anesthetic gases in postanesthesia care units, intensive care units, and other patient care areas should also be recognized. Studies have documented excessive levels of waste anesthetic gases in poorly ventilated postanesthesia care areas.<sup>239-241</sup> However, no studies have documented significant adverse health effects.

## Xenon and Other Noble Gases

Modern inhaled anesthetics represent vast improvements over earlier inhaled agents, with N<sub>2</sub>O representing the longest surviving widely used anesthetic. The noble gas xenon was first shown to produce general anesthesia in 1951,<sup>242</sup> and subsequent studies have revealed that in comparison with other inhaled anesthetics, it approaches being the ideal agent.<sup>243-245</sup> It is most comparable to N<sub>2</sub>O, but superior in a number of ways. Xenon is present as a minor constituent of air (50 parts per billion), and is isolated by distillation of liquefied air, along with liquefied nitrogen and oxygen. Xenon is entirely unreactive in the biosphere and is the only inhaled anesthetic that is not an environmental pollutant, although its distillation from air uses considerable energy and thus creates CO<sub>2</sub> and other pollutants as byproducts.<sup>219</sup> It is odorless, tasteless, nonflammable, and has a limitless shelf-life. Its solubility in blood ( $\lambda_{b/g} = 0.14$ ) and body tissues is lower than that of any other inhaled anesthetic, including N<sub>2</sub>O. As a result, it has extraordinarily rapid onset and respiratory clearance, with emergence times 2- to 3-fold faster when it replaces N<sub>2</sub>O in clinical settings.<sup>246-248</sup> It undergoes no biotransformation or reactions with CO<sub>2</sub> absorbents or ultraviolet light. Moreover, xenon has favorable pharmacodynamic effects in comparison to most inhaled anesthetics. It produces minimal cardiovascular depression and is not arrhythmogenic.<sup>248-251</sup> As with N<sub>2</sub>O, xenon has analgesic activity and reduces intraoperative opioid requirements.<sup>252</sup> It does not trigger malignant hyperthermia or produce any known toxicity.<sup>253</sup> In fact, xenon has been shown to have cardioprotective and neuroprotective activities in preclinical models.<sup>243,245</sup> Clinical trials in adult cardiac surgery patients,<sup>254-256</sup> partial nephrectomy patients,<sup>257</sup> and comatose survivors of cardiac arrest<sup>258,259</sup> have demonstrated that xenon reduces pressor requirements and modestly reduces the extent of organ damage, relative to other anesthetics. However, in these clinical settings and in others, xenon does not improve neurocognitive function or survival.<sup>260-262</sup>

Given all these advantages, why is xenon not a commonly used inhaled anesthetic? The main reason is its cost.<sup>263</sup> At more than \$15/L in the gas form, xenon is greater than 100-fold more expensive than N<sub>2</sub>O and far more expensive per patient than either desflurane or sevoflurane, which are currently the most expensive VAs. Xenon has a MAC-immobility of 0.61 atm, and even with a strict closed-circuit technique, greater than 10 L are needed to anesthetize a typical patient. To perform closed circuit anesthesia with xenon-oxygen also requires lengthy preanesthetic denitrogenation to prevent N<sub>2</sub> from accumulating in the rebreathing circuit.<sup>264</sup> Transitioning from 100% oxygen during denitrogenation to closed circuit xenon-oxygen anesthesia is another slow process because xenon is added to the circuit as oxygen is metabolized in the patient at 200 to 250 mL/min. High-flow xenon is otherwise necessary to make this transition short. To make xenon a more affordable anesthetic, specialized anesthesia machines have been designed to enable its efficient delivery,<sup>265</sup> and new waste-scavenging systems are being introduced with cryogenic traps that can condense xenon in a liquid form from waste gases.<sup>266</sup> This process allows relatively inexpensive recycling of xenon after it has been redistilled to a pure form.

In addition to cost, xenon presents a few other downsides. Xenon gas has a much higher density (5.9 g/L) than either N<sub>2</sub>O (1.9 g/L) or air (1.2 g/L), resulting in increased flow resistance and work of breathing.<sup>267</sup> Thus it may be a poor choice for patients with compromised respiratory function. As with N<sub>2</sub>O, high xenon partial pressures needed for anesthesia cause expansion of trapped air spaces and vascular air emboli.<sup>268</sup> Compared with propofol infusion or sevoflurane inhalation, xenon anesthesia results in a higher incidence of nausea and vomiting.<sup>269,270</sup>

Currently, xenon remains an experimental anesthetic, with clinical research focusing on its potential as an organ protectant, and the development of technologies to reduce its cost. Shifting the cost-benefit balance toward more xenon use in patients will depend on whether clinical studies end up supporting xenon's beneficial efficacy. Other noble gases also share some of xenon's neuroprotective actions in experimental model systems and are also under investigation as potential clinical anesthetics.<sup>271</sup>

 Complete references available online at [expertconsult.com](http://expertconsult.com).

## References

- Mapleson WW. *Br J Anaesth.* 1973;45:319.
- Bovill JG. *Handb Exp Pharmacol.* 2008;182:121.
- Eger 2nd Ed. *Anesth Analg.* 1987;66:971.
- Eger 2nd Ed. Shargel R. *Anesthesiology.* 1963;24:625.
- Cromwell TH, et al. *Anesthesiology.* 1971;35:401.
- Yasuda N, et al. *Anesth Analg.* 1989;69:370.
- Stoepling RK, et al. *Anesthesiology.* 1970;33(5).
- Dwyer R, et al. *Anesthesiology.* 1992;77:888.
- Gion H, Saidman LJ. *Anesthesiology.* 1971;35:361.
- Rampil IJ, et al. *Anesthesiology.* 1991;74:429.
- Katoh T, et al. *Anesth Analg.* 1993;77:1012.
- Steward A, et al. *Br J Anaesth.* 1973;45:282.
- Levitt DG. *BMC Anesthesiol.* 2002;2:5.
- Wissing H, et al. *Br J Anaesth.* 2000;84:443.
- Kennedy RR, et al. *Anesth Analg.* 2002;95:1616.
- Munson ES, Eger 2nd Ed. *Anesthesiology.* 1970;33:515.
- Allott PR, et al. *Br J Anaesth.* 1973;45:294.
- Munson ES, et al. *Anesth Analg.* 1978;57:224.
- Eger 2nd Ed, et al. *Anesth Analg.* 1998;86:1070.
- Yamamura H, et al. *Anaesthesia.* 1963;18:427.
- Kennedy RR, Baker AB. *Anaesth Intensive Care.* 2001;29:535.
- Eger 2nd Ed. Severinghaus JW. *Anesthesiology.* 1964;25:620.
- Stoepling RK, Longnecker DE. *Anesthesiology.* 1972;36:352.
- Stoepling RK, Eger 2nd Ed. *Anesthesiology.* 1969;30:273.
- Epstein RM, et al. *Anesthesiology.* 1964;25:364.
- Taheri S, Eger 2nd Ed. *Anesth Analg.* 1999;89:774.
- Hendrickx JF, et al. *Br J Anaesth.* 2006;96:391.
- Peyton PJ, Horriat M, Robinson GJ, Pierce R, Thompson BR. Magnitude of the second gas effect on arterial sevoflurane partial pressure. *Anesthesiology.* 2008;108:381-387.
- Korman B, et al. *Anesthesiology.* 2018;129.
- Barrett EJ, Rattigan S. *Diabetes.* 61:2661.
- Larsen OA, et al. *Acta Physiol Scand.* 1966;66:337.
- Matsukawa T, et al. *Anesthesiology.* 1995;82:662.
- Watt SJ, et al. *Anaesthesia.* 1996;51:24.
- Westenskow DR, et al. *Br J Anaesth.* 1986;58:555.
- Van Zundert T, et al. *Anaesth Intensive Care.* 38:76.
- Gallagher TM, Black GW. *Anaesthesia.* 1985;40:1073.
- Carpenter RL, et al. *Anesth Analg.* 1986;65:575.
- Yasuda N, et al. *Anesthesiology.* 1991;74:489.
- Hendrickx J, et al. *Eur J Anaesthesiol.* 2016;33:611.
- Eger EI, Brandstater B. *Anesthesiology.* 1965;26:756.
- Eger 2nd Ed. *Anesth Analg.* 2001;93:947.
- Hunter T, et al. *Paediatr Anaesth.* 2005;15:750.
- Baum JA. *Low flow anaesthesia: the theory and practice of low flow, minimal flow and closed system anaesthesia.* 3rd ed. Boston, Mass: Butterworth-Heinemann; 2001.

44. Levy RJ, et al. *Anesth Analg*. 2010;110:747.
45. Severinghaus JW. *J Clin Invest*. 1954;33:1183.
46. Lowe H, Ernst E. *The quantitative practice of anaesthesia: use of closed circuit*. Baltimore, MD: Williams & Wilkins; 1981.
47. Lerou JG, et al. *Anesthesiology*. 1991;75:230.
48. Munson ES, et al. *Anesthesiology*. 1973;38:251.
49. Gibbons RT, et al. *Anesth Analg*. 1977;56:32.
50. Eger 2nd EI, et al. *Anesthesiology*. 1970;32:396.
51. Munson ES, Merrick HC. *Anesthesiology*. 1966;27:783.
52. Eger 2nd EI, Saidman LJ. *Anesthesiology*. 1965;26:61.
53. Perreault L, et al. *Anesthesiology*. 1982;57:325.
54. Wolf GL, et al. *Anesthesiology*. 1983;59:547.
55. Miller CF, Furman WR. *Anesthesiology*. 1983;58:281.
56. Singh M, et al. *J Surg Tech Case Rep*. 2015;7:20–22.
57. Stanley TH, et al. *Anesthesiology*. 1974;41:256.
58. Algren JT, et al. *Paediatr Anaesth*. 1998;8:31.
59. Kaplan R, et al. *Anesthesiology*. 1981;55:71.
60. Lemmens HJ, et al. *Anesth Analg*. 2008;107:1864.
61. Leeson S, et al. *Anesth Analg*. 2014;119:829.
62. Hendrickx JF, et al. *BMC Anesthesiol*. 2006;6:7.
63. Nordmann GR, et al. *Br J Anaesth*. 2006;96:779.
64. Cullen BF, Eger 2nd EI. *Anesthesiology*. 1972;36:168.
65. Fassoulaki A, et al. *Anesthesiology*. 1991;74:479.
66. Lester MJ, et al. *Anesth Analg*. 1991;73:209.
67. Yoshimura N, et al. *Anesthesiology*. 1976;44:372.
68. Neumann MA, et al. *Anesthesiology*. 1998;88:914.
69. Fink BR. *Anesthesiology*. 1955;16:511.
70. Rackow H, et al. *J Appl Physiol*. 1961;16:723.
71. Kharasch ED, et al. *Eur J Clin Pharmacol*. 2000;55:853.
72. Kenna JG. *J Hepatol*. 1997;26(suppl 1):5.
73. Kharasch ED, et al. *Lancet*. 1996;347:1367.
74. Garton KJ, et al. *Drug Metab Dispos*. 1995;23:1426.
75. Kenna JG. *J Hepatol*. 1997;26(suppl 1):5.
76. Gut J, et al. *Pharmacol Ther*. 1993;58(133).
77. Joshi PH, Conn HO. *Ann Int Med*. 1974;80:395.
78. Kharasch ED, et al. *Anesthesiology*. 1995;82:689.
79. Cousins MJ, Mazze RI. *JAMA*. 1973;225:1611.
80. Kharasch ED, et al. *Anesthesiology*. 2006;105:726.
81. Kharasch ED, et al. *Anesth Analg*. 2001;93:1511.
82. Christ DD, et al. *Drug Metab Dispos*. 1988;16:135.
83. Mazze RI, et al. *Anesthesiology*. 1982;57:5.
84. Kharasch ED, Thummel KE. *Anesthesiology*. 1993;79:795.
85. Christ DD, et al. *Anesthesiology*. 1988;69:833.
86. Mazze RI, et al. *Anesth Analg*. 2000;90:683.
87. Brunt EM, et al. *Hepatology*. 1991;13:1017.
88. Mazze RI, et al. *Anesthesiology*. 1974;40:536.
89. Sutton TS, et al. *Anesth Analg*. 1991;73:180.
90. Martin JL, et al. *Anesthesiology*. 1995;83:1125.
91. Jones RM, et al. *Br J Anaesth*. 1990;64:482.
92. Anderson JS, et al. *Anesth Analg*. 2007;104:1452.
93. Holaday DA, Smith FR. *Anesthesiology*. 1981;54:100.
94. Kharasch ED, et al. *Anesthesiology*. 1995;82:1379.
95. Kobayashi Y, et al. *Anesth Analg*. 1992;74:753.
96. Turillazzi E, et al. *Toxicol Pathol*. 2007;35:840.
97. Terrell RC. *Anesthesiology*. 2008;108:531.
98. Krishna DR, Klotz U. *Clin Pharmacokinet*. 1994;26:144.
99. Lohr JW, et al. *Pharmacol Rev*. 1998;50:107.
100. Wilkinson GR. *N Engl J Med*. 2005;352:2211.
101. Kharasch ED. *Acta Anaesthesiol Belg*. 1996;47:7.
102. Weiss CF, et al. *N Engl J Med*. 1960;262:787.
103. Young WS, Lietman PS. *J Pharmacol Exp Therap*. 1978;204:203.
104. Kalow W. *Hum Genomics*. 2004;1:375.
105. Ingelman-Sundberg M, et al. *Trends Pharmacol Sci*. 1999;20:342.
106. Summary of the national Halothane Study. Possible association between halothane anesthesia and postoperative hepatic necrosis. *JAMA*. 1966;197.
107. Ray DC, Drummond GB. *Br J Anaesth*. 1991;67:84.
108. Warner LO, et al. *Anesth Analg*. 1984;63:838.
109. Wark HJ. *Anaesthesia*. 1983;38:237.
110. Wark H, et al. *Br J Anaesth*. 1986;58:1224.
111. Tung D, et al. *Can J Anaesth*. 2005;52:133.
112. Ihtiyar E, et al. *Ind J Gastroenterol*. 2006;25:41.
113. Peiris LJ, et al. *J Clin Anesth*. 2012;24:477.
114. Turner GB, et al. *Eur J Gastroenterol Hepatol*. 2000;12:955.
115. Lewis JH, et al. *Ann Int Med*. 1983;98:984.
116. Lischner MW, et al. *Arch Int Med*. 1967;120:725.
117. Kharasch ED. *Anesth Analg*. 1995;81:S27.
118. Kharasch ED, et al. *Anesthesiology*. 1995;82:1369.
119. Ronis MJ, et al. *Biochem Pharmacol*. 1998;55:123.
120. Hotchkiss JA, et al. *Toxicol Lett*. 1995;78:1.
121. Chen TL, et al. *Can J Anaesth*. 2000;47:680.
122. Knights KM, et al. *Br J Clin Pharmacol*. 2013;76:587.
123. Mazze RI. *Anesthesiology*. 2006;105:843.
124. Mazze RI, et al. *Anesthesiology*. 1972;36:571.
125. Baden JM, et al. *Anesthesiology*. 1982;56:203.
126. Mazze RI, et al. *J Pharmacol Exp Therap*. 1974;190:523.
127. Cousins MJ, et al. *J Pharmacol Exp Therap*. 1974;190:530.
128. Taves DR, et al. *JAMA*. 1970;214:91.
129. Mazze RI, et al. *JAMA*. 1971;216:278.
130. Mazze RI, et al. *Anesthesiology*. 1971;35:247.
131. Murray JM, Trinick TR. *Anesth Analg*. 1992;74:236.
132. Spencer EM, et al. *Anesth Analg*. 1991;73:731.
133. Anders MW. *Annu Rev Pharmacol Toxicol*. 2005;45:147.
134. Keller KA, et al. *Anesthesiology*. 1995;83:1220.
135. Gonsowski CT, et al. *Anesthesiology*. 1994;80:566.
136. Kharasch ED, et al. *Anesthesiology*. 2002;96:173.
137. Bito H, Ikeda K. *Anesthesia Analg*. 1996;82:173.
138. Kharasch ED, et al. *Anesthesiology*. 1997;86:1238.
139. Bito H, et al. *Anesthesiology*. 1997;86:1231.
140. Conzen PF, et al. *Anesthesiology*. 2002;97:578.
141. Eger 2nd EI, et al. *Anesthesia Analg*. 1997;85:1154.
142. Ebert TJ, et al. *Anesthesiology*. 1998;88:601.
143. Higuchi H, et al. *Anesthesiology*. 1998;89:307.
144. Higuchi H, et al. *Anesth Analg*. 2001;92:650.
145. Kharasch ED, et al. *Anesthesiology*. 2005;103:1183.
146. Kharasch ED, et al. *Anesthesiology*. 1997;86:160.
147. Kharasch ED, et al. *Anesthesiology*. 1998;88:1624.
148. Altuntas TG, et al. *Chem Res Toxicol*. 2004;17:435.
149. Eger 2nd EI, et al. *Anesth Analg*. 1997;85:1164.
150. Wissing H, et al. *Anesthesiology*. 2001;95:1205.
151. Keijzer C, et al. *Acta Anaesthesiol Scand*. 2005;49:815.
152. Baxter PJ, et al. *Anesthesiology*. 1998;89:929.
153. Fang ZX, et al. *Anesthesia Analg*. 1995;80:1187.
154. Woehlck HJ, et al. *Anesthesiology*. 1997;87:228.
155. Berry PD, et al. *Anesthesiology*. 1999;90:613.
156. Wu J, et al. *Anesthesiology*. 2004;101:534.
157. Lester M, et al. *Anesth Analg*. 2004;99:769.
158. Baum J, van Aken H. *Eur J Anaesthesiol*. 2000;17:597.
159. Murray JM, et al. *Anesthesiology*. 1999;91:1342.
160. Kobayashi S, et al. *J Anesth*. 2004;18:277.
161. Straus MM, et al. *Anesthesia*. 2004;59:584.
162. Kobayashi S, et al. *J Clin Anesth*. 2003;15:33.
163. Sanders RD, et al. *Anesthesiology*. 2008;109:707.
164. Reynolds E. *Lancet neurology*. 2006;5:949.
165. Doran M, et al. *BMJ*. 2004;328:1364.
166. Keddie S, et al. *J Neurol*. 2018.
167. Garakani A, et al. *Am J Addict*. 2016;25:358.
168. Kaar SJ, et al. *J Psychopharmacol*. 2016;30:395.
169. Fiskerstrand T, et al. *J Pharmacol Exp Therap*. 1997;282:1305.
170. Duma A, et al. *Anesth Analg*. 2015;120:1325.
171. Amos RJ, et al. *Lancet*. 1982;2:835.
172. Sesso RM, et al. *Neuroradiology*. 1999;41:588.
173. Hadzic A, et al. *Anesthesiology*. 1995;83:863.
174. McNeely JK, et al. *Anesthesiology*. 2000;93:1549.
175. Ilinczky S, et al. *Eur J Neurol*. 2002;9:101.
176. Selzer RR, et al. *N Engl J Med*. 2003;349:45.
177. McCully KS. *Am J Pathology*. 1969;56:111.
178. Nygard O, et al. *N Engl J Med*. 1997;337:230.
179. Mayer EL, et al. *J Am Coll Cardiol*. 1996;27:517.
180. Kaul S, et al. *J Am Coll Cardiol*. 2006;48:914.
181. Ntaios G, et al. *Arch Cardiovasc Dis*. 2009;102:847.
182. Badner NH, et al. *Anesth Analg*. 2000;91:1073.
183. Myles PS, et al. *Anesthesiology*. 2007;107:221.
184. Leslie K, et al. *Anesth Analg*. 2011;112:387.
185. Myles PS, et al. *Lancet*. 2014;384:1446.
186. Leslie K, et al. *Anesth Analg*. 2013.
187. Indraratna P, et al. *Heart Lung Circ*. 2017;26:e41.
188. Nagele P, et al. *Anesthesiology*. 2008;109:36.

189. Nagele P, et al. *Pharmacogenet Genomics*. 2009;19:325.
190. Rao LK, et al. *Anaesthesia*. 2010;65:710.
191. Nunn JF. *Br J Anaesth*. 1987;59:3.
192. Myles PS, et al. *Anaesth Intensive Care*. 2004;32:165.
193. Rappaport B, et al. *N Engl J Med*. 2011;364:1387.
194. Hudson AE, Hemmings Jr HC. *Br J Anaesth*. 2011;107:30.
195. Jevtovic-Todorovic V, et al. *J Neurosci*. 2003;23:876.
196. Loepke AW, Soriano SG. *Anesth Analg*. 2008;106:1681.
197. Slikker Jr W, et al. *Toxicol Sci*. 2007;98:145.
198. Zou X, et al. *Neurotoxicol Teratol*. 2011;33:592.
199. Brambrink AM, et al. *Anesthesiology*. 2010;112:834.
200. Brambrink AM, et al. *Anesthesiology*. 2012;116:372.
201. Schenning KJ, et al. *Neurotoxicol Teratol*. 2017;60:63.
202. Gascon E, et al. *Eur J Anaesthesiol*. 2007;24:213.
203. Mellon RD, et al. *Anesth Analg*. 2007;104:509.
204. Vutskits L, et al. *Paediatr Anaesth*. 2012;22:973.
205. Graham MR, et al. *Anesthesiology*. 2016;125:667.
206. Glatz P, et al. *JAMA Pediatr*. 2017;171:e163470.
207. Warner DO, et al. *Anesthesiology*. 2018;129(1):89.
208. Davidson AJ, Sun LS. *Anesthesiology*. 2018;128:840.
209. Schneuer FJ, et al. *Paediatr Anaesth*. 2018;28(6):528.
210. Davidson AJ, et al. *Lancet*. 2016;387:239.
211. Axelrod D, et al. *Greening the Operating Room and Perioperative Arena: Environmental Sustainability for Anesthesia Practice*. American Society of Anesthesiologists; 2014.
212. Ravishankara AR, et al. *Science*. 2009;326:123.
213. Langbein T, et al. *Br J Anaesth*. 1999;82:66.
214. Ryan SM, Nielsen CJ. *Anesth Analg*. 2010;111:92.
215. *Climate Change 2007: The Physical Science Basis*. New York: Cambridge University Press; 2007.
216. Austin J, et al. *Nature*. 1992;360:221.
217. Forster P, et al. In: Solomon S, Qin D, Manning M, eds. *Changes in Atmospheric Constituents and in Radiative Forcing, Climate Change 2007: The Physical Science Basis*. Cambridge: Contribution of Working Group I to the Fourth Assessment Report of the Intergovernmental Panel on Climate Change; 2007.
218. Ryan S, Sherman J. *Anesth Analg*. 2012;114:921.
219. Ishizawa Y. *Anesth Analg*. 2011;112:213.
220. Gutierrez MJF, et al. *Waste Manag Res*. 2005;23:133.
221. Maskell K, et al. *Lancet*. 1993;342:1027.
222. Schmeltekopf AL, et al. *Geophys Res Lett*. 1975;2:393.
223. Sherman SJ, Cullen BF. *Anesthesiology*. 1988;68:816.
224. Hammitt JK, et al. *Nature*. 1987;330:711.
225. Langbein T, et al. *Br J Anaesth*. 1999;82:66.
226. Brown AC, et al. *Nature*. 1989;341:635.
227. *Executive summary, scientific assessment of ozone depletion: 2002*. Geneva: World Meteorological Organization; 2002. Global Ozone Research and Monitoring Project Report No. 47.
228. Barwise JA, et al. *Anesth Analg*. 2011;113:1064.
229. McGregor DG. *Mayo Clinic*. 2000;75:273.
230. Burn AG. *Best Pract Res Clin Anaesthesiol*. 2003;17:147.
231. Vieira E, et al. *Anesth Analg*. 1980;59:175.
232. Fujinaga M, et al. *Anesthesiology*. 1988;69:401.
233. Yilmaz S, Calbayram NC. *J Clin Anesth*. 2016;35:326.
234. Spence AA. *Br J Anaesth*. 1987;59:96.
235. Szyfter K, et al. *J Appl Genet*. 2004;45:369.
236. Friedman JM. *Teratology*. 1988;37:69.
237. Kuczkowski KM. *Obstet Gynecol Surv*. 2004;59:52.
238. Reitman E, Flood P. *Br J Anaesth*. 2011;107(suppl 1):i72.
239. Sessler DI, Badgwell JM. *Anesth Analg*. 1998;87:1083.
240. McGregor DG, et al. *Anesth Analg*. 1999;89:472.
241. Krenzischek DA, et al. *J Perianesth Nurs*. 2002;17:227.
242. Cullen SC, Gross EG. *Science*. 1951;113:580.
243. Preckel B, et al. *Anesthesiology*. 2006;105:187.
244. Sanders RD, et al. *Br J Anaesth*. 2003;91:709.
245. Sanders RD, Maze M. *Curr Opin Anaesthesiol*. 2005;18:405.
246. Goto T, et al. *Anesthesiology*. 1997;86:1273.
247. Rossaint R, et al. *Anesthesiology*. 2003;98:6.
248. Law LS, Lo EA, Gan TJ. Xenon Anesthesia: A Systematic Review and Meta-Analysis of Randomized Controlled Trials. *Anesth Analg*. 2016;122:678–697.
249. Goto T, et al. *Anaesthesia*. 2004;59:1178.
250. Wappler F, et al. *Anesthesiology*. 2007;106:463.
251. Baumert JH, et al. *Br J Anaesth*. 2008;100:605.
252. Lachmann B, et al. *Lancet*. 1990;335(1413).
253. Wappler F. *Curr Opin Anaesthesiol*. 2010;23:417.
254. Al Tmimi L, et al. *Anesth Analg*. 2017;125:1118.
255. Al Tmimi L, et al. *Trials*. 2015;16:449.
256. Hofland J, et al. *Anesthesiology*. 2017;127:918.
258. Arola O, et al. *J Am Coll Cardiol*. 2017;70:2652.
259. Laitio R, et al. *JAMA*. 2016;315:1120.
260. Coburn M, et al. *Br J Anaesth*. 2007;98:756.
261. Coburn M, et al. *Eur J Anaesthesiol*. 2005;22:870.
262. Coburn M, et al. *Br J Anaesth*. 2018;120:127.
263. Nakata Y, et al. *J Clin Anesth*. 1999;11:477.
264. Rawat S, Dingley J. *Anesth Analg*. 2010;110:101.
265. Dingley J, et al. *Anesthesiology*. 2001;94:173.
266. Dingley J, Mason RS. *Anesth Analg*. 2007;105:1312.
267. Zhang P, et al. *Can J Anaesthesia = Journal canadien d'anesthesie*. 1995;42:547.
268. Lockwood G. *Br J Anaesth*. 2002;89:282.
269. Coburn M, et al. *Br J Anaesth*. 2008;100:787.
270. Fahlenkamp AV, et al. *PLoS One*. 2016;11:e0153807.
271. Dickinson R, Franks NP. *Crit Care*. 2010;14:229.

## References

- Mapleson WW. Circulation-time models of the uptake of inhaled anaesthetics and data for quantifying them. *Br J Anaesth.* 1973;45:319–334.
- Bovill JG. Inhalation anaesthesia: from diethyl ether to xenon. *Handb Exp Pharmacol.* 2008;121–142.
- Eger EI 2nd. Partition coefficients of I-653 in human blood, saline, and olive oil. *Anesth Analg.* 1987;66:971–973.
- Eger EI 2nd, Shargel R. The solubility of methoxyflurane in human blood and tissue homogenates. *Anesthesiology.* 1963;24:625–627.
- Cromwell TH, Eger EI 2nd, Stevens WC, Dolan WM. Forane uptake, excretion, and blood solubility in man. *Anesthesiology.* 1971;35:401–408.
- Yasuda N, Targ AG, Eger EI 2nd. Solubility of I-653, sevoflurane, isoflurane, and halothane in human tissues. *Anesth Analg.* 1989;69:370–373.
- Stoelting RK, Longnecker DE, Eger EI 2nd. Minimum alveolar concentrations in man on awakening from methoxyflurane, halothane, ether and fluroxene anesthesia: MAC awake. *Anesthesiology.* 1970;33:5–9.
- Dwyer R, Bennett HL, Eger EI 2nd, Heilbron D. Effects of isoflurane and nitrous oxide in subanesthetic concentrations on memory and responsiveness in volunteers. *Anesthesiology.* 1992;77:888–898.
- Gion H, Saidman LJ. The minimum alveolar concentration of enflurane in man. *Anesthesiology.* 1971;35:361–364.
- Rampil IJ, Lockhart SH, Zwass MS, et al. Clinical characteristics of desflurane in surgical patients: minimum alveolar concentration. *Anesthesiology.* 1991;74:429–433.
- Katoh T, Suguro Y, Kimura T, Ikeda K. Cerebral awakening concentration of sevoflurane and isoflurane predicted during slow and fast alveolar wash-out. *Anesth Analg.* 1993;77:1012–1017.
- Steward A, Allott PR, Cowles AL, Mapleson WW. Solubility coefficients for inhaled anaesthetics for water, oil and biological media. *Br J Anaesth.* 1973;45:282–293.
- Levitt DG. PKQuest: volatile solutes—application to enflurane, nitrous oxide, halothane, methoxyflurane and toluene pharmacokinetics. *BMC Anesthesiol.* 2002;2:5.
- Wissing H, Kuhn I, Rietbrock S, Fuhr U. Pharmacokinetics of inhaled anaesthetics in a clinical setting: comparison of desflurane, isoflurane and sevoflurane. *Br J Anaesth.* 2000;84:443–449.
- Kennedy RR, French RA, Spencer C. Predictive accuracy of a model of volatile anesthetic uptake. *Anesth Analg.* 2002;95: 1616–1621.
- Munson ES, Eger EI 2nd. The effects of hyperthermia and hypothermia on the rate of induction of anesthesia: calculations using a mathematical model. *Anesthesiology.* 1970;33:515–519.
- Allott PR, Steward A, Flook V, Mapleson WW. Variation with temperature of the solubilities of inhaled anaesthetics in water, oil and biological media. *Br J Anaesth.* 1973;45:294–300.
- Munson ES, Eger EI 2nd, Tham MK, Embro WJ. Increase in anesthetic uptake, excretion, and blood solubility in man after eating. *Anesth Analg.* 1978;57:224–231.
- Eger EI 2nd, Ionescu P, Gong D. Circuit absorption of halothane, isoflurane, and sevoflurane. *Anesth Analg.* 1998;86:1070–1074.
- Yamamura H, Wakasugi B, Okuma Y, Maki K. The effects of ventilation on the absorption and elimination of inhalation anaesthetics. *Anesthesia.* 1963;18:427–438.
- Kennedy RR, Baker AB. The effect of cardiac output changes on end-tidal volatile anaesthetic concentrations. *Anesth Intensive Care.* 2001;29:535–538.
- Eger EI 2nd, Severinghaus JW. Effect of uneven pulmonary distribution of blood and gas on induction with inhalation anaesthetics. *Anesthesiology.* 1964;25:620–626.
- Stoelting RK, Longnecker DE. The effect of right-to-left shunt on the rate of increase of arterial anesthetic concentration. *Anesthesiology.* 1972;36:352–356.
- Stoelting RK, Eger EI 2nd. An additional explanation for the second gas effect: a concentrating effect. *Anesthesiology.* 1969;30:273–277.
- Epstein RM, Rackow H, Salanitre E, Wolf GL. Influence of the concentration effect on the uptake of anesthetic mixtures: the second gas effect. *Anesthesiology.* 1964;25:364–371.
- Taheri S, Eger EI 2nd. A demonstration of the concentration and second gas effects in humans anesthetized with nitrous oxide and desflurane. *Anesth Analg.* 1999;89:774–780.
- Hendrickx JF, Carette R, Lemmens HJ, De Wolf AM. Large volume N<sub>2</sub>O uptake alone does not explain the second gas effect of N<sub>2</sub>O on sevoflurane during constant inspired ventilation. *Br J Anaesth.* 2006;96:391–395.
- Peyton PJ, Horriat M, Robinson GJ, Pierce R, Thompson BR. Magnitude of the second gas effect on arterial sevoflurane partial pressure. *Anesthesiology.* 2008;108:381–387.
- Korman B, Dash RK, Peyton PJ. Can mathematical modeling explain the measured magnitude of the second gas effect? *Anesthesiology.* 2018;129.
- Barrett EJ, Rattigan S. Muscle perfusion: its measurement and role in metabolic regulation. *Diabetes.* 61: 2661–2668.
- Larsen OA, Lassen NA, Quaade F. Blood flow through human adipose tissue determined with radioactive xenon. *Acta Physiol Scand.* 1966;66:337–345.
- Matsukawa T, Sessler DI, Sessler AM, et al. Heat flow and distribution during induction of general anesthesia. *Anesthesiology.* 1995;82:662–673.
- Watt SJ, Cook LB, Ohri S, Lockwood GG. The relationship between anaesthetic uptake and cardiac output. *Anaesthesia.* 1996;51:24–28.
- Westenskow DR, Zbinden AM, Thomson DA, Kohler B. Control of end-tidal halothane concentration. Part A: anaesthesia breathing system and feedback control of gas delivery. *Br J Anaesth.* 1986;58:555–562.
- Van Zundert T, Hendrickx J, Brebels A, De Cooman S, Gatt S, De Wolf A. Effect of the mode of administration of inhaled anaesthetics on the interpretation of the F(A)/F(I) curve—a GasMan simulation. *Anaesth Intensive Care.* 38:76–81.
- Gallagher TM, Black GW. Uptake of volatile anaesthetics in children. *Anaesthesia.* 1985;40:1073–1077.
- Carpenter RL, Eger 2nd EI, Johnson BH, Unadkat JD, Sheiner LB. Pharmacokinetics of inhaled anesthetics in humans: measurements during and after the simultaneous administration of enflurane, halothane, isoflurane, methoxyflurane, and nitrous oxide. *Anesth Analg.* 1986;65:575–582.
- Yasuda N, Lockhart SH, Eger EI 2nd, et al. Kinetics of desflurane, isoflurane, and halothane in humans. *Anesthesiology.* 1991;74:489–498.
- Hendrickx J, Peyton P, Carette R, De Wolf A. Inhaled anaesthetics and nitrous oxide: complexities overlooked: things may not be what they seem. *Eur J Anaesthesiol.* 2016;33:611–619.
- Eger EI, Brandstater B. Minimal alveolar anesthetic concentration: a standard of anesthetic potency. *Anesthesiology.* 1965;26:756–763.
- Eger EI 2nd. Age, minimum alveolar anesthetic concentration, and minimum alveolar anesthetic concentration—awake. *Anesth Analg.* 2001;93:947–953.
- Hunter T, Lerman J, Bissonnette B. The temperature and humidity of inspired gases in infants using a pediatric circle system: effects of high and low-flow anesthesia. *Paediatr Anaesth.* 2005;15:750–754.
- Baum JA. *Low Flow Anaesthesia: The Theory and Practice of Low Flow, Minimal Flow and Closed System Anaesthesia.* 2nd ed. Boston, MA: Butterworth-Heinemann; 2001.
- Levy RJ, Nasr VG, Rivera O, et al. Detection of carbon monoxide during routine anesthetics in infants and children. *Anesth Analg.* 2010;110:747–753.
- Severinghaus JW. The rate of uptake of nitrous oxide in man. *J Clin Invest.* 1954;33:1183–1189.
- Lowe H, Ernst E. *The Quantitative Practice of Anesthesia: Use of Closed Circuit.* Baltimore: Williams & Wilkins; 1981.
- Lerou JG, Dirksen R, Beneken Kolmer HH, Booij LH, Borm GF. A system model for closed-circuit inhalation anesthesia. II. Clinical validation. *Anesthesiology.* 1991;75:230–237.
- Munson ES, Eger EI 2nd, Bowers DL. Effects of anesthetic-depressed ventilation and cardiac output on anesthetic uptake: a computer nonlinear stimulation. *Anesthesiology.* 1973;38:251–259.
- Gibbons RT, Steffey EP, Eger EI 2nd. The effect of spontaneous versus controlled ventilation on the rate of rise of alveolar halothane concentration in dogs. *Anesth Analg.* 1977;56:32–34.
- Eger EI 2nd, Smith NT, Stoelting RK, Cullen DJ, Kadis LB, Whitcher CE. Cardiovascular effects of halothane in man. *Anesthesiology.* 1970;32:396–409.
- Munson ES, Merrick HC. Effect of nitrous oxide on venous air embolism. *Anesthesiology.* 1966;27:783–787.

52. Eger EI 2nd, Saidman LJ. Hazards of nitrous oxide anesthesia in bowel obstruction and pneumothorax. *Anesthesiology*. 1965;26:61–66.
53. Perreault L, Normandin N, Plamondon L, et al. Tympanic membrane rupture after anesthesia with nitrous oxide. *Anesthesiology*. 1982;57:325–326.
54. Wolf GL, Capuano C, Hartung J. Nitrous oxide increases intraocular pressure after intravitreal sulfur hexafluoride injection. *Anesthesiology*. 1983;59:547–548.
55. Miller CF, Furman WR. Symptomatic pneumocephalus after translabyrinthine acoustic neuroma excision and nitrous oxide anesthesia. *Anesthesiology*. 1983;58:281–283.
56. Singh M, Vasudeva VS, Rios Diaz AJ, Dunn IF, Caterson EJ. Intraoperative development of tension pneumocephalus in a patient undergoing repair of a cranial-dural defect under nitrous oxide anesthesia. *J Surg Tech Case Rep*. 2015;7:20–22.
57. Stanley TH, Kawamura R, Graves C. Effects of nitrous oxide on volume and pressure of endotracheal tube cuffs. *Anesthesiology*. 1974;41:256–262.
58. Algren JT, Gursoy F, Johnson TD, Skjonsby BS. The effect of nitrous oxide diffusion on laryngeal mask airway cuff inflation in children. *Paediatr Anaesth*. 1998;8:31–36.
59. Kaplan R, Abramowitz MD, Epstein BS. Nitrous oxide and air-filled balloon-tipped catheters. *Anesthesiology*. 1981;55:71–73.
60. Lemmens HJ, Saidman LJ, Eger EI 2nd, Lester MJ. Obesity modestly affects inhaled anesthetic kinetics in humans. *Anesth Analg*. 2008;107:1864–1870.
61. Leeson S, Roberson RS, Philip JH. Hypoventilation after inhaled anesthesia results in reanesthetization. *Anesth Analg*. 2014;119:829–835.
62. Hendrickx JF, Lemmens HJ, Shafer SL. Do distribution volumes and clearances relate to tissue volumes and blood flows? A computer simulation. *BMC Anesthesiol*. 2006;6:7.
63. Nordmann GR, Read JA, Sale SM, Stoddart PA, Wolf AR. Emergence and recovery in children after desflurane and isoflurane anaesthesia: effect of anaesthetic duration. *Br J Anaesth*. 2006;96:779–785.
64. Cullen BF, Eger EI 2nd. Diffusion of nitrous oxide, cyclopropane, and halothane through human skin and amniotic membrane. *Anesthesiology*. 1972;36:168–173.
65. Fassoulaki A, Lockhart SH, Freire BA, et al. Percutaneous loss of desflurane, isoflurane, and halothane in humans. *Anesthesiology*. 1991;74:479–483.
66. Lester MJ, Taheri S, Eger EI 2nd, Liu J, Rampil IJ, Dwyer R. Visceral losses of desflurane, isoflurane, and halothane in swine. *Anesth Analg*. 1991;73:209–212.
67. Yoshimura N, Holaday DA, Fiserova-Bergerova V. Metabolism of methoxyflurane in man. *Anesthesiology*. 1976;44:372–379.
68. Neumann MA, Weiskopf RB, Gong DH, Eger EI 2nd, Ionescu P. Changing from isoflurane to desflurane toward the end of anesthesia does not accelerate recovery in humans. *Anesthesiology*. 1998;88:914–921.
69. Fink BR. Diffusion anoxia. *Anesthesiology*. 1955;16:511–519.
70. Rackow H, Salanitre E, Frumin MJ. Dilution of alveolar gases during nitrous oxide excretion in man. *J Appl Physiol*. 1961;16:723–728.
71. Kharasch ED. Adverse drug reactions with halogenated anesthetics. *Clin Pharmacol Ther*. 2008;84:158–162.
72. Kharasch ED, Hankins DC, Fenstamaker K, Cox K. Human halothane metabolism, lipid peroxidation, and cytochromes P(450)2A6 and P(450)3A4. *Eur J Clin Pharmacol*. 2000;55:853–859.
73. Kharasch ED, Hankins D, Mautz D, Thummel KE. Identification of the enzyme responsible for oxidative halothane metabolism: implications for prevention of halothane hepatitis. *Lancet*. 1996;347:1367–1371.
74. Garton KJ, Yuen P, Meinwald J, Thummel KE, Kharasch ED. Stereoselective metabolism of enflurane by human liver cytochrome P450 2E1. *Drug Metab Dispos*. 1995;23:1426–1430.
75. Kenna JG. Immunoallergic drug-induced hepatitis: lessons from halothane. *J Hepatol*. 1997;26(suppl 1):5–12.
76. Gut J, Christen U, Huwyler J. Mechanisms of halothane toxicity: novel insights. *Pharmacol Ther*. 1993;58:133–155.
77. Joshi PH, Conn HO. The syndrome of methoxyflurane-associated hepatitis. *Ann Intern Med*. 1974;80:395–401.
78. Kharasch ED, Hankins DC, Thummel KE. Human kidney methoxyflurane and sevoflurane metabolism. Intrarenal fluoride production as a possible mechanism of methoxyflurane nephrotoxicity. *Anesthesiology*. 1995;82:689–699.
79. Cousins MJ, Mazze RI. Methoxyflurane nephrotoxicity. A study of dose response in man. *JAMA*. 1973;225:1611–1616.
80. Kharasch ED, Schroeder JL, Liggitt HD, Park SB, Whittington D, Sheffels P. New insights into the mechanism of methoxyflurane nephrotoxicity and implications for anesthetic development (part 1): identification of the nephrotoxic metabolic pathway. *Anesthesiology*. 2006;105:726–736.
81. Kharasch ED, Frink EJ Jr, Artru A, Michalowski P, Rooke GA, Nogami W. Long-duration low-flow sevoflurane and isoflurane effects on postoperative renal and hepatic function. *Anesth Analg*. 2001;93:1511–1520; table of contents.
82. Christ DD, Satoh H, Kenna JG, Pohl LR. Potential metabolic basis for enflurane hepatitis and the apparent cross-sensitization between enflurane and halothane. *Drug Metab Dispos*. 1988;16:135–140.
83. Mazze RI, Woodruff RE, Heerdt ME. Isoniazid-induced enflurane del fluorination in humans. *Anesthesiology*. 1982;57:5–8.
84. Kharasch ED, Thummel KE. Identification of cytochrome P450 2E1 as the predominant enzyme catalyzing human liver microsomal defluorination of sevoflurane, isoflurane, and methoxyflurane. *Anesthesiology*. 1993;79:795–807.
85. Christ DD, Kenna JG, Kammerer W, Satoh H, Pohl LR. Enflurane metabolism produces covalently bound liver adducts recognized by antibodies from patients with halothane hepatitis. *Anesthesiology*. 1988;69:833–838.
86. Mazze RI, Callan CM, Galvez ST, Delgado-Herrera L, Mayer DB. The effects of sevoflurane on serum creatinine and blood urea nitrogen concentrations: a retrospective, twenty-two-center, comparative evaluation of renal function in adult surgical patients. *Anesth Analg*. 2000;90:683–688.
87. Brunt EM, White H, Marsh JW, Holtmann B, Peters MG. Fulminant hepatic failure after repeated exposure to isoflurane anesthesia: a case report. *Hepatology*. 1991;13:1017–1021.
88. Mazze RI, Cousins MJ, Barr GA. Renal effects and metabolism of isoflurane in man. *Anesthesiology*. 1974;40:536–542.
89. Sutton TS, Koblin DD, Gruenke LD, et al. Fluoride metabolites after prolonged exposure of volunteers and patients to desflurane. *Anesth Analg*. 1991;73:180–185.
90. Martin JL, Plevak DJ, Flannery KD, et al. Hepatotoxicity after desflurane anesthesia. *Anesthesiology*. 1995;83:1125–1129.
91. Jones RM, Koblin DD, Cashman JN, Eger EI 2nd, Johnson BH, Damask MC. Biotransformation and hepato-renal function in volunteers after exposure to desflurane (I-653). *Br J Anaesth*. 1990;64:482–487.
92. Anderson JS, Rose NR, Martin JL, Eger EI, Njoku DB. Desflurane hepatitis associated with hapten and autoantigen-specific IgG4 antibodies. *Anesth Analg*. 2007;104:1452–1453; table of contents.
93. Holaday DA, Smith FR. Clinical characteristics and biotransformation of sevoflurane in healthy human volunteers. *Anesthesiology*. 1981;54:100–106.
94. Kharasch ED, Armstrong AS, Gunn K, Artru A, Cox K, Karol MD. Clinical sevoflurane metabolism and disposition. II. The role of cytochrome P450 2E1 in fluoride and hexafluoroisopropanol formation. *Anesthesiology*. 1995;82:1379–1388.
95. Kobayashi Y, Ochiai R, Takeda J, Sekiguchi H, Fukushima K. Serum and urinary inorganic fluoride concentrations after prolonged inhalation of sevoflurane in humans. *Anesth Analg*. 1992;74:753–757.
96. Turillazzi E, D'Errico S, Neri M, Riezzo I, Fineschi V. A fatal case of fulminant hepatic necrosis following sevoflurane anesthesia. *Toxicol Pathol*. 2007;35:840–845.
97. Terrell RC. The invention and development of enflurane, isoflurane, sevoflurane, and desflurane. *Anesthesiology*. 2008;108:531–533.
98. Krishna DR, Klotz U. Extrahepatic metabolism of drugs in humans. *Clin Pharmacokinet*. 1994;26:144–160.
99. Lohr JW, Willsky GR, Acara MA. Renal drug metabolism. *Pharmacol Rev*. 1998;50:107–141.
100. Wilkinson GR. Drug metabolism and variability among patients in drug response. *N Engl J Med*. 2005;352:2211–2221.
101. Kharasch ED. Metabolism and toxicity of the new anesthetic agents. *Acta Anaesthesiol Belg*. 1996;47:7–14.
102. Weiss CF, Glazko AJ, Weston JK. Chloramphenicol in the newborn infant. A physiologic explanation of its toxicity when given in excessive doses. *N Engl J Med*. 1960;262:787–794.

103. Young WS, Lietman PS. Chloramphenicol glucuronyl transferase: assay, ontogeny and inducibility. *J Pharmacol Exp Ther*. 1978;204:203–211.
104. Kalow W. Human pharmacogenomics: the development of a science. *Hum Genomics*. 2004;1:375–380.
105. Ingelman-Sundberg M, Oscarson M, McLellan RA. Polymorphic human cytochrome P450 enzymes: an opportunity for individualized drug treatment. *Trends Pharmacol Sci*. 1999;20:342–349.
106. Summary of the National Halothane Study. Possible association between halothane anesthesia and postoperative hepatic necrosis. *JAMA*. 1966;197:775–788.
107. Ray DC, Drummond GB. Halothane hepatitis. *Br J Anaesth*. 1991;67:84–99.
108. Warner LO, Beach TP, Garvin JP, Warner EJ. Halothane and children: the first quarter century. *Anesth Analg*. 1984;63:838–840.
109. Wark HJ. Postoperative jaundice in children. The influence of halothane. *Anaesthesia*. 1983;38:237–242.
110. Wark H, O'Halloran M, Overton J. Prospective study of liver function in children following multiple halothane anaesthetics at short intervals. *Br J Anaesth*. 1986;58:1224–1228.
111. Tung D, Yoshida EM, Wang CS, Steinbrecher UP. Severe desflurane hepatotoxicity after colon surgery in an elderly patient. *Can J Anaesth*. 2005;52:133–136.
112. Ihtiyar E, Algin C, Haciolcu A, Isiksoy S. Fatal isoflurane hepatotoxicity without re-exposure. *Indian J Gastroenterol*. 2006;25:41–42.
113. Peiris LJ, Agrawal A, Morris JE, Basnyat PS. Isoflurane hepatotoxicity-induced liver failure: a case report. *J Clin Anesth*. 2012;24:477–479.
114. Turner GB, O'Rourke D, Scott GO, Beringer TR. Fatal hepatotoxicity after re-exposure to isoflurane: a case report and review of the literature. *Eur J Gastroenterol Hepatol*. 2000;12:955–959.
115. Lewis JH, Zimmerman HJ, Ishak KG, Mullick FG. Enflurane hepatotoxicity. A clinicopathologic study of 24 cases. *Ann Intern Med*. 1983;98:984–992.
116. Lischner MW, MacNabb GM, Galambos JT. Fatal hepatic necrosis following surgery. Possible relation to methoxyflurane anesthesia. *Arch Intern Med*. 1967;120:725–728.
117. Kharasch ED. Biotransformation of sevoflurane. *Anesth Analg*. 1995;81:S27–38.
118. Kharasch ED, Karol MD, Lanni C, Sawchuk R. Clinical sevoflurane metabolism and disposition. I. Sevoflurane and metabolite pharmacokinetics. *Anesthesiology*. 1995;82:1369–1378.
119. Ronis MJ, Huang J, Longo V, Tindberg N, Ingelman-Sundberg M, Badger TM. Expression and distribution of cytochrome P450 enzymes in male rat kidney: effects of ethanol, acetone and dietary conditions. *Biochem Pharmacol*. 1998;55:123–129.
120. Hotchkiss JA, Kim H, Hahn FF, Novak RF, Dahl AR. Pyridine induction of Sprague-Dawley rat renal cytochrome P4502E1: immunohistochemical localization and quantitation. *Toxicol Lett*. 1995;78:1–7.
121. Chen TL, Chen TG, Tai YT, et al. Propofol inhibits renal cytochrome P450 activity and enflurane defluorination in vitro in hamsters. *Can J Anaesth*. 2000;47:680–686.
122. Knights KM, Rowland A, Miners JO. Renal drug metabolism in humans: the potential for drug-endobiotic interactions involving cytochrome P450 (CYP) and UDP-glucuronosyltransferase (UGT). *Br J Clin Pharmacol*. 2013.
123. Mazze RI. Methoxyflurane revisited: tale of an anesthetic from cradle to grave. *Anesthesiology*. 2006;105:843–846.
124. Mazze RI, Cousins MJ, Kosek JC. Dose-related methoxyflurane nephrotoxicity in rats: a biochemical and pathologic correlation. *Anesthesiology*. 1972;36:571–587.
125. Baden JM, Rice SA, Mazze RI. Deuterated methoxyflurane anesthesia and renal function in Fischer 344 rats. *Anesthesiology*. 1982;56:203–206.
126. Mazze RI, Hitt BA, Cousins MJ. Effect of enzyme induction with phenobarbital on the in vivo and in vitro defluorination of isoflurane and methoxyflurane. *J Pharmacol Exp Ther*. 1974;190:523–529.
127. Cousins MJ, Mazze RI, Kosek JC, Hitt BA, Love FV. The etiology of methoxyflurane nephrotoxicity. *J Pharmacol Exp Ther*. 1974;190:530–541.
128. Taves DR, Fry BW, Freeman RB, Gillies AJ. Toxicity following methoxyflurane anesthesia. II. Fluoride concentrations in nephrotoxicity. *JAMA*. 1970;214:91–95.
129. Mazze RI, Shue GL, Jackson SH. Renal dysfunction associated with methoxyflurane anesthesia. A randomized, prospective clinical evaluation. *JAMA*. 1971;216:278–288.
130. Mazze RI, Trudell JR, Cousins MJ. Methoxyflurane metabolism and renal dysfunction: clinical correlation in man. *Anesthesiology*. 1971;35:247–252.
131. Murray JM, Trinick TR. Plasma fluoride concentrations during and after prolonged anesthesia: a comparison of halothane and isoflurane. *Anesth Analg*. 1992;74:236–240.
132. Spencer EM, Willatts SM, Prys-Roberts C. Plasma inorganic fluoride concentrations during and after prolonged (greater than 24 h) isoflurane sedation: effect on renal function. *Anesth Analg*. 1991;73:731–737.
133. Anders MW. Formation and toxicity of anesthetic degradation products. *Annu Rev Pharmacol Toxicol*. 2005;45:147–176.
134. Keller KA, Callan C, Prokocimer P, et al. Inhalation toxicity study of a haloalkene degradant of sevoflurane, compound A (PIFE), in Sprague-Dawley rats. *Anesthesiology*. 1995;83:1220–1232.
135. Gonsowski CT, Laster MJ, Eger EI 2nd, Ferrell LD, Kerschmann RL. Toxicity of compound A in rats. Effect of increasing duration of administration. *Anesthesiology*. 1994;80:566–573.
136. Kharasch ED, Powers KM, Artru AA. Comparison of Amsorb, sodalime, and Baralyme degradation of volatile anesthetics and formation of carbon monoxide and compound a in swine in vivo. *Anesthesiology*. 2002;96:173–182.
137. Bito H, Ikeda K. Renal and hepatic function in surgical patients after low-flow sevoflurane or isoflurane anesthesia. *Anesth Analg*. 1996;82:173–176.
138. Kharasch ED, Frink EJ Jr, Zager R, Bowdle TA, Artru A, Nogami WM. Assessment of low-flow sevoflurane and isoflurane effects on renal function using sensitive markers of tubular toxicity. *Anesthesiology*. 1997;86:1238–1253.
139. Bito H, Ikeuchi Y, Ikeda K. Effects of low-flow sevoflurane anesthesia on renal function: comparison with high-flow sevoflurane anesthesia and low-flow isoflurane anesthesia. *Anesthesiology*. 1997;86:1231–1237.
140. Conzen PF, Kharasch ED, Czerner SF, et al. Low-flow sevoflurane compared with low-flow isoflurane anesthesia in patients with stable renal insufficiency. *Anesthesiology*. 2002;97:578–584.
141. Eger EI 2nd, Gong D, Koblin DD, et al. Dose-related biochemical markers of renal injury after sevoflurane versus desflurane anesthesia in volunteers. *Anesth Analg*. 1997;85:1154–1163.
142. Ebert TJ, Frink EJ Jr, Kharasch ED. Absence of biochemical evidence for renal and hepatic dysfunction after 8 hours of 1.25 minimum alveolar concentration sevoflurane anesthesia in volunteers. *Anesthesiology*. 1998;88:601–610.
143. Higuchi H, Sumita S, Wada H, et al. Effects of sevoflurane and isoflurane on renal function and on possible markers of nephrotoxicity. *Anesthesiology*. 1998;89:307–322.
144. Higuchi H, Adachi Y, Wada H, Kanno M, Satoh T. The effects of low-flow sevoflurane and isoflurane anesthesia on renal function in patients with stable moderate renal insufficiency. *Anesth Analg*. 2001;92:650–655.
145. Kharasch ED, Schroeder JL, Sheffels P, Liggitt HD. Influence of sevoflurane on the metabolism and renal effects of compound A in rats. *Anesthesiology*. 2005;103:1183–1188.
146. Kharasch ED, Thorning D, Garton K, Hankins DC, Kilty CG. Role of renal cysteine conjugate beta-lyase in the mechanism of compound A nephrotoxicity in rats. *Anesthesiology*. 1997;86:160–171.
147. Kharasch ED, Hoffman GM, Thorning D, Hankins DC, Kilty CG. Role of the renal cysteine conjugate beta-lyase pathway in inhaled compound A nephrotoxicity in rats. *Anesthesiology*. 1998;88:1624–1633.
148. Altuntas TG, Park SB, Kharasch ED. Sulfoxidation of cysteine and mercapturic acid conjugates of the sevoflurane degradation product fluoromethyl-2,2-difluoro-1-(trifluoromethyl)vinyl ether (compound A). *Chem Res Toxicol*. 2004;17:435–445.
149. Eger EI 2nd, Ionescu P, Laster MJ, Gong D, Weiskopf RB, Kerschmann RL. Quantitative differences in the production and toxicity of  $\text{CF}_2=\text{BrCl}$  versus  $\text{CH}_2\text{F}-\text{O}-\text{C}(\text{=CF}_2)(\text{CF}_3)$  (compound A): the safety of halothane does not indicate the safety of sevoflurane. *Anesth Analg*. 1997;85:1164–1170.
150. Wissing H, Kuhn I, Warnken U, Dudziak R. Carbon monoxide production from desflurane, enflurane, halothane, isoflurane, and sevoflurane with dry soda lime. *Anesthesiology*. 2001;95:1205–1212.
151. Keijzer C, Perez RS, de Lange JJ. Carbon monoxide production from desflurane and six types of carbon dioxide absorbents in a patient model. *Acta Anaesthesiol Scand*. 2005;49:815–818.

152. Baxter PJ, Garton K, Kharasch ED. Mechanistic aspects of carbon monoxide formation from volatile anesthetics. *Anesthesiology*. 1998;89:929–941.
153. Fang ZX, Eger EI 2nd, Laster MJ, Chortkoff BS, Kandel L, Ionescu P. Carbon monoxide production from degradation of desflurane, enflurane, isoflurane, halothane, and sevoflurane by soda lime and Baralyme. *Anesth Analg*. 1995;80:1187–1193.
154. Woehlck HJ, Dunning M 3rd, Connolly LA. Reduction in the incidence of carbon monoxide exposures in humans undergoing general anesthesia. *Anesthesiology*. 1997;87:228–234.
155. Berry PD, Sessler DI, Larson MD. Severe carbon monoxide poisoning during desflurane anesthesia. *Anesthesiology*. 1999;90:613–616.
156. Wu J, Previte JP, Adler E, Myers T, Ball J, Gunter JB. Spontaneous ignition, explosion, and fire with sevoflurane and barium hydroxide lime. *Anesthesiology*. 2004;101:534–537.
157. Laster M, Roth P, Eger EI 2nd. Fires from the interaction of anesthetics with desiccated absorbent. *Anesth Analg*. 2004;99:769–774; table of contents.
158. Baum J, van Aken H. Calcium hydroxide lime—a new carbon dioxide absorbent: a rationale for judicious use of different absorbents. *Eur J Anaesthesiol*. 2000;17:597–600.
159. Murray JM, Renfrew CW, Bedi A, McCrystal CB, Jones DS, Fee JP. Amsorb: a new carbon dioxide absorbent for use in anesthetic breathing systems. *Anesthesiology*. 1999;91:1342–1348.
160. Kobayashi S, Bito H, Morita K, Katoh T, Sato S. Amsorb Plus and Dragersorb Free, two new-generation carbon dioxide absorbents that produce a low compound A concentration while providing sufficient CO<sub>2</sub> absorption capacity in simulated sevoflurane anesthesia. *J Anesth*. 2004;18:277–281.
161. Struys MM, Bouche MP, Rolly G, et al. Production of compound A and carbon monoxide in circle systems: an in vitro comparison of two carbon dioxide absorbents. *Anaesthesia*. 2004;59:584–589.
162. Kobayashi S, Bito H, Obata Y, Katoh T, Sato S. Compound A concentration in the circle absorber system during low-flow sevoflurane anesthesia: comparison of Dragersorb Free, Amsorb, and Sodasorb II. *J Clin Anesth*. 2003;15:33–37.
163. Sanders RD, Weimann J, Maze M. Biologic effects of nitrous oxide: a mechanistic and toxicologic review. *Anesthesiology*. 2008;109:707–722.
164. Reynolds E. Vitamin B12, folic acid, and the nervous system. *Lancet Neurol*. 2006;5:949–960.
165. Doran M, Rassam SS, Jones LM, Underhill S. Toxicity after intermittent inhalation of nitrous oxide for analgesia. *BMJ*. 2004;328:1364–1365.
166. Keddie S, Adams A, Kelso ARC, et al. No laughing matter: subacute degeneration of the spinal cord due to nitrous oxide inhalation. *J Neurol*. 2018.
167. Garakani A, Jaffe RJ, Savla D, et al. Neurologic, psychiatric, and other medical manifestations of nitrous oxide abuse: a systematic review of the case literature. *Am J Addict*. 2016;25:358–369.
168. Kaar SJ, Ferris J, Waldron J, Devaney M, Ramsey J, Winstock AR. Up: the rise of nitrous oxide abuse. An international survey of contemporary nitrous oxide use. *J Psychopharmacol*. 2016;30:395–401.
169. Fiskerstrand T, Ueland PM, Refsum H. Folate depletion induced by methotrexate affects methionine synthase activity and its susceptibility to inactivation by nitrous oxide. *J Pharmacol Exp Ther*. 1997;282:1305–1311.
170. Duma A, Cartmill C, Blood J, Sharma A, Kharasch ED, Nagele P. The hematological effects of nitrous oxide anesthesia in pediatric patients. *Anesth Analg*. 2015;120:1325–1330.
171. Amos RJ, Amess JA, Hinds CJ, Mollin DL. Incidence and pathogenesis of acute megaloblastic bone-marrow change in patients receiving intensive care. *Lancet*. 1982;2:835–838.
172. Sesso RM, Iunes Y, Melo AC. Myeloneuropathy following nitrous oxide anaesthesia in a patient with macrocytic anaemia. *Neuroradiology*. 1999;41:588–590.
173. Hadzic A, Glab K, Sanborn KV, Thys DM. Severe neurologic deficit after nitrous oxide anesthesia. *Anesthesiology*. 1995;83:863–866.
174. McNeely JK, Buczulinski B, Rosner DR. Severe neurological impairment in an infant after nitrous oxide anesthesia. *Anesthesiology*. 2000;93:1549–1550.
175. Iliniczky S, Jelencsik I, Kenez J, Szirmai I. MR findings in subacute combined degeneration of the spinal cord caused by nitrous oxide anaesthesia—two cases. *Eur J Neurol*. 2002;9:101–104.
176. Selzer RR, Rosenblatt DS, Laxova R, Hogan K. Adverse effect of nitrous oxide in a child with 5,10-methylenetetrahydrofolate reductase deficiency. *N Engl J Med*. 2003;349:45–50.
177. McCully KS. Vascular pathology of homocysteine: implications for the pathogenesis of arteriosclerosis. *Am J Pathol*. 1969;56:111–128.
178. Nygard O, Nordrehaug JE, Refsum H, Ueland PM, Farstad M, Vollset SE. Plasma homocysteine levels and mortality in patients with coronary artery disease. *N Engl J Med*. 1997;337:230–236.
179. Mayer EL, Jacobsen DW, Robinson K. Homocysteine and coronary atherosclerosis. *J Am Coll Cardiol*. 1996;27:517–527.
180. Kaul S, Zadeh AA, Shah PK. Homocysteine hypothesis for atherosclerotic cardiovascular disease: not validated. *J Am Coll Cardiol*. 2006;48:914–923.
181. Ntaios G, Savopoulos C, Grekas D, Hatzitolios A. The controversial role of B-vitamins in cardiovascular risk: an update. *Arch Cardiovasc Dis*. 2009;102:847–854.
182. Badner NH, Beattie WS, Freeman D, Spence JD. Nitrous oxide-induced increased homocysteine concentrations are associated with increased postoperative myocardial ischemia in patients undergoing carotid endarterectomy. *Anesth Analg*. 2000;91:1073–1079.
183. Myles PS, Leslie K, Chan MT, et al. Avoidance of nitrous oxide for patients undergoing major surgery: a randomized controlled trial. *Anesthesiology*. 2007;107:221–231.
184. Leslie K, Myles PS, Chan MT, et al. Nitrous oxide and long-term morbidity and mortality in the ENIGMA trial. *Anesth Analg*. 2011;112:387–393.
185. Myles PS, Leslie K, Chan MT, et al. The safety of addition of nitrous oxide to general anaesthesia in at-risk patients having major non-cardiac surgery (ENIGMA-II): a randomised, single-blind trial. *Lancet*. 2014;384:1446–1454.
186. Leslie K, Myles P, Devereaux PJ, et al. Nitrous oxide and serious morbidity and mortality in the POISE trial. *Anesth Analg*. 2013.
187. Indraratna P, Alexopoulos C, Celermajer D, Alford K. Acute ST-elevation myocardial infarction, a unique complication of recreational nitrous oxide use. *Heart Lung Circ*. 2017;26:e41–e43.
188. Nagele P, Zeugswetter B, Wiener C, et al. Influence of methylenetetrahydrofolate reductase gene polymorphisms on homocysteine concentrations after nitrous oxide anesthesia. *Anesthesiology*. 2008;109:36–43.
189. Nagele P, Zeugswetter B, Eberle C, Hupfl M, Mittlbock M, Fodinger M. A common gene variant in methionine synthase reductase is not associated with peak homocysteine concentrations after nitrous oxide anesthesia. *Pharmacogenet Genomics*. 2009;19:325–329.
190. Rao LK, Francis AM, Wilcox U, Miller JP, Nagele P. Pre-operative vitamin B infusion and prevention of nitrous oxide-induced homocysteine increase. *Anesthesia*. 2010;65:710–715.
191. Nunn JF. Clinical aspects of the interaction between nitrous oxide and vitamin B12. *Br J Anaesth*. 1987;59:3–13.
192. Myles PS, Leslie K, Silbert B, Paech MJ, Peyton P. A review of the risks and benefits of nitrous oxide in current anaesthetic practice. *Anaesth Intensive Care*. 2004;32:165–172.
193. Rappaport B, Mellon RD, Simone A, Woodcock J. Defining safe use of anesthesia in children. *N Engl J Med*. 2011;364:1387–1390.
194. Hudson AE, Hemmings HC Jr. Are anaesthetics toxic to the brain? *Br J Anaesth*. 2011;107:30–37.
195. Jevtovic-Todorovic V, Hartman RE, Izumi Y, et al. Early exposure to common anesthetic agents causes widespread neurodegeneration in the developing rat brain and persistent learning deficits. *J Neurosci*. 2003;23:876–882.
196. Loepke AW, Soriano SG. An assessment of the effects of general anesthetics on developing brain structure and neurocognitive function. *Anesth Analg*. 2008;106:1681–1707.
197. Slikker W Jr, Zou X, Hotchkiss CE, et al. Ketamine-induced neuronal cell death in the perinatal rhesus monkey. *Toxicol Sci*. 2007;98:145–158.
198. Zou X, Liu F, Zhang X, et al. Inhalation anesthetic-induced neuronal damage in the developing rhesus monkey. *Neurotoxicol Teratol*. 2011;33:592–597.
199. Brambrink AM, Evers AS, Avidan MS, et al. Isoflurane-induced neuroapoptosis in the neonatal rhesus macaque brain. *Anesthesiology*. 2010;112:834–841.
200. Brambrink AM, Evers AS, Avidan MS, et al. Ketamine-induced neuroapoptosis in the fetal and neonatal rhesus macaque brain. *Anesthesiology*. 2012;116:372–384.

201. Schenning KJ, Noguchi KK, Martin LD, et al. Isoflurane exposure leads to apoptosis of neurons and oligodendrocytes in 20- and 40-day old rhesus macaques. *Neurotoxicol Teratol*. 2017;60:63–68.
202. Gascon E, Klauser P, Kiss JZ, Vutskits L. Potentially toxic effects of anaesthetics on the developing central nervous system. *Eur J Anaesthesiol*. 2007;24:213–224.
203. Mellon RD, Simone AF, Rappaport BA. Use of anesthetic agents in neonates and young children. *Anesth Analg*. 2007;104:509–520.
204. Vutskits L, Davis PJ, Hansen TG. Anesthetics and the developing brain: time for a change in practice? A pro/con debate. *Paediatr Anaesth*. 2012;22:973–980.
205. Graham MR, Brownell M, Chateau DG, Dragan RD, Burchill C, Fransoo RR. Neurodevelopmental assessment in kindergarten in children exposed to general anesthesia before the age of 4 years: a retrospective matched cohort study. *Anesthesiology*. 2016;125:667–677.
206. Glatz P, Sandin RH, Pedersen NL, Bonamy AK, Eriksson LI, Granath F. Association of anesthesia and surgery during childhood with long-term academic performance. *JAMA Pediatr*. 2017;171:e163470.
207. Warner DO, Zaccariello MJ, Katusic SK, et al. Neuropsychological and behavioral outcomes after exposure of young children to procedures requiring general anesthesia: the Mayo Anesthesia Safety in Kids (MASK) study. *Anesthesiology*. 2018.
208. Davidson AJ, Sun LS. Clinical evidence for any effect of anesthesia on the developing brain. *Anesthesiology*. 2018;128:840–853.
209. Schneuer FJ, Bentley JP, Davidson AJ, et al. The impact of general anesthesia on child development and school performance: a population-based study. *Paediatr Anaesth*. 2018.
210. Davidson AJ, Disma N, de Graaff JC, et al. Neurodevelopmental outcome at 2 years of age after general anaesthesia and awake-regional anaesthesia in infancy (GAS): an international multicentre, randomised controlled trial. *Lancet*. 2016;387:239–250.
211. Axelrod D, Bell C, Feldman J, et al. *Greening the Operating Room and Perioperative Arena: Environmental Sustainability for Anesthesia Practice*. American Society of Anesthesiologists; 2014.
212. Ravishankara AR, Daniel JS, Portmann RW. Nitrous oxide (N<sub>2</sub>O): the dominant ozone-depleting substance emitted in the 21st century. *Science*. 2009;326:123–125.
213. Langbein T, Sonntag H, Trapp D, et al. Volatile anaesthetics and the atmosphere: atmospheric lifetimes and atmospheric effects of halothane, enflurane, isoflurane, desflurane and sevoflurane. *Br J Anaesth*. 1999;82:66–73.
214. Ryan SM, Nielsen CJ. Global warming potential of inhaled anaesthetics: application to clinical use. *Anesth Analg*. 2010;111:92–98.
215. *Climate Change 2007: The Physical Science Basis*. New York: Cambridge University Press; 2007.
216. Austin J, Butchart N, Shine KP. Possibility of an arctic ozone hole in a double-CO<sub>2</sub> climate. *Nature*. 1992;360:221–225.
217. Forster P, Ramaswamy V, Artaxo P, et al. In: Solomon S, Qin D, Manning M, eds. *Changes in Atmospheric Constituents and in Radiative Forcing, Climate Change 2007: The Physical Science Basis*. Cambridge: Contribution of Working Group I to the Fourth Assessment Report of the Intergovernmental Panel on Climate Change; 2007.
218. Ryan S, Sherman J. Sustainable anesthesia. *Anesth Analg*. 2012;114:921–923.
219. Ishizawa Y. Special article: general anesthetic gases and the global environment. *Anesth Analg*. 2011;112:213–217.
220. Gutierrez MJF, Baxter D, Hunter C, Svoboda K. Nitrous oxide (N<sub>2</sub>O) emissions from waste and biomass to energy plants. *Waste Manag Res*. 2005;23:133–147.
221. Maskell K, Mintzer IM, Callander BA. Basic science of climate change. *Lancet*. 1993;342:1027–1031.
222. Schmeltekopf AL, Goldan PD, Henderson WR, et al. Measurements of stratospheric CFC13, CF2Cl<sub>2</sub>, and N<sub>2</sub>O. *Geophys Res Lett*. 1975;2:393–396.
223. Sherman SJ, Cullen BF. Nitrous oxide and the greenhouse effect. *Anesthesiology*. 1988;68:816–817.
224. Hammitt JK, Camm F, Connell PS, et al. Future emission scenarios for chemicals that may deplete stratospheric ozone. *Nature*. 1987;330:711–716.
225. Langbein T, Sonntag H, Trapp D, et al. Volatile anaesthetics and the atmosphere: atmospheric lifetimes and atmospheric effects of halothane, enflurane, isoflurane, desflurane and sevoflurane. *Br J Anaesth*. 1999;82:66–73.
226. Brown AC, Canosa-Mas CE, Parr AD, Pierce JM, Wayne RP. Tropospheric lifetimes of halogenated anaesthetics. *Nature*. 1989;341:635–637.
227. Executive Summary. *Scientific Assessment of Ozone Depletion: 2002*. Geneva: World Meteorological Organization; 2002. Global Ozone Research and Monitoring Project Report No. 47.
228. Barwise JA, Lancaster LJ, Michaels D, Pope JE, Berry JM. Technical communication: an initial evaluation of a novel anesthetic scavenging interface. *Anesth Analg*. 2011;113:1064–1067.
229. McGregor DG. Occupational exposure to trace concentrations of waste anesthetic gases. *Mayo Clin Proc*. 2000;75:273–277.
230. Burn AG. Occupational hazards of inhalational anaesthetics. *Best Pract Res Clin Anaesthesiol*. 2003;17:147–161.
231. Vieira E, Cleaton-Jones P, Austin JC, Moyes DG, Shaw R. Effects of low concentrations of nitrous oxide on rat fetuses. *Anesth Analg*. 1980;59:175–177.
232. Fujinaga M, Mazze RI, Baden JM, Fintel AG, Shepard TH. Rat whole embryo culture: an in vitro model for testing nitrous oxide teratogenicity. *Anesthesiology*. 1988;69:401–404.
233. Yilmaz S, Calbayram NC. Exposure to anesthetic gases among operating room personnel and risk of genotoxicity: a systematic review of the human biomonitoring studies. *J Clin Anesth*. 2016;35:326–331.
234. Spence AA. Environmental pollution by inhalation anaesthetics. *Br J Anaesth*. 1987;59:96–103.
235. Szyfter K, Szulc R, Mikstacki A, Stachecki I, Rydzanicz M, Jaloszynski P. Genotoxicity of inhalation anaesthetics: DNA lesions generated by sevoflurane in vitro and in vivo. *J Appl Genet*. 2004;45:369–374.
236. Friedman JM. Teratogen update: anesthetic agents. *Teratology*. 1988;37:69–77.
237. Kuczkowski KM. Nonobstetric surgery during pregnancy: what are the risks of anesthesia? *Obstet Gynecol Surv*. 2004;59:52–56.
238. Reitman E, Flood P. Anaesthetic considerations for non-obstetric surgery during pregnancy. *Br J Anaesth*. 2011;107(suppl 1):i72–i78.
239. Sessler DI, Badgwell JM. Exposure of postoperative nurses to exhaled anesthetic gases. *Anesth Analg*. 1998;87:1083–1088.
240. McGregor DG, Senjem DH, Mazze RI. Trace nitrous oxide levels in the postanesthesia care unit. *Anesth Analg*. 1999;89:472–475.
241. Krenzischek DA, Schaefer J, Nolan M, et al. Phase I collaborative pilot study: waste anesthetic gas levels in the PACU. *J Perianesth Nurs*. 2002;17:227–239.
242. Cullen SC, Gross EG. The anesthetic properties of xenon in animals and human beings, with additional observations on krypton. *Science*. 1951;113:580–582.
243. Preckel B, Weber NC, Sanders RD, Maze M, Schlack W. Molecular mechanisms transducing the anesthetic, analgesic, and organ-protective actions of xenon. *Anesthesiology*. 2006;105:187–197.
244. Sanders RD, Franks NP, Maze M. Xenon: no stranger to anaesthesia. *Br J Anaesth*. 2003;91:709–717.
245. Sanders RD, Maze M. Xenon: from stranger to guardian. *Curr Opin Anaesthesiol*. 2005;18:405–411.
246. Goto T, Saito H, Shinkai M, Nakata Y, Ichinose F, Morita S. Xenon provides faster emergence from anesthesia than does nitrous oxide-sevoflurane or nitrous oxide-isoflurane. *Anesthesiology*. 1997;86:1273–1278.
247. Rossaint R, Reyle-Hahn M, Schulte Am Esch J, et al. Multicenter randomized comparison of the efficacy and safety of xenon and isoflurane in patients undergoing elective surgery. *Anesthesiology*. 2003;98:6–13.
248. Law LS, Lo EA, Gan TJ. Xenon anesthesia: a systematic review and meta-analysis of randomized controlled trials. *Anesth Analg*. 2016;122:678–697.
249. Goto T, Hanne P, Ishiguro Y, Ichinose F, Niimi Y, Morita S. Cardiovascular effects of xenon and nitrous oxide in patients during fentanyl-midazolam anaesthesia. *Anaesthesia*. 2004;59:1178–1183.
250. Wappler F, Rossaint R, Baumert J, et al. Multicenter randomized comparison of xenon and isoflurane on left ventricular function in patients undergoing elective surgery. *Anesthesiology*. 2007;106:463–471.
251. Baumert JH, Hein M, Hecker KE, Satlow S, Neef P, Rossaint R. Xenon or propofol anaesthesia for patients at cardiovascular risk in non-cardiac surgery. *Br J Anaesth*. 2008;100:605–611.

252. Lachmann B, Armbruster S, Schairer W, et al. Safety and efficacy of xenon in routine use as an inhalational anaesthetic. *Lancet*. 1990;335:1413–1415.
253. Wappler F. Anesthesia for patients with a history of malignant hyperthermia. *Curr Opin Anaesthesiol*. 2010;23:417–422.
254. Al Tmimi L, Devroe S, Dewinter G, et al. Xenon as an adjuvant to propofol anesthesia in patients undergoing off-pump coronary artery bypass graft surgery: a pragmatic randomized controlled clinical trial. *Anesth Analg*. 2017;125:1118–1128.
255. Al Tmimi L, Van de Velde M, Herijgers P, et al. Xenon for the prevention of postoperative delirium in cardiac surgery: study protocol for a randomized controlled clinical trial. *Trials*. 2015;16:449.
256. Hofland J, Ouattara A, Fellahi JL, et al. Effect of xenon anesthesia compared to sevoflurane and total intravenous anesthesia for coronary artery bypass graft surgery on postoperative cardiac troponin release: an international, multicenter, phase 3, single-blinded, randomized noninferiority trial. *Anesthesiology*. 2017;127:918–933.
257. Stevanovic A, Schaefer P, Coburn M, et al. Renal function following xenon anesthesia for partial nephrectomy—an explorative analysis of a randomized controlled study. *PLoS One*. 2017;12:e0181022.
258. Arola O, Saraste A, Laitio R, et al. Inhaled xenon attenuates myocardial damage in comatose survivors of out-of-hospital cardiac arrest: the xe-hypotheca trial. *J Am Coll Cardiol*. 2017;70:2652–2660.
259. Laitio R, Hynninen M, Arola O, et al. Effect of inhaled xenon on cerebral white matter damage in comatose survivors of out-of-hospital cardiac arrest: a randomized clinical trial. *JAMA*. 2016;315:1120–1128.
260. Coburn M, Baumert JH, Roertgen D, et al. Emergence and early cognitive function in the elderly after xenon or desflurane anaesthesia: a double-blinded randomized controlled trial. *Br J Anaesth*. 2007;98:756–762.
261. Coburn M, Kunitz O, Baumert JH, Hecker K, Rossaint R. Patients' self-evaluation after 4–12 weeks following xenon or propofol anaesthesia: a comparison. *Eur J Anaesthesiol*. 2005;22:870–874.
262. Coburn M, Sanders RD, Maze M, et al. The hip fracture surgery in elderly patients (HIPELD) study to evaluate xenon anaesthesia for the prevention of postoperative delirium: a multicentre, randomized clinical trial. *Br J Anaesth*. 2018;120:127–137.
263. Nakata Y, Goto T, Niimi Y, Morita S. Cost analysis of xenon anesthesia: a comparison with nitrous oxide-isoflurane and nitrous oxide-sevoflurane anesthesia. *J Clin Anesth*. 1999;11:477–481.
264. Rawat S, Dingley J. Closed-circuit xenon delivery using a standard anesthesia workstation. *Anesth Analg*. 2010;110:101–109.
265. Dingley J, Findlay GP, Foex BA, Mecklenburgh J, Esmail M, Little RA. A closed xenon anesthesia delivery system. *Anesthesiology*. 2001;94:173–176.
266. Dingley J, Mason RS. A cryogenic machine for selective recovery of xenon from breathing system waste gases. *Anesth Analg*. 2007;105:1312–1318; table of contents.
267. Zhang P, Ohara A, Mashimo T, Imanaka H, Uchiyama A, Yoshiya I. Pulmonary resistance in dogs: a comparison of xenon with nitrous oxide. *Can J Anaesth*. 1995;42:547–553.
268. Lockwood G. Expansion of air bubbles in aqueous solutions of nitrous oxide or xenon. *Br J Anaesth*. 2002;89:282–286.
269. Coburn M, Kunitz O, Apfel CC, Hein M, Fries M, Rossaint R. Incidence of postoperative nausea and emetic episodes after xenon anaesthesia compared with propofol-based anaesthesia. *Br J Anaesth*. 2008;100:787–791.
270. Fahlenkamp AV, Stoppe C, Cremer J, et al. Nausea and vomiting following balanced xenon anesthesia compared to sevoflurane: a post-hoc explorative analysis of a randomized controlled trial. *PLoS One*. 2016;11:e0153807.
271. Dickinson R, Franks NP. Bench-to-bedside review: molecular pharmacology and clinical use of inert gases in anesthesia and neuroprotection. *Crit Care*. 2010;14:229.

OLEG V. EVGENOV, YAFEN LIANG, YANDONG JIANG, and JAMES L. BLAIR

## KEY POINTS

- Inhaled anesthetics affect every part of physiology of the lungs and their pulmonary pharmacology is complex.
- Volatile anesthetics produce bronchodilation through decreases in cytoplasmic ionized calcium concentration and/or a reduction in calcium sensitivity of airway smooth muscle. Volatile anesthetics also attenuate an increase in pulmonary airway resistance induced by chemical and mechanical stimulation.
- Inhaled anesthetics reduce the rate of mucous clearance and affect function of type II alveolar cells; these effects can potentially contribute to postoperative pulmonary complications.
- Volatile anesthetics produce a biphasic response in pulmonary vascular smooth muscle. Although inhibition of hypoxic pulmonary vasoconstriction by volatile anesthetic is an overall small effect, it can contribute to worsening of hypoxemia in patients with underlying pulmonary disease.
- Volatile anesthetics depress respiratory function through a diminished respiratory drive and an increase in upper airway collapsibility. Following extubation, even at residual concentrations, volatile anesthetics can severely impair peripheral chemoreceptor inputs and hypoxic arousal reflexes.
- Volatile anesthetics produce dose-dependent reductions in tidal volume and minute ventilation, cause tachypnea, and blunt ventilatory response to hypercapnia and hypoxia.
- During anesthesia with volatile agents, diaphragmatic function remains relatively well preserved, whereas inspiratory rib cage muscles are significantly depressed resulting in insufficiency of breathing or paradoxical breathing.
- Volatile anesthetics can compromise upper airway patency. Even at low concentrations, upper airway obstruction can occur in susceptible patients, including elderly, obese, or critically ill patients.
- Volatile anesthetics vary in their ability to irritate airways and augment defensive airway reflexes. Sevoflurane causes the least amount of subjective airway irritation and is the anesthetic of choice for inhaled induction of anesthesia in infants and children.
- Preclinical and clinical evidence suggests therapeutic potential of isoflurane and sevoflurane in acute lung injury.
- Although concerns have been recently raised regarding the use of nitrous oxide, a lack of strong evidence does not justify abandoning it from clinical practice, especially considering its favorable cost-effectiveness.
- Xenon produces a fast on and off action and is a promising alternative for sedation in the critical care setting.

## Introduction

Pulmonary pharmacology of inhaled anesthetics is complex. This chapter focuses in depth on pulmonary pharmacology of isoflurane, sevoflurane, desflurane, nitrous oxide, and xenon. The older anesthetics (including halothane, enflurane, and ether) are no longer in use in the developed countries, and are discussed here only for comparison. The lungs are unique in their exposure to a wide variety of physical forces including ventilation, blood flow, and surface tension as well as derangements of function caused by disease and environmental factors. The effects of inhaled anesthetics on ventilatory control, airway tone, mucociliary function, surfactant production, pulmonary vascular

resistance (PVR), and acute lung injury (ALI) are examined in detail in this chapter.

The physical properties of commonly used inhalational anesthetics and clinical concerns are presented in [Table 21.1](#).

## Inhaled Anesthetics

### ASTHMA AND BRONCHOSPASM OVERVIEW

Asthma is a chronic airway disease with an estimated worldwide annual death rate of 250,000. Asymptomatic asthma patients have relatively infrequent perioperative respiratory complications; however, bronchospasm

**TABLE 21.1** The Physical Properties of Commonly Used Inhalational Anesthetics and Their Clinical Concerns

Property	Halothane	Isoflurane	Sevoflurane	Desflurane	Nitrous oxide	Xenon
Boiling point (°C)	50.2	49	59	24	-88	-108
Vapor pressure (mm Hg) at 20°C	241	238	157	669	38,770	-
Blood:gas partition coefficient	2.5	1.46	0.65	0.42	0.46	0.115
Oil:gas partition coefficient	224	91	47	19	1.4	1.9
Minimal alveolar concentration (MAC)	0.74	1.17	1.8	6.6	104	63-71
Metabolized in the body (%)	25	0.2	2-4	0.02	0	0
Clinical concerns	Hepatotoxicity		Compound A	Airway irritation	Gas expansion	Apnea

develops in about 9% of asthmatics in the perioperative period.<sup>1</sup> Twenty-five percent of asthmatics may present with wheezing after induction of anesthesia,<sup>2</sup> and 1.7% of asthma patients sustain a poor respiratory outcome.<sup>3</sup> In addition, acute bronchospasm can occur at induction, intubation, or during maintenance of anesthesia without prior history of asthma or COPD. According to the ASA Closed Claims Project<sup>4</sup> 40 cases of bronchospasm resulted in settled malpractice claims, with 88% involving brain damage or death. Importantly, only half of the patients had preexisting asthma or COPD. Adverse respiratory events accounted for 28% of claims related to anesthesia-related brain damage and death in the United States; they were associated with the highest mean cost per closed claim. In France, 7% of anesthesia-related deaths were also attributed to bronchospasm.<sup>5</sup> A nonallergic mechanism was involved in nearly 80% of cases. Although bronchospasm caused by airway irritation occurred more frequently in patients who had one or more predisposing factors including asthma, heavy tobacco smoking, or bronchitis, only 50% and 60% of patients with nonallergic and allergic bronchospasm, respectively, had history of asthma.

## PHYSIOLOGY OF BRONCHIAL SMOOTH MUSCLE

Airway resistance is increased, at least in part, by an increase in bronchiolar smooth muscle (BSM) tone. BSM extends down to the terminal bronchioles and is controlled primarily by autonomic nervous system activity. Nonadrenergic, noncholinergic mechanisms, activated by the stimulation of the afferent bronchopulmonary sensory C fibers, play a role in BSM constriction to tachykinins, vasoactive intestinal peptide (VIP), adenosine, and calcitonin gene-related peptides.

Asthmatic bronchiolar constriction involves complex interactions of airway nerves, smooth muscle, epithelium, and inflammatory cells. In contrast, reflex bronchoconstriction caused by airway irritation is mediated by sensory afferents in the nucleus of the solitary tract (NTS), projecting to vagal preganglionic neurons (VPN). Glutamate modulates stimulation of NTS and VPN, whereas  $\gamma$  aminobutyric acid (GABA) is inhibitory from NTS projecting to VPN. VPN projections to the airways release acetylcholine (ACh) predominantly onto M3 receptors, inducing bronchoconstriction. Baseline airway tone is also mediated by the vagus nerve. The muscarinic acetylcholine receptors (mAChRs, M1-M5) on BSM are G protein-coupled receptors, three

of which (M1, M2, and M3) are expressed in the lungs of humans and of most mammals.<sup>6</sup> Belmonte and colleagues<sup>7</sup> reviewed the essentials of muscarinic control of mAChRs in the lungs. Neuronal inhibitory M2 muscarinic ACh receptors on parasympathetic nerves are responsible for limiting ACh release from these nerves (Fig. 21.1).

## ROLE OF CALCIUM

Alterations in cytoplasmic ionized calcium concentration ( $[\text{Ca}^{2+}]$ ) and calcium ( $\text{Ca}^{2+}$ ) influx result from the interplay of cyclic nucleotides in BSM that alters myosin light chain (MLC) and MLC kinase activity.  $\text{Ca}^{2+}$ /calmodulin-dependent MLC kinase is critical for tonic smooth muscle contraction.<sup>8</sup> Agonist activation of BSM also involves a second messenger, cADP ribose, resulting in inositol triphosphate ( $\text{IP}_3$ )-mediated release of  $\text{Ca}^{2+}$  from sarcoplasmic reticulum via activated ryanodine channels.<sup>9</sup> This release is followed by an increase in sodium ( $\text{Na}^+$ ) influx across the cell membrane. This localized increase in  $\text{Na}^+$  may switch the  $\text{Na}^+/\text{Ca}^{2+}$  exchanger into reverse mode, leading to even more  $\text{Ca}^{2+}$  influx and greater bronchial constriction. Several different cyclic adenosine monophosphate (cAMP) signaling compartments exist in airway smooth muscle that are responsive to different hormones and neurotransmitters.<sup>10</sup> The mechanical stretch of human BSM cells also causes contraction via an influx of  $\text{Ca}^{2+}$  through unique stretch-activated nonselective cation channels.<sup>11</sup> Adenosine indirectly enhances contraction of airway smooth muscle via the activation of mast cells and via nerves by directly stimulating adenosine type I receptors on airway smooth muscle, thereby rapidly mobilizing  $[\text{Ca}^{2+}]$  stores through G proteins and  $\text{IP}_3$  signaling. Agonist-induced stimulation of *particulate guanylyl cyclase* relaxes bronchial smooth muscle by attenuating inward  $\text{Ca}^{2+}$  current, whereas stimulation of *soluble guanylyl cyclase* by substances such as nitric oxide (NO) reduces  $[\text{Ca}^{2+}]$  concentration and  $\text{Ca}^{2+}$  sensitivity.<sup>12</sup>

## HISTAMINE

Release of histamine in the airway produces reflex bronchoconstriction from actions on H1 receptors on BSM, eliciting activation of phospholipase C and protein kinase C (PKC) downstream mediators, leading to release of  $\text{Ca}^{2+}$  from intracellular stores. This leads to calcium ion entry through calcium channels, cation channels of the transient receptor potential (TRP1) channel type, and stimulation of a  $\text{Na}^+$ /

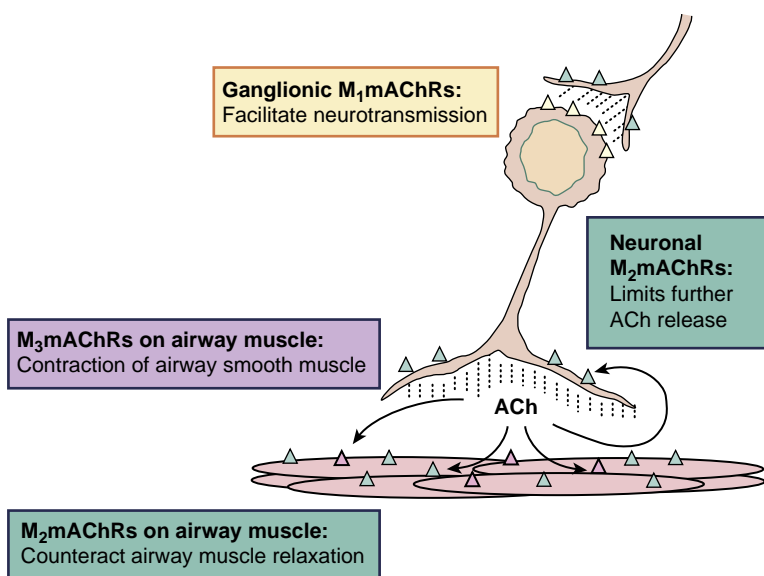


**Fig. 21.1 Muscarinic acetylcholine receptors (mAChRs) on pulmonary parasympathetic nerves (PSN) and airway smooth muscle (ASM).** Acetylcholine (ACh) released by PSN stimulates M<sub>2</sub> mAChRs on ASM resulting in contraction. M<sub>2</sub> mAChRs on ASM facilitate M<sub>3</sub> mAChR-mediated contraction by counteracting the cyclic adenosine monophosphate relaxant pathway. Release of ACh by nerves is tightly controlled by M<sub>2</sub> mAChRs found on PSN endings. M<sub>1</sub> mAChRs found within parasympathetic ganglia are thought to facilitate cholinergic neurotransmission that is mediated primarily by nicotinic Ach receptors.<sup>7</sup> (Redrawn from Belmonte KE. Cholinergic pathways in the lungs and anticholinergic therapy for chronic obstructive pulmonary disease. *Proc Am Thorac Soc*. 2005;2(4):297–304. Used with permission.)

$\text{Ca}^{2+}$  exchanger. Nicotinic acid adenine dinucleotide phosphate has also been suggested as a potential second messenger in histamine-induced  $\text{Ca}^{2+}$  release from lysosome-like acidic compartments, functionally coupled to the endoplasmic reticulum via H1 receptor in endothelial cells.<sup>13</sup> This increase in bronchomotor tone is attenuated by the cholinergic antagonist atropine. The histamine-degrading enzyme, histamine N-methyltransferase, has been localized to human airway epithelium and may play a protective role against histamine-mediated bronchoconstriction.<sup>14</sup> Histamine-induced bronchoconstriction, measured as altered pulmonary resistance (RL) and dynamic pulmonary compliance ( $C_{\text{dyn}}$ ) in response to intravenous (IV) histamine was studied in dogs to determine the bronchodilatory effects of halothane, sevoflurane, isoflurane, and enflurane. All the volatile anesthetics demonstrated an inhibitory effect on increases in RL and decreases in  $C_{\text{dyn}}$  caused by histamine.<sup>15</sup>

## ADRENERGIC RECEPTORS

Adrenergic receptors in BSM are classified into  $\alpha$  and  $\beta_2$  types. The  $\alpha_2$  agonists clonidine and dexmedetomidine have been shown to produce bronchodilation in central airways,<sup>16</sup> which may be mediated through  $\alpha_2$  central vagolytic effects. Clinically, the  $\beta_2$ -receptor subtypes play an important role in BSM responsiveness. Stimulation of  $\beta_2$  adrenoceptors causes cAMP-mediated relaxation via activation of protein kinase A and subsequent  $\text{Ca}^{2+}$  efflux out of the cell and into the SR. Interestingly, asthma, as well as allergy- and methacholine-induced bronchospasm, do not appear to be genetically linked to a dominant  $\beta_2$  adrenoceptor gene.<sup>17</sup>

Respiratory epithelium releases substances that modulate BSM tone. Removal of the epithelium enhances contractile responses to ACh, histamine, or serotonin in large airways and decreases relaxation responses to isoproterenol in small

airways. These responses are similar to the effect of endothelial damage on vascular smooth muscle tone. Notably, cardiopulmonary bypass does significantly affect porcine bronchiolar epithelium-mediated bronchomotor activity, in contrast to vascular endothelium-mediated smooth muscle dysfunction.<sup>18</sup> While endogenous epithelial factors have been identified, endogenous NO produced in respiratory epithelium likely plays a bronchodilatory role similar to that of vascular endothelium. Endothelin-1 is a potent constrictor of vascular smooth muscle and BSM that activates the IP<sub>3</sub> pathway and produces greater pulmonary effects compared to the systemic circulation.<sup>19</sup> Clinically, evaluation of the effects of the inhalational agents may be framed against a background of the major physiologic mechanisms governing normal and pathophysiologic BSM activity. These include airway disease (asthma and COPD), the overarching complex chemistry of calcium release as the BSM stimulus-contraction coupler, intrinsic factors (afferent and efferent ACh signaling,  $\alpha_2$  receptor signaling, NO and endothelin-1, allergy and histamine release), and extrinsic factors (physical and chemical irritants, e.g., endotracheal tubes), capable of promoting reflex bronchoconstriction.

## Effects of Inhaled Anesthetics

In general, all volatile anesthetics are bronchodilators, making them a good choice for patients with increased airway resistance. Using computed tomography (CT), Brown and colleagues demonstrated that halothane causes dose-dependent bronchodilation in a dog (Fig. 21.2).<sup>20</sup>

Eliminating indirect effects of arterial carbon dioxide ( $\text{CO}_2$ ) tension is important when examining the actions of volatile anesthetics on bronchial tone, especially during spontaneous ventilation. This is because hypercapnia-induced bronchodilation and hypocapnia-induced bronchoconstriction are both attenuated by isoflurane.<sup>21</sup> Thus a concentration-dependent bronchodilator effect

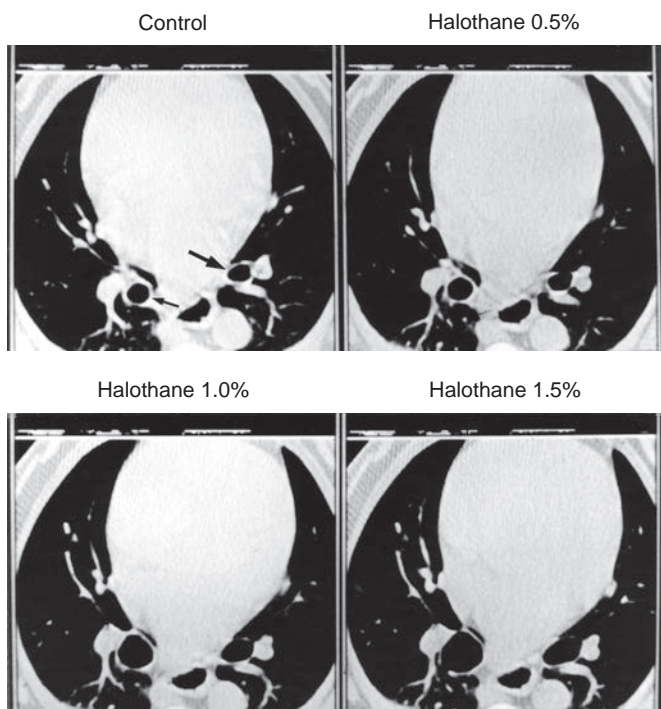


**Fig. 21.2 High-resolution computed tomography scans from one dog.** Upper left: Control. Upper right: During 0.5% halothane. Lower left: During 1.0% halothane. Lower right: During 1.5% halothane. Note the progressive dilation of the airways as indicated by the arrows. (Reproduced from Brown RH, Mitzner W, Zerhouni E, et al. Direct *in vivo* visualization of bronchodilation induced by inhalational anesthesia using high-resolution computed tomography. *Anesthesiology*. 1993;78:295. Used with permission.)

of volatile anesthetics may be indirectly attributable to increase in  $\text{CO}_2$  tension. The structure of the respiratory epithelium changes from pseudostratified columnar cells of the large airways to thinner, cuboidal cells of the bronchioles, and thus a relatively large amount of histologic heterogeneity exists between these regions. The specific effects of volatile anesthetics on the bronchioles depend on the location in and the structure of the respiratory tree. *In vitro*, isoflurane preferentially relaxes the bronchioles rather than the bronchi.<sup>22</sup> Isoflurane and halothane dilate fourth order bronchi at equivalent minimum alveolar concentration (MAC) values.<sup>23</sup> Similarly, at up to 1 MAC, isoflurane, sevoflurane, and desflurane attenuate methacholine-induced bronchoconstriction in open-chest, pentobarbital-anesthetized rats.<sup>24</sup> Isoflurane and sevoflurane also appear to have greater inhibitory effects on bronchial contraction as compared with tracheal smooth muscle contraction.<sup>25</sup> Furthermore, halothane, desflurane, and isoflurane relax distal airways (e.g., bronchioles) to a greater extent than proximal airways (e.g., bronchi).<sup>26</sup> These differential effects appear to be related to the type of voltage-dependent  $\text{Ca}^{2+}$  (VDC) channels that are present in these regions.

Inhalation of 1 or 2 MAC halothane, enflurane, sevoflurane, and isoflurane did not alter baseline pulmonary resistance and dynamic pulmonary compliance, but these anesthetics significantly attenuated increases in airway resistance and decreases in dynamic respiratory compliance in response to intravenous histamine. Halothane was the most effective bronchodilator, whereas responses to

isoflurane, enflurane, and sevoflurane were similar.<sup>15</sup> In an isolated lung model, desflurane produced bronchodilation at 1 MAC but increased airway resistance at 2 MAC,<sup>27</sup> presumably resulting in part from significant increases in inspired gas density at higher MAC. Isoflurane, sevoflurane, and desflurane at 1.0, 1.5, and 2.0 MAC in 25%  $\text{O}_2$  were all examined in a two-chamber test lung model with fixed resistance. All anesthetics demonstrated increased density and calculated resistance at higher MAC, with desflurane producing the highest increase in resistance at 2.0 MAC.<sup>28</sup> In a randomized clinical trial evaluating the same agents at 1.0 and 1.5 MAC, total inspiratory resistance ( $R[\text{rs}]$ ), minimal resistance ( $R[\text{min}]$ ), and effective resistance ( $D[\text{Rrs}]$ ) were calculated using the end-inspiratory occlusion technique. No significant differences of those parameters were observed during administration of the three agents at 1 MAC for 30 min. At 1.5 MAC, desflurane caused a maximum increase in  $R(\text{rs})$  by 26% and in  $R(\text{min})$  by 30% above baseline, in contrast to isoflurane and sevoflurane, which did not have a significant effect on  $R(\text{rs})$  and  $R(\text{min})$ .<sup>29</sup> Presumably, this increased resistance is due at least in part to the greater net viscosity of the higher absolute concentration of desflurane at 1.5 MAC. Other factors may also cause the reduction in the bronchodilation of desflurane at higher concentrations, especially in smokers.<sup>30</sup> Halothane, enflurane, and sevoflurane are equivalent at dilating third- or fourth-generation bronchi as directly measured with a fiberoptic bronchoscope *in vivo*.<sup>31</sup>

It appears that desflurane can both augment or inhibit bronchoconstriction (see below). At 1 MAC desflurane and sevoflurane blocked, to a similar degree, the increase in central airway resistance after a cholinergic challenge in rabbits. Both anesthetics reduced basal bronchial tone by 30% to 40%. This effect was consistently observed in the presence or absence of allergic airway inflammation and bronchial hyperresponsiveness.<sup>32</sup> When the mechanism of constriction is centrally mediated, such as with a cholinergic challenge,<sup>22,24,33,34</sup> desflurane appears to play a beneficial role in attenuating bronchoconstriction. However, when the mechanism of airway constriction is due to non-adrenergic, noncholinergic activation with tachykinins, desflurane may augment and worsen constriction.<sup>35,36</sup> Thus clinicians tend to avoid using desflurane in patients with reactive airway disease.

## EFFECTS OF INHALED ANESTHETICS ON BRONCHOMOTOR TONE IN HUMANS AND THE WORK OF BREATHING

Sevoflurane (1 MAC) reduced respiratory system resistance by 15% in patients undergoing elective surgery, whereas desflurane had no effect.<sup>30</sup> Rooke and associates<sup>37</sup> compared the bronchodilating effects of halothane, isoflurane, sevoflurane, desflurane, and thiopental–nitrous oxide in healthy patients undergoing induction of anesthesia and tracheal intubation. In contrast to thiopental–nitrous oxide, all volatile agents with the exception of desflurane significantly reduced respiratory resistance (Fig. 21.3).

The work of breathing is defined as pressure or force multiplied by the tidal volume during inspiration. Respiratory work is further divided into elastic work (required to overcome the recoil of the lung) and resistive work (required to

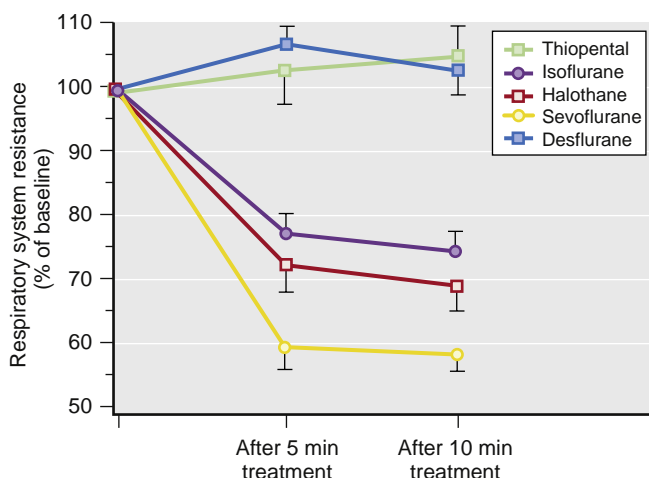


**Fig. 21.3** Percent change in respiratory system resistance in patients after 5 and 10 minutes of maintenance anesthesia with either 0.25 mg/kg/min thiopental plus 50% nitrous oxide or 1.1 minimum alveolar concentration (MAC) sevoflurane, halothane, or isoflurane, or approximately 1 MAC desflurane. All volatile anesthetics except desflurane decreased resistance. Sevoflurane decreased resistance more than isoflurane. (Modified from Rooke GA, Choi JH, Bishop MJ. The effect of isoflurane, halothane, sevoflurane, and thiopental/nitrous oxide on respiratory system resistance after tracheal intubation. *Anesthesiology*. 1997;86:1294; and Goff MJ, Arain SR, Ficke DJ, et al. Absence of bronchodilation during desflurane anesthesia: a comparison to sevoflurane and thiopental. *Anesthesiology*. 2000;93:404. Used with permission.)

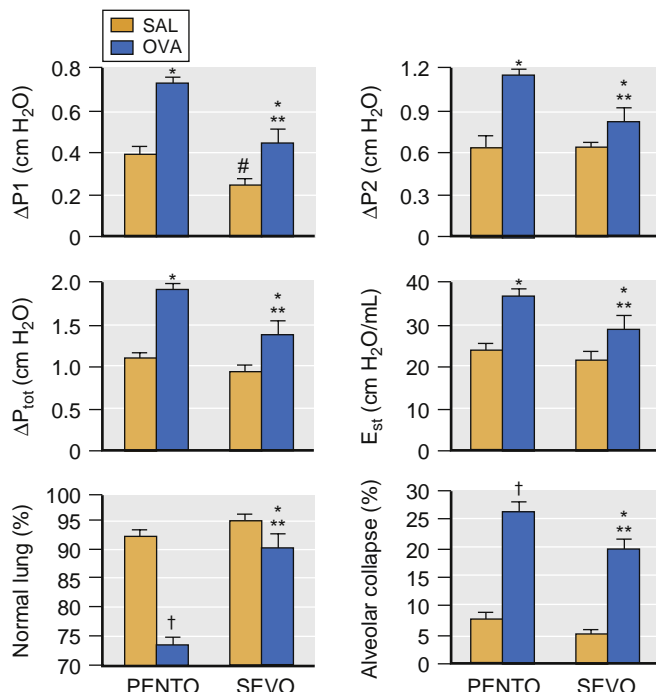


**Fig. 21.4** Mean ± standard error of the mean for pressure to overcome airway resistance ( $\Delta P_1$ ), viscoelastic lung properties ( $\Delta P_2$ ), total of  $\Delta P_1$  and  $\Delta P_2$  ( $\Delta P_{tot}$ ), and static lung elastance ( $E_{st}$ ). Also shown are the percent of normal area and the percent of alveolar collapse in mice repeatedly challenged with intratracheal instillation of saline (SAL) or ovalbumin (OVA). Animals were anesthetized with pentobarbital sodium (PENTO) or sevoflurane (SEVO), 1 minimum alveolar concentration (MAC). \* $P < .05$  versus corresponding SAL group; \*\* $P < .001$  versus OVA-PENTO group; † $P < .05$  versus SAL-PENTO group; † $P < .01$  versus the SAL-PENTO group. (Modified from Burbaran SM, Xisto DG, Ferreira HC, et al. Lung mechanics and histology during sevoflurane anesthesia in a model of chronic allergic rhinitis. *Anesth Analg*. 2007;104:631. Used with permission.)

to overcome airway flow resistance and viscoelastic resistance of pulmonary tissues). The work of breathing is usually derived from transpulmonary pressure volume curves. Volatile anesthetics increase the work of breathing in adults and children. In rats, sevoflurane reduced pulmonary compliance at the lung periphery rather than at the airway level, thereby increasing viscoelastic and elastic pressures in the lung.<sup>38</sup> In addition, in a murine model of chronic asthma, sevoflurane significantly decreased resistance in central and distal airways and also lowered resistance in the lung periphery. These data suggest that sevoflurane exerts a beneficial effect in the presence of chronic airway obstruction and indicate that sevoflurane might reduce the work of breathing in comparison to other drugs (Fig. 21.4).<sup>39</sup>

Studies in humans demonstrate a ceiling effect where low concentrations of volatile anesthetics significantly reduce *upper airway resistance*, reflecting changes in airway smooth muscle tone in the major airways. In contrast, distal airways and lung parenchyma lack a smooth muscle component (with *lower airway and alveolar resistance* being more a measure of viscoelastic changes in the lung). Increasing concentrations of inhalational agents have diminished effect on these more distal pulmonary components and thus do not further reduce total lung resistance (Fig. 21.5).<sup>40</sup>

Expiration is passively affected by the recoil characteristics of the lung during normal breathing. In anesthetized patients, the ventilatory response to expiratory resistance is reduced to a greater extent than the response to inspiratory resistance. Conscious and anesthetized humans exhibit decreases in respiratory rate when expiratory resistive loads are applied, but only anesthetized subjects develop rib cage–abdominal wall motion dyssynchrony that causes less effective ventilation and reduction in minute alveolar ventilation. This concept may be particularly important in spontaneously breathing anesthetized patients who demonstrate expiratory obstruction, such as in cases of asthma, COPD, airway secretions, or during hypopharyngeal obstruction or partial breathing circuit occlusion.

Experimental studies demonstrating the equal potency of sevoflurane and isoflurane and the higher potency of halothane for bronchodilation must be extrapolated with caution because histamine-mediated experimental bronchospasm may not closely mimic tracheal intubation-induced bronchospasm in humans. Indeed, Arakawa and colleagues<sup>41</sup> showed that similar inspired concentrations of halothane, isoflurane, and sevoflurane produced nearly identical reductions in airway resistance in a patient with *status asthmaticus*. Volatile anesthetics may thus be an effective therapeutic modality in *status asthmaticus* when conventional therapy has failed.<sup>42,43</sup>

$\beta$ -Adrenoceptor agonists may be beneficial for treating acute bronchospasm in patients anesthetized with halothane,<sup>44,45</sup> but their use may not be beneficial with other volatile anesthetics. For example, the  $\beta_2$ -adrenergic agonist fenoterol reduced respiratory system resistance after endotracheal intubation but did not further decrease resistance when administered in the presence of 1.3% isoflurane.<sup>46</sup> These findings should be interpreted with caution because the technique used to determine respiratory system resistance incorporates alterations in lung and chest wall resistance, as well as tissue viscosity. The most important functional change that occurs in the presence of lung disease is increased resistance. Resistance to airflow is

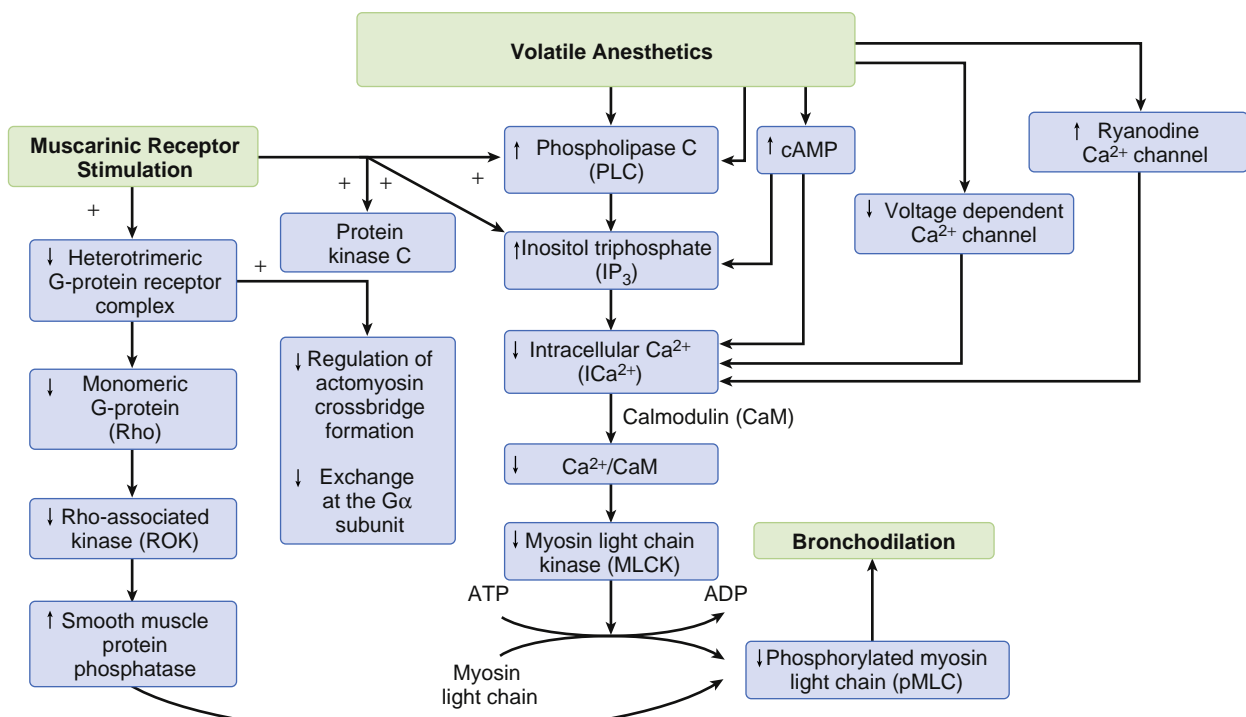


**Fig. 21.5** Isoflurane (ISO) at 0.6% reduced respiratory system elastance (E in  $\text{cm H}_2\text{O/L}$ ) and resistance (R in  $\text{cm H}_2\text{O/L/s}$ ). Total represents the total respiratory system (lung and chest wall). Values are mean  $\pm$  standard deviation (SD). No further reductions with increasing concentrations of isoflurane were observed. \* $P < .05$  versus baseline; ADP, adenosine diphosphate; ATP, adenosine triphosphate; cAMP, cyclic adenosine monophosphate. (Modified from Ruiz P, Chartrand D. The effect of isoflurane 0.6% on respiratory mechanics in anesthetized-paralyzed humans is not increased at concentrations of 0.9% and 1.2%. *Can J Anaesth*. 2003;50:67. Used with permission.)

typically thought of as being determined by the flow rate and airway smooth muscle tension. However, nonmuscle elements, such as lung inflammation, airway thickening, altered lung volumes, lung recoil, airway wall remodeling, mucous hypersecretion, and loss of lung elastance, also play a clinically significant role in the amount of airway narrowing. The role of volatile anesthetics in altering many of these non-smooth-muscle elements responsible for airway resistance needs further elucidation.

The effects of volatile anesthetics on bronchomotor tone are also dependent on the substance used to produce contraction in vitro.<sup>47</sup> Relaxation of tracheal smooth muscle by halothane and isoflurane is greatest in the presence of the endogenous mediator serotonin (resulting from anaphylactoid or immunologic reactions) compared with ACh (representing the neutrally derived mediator of reflex bronchospasm). Thus inhaled anesthetics may remain effective bronchodilators, even in the presence of severe serotonin- or histamine-induced bronchospasm that is refractory to  $\beta_2$ -adrenoceptor therapy. It is important to note that in anesthetized patients, volatile anesthetic-induced decreases in bronchomotor tone and neurally mediated airway reflexes may be partially opposed by a simultaneous reduction in functional residual capacity (FRC). The well-known increased risk for morbidity and mortality in patients with asthma may be at least partially attributed to these FRC-mediated increases in airway resistance. Low temperature abolished the inhibitory effects of volatile anesthetics on carbamyl-induced contraction of airway smooth muscle in dogs,<sup>48</sup> suggesting that intraoperative hypothermia may also attenuate volatile anesthetic-induced bronchodilation.

Bronchospasm may occur in conditions and with respiratory diseases other than asthma. For example, healthy patients undergoing surgical stimulation of lung parenchyma or airways including tracheal stimulation by an endotracheal tube are at risk of developing bronchospasm. Preoperative medications, sedatives, neuromuscular blockers, and volatile anesthetics are all important factors that may trigger or attenuate bronchospasms. Regardless of the airway sensitivity prior to induction, the different pathways involved in an individual patient may yield different responses to the volatile anesthetics. Iwasaki and colleagues<sup>49</sup> demonstrated that sevoflurane-induced relaxation of airway smooth muscle and VDC channels were dependent on the type of hyperreactive airway model. Sevoflurane had smaller effects in a model of chronic tobacco smoking (enlarged alveolar ducts and less mucociliary hyperreactivity), compared with an antigen-acute asthmatic (ovalbumin-sensitized) model. The morphologic changes in the peripheral airway may be responsible to some degree for a decrease in the efficacy of volatile anesthetics as bronchodilators in tobacco smokers, but sevoflurane and isoflurane still decrease respiratory system resistance in patients with COPD.<sup>50</sup>

In children undergoing elective imaging studies, sevoflurane produced progressive reductions in the cross-sectional area of upper airway, resulting in pharyngeal airway collapse<sup>51</sup> (also see Chapter 93). As observed with isoflurane in animal models, the effects of sevoflurane were not uniformly distributed along the upper airway. In healthy children, sevoflurane slightly decreased airway resistance, but desflurane had the opposite effect, presumably via reduced airway size.<sup>52</sup>

Children with documented airway susceptibility, such as those with asthma or a recent upper respiratory tract infection, exhibit significant increases in airway resistance. In these pediatric patients, desflurane should be avoided.

## MECHANISMS OF ACTION OF VOLATILE ANESTHETICS

Volatile anesthetics attenuate airway smooth muscle tone by reducing smooth muscle contractility. This action is the result of the direct effects on bronchial epithelium and airway smooth muscle cells, combined with the indirect inhibition of reflex neural pathways. Several intracellular mediators responsible for  $\text{Ca}^{2+}$  mobilization are potential sites for the action of volatile anesthetics. Inhibition of cell membrane-associated VDC channels reduces  $\text{Ca}^{2+}$  entry into the cytosol.<sup>53</sup> Volatile anesthetic-induced increases in cAMP concentrations cause decreases in intracellular-free  $\text{Ca}^{2+}$  by stimulating  $\text{Ca}^{2+}$  efflux and increasing  $\text{Ca}^{2+}$  uptake into the sarcoplasmic reticular (SR). In addition, a decrease in  $\text{Ca}^{2+}$  sensitivity attributable to inhibition of PKC activity, inhibition of G-protein function, and attenuation of Rho/Rho-kinase signaling pathways also play important roles.<sup>53,54</sup> Volatile anesthetics may also alter pulmonary resistance by affecting the density of the gas mixture.<sup>28</sup> In an experimental lung model of fixed pulmonary resistance, high concentrations of volatile anesthetics increased the density of the gas mixture and the calculated resistance, with desflurane producing the largest increase (Fig. 21.6).<sup>28</sup> Such an effect is particularly profound for  $^{55}\text{Xe}$  which has a molecular weight of 131.2 Daltons, making it four times as dense as room air.<sup>55</sup>

The effects of volatile anesthetics on proximal, compared with distal, airways may be related to the differential effects on VDC channels and the relative distribution of these channels. Long-lasting (L-type) VDC channels appear to be the predominant mechanism for  $\text{Ca}^{2+}$  entry in tracheal smooth muscle, whereas both transient (T-type) and L-type VDC channels are present in bronchial smooth muscle.<sup>25,56</sup> Isoflurane and sevoflurane inhibit both types of VDC channels in a dose-dependent fashion, and their effects on T-type VDC channels in bronchial smooth muscle are even more pronounced (Fig. 21.7).<sup>25</sup>

The differential effects of volatile anesthetics on tracheal smooth muscle, compared with bronchial smooth muscle, may also be related to actions on  $\text{Ca}^{2+}$ -activated chloride channel activity<sup>57,58</sup> or differential sensitivities of  $\text{K}^+$  channel subtypes.<sup>57</sup>

The proposed signaling pathways underlying volatile anesthetic-induced bronchodilation are depicted in Fig. 21.8.<sup>59,60</sup>

Volatile anesthetic-induced reductions in  $\text{ICa}^{2+}$  result from the inhibition of both VDC and receptor-gated  $\text{Ca}^{2+}$  channels. In addition, volatile anesthetics deplete  $\text{Ca}^{2+}$  stores in SR by increasing  $\text{Ca}^{2+}$  leakage.  $\text{Ca}^{2+}$  influx occurring in response to depleted SR  $\text{Ca}^{2+}$  stores is known as store-operated  $\text{Ca}^{2+}$  entry (SOCE). By depleting  $\text{Ca}^{2+}$  stores in SR, volatile anesthetics may be expected to enhance SOCE. Nevertheless, at clinically relevant concentrations, volatile anesthetics (isoflurane more than sevoflurane) also inhibit SOCE in airway smooth muscle to further reduce available  $\text{Ca}^{2+}$ .<sup>61</sup>

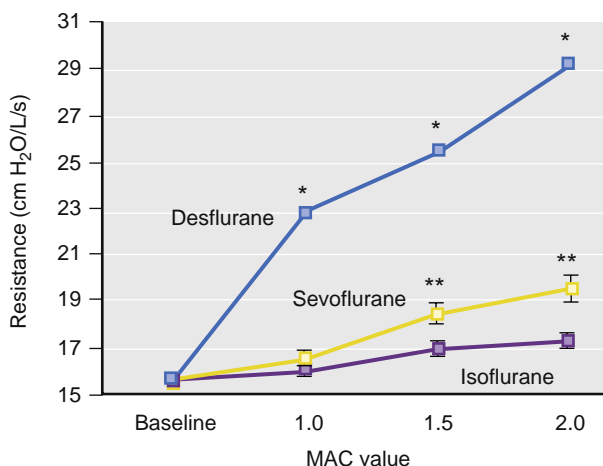


**Fig. 21.6** Comparison of the effect of different volatile anesthetics at equivalent concentrations on total pulmonary resistance. At 1 minimum alveolar concentration (MAC), only desflurane significantly increased pulmonary resistance, compared with isoflurane and sevoflurane. At 1.5 and 2 MAC, sevoflurane significantly increased total pulmonary resistance compared with isoflurane, whereas desflurane caused a more pronounced increase than the other two agents. \*Increased pulmonary resistance in comparison with sevoflurane and isoflurane; \*\*increased pulmonary resistance in comparison with isoflurane. (Reproduced from Nyktari VG, Papaioannou AA, Prinianakis G, et al. Effect of the physical properties of isoflurane, sevoflurane, and desflurane on pulmonary resistance in a laboratory lung model. *Anesthesiology*. 2006;104:1202. Used with permission.)

Volatile anesthetic-induced reductions in SR  $\text{Ca}^{2+}$  appear to occur through enhancement of  $\text{IP}_3$ <sup>62</sup> and ryanodine-receptor channel activities.<sup>59</sup> Kai and co-workers<sup>53</sup> demonstrated that halothane attenuates ACh-induced  $\text{Ca}^{2+}$  sensitization in canine tracheal smooth muscle to a greater extent than does sevoflurane, whereas isoflurane has effect at concentrations equivalent to 2 MAC. This effect appears to be mediated, at least in part, by an increase in smooth muscle protein phosphatase,<sup>60</sup> modulation of G proteins (specifically  $\text{G}_q$  and  $\text{G}_i$  that exert actions on cyclic guanosine monophosphate [cGMP]),<sup>53</sup> or modulation of the Rho/Rho-kinase signaling pathways.<sup>63,64</sup> Volatile anesthetics interact with the muscarinic receptor-heterotrimeric G protein complex to prevent agonist-promoted nucleotide exchange at the  $\text{G}\alpha$  subunit of the G protein.<sup>65,66</sup> Halothane, sevoflurane, and, minimally, isoflurane exert direct effects on muscarinic receptor-mediated contraction of isolated airway smooth muscle.<sup>67</sup> The inhibitory effects of volatile agents on the biochemical coupling between the  $\text{M}_3$  muscarinic receptor and the  $\text{G}\alpha_q$  heterotrimeric G protein is completely reversible with time. Isoflurane-induced relaxation of precontracted bronchial smooth muscles is significantly augmented by pretreatment with a Rho-kinase inhibitor, whereas sevoflurane-inhibited guanosine-5'-triphosphate (GTP)  $\gamma$  S-stimulated contraction and membrane translocation of both Rho and Rho-kinase in a concentration-dependent manner. These latter actions play important roles in  $\text{Ca}^{2+}$  sensitization.<sup>54</sup> The final pathway in airway smooth muscle contraction is the generation of force and shortening of smooth muscles regulated by myosin cross-bridge number and kinetics. Isoflurane modulates both cross-bridge number and cycling rates of isolated rat airway smooth muscle.<sup>67</sup>

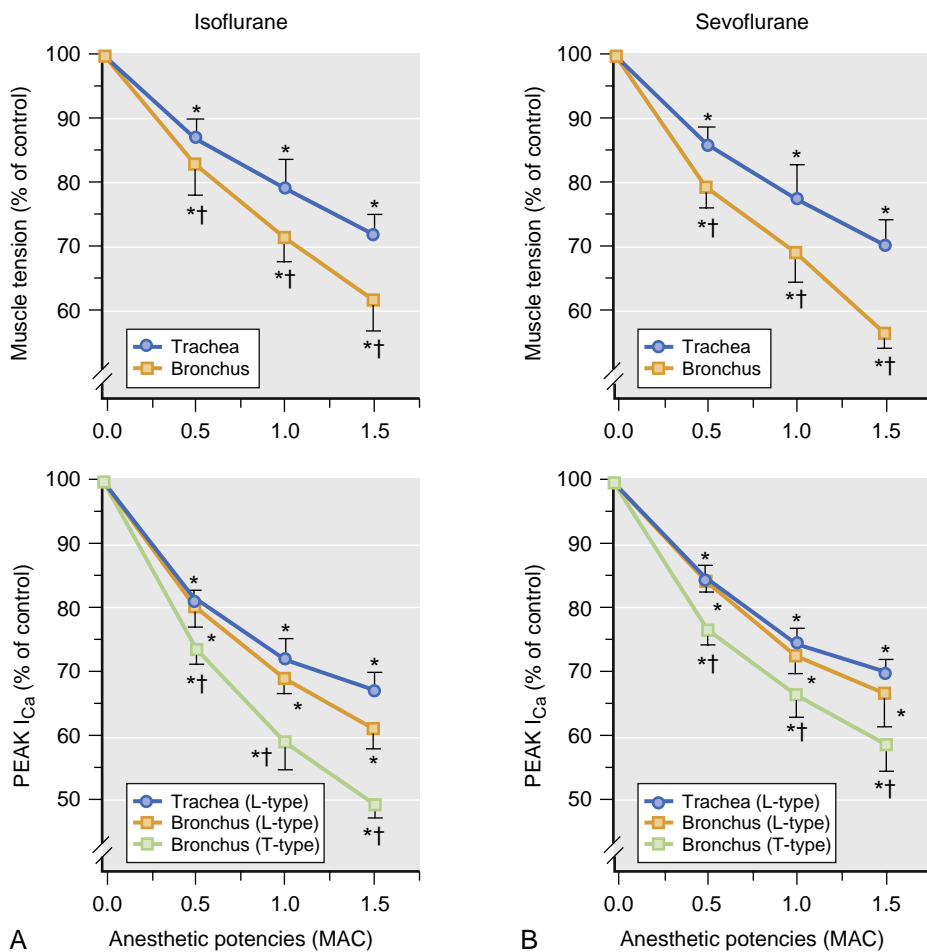


**Fig. 21.7** Effect of isoflurane and sevoflurane on porcine tracheal versus bronchial smooth muscle tension or inward calcium ( $\text{Ca}^{2+}$ ) current intercellular calcium ( $\text{ICa}^{2+}$ ) through T- and L-type voltage-dependent  $\text{Ca}^{2+}$  (VDC) channels. No differences were observed in the inhibition of L-type VDC channels. Both anesthetics had greater inhibitory effects on T-type VDC channels in bronchial smooth muscle. Symbols represent mean  $\pm$  standard deviation (SD). (A)  $^*P < .05$  versus 0 minimum alveolar concentration (MAC).  $^{\dagger}P < .05$  versus tracheal smooth muscle. (B)  $^*P < .05$  versus L-type VDC channels. (Reproduced from Yamakage M, Chen X, Tsujiguchi N, et al. Different inhibitory effects of volatile anesthetics on T- and L-type voltage dependent  $\text{Ca}^{2+}$  channels in porcine tracheal and bronchial smooth muscles. *Anesthesiology*. 2001;94:683. Used with permission.)

The bronchodilatory effect of volatile anesthetics is also mediated by GABA A ( $\text{GABA}_A$ ) receptors in the brainstem or GABA B ( $\text{GABA}_B$ ) receptors on preganglionic cholinergic nerves in the lung similar to the observations with propofol.<sup>68</sup> Indeed,  $\text{GABA}_A$  and  $\text{GABA}_B$  receptors, as well as glutamic decarboxylase (enzyme responsible for GABA synthesis), are located in airway epithelial and smooth muscle cells. GABA levels increase and localize to airway smooth muscle after contractile stimuli in upper airways. Furthermore, a GABA agonist reversed augmentation of cholinergic-induced tracheal ring contraction.<sup>68,69</sup>

Inhaled but not intravenous halothane attenuated bronchoconstricting effects of low inhaled concentrations of  $\text{CO}_2$  in rat distal bronchi, suggesting that halothane exerts a direct action on airway muscle tone or local neural reflex arcs rather than centrally controlled reflex pathways. Consistent with this hypothesis, halothane-, isoflurane-, sevoflurane-, and desflurane-induced dilation of distal bronchial segments is partially dependent on the presence of bronchial epithelium.<sup>23,70</sup> Prostanoids (e.g., prostaglandin E<sub>2</sub> or I<sub>2</sub>) or NO may be responsible for the bronchodilatory effects of volatile anesthetics under

these conditions. Focal epithelial damage or inflammation may occur in small airways in patients with asthma or allergen exposure, resulting in a reduced bronchodilatory response to volatile anesthetics.<sup>71</sup> Nevertheless, the most pronounced bronchodilatory action of volatile anesthetics in patients with chronic reactive airway disease occurs primarily in the proximal rather than distal airways.

Direct stimulation of intrinsic airway nerves in vitro produces a contractile response that is inhibited by atropine. Volatile anesthetic-induced bronchodilation also occurs by modulation of this airway cholinergic neural transmission mediated through prejunctional and postjunctional mechanisms.<sup>72,73</sup> The combination of atropine and halothane did not increase airway caliber over that attained with either drug alone, suggesting that halothane dilates airways by blocking vagal tone during unstimulated conditions.<sup>74</sup> Potent tracheal constriction also occurs in response to the endogenously produced endothelin-1. Isoflurane attenuated the endothelin-1-induced airway smooth muscle contraction in rat tracheal rings, suggesting another potential mechanism for airway smooth muscle relaxation.<sup>75</sup>

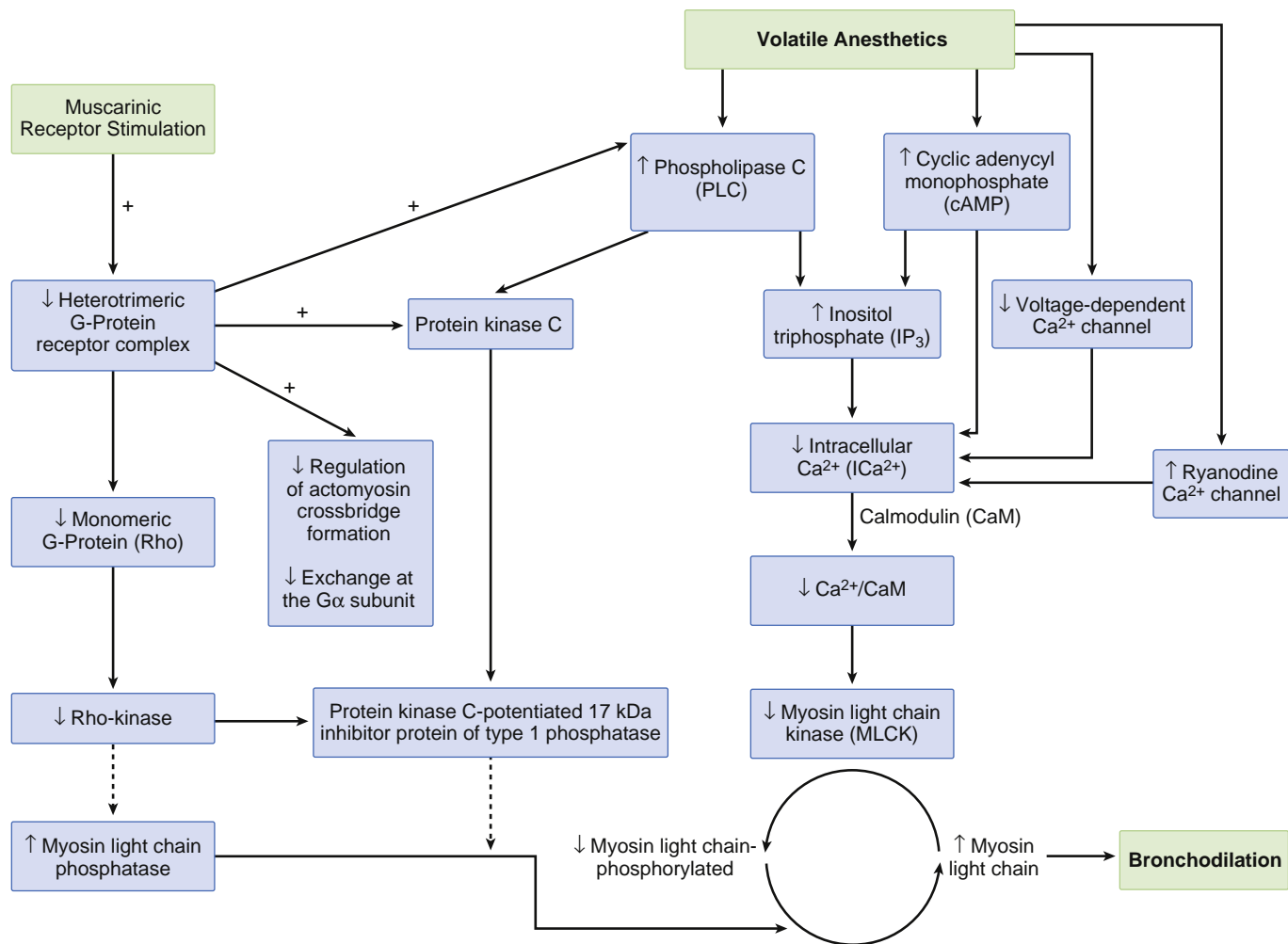


**Fig. 21.8** Proposed signaling pathways underlying volatile anesthetic-induced bronchodilation and/or inhibition of muscarinic agonist-induced contraction of airway smooth muscle. +, Excitatory action of muscarinic-receptor agonist. ↑, Activation or increase attributable to the volatile anesthetic. ↓, Inhibition or decrease attributable to the volatile anesthetic. Volatile anesthetics play a role in decreasing intracellular calcium (ICa<sup>2+</sup>) levels and decreasing calcium (Ca<sup>2+</sup>) sensitivity.

## Mucociliary Function and Surfactant

### NORMAL MUCOCILIARY FUNCTION

The upward clearance of mucus from the tracheobronchial tree is responsible for removal of foreign particulate matter, microorganisms, and dead cells and is a primary pulmonary defense mechanism. Although ciliated respiratory epithelium cells are present throughout the respiratory tree, the density of ciliated respiratory epithelium progressively decreases from the trachea to the terminal bronchioles. Cilia are hair-like appendages, consisting of hundreds of proteins organized around a microtubular architecture. They are anchored to the apical cytoplasm by a basal body and extend from the cell surface into the extracellular space.<sup>76,77</sup> Cilia are classified as either motile or immotile (primary). Motile cilia were thought to be responsible for generating extracellular fluid movement or propelling individual cells, whereas primary cilia were believed to be vestigial. However, primary cilia are important environmental sensors. In human bronchial epithelium, they play a key role

in sensing and transducing extracellular mechanochemical signals and are also capable of identifying smooth muscle injury.<sup>78</sup> Indeed, ciliopathies are responsible for a variety of pediatric disorders such as primary ciliary dyskinesia and autosomal recessive polycystic kidney disease.<sup>76,79</sup> Christopher et al. studied the effects of temperature (15°C-37°C) with varying combinations with fentanyl, dexmedetomidine, and isoflurane on the cilia of mouse tracheal epithelia. There was a linear correlation between cilia motility and temperature. Fentanyl exerted stimulatory effects on cilia, while dexmedetomidine and isoflurane both inhibited cilia function. When added together, fentanyl, dexmedetomidine, and isoflurane were all cilia inhibitory. In contrast, fentanyl plus dexmedetomidine did not significantly alter ciliary function, with results suggesting complex drug-drug and drug-temperature interactions not predicted by simple summation of effects.<sup>80</sup>

Ciliary motion consists of a rapid stroke in a cephalad direction, followed by a slower caudal recovery stroke. Movements of cilia are closely coordinated to move matter efficiently toward the trachea in a wave motion known as *metachronism*. Each motile cilium is organized

in nine peripheral microtubule pairs surrounding a central pair (9+2). During a beat, dynein arms undergo an adenosine triphosphate (ATP)–dependent attachment, retraction, and release cycle with the adjacent doublet, which results in a sliding motion. The basal bodies of the motile cilia are anchored to the microtubules, nexin links, and radial spokes and are further restricted by the ciliary membrane. This anatomic constraint converts the sliding motion into a bend.

The quantity and physical properties of the mucous layer may also promote the coordination of ciliary beats. Mucus is a mixture of water, electrolytes, and macromolecules (e.g., lipids, mucins, enzymes) secreted by goblet cells and mucosal glands. Thicker layers of mucus slow the removal of surface particles from the airway, whereas low-viscosity mucus promotes more rapid ciliary transport. Impaired mucociliary function in the upper airways correlates with low levels of nasal NO, although the clinical significance of this finding is unclear.<sup>81</sup> Direct nervous system control of ciliary coordination has not been demonstrated in vertebrates, but mucociliary clearance is closely related to autonomic nervous system activity, most likely related to changes in physical characteristics of respiratory secretions (also see Chapter 103).<sup>82</sup>

Several factors affect mucociliary function in mechanically ventilated patients contributing to lung atelectasis and hypoxemia. For example, insufficiently humidified inspired gases reduce ciliary movement and desiccate mucus. In dogs, the flow rate of tracheal mucus was maintained within the basal range during a 40-minute exposure to inspired dry air at a temperature higher than 32°C. However, 3 hours of inhalation of dry air caused a complete cessation of the flow of tracheal mucus, which was restored by the subsequent use of inspired gases with 100% relative humidity at 38°C. Several anesthesia-related factors also reduce the rate of mucous movement, including high-inspired oxygen (O<sub>2</sub>) concentrations, adjuvant medications (e.g., corticosteroids, atropine,  $\beta$ -adrenoreceptor antagonists) that affect bronchial tone, the presence of an endotracheal tube, and positive-pressure ventilation.<sup>83</sup>

## EFFECTS OF INHALED ANESTHETICS ON MUCOCILIARY FUNCTION

Volatile anesthetics and nitrous oxide diminish the rates of mucous clearance by decreasing ciliary beat frequency, disrupting metachronism, and altering the physical characteristics or quantity of mucus. In contrast to many intravenous anesthetics,<sup>84,85</sup> halothane, enflurane, isoflurane, and sevoflurane all reduce ciliary movement and beat frequency *in vitro*.<sup>84-87</sup> Among the volatile anesthetics, sevoflurane exhibited the weakest cilino-inhibitory effects in rat cultured tracheal epithelial cells *in vitro* (Fig. 21.9).<sup>87</sup>

Gamsu and colleagues<sup>88</sup> measured the rate of tantalum (a powder that adheres to airway mucus) clearance from the lungs of postoperative patients who received general anesthesia for intraabdominal or lower extremity surgeries. Tantalum retention was closely correlated with the retention of mucus and shown for as long as 6 days after intraabdominal surgery. The administration of halothane (1%–2%) and nitrous oxide (60%) rapidly decreased the rate of mucous movement in females undergoing gynecologic

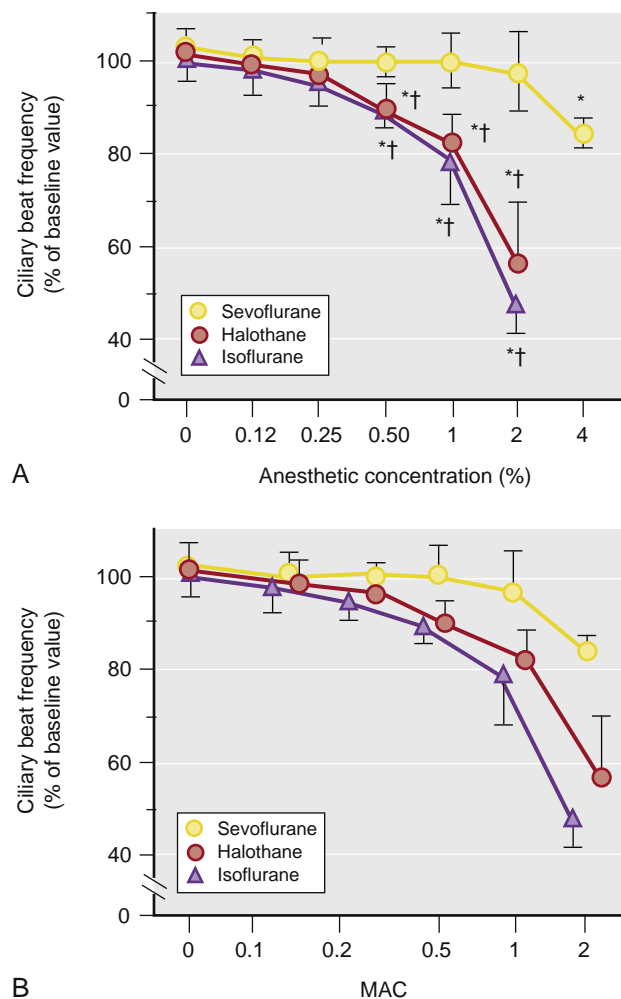


**Fig. 21.9 Effects of sevoflurane, halothane, and isoflurane on ciliary beat frequency (CBF) in cultured rat tracheal epithelial cells.** CBF was measured at baseline and 30 minutes after exposure to various anesthetic concentrations. Values represent mean  $\pm$  standard deviation. (A) Plot of percent baseline CBF versus anesthetic concentration. \* $P < .05$  versus 0% vehicle, † $P < .05$  versus sevoflurane at the same concentration. (B) Percent baseline CBF versus minimum alveolar concentration (MAC). (Modified from Matsuura S, Shirakami G, Iida H, et al. The effect of sevoflurane on ciliary motility in rat cultured tracheal epithelial cells: a comparison with isoflurane and halothane. *Anesth Analg*. 2006;102:1703. Used with permission.)

surgery. Little or no mucous motion was observed after 90 minutes of halothane–nitrous oxide inhalation.<sup>89</sup> Bronchial mucosal transport velocity was also determined using radiolabeled albumin microspheres distally deposited in the mainstem bronchi using a fiberoptic bronchoscope in healthy patients. In contrast to the findings of the study with halothane, mucous velocity was unchanged during the administration of 1.5 MAC isoflurane.<sup>90</sup>

Impairment of ciliary beat frequency, mucociliary clearance, and bronchial mucous transport contribute to pulmonary complications, including retention of secretions, atelectasis, and lower respiratory tract infection. A reduction in bronchial mucous transport of as little as 3.5 mm/min (normally 10 mm/min) was associated with an increase in pulmonary complications in patients who were mechanically ventilated for 4 days in the intensive care unit (ICU).<sup>91</sup> Thus pulmonary therapy directed at enhancing

clearance of secretions from the airways may be beneficial in the immediate postoperative period, regardless of the type of volatile anesthetic chosen.

Compared to nonsmokers, tobacco smokers have significantly slower bronchial mucous transport velocities and are prone to more frequent pulmonary complications when undergoing major abdominal or thoracic surgeries.<sup>92</sup> The specific effects of volatile anesthetics on mucous movement in smokers have not been well studied. However, it is likely that an additive or synergistic negative effect on mucous transport may be present. Impairment of mucociliary function also occurs after lung transplantation. The mechanism for this dysfunction may be related to alterations in the surface properties of mucus and significant impairment of mucociliary transport distal to bronchial transection and re-anastomosis.<sup>93</sup> The effects of volatile anesthetics on mucous transport in lung transplant patients have not been described, but the baseline reductions in mucociliary movement would certainly predispose to postoperative respiratory complications.

## EFFECTS OF INHALED ANESTHETICS ON SURFACTANT

Pulmonary surfactant decreases the work of breathing by reducing surface tension at the fluid-gas interface. Surfactant is a mixture of proteins and phospholipids synthesized by alveolar type II cells. Similar to mucus, surfactant plays a role in removing foreign particles from airways while also enhancing the bactericidal actions of alveolar macrophages. Halothane<sup>94</sup> and isoflurane<sup>95</sup> produced a transient dose-dependent reduction in phosphatidylcholine (a major component of surfactant) synthesis by alveolar cells during a 4-hour exposure. High concentrations of halothane also disrupted the energy metabolism of cultured alveolar cells as indicated by reduced ATP content and enhanced glycolytic metabolism. Halothane and isoflurane potentiated a hydrogen peroxide-induced reduction of phosphatidylcholine content in alveolar type II cells<sup>95,96</sup> by affecting cell energetics. Halothane decreased the  $\text{Na}^+/\text{K}^+$ -adenosine triphosphatase ( $\text{Na}^+/\text{K}^+$ -ATPase), and  $\text{Na}^+$  channel activity in alveolar type II cells, probably related to alterations in  $\text{ICa}^{2+}$  or ATP depletion. A similar decrease in type II alveolar cell  $\text{Na}^+/\text{K}^+$ -ATPase occurs after the administration of isoflurane.<sup>97</sup> Transepithelial  $\text{Na}^+$  transport helps regulate alveolar fluid balance, and, as a result, impairment of this transport system may contribute to alveolar edema. This observation may be especially relevant in surgical patients because volatile anesthetics decrease alveolar epithelial fluid clearance.<sup>98</sup>

The phospholipid composition of surfactant is critical to its functional integrity. Another crucial component of surfactant is the hydrophobic surfactant-associated protein C synthesized by alveolar type II cells. This protein facilitates the adsorption and spreading of phospholipids to form the surfactant monolayer and enhances the lipid uptake into alveolar type II cells. Exogenous surfactants that contain surfactant-associated protein C are effective at decreasing barotrauma and mortality in vivo. Clinically relevant concentrations of halothane increase surfactant-associated protein C messenger ribonucleic acid (mRNA) in vitro but cause the opposite effect in mechanically ventilated rats.<sup>99</sup>

Extrapolation of these findings to patients should be approached with caution, but halothane and mechanical ventilation may play a potentially additive and deleterious role on surfactant production and homeostasis of the alveolar space, particularly in the presence of ALI. In a rat model, sevoflurane produced deterioration in surfactant composition and viscosity with impaired lung mechanics promoting alveolar collapse<sup>100</sup>; again, caution is warranted in extrapolating these findings to humans. Bilgi and colleagues compared the effects of low-flow and high-flow inhalational anesthesia with nitrous oxide and desflurane on mucociliary activity and pulmonary function tests in humans. The forced vital capacity and forced expiratory volume and mucociliary clearance of saccharin powder were better preserved with low-flow rather than a high-flow technique, suggesting that heated and humidified gases may have a greater impact than the inhaled anesthetics themselves.<sup>101</sup>

Prolonged administration of volatile anesthetics may produce mucous pooling and impair alveolar cell surfactant metabolism. These actions may result in adverse effects on pulmonary function including development of atelectasis and infections. Patients with excessive or abnormal mucous or surfactant production and patients with ALI, chronic bronchitis, asthma, cystic fibrosis, and chronic mechanical ventilation are at the greatest risk. Clinical studies of the effects of volatile anesthetics on mucociliary function, surfactant metabolism, and immunomodulation in patients with compromised pulmonary function are still sparse.

## PULMONARY VASCULAR RESISTANCE

### Regulation of Pulmonary Vascular Tone

The pulmonary vascular bed is a low-pressure, high-flow system. Normal pulmonary arterial (PA) pressure is approximately one-fifth of the systemic arterial pressure. Correspondingly, PVR is lower than systemic vascular resistance. The main pulmonary artery and its major branches have a thinner media and less vascular smooth muscle than the aorta and major proximal arterial vessels. Changes in pulmonary vascular smooth muscle tone alter PVR by affecting the slope of pressure-flow relation. Such direct changes may be produced by a rapid rise in cytoplasmic  $\text{ICa}^{2+}$  of the pulmonary vascular smooth muscle cell or by alterations in sympathetic nervous system activity, arterial  $\text{O}_2$  and  $\text{CO}_2$  tension, acid-base balance, or plasma catecholamine concentrations. Hypercapnia at constant pH (i.e., isohydria) does not alter tone in isolated pulmonary arteries, but normocapnic acidosis relaxes isolated pulmonary arteries by an endothelium-independent mechanism.<sup>102</sup> However, pulmonary endothelial dysfunction potentiates hypercapnia-induced vasoconstriction.<sup>103</sup> Changes in PA pressure and PVR exert important effects on pulmonary gas or fluid exchange. An increase in PVR occurring in conjunction with a corresponding increase in PA pressure promotes interstitial fluid transudation. An acute increase in PVR can be caused by large tidal volumes, high positive end-expiratory pressure, alveolar hypoxia, hypercarbia, acidosis, and critical closing pressure. Hypoxia and acidosis have a synergistic effect increasing PVR. In contrast to acute pulmonary hypertension, the development of chronic pulmonary hypertension involves endothelial dysfunction with persistent vasoconstriction due to imbalance between

endogenous vasoconstrictors (including thromboxane A<sub>2</sub>, angiotensin 2, and endothelin 1) and vasodilators (including NO and prostacyclin), smooth muscle proliferation, platelet aggregation, vascular remodeling and thrombosis, and formation of plexiform lesions that irreversibly obliterate pulmonary arterioles. Clinically, the use of positive inotropic medications (e.g., milrinone) or expanded blood volume can passively decrease PVR by increasing cardiac output. Volatile anesthetics may also have indirect effects on PVR through a reduction in lung volumes during spontaneous ventilation. To assess the total effect of the volatile anesthesia, the volume status and mechanical ventilation on the pulmonary pressures, and right heart function, either transthoracic or transesophageal echocardiography should be considered.

Endogenously produced NO plays an important role in the regulation of PVR both in the healthy, normoxic lung and during hypoxia. NO is generated via oxidation of a terminal guanidinium nitrogen on the amino acid L-arginine. The reaction utilizes molecular O<sub>2</sub> and NADPH as substrates, requires the presence of tetrahydrobiopterin, flavoproteins, calmodulin, and thiols as cofactors, and yields NO in addition to the co-product L-citrulline.<sup>104</sup> This oxidation is catalyzed by a single enzyme protein, NO synthase (NOS), which exists in three distinct isoforms. Constitutive calcium-dependent isoforms of the enzyme were originally purified from neuronal tissue (nNOS) and vascular endothelium (eNOS).<sup>105,106</sup> When stimulated by bacterial endotoxin and proinflammatory cytokines, a third calcium-independent isoform (iNOS) is induced in various cell types including endothelial and vascular smooth muscle cells, macrophages, and fibroblasts. Once expressed, iNOS is independent of calcium, and NO production continues at a maximum rate. All three NOS isoforms are widely distributed in the lung, extensively involved in vascular homeostasis, and intimately linked to the pulmonary O<sub>2</sub> environment.<sup>107</sup>

NO diffuses away from its point of synthesis and interacts with various intracellular molecular sites both within the generating cells and the target cells. The best-characterized target for NO is iron, bound within certain proteins, either as a heme group or as an iron-sulfur complex. The interaction of NO with the heme component of soluble guanylate cyclase stimulates enzymatic conversion of guanosine triphosphate to cGMP.<sup>104</sup> In turn, increased intracellular levels of cGMP cause relaxation of systemic and pulmonary vascular and nonvascular smooth muscles by several mechanisms. Besides lowering free intracellular calcium and attenuating calcium transients, cGMP causes hyperpolarization of muscle cells through activation of potassium channels.

Inhalation of gaseous NO produces selective pulmonary vasodilation in well-ventilated lung areas and may be beneficial in the treatment of neonatal pulmonary hypertension resulting from a variety of congenital heart diseases, hypoplastic lung, and meconium aspiration. Inhaled NO has also some benefits in the treatment of acute pulmonary hypertension in adults, provided that the PVR is not fixed by remodeling and hypertrophy of pulmonary vasculature. Additionally, the use of inhaled NO to reduce PVR in pediatric and adult patients during cardiac surgeries has become common (also see Chapters 67, 94, and 104).<sup>108</sup>

Prostacyclin is another endogenous vasodilator produced by the endothelium that causes smooth muscle relaxation through adenylyl cyclase stimulation and production of cAMP. Prostacyclin is used in inhaled or injected formulations to produce pulmonary vasodilation in patients with chronic PA hypertension. Another group of pulmonary vasodilators, including sildenafil and tadalafil, acts by inhibiting cGMP-specific phosphodiesterase type 5 (an enzyme that is responsible for cGMP degradation) and is used for therapy of refractory PA hypertension. Finally, riociguat, a novel drug that directly stimulates soluble guanylate cyclase independently of NO, has been recently approved for treating patients with chronic pulmonary hypertension and chronic thromboembolic pulmonary hypertension.<sup>109</sup>

## MECHANISMS OF HYPOXIC PULMONARY VASOCONSTRICITION

Changes in PVR affect the regional distribution of blood flow within the lung and produce changes in ventilation-perfusion matching and gas exchange. The distribution of PA blood flow and ventilation in the lung is mainly a gravity-dependent phenomenon that is primarily mediated by the asymmetric branching of airways and blood vessels, thereby establishing regional heterogeneity.<sup>110</sup> An increase in PVR occurring within an area of atelectasis optimizes gas exchange by shifting blood flow away from the atelectatic segment to well-ventilated regions of the lung. This phenomenon, termed hypoxic pulmonary vasoconstriction (HPV), is unique to the pulmonary circulation because other vascular beds (e.g., coronary and cerebral) dilate in response to hypoxia. Thus HPV maintains oxygenation, while medications (including volatile anesthetics) that interfere with HPV may adversely affect gas exchange. HPV plays an especially important role in the presence of atelectasis, pneumonia, reactive airway disease, acute respiratory distress syndrome (ARDS), or one-lung ventilation (OLV). It usually does not contribute to pulmonary blood flow heterogeneity under normal conditions in supine humans.<sup>111</sup>

HPV is a locally mediated phenomenon that occurs when alveolar O<sub>2</sub> tension falls below approximately 60 mm Hg and is maximal when O<sub>2</sub> tension is approximately 30 mm Hg. HPV was first identified in 1894, and the precise mechanism is only now becoming clear. Specialized O<sub>2</sub>-sensing cells modulate respiratory and circulatory function to maintain a normal O<sub>2</sub> supply. Hypercapnia-induced acidosis increases PVR in intact animals and in isolated, perfused lungs. Acidosis-induced increases in PVR are relatively small at normal alveolar O<sub>2</sub> tensions but are dramatically enhanced during alveolar hypoxia. Local acidosis and increases in alveolar CO<sub>2</sub> tension augment HPV and further improve arterial oxygenation in healthy lungs. High CO<sub>2</sub> concentrations reduce NO levels,<sup>112</sup> but whether this action plays a part in hypercarbia-induced improvements in the ventilation-perfusion ratio is unclear.<sup>113</sup>

Although the hypoxia-mediated endothelial-derived vasoconstrictor has yet to be identified,<sup>114</sup> hypoxia releases Ca<sup>2+</sup> from smooth muscle SR via ryanodine receptors,<sup>115</sup> enhances Ca<sup>2+</sup> sensitization,<sup>114-116</sup> and modulates voltage-gated K<sup>+</sup> channels in smooth muscles.<sup>117</sup> Other mediators of the hypoxic-response coupling have been identified.<sup>116,118</sup>

Wang and colleagues<sup>119</sup> have recently demonstrated that both connexin 40-mediated retrograde endothelial signal conduction for  $O_2$  sensing, as well as  $Ca^{2+}$  influx at TRP1 channel V4 on pulmonary arterioles<sup>120</sup> are required for HPV. Ultimately, there are a number of contenders for the role of HPV oxygen sensor, yet there is still no consensus on how this happens *in vivo*, with most of the proposed mechanisms interlinked, depending on the phase of HPV, the degree of hypoxia, involvement of anesthetic or other agents.<sup>121</sup>

## INHALED ANESTHETICS AND HYPOXIC PULMONARY VASOCONSTRICITION

All volatile anesthetics dilate the pulmonary vascular bed. In a thorough review, Akata<sup>122</sup> discussed the mechanisms by which inhaled anesthetics produce this vasodilation, including a reduction in free cytosolic  $Ca^{2+}$  and inhibition of myofilament  $Ca^{2+}$  sensitivity. However, the vasodilator effect of volatile anesthetics is modest in normal lungs, and the small attenuation of PVR is usually offset by a concomitant reduction in cardiac output. The net effect of these hemodynamic changes results in minor, if any, changes in PA pressure concomitant with a small decrease in total pulmonary blood flow. In contrast to their action as direct pulmonary vasodilators, volatile anesthetics also attenuate  $K_{ATP}$  channel-mediated and endothelium-dependent pulmonary vasodilation in chronically instrumented dogs.<sup>123-125</sup> This inhibition of pulmonary vasodilation is not a uniform observation under all experimental conditions. For example, isoflurane and halothane, but not enflurane, enhance isoproterenol-mediated vasodilation.<sup>126,127</sup> Unlike the findings with other volatile anesthetics,  $K_{ATP}$  channel-mediated pulmonary vasodilation in response to a  $K^+$  channel agonist (lemakalim) is preserved during sevoflurane anesthesia.<sup>125</sup> Indeed, evidence suggests that

halothane, enflurane, and isoflurane, but not sevoflurane, differentially modulate pulmonary vascular tension through  $Ca^{2+}$ -activated or voltage-sensitive  $K^+$  channels, at least in isolated rabbit lungs.<sup>128</sup> Halothane- and enflurane-induced constriction of pulmonary vessels was potentiated by voltage-gated potassium (Kv) channel inhibition in this isolated rabbit lung preparation. In contrast, isoflurane did not affect pulmonary vessels when Kv channels were inhibited. Further, sevoflurane dilated pulmonary vessels and this dilation was unaffected by  $K^+$  channel subtype inhibitors (Fig. 21.10).<sup>128</sup>

Smooth muscle TASK-1 channels also appear to contribute to volatile anesthetic-induced PA dilation.<sup>129</sup> Rather than causing immediate vasodilation, volatile anesthetics produce a paradoxical initial dose-dependent increase in force in isolated PA strips as a result of  $Ca^{2+}$  release from intracellular stores (Fig. 21.11).<sup>122,130,131</sup> Subsequently, a decrease in force, associated with a  $Ca^{2+}$ /calmodulin-dependent protein kinase II activation, occurs.<sup>130,131</sup> Extrapolation of these results to humans must be approached with caution, but these studies suggest that vasodilatory responses of volatile anesthetics may be more profound in patients with reduced SR  $Ca^{2+}$  stores (e.g., neonates) or those with depressed protein kinase activity (e.g., primary pulmonary hypertension).

In general, all volatile anesthetics attenuate HPV in isolated perfused lungs or in an *in situ* preparation with constant perfusion (Fig. 21.12),<sup>121,132</sup> whereas most intravenous anesthetics do not have such an effect.<sup>118</sup> The combined administration of a  $Ca^{2+}$ -channel blocker and a volatile anesthetic further reduces HPV by up to 40%, compared with either drug alone, suggesting that these drugs inhibit HPV through differing mechanisms. The mechanisms of HPV inhibition by volatile anesthetics are unclear but may be related to arachidonic acid metabolites<sup>133</sup>

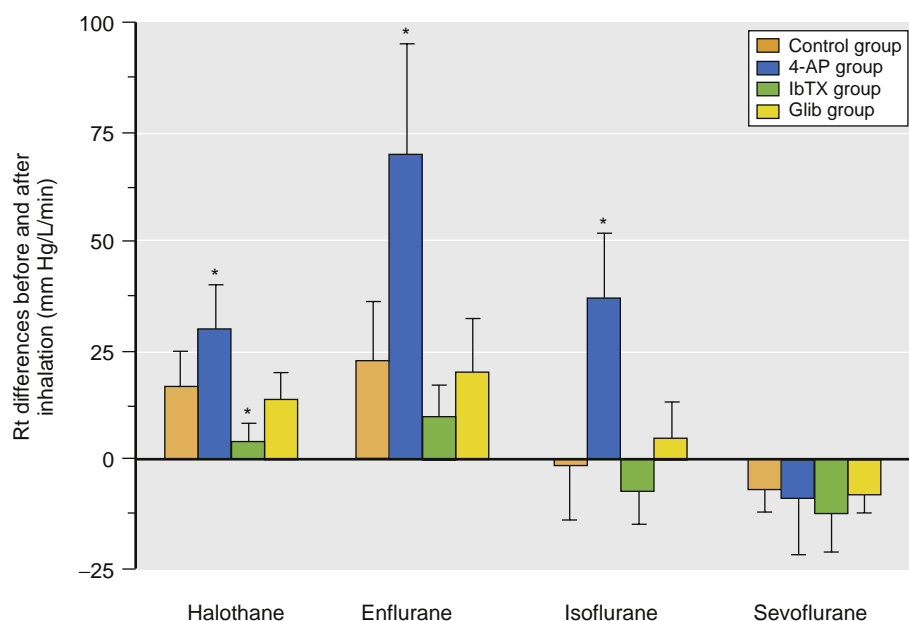


**Fig. 21.10 Total pulmonary vascular resistance (Rt) before and after anesthetic inhalation.** Data are mean  $\pm$  standard deviation. \* $P < .01$  versus control group. 4AP, voltage-sensitive  $K^+$  channel inhibitor; Glib, glibenclamide, an adenosine triphosphate-sensitive  $K^+$  channel inhibitor; IbTX, calcium-activated  $K^+$  channel inhibitor; Rt difference, resistance after the administration of anesthetic minus resistance before administering the anesthetic. (Modified from Liu R, Ishibe Y, Okazaki N, et al. Volatile anesthetics regulate pulmonary vascular tensions through different potassium channel subtypes in isolated rabbit lungs. *Can J Anaesth*. 2003;50:301. Used with permission.)

or endothelial-derived vasodilating factors.<sup>134</sup> However, other evidence suggests that anesthetic-induced inhibition of HPV may occur independent of pulmonary vascular endothelium, NO, or guanylate cyclase.<sup>135,136</sup> Volatile anesthetics also disrupt  $\text{Ca}^{2+}$  homeostasis in vascular smooth muscle and thereby interfere with pulmonary vasoconstriction. Halothane and isoflurane attenuated

endothelium-dependent vasodilation by inhibiting cGMP accumulation<sup>137</sup> and a  $\text{K}_{\text{ATP}}$  channel-mediated interaction between NO and prostacyclin in isolated canine PA rings.<sup>138</sup> In contrast, isoflurane modulated the HPV response, at least in part, through  $\text{Ca}^{2+}$ -activated and voltage-sensitive  $\text{K}^{+}$  channels. Attenuation of HPV by sevoflurane occurred independent of  $\text{K}^{+}$ -channel function.<sup>139</sup>

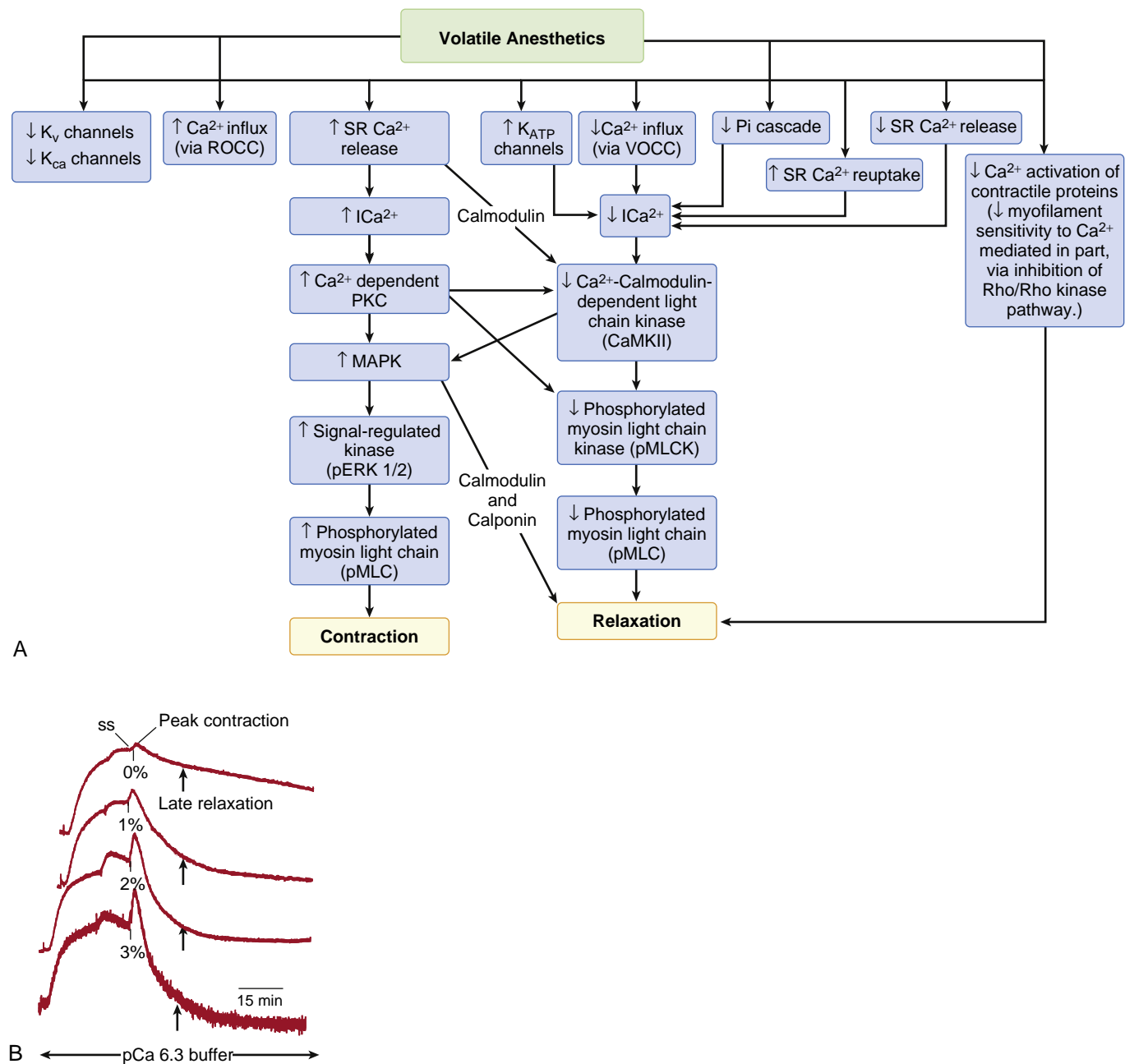


**Fig. 21.11** (A) Proposed signaling pathways underlying volatile anesthetic-induced contraction and relaxation in pulmonary artery smooth muscle. Intracellular calcium ( $\text{ICa}^{2+}$ ) may be increased by release from the sarcoplasmic reticulum (SR), by the inhibition of voltage-sensitive potassium ( $\text{K}_v$ ) or calcium-activated potassium ( $\text{K}_{\text{ca}}$ ) channels, or by receptor-operated  $\text{Ca}^{2+}$  channels (ROCC). Increased  $\text{ICa}^{2+}$  results in an initial dose-dependent increase in force (associated with activation of protein kinase C [PKC] and increased mitogen-activated protein kinase [MAPK]). Volatile anesthetics also decrease  $\text{ICa}^{2+}$  by activating adenosine triphosphate-regulated potassium ( $\text{K}_{\text{ATP}}$ ) channels, thereby inhibiting  $\text{Ca}^{2+}$  influx via voltage-operated  $\text{Ca}^{2+}$  channels (VOCC), decreasing SR-induced release of  $\text{Ca}^{2+}$ , inhibiting the phosphatidylinositol (Pi) cascade, and enhancing SR-mediated reuptake of  $\text{Ca}^{2+}$ . The resultant decrease in force is associated with activation of  $\text{Ca}^{2+}$ -calmodulin-dependent protein kinase II (CaMKII). It is important to note that there are many agent-specific effects of volatile anesthetics on each component of these pathways. pERK, Phosphorylated extracellular signal-regulated kinase. (B) Example of a biphasic (contraction/relaxation) effect of halothane on pulmonary arterial smooth muscle. 0%, 1%, 2%, and 3%, Halothane dose dependently enhanced  $\text{Ca}^{2+}$ -activated peak force and late relaxation. (Data from Akata,<sup>122</sup> Su and Vo,<sup>130</sup> and Zhong and Su.<sup>131</sup>)

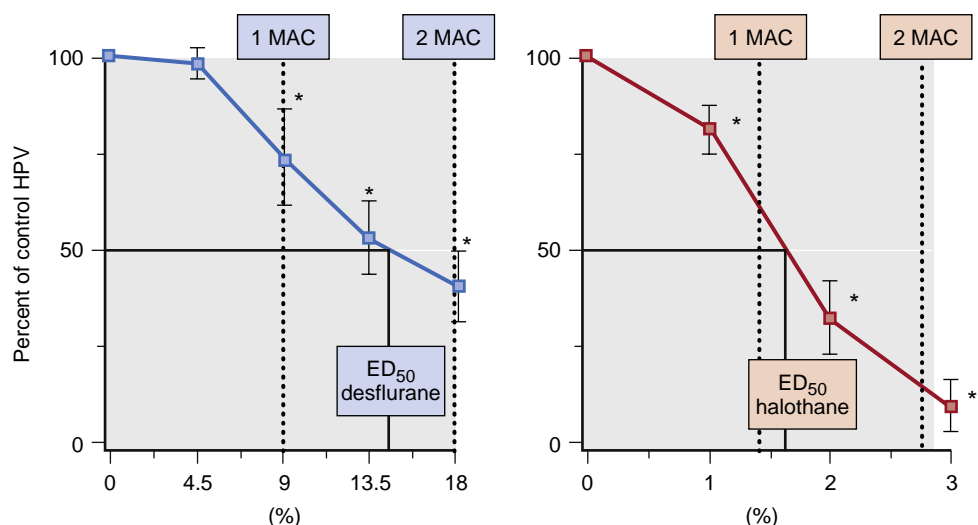


**Fig. 21.12** Concentration-dependent inhibition of hypoxic pulmonary vasoconstriction (HPV) in isolated rabbit lungs by desflurane (blue squares) and halothane (red squares). Values are mean  $\pm$  standard error of the mean and expressed as a percentage of control. \* $P < .05$  versus control HPV. The 50% effective dose ( $ED_{50}$ ) values were within the range of 1 and 2 minimum alveolar concentrations (MAC) for rabbits for both agents. (Reproduced from Loer SA, Scheeren T, Tarnow J. Desflurane inhibits hypoxic pulmonary vasoconstriction in isolated rabbit lungs. *Anesthesiology*. 1995;83:552. Used with permission.)

The relative efficacy of volatile anesthetics on HPV in vivo is difficult to assess because several other factors impair HPV, including temperature, pH,  $CO_2$  tension, degree of hypoxia, size of the hypoxic area, surgical trauma, and medications. During OLV, the direct inhibitory effects of volatile anesthetics on HPV may increase perfusion in the nonventilated lung and worsen hypoxemia. However, volatile anesthetics may also affect HPV, lung perfusion, and oxygenation by indirect actions on cardiac output and mixed venous  $O_2$  saturation.<sup>140</sup> Baseline PA blood flow and pressure also modulate the effects of HPV. Elevated PA pressures may cause passive distension of constricted vascular beds and thereby reverse HPV. Alternatively, reflex pulmonary and systemic vasoconstriction in response to hypotension may increase PVR in healthy lung segments, leading to a shift of pulmonary blood flow to hypoxic areas of lung.<sup>121</sup>

Early studies suggested that nitrous oxide attenuates HPV in animal models in vivo. As opposed to the findings with isoflurane,<sup>133</sup> sevoflurane or desflurane did not inhibit HPV in chronically instrumented dogs subjected to gradual occlusion of the right main PA (Fig. 21.13).<sup>141</sup> Nitrous oxide,<sup>142</sup> desflurane, and isoflurane,<sup>143</sup> but not xenon,<sup>142</sup> reduced the mixed venous  $O_2$  saturation, cardiac output, and arterial oxygenation during OLV in pigs. However, nitrous oxide,<sup>142</sup> xenon,<sup>142</sup> desflurane,<sup>143,144</sup> and isoflurane<sup>143,145</sup> did not alter perfusion of the nonventilated lung or reduce the shunt fraction during OLV. In animals with a preexisting impairment of gas exchange attributable to a pneumoperitoneum, sevoflurane, but not isoflurane, caused more profound abnormalities in gas exchange than did propofol.<sup>146</sup> Thus although reductions in HPV by volatile anesthetics have been relatively small in vivo, preexisting pulmonary disease may worsen anesthetic-induced gas exchange abnormalities.

## EFFECTS OF VOLATILE ANESTHETICS ON PULMONARY VASCULATURE IN HUMANS

General anesthesia often impairs pulmonary gas exchange. In addition to specific effects of volatile anesthetics, many

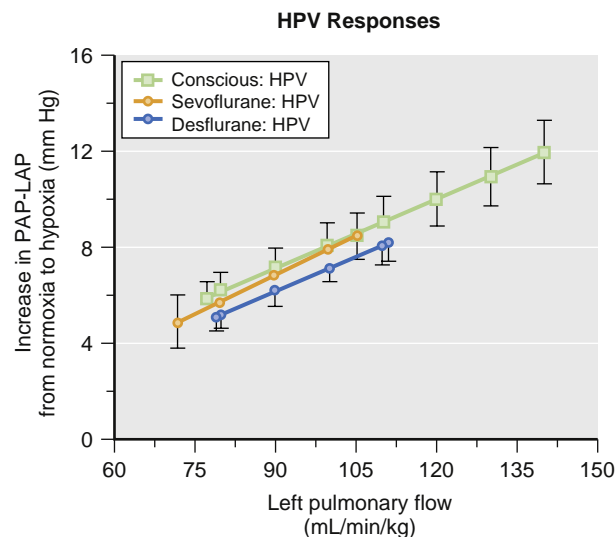


**Fig. 21.13** Composite hypoxic pulmonary vasoconstriction (HPV) responses (increase in pulmonary artery pressure [PAP] minus left atrial pressure [LAP] as a function of left pulmonary flow) in the same seven chronically instrumented dogs in the conscious state and during sevoflurane and desflurane anesthesia. Neither anesthetic affected the magnitude of HPV when compared with the response in the conscious state. (From Lesitsky MA, Davis S, Murray PA. Preservation of hypoxic pulmonary vasoconstriction during sevoflurane and desflurane anesthesia compared to the conscious state in chronically instrumented dogs. *Anesthesiology*. 1998;89:1501. Used with permission.)

other factors including gravity, posture, atelectasis, differences in vessel conductance between lung regions, intrathoracic pressure, and HPV may all affect the distribution of pulmonary blood flow and ventilation during the administration of volatile anesthetics. Alterations in regional ventilation are related to variations in alveolar compliance, inspiratory rate, flow rate, pleural pressures, and ventilatory modes.<sup>147</sup> In spontaneously breathing healthy volunteers, sevoflurane (1 MAC for 20 minutes) administered via a facemask did not alter the relative distribution of either ventilation or perfusion in a ventral to dorsal direction

measured by single photon-emission CT.<sup>147</sup> Similarly, no change in the distribution of ventilation, as measured by using electrical impedance tomography, occurred in spontaneously breathing adults receiving 0.7 MAC of sevoflurane via a laryngeal mask airway (LMA).<sup>145</sup> Interestingly, sevoflurane reduced regional heterogeneity of the perfusion distribution and increased regional heterogeneity of the ventilation/perfusion ( $\dot{V}/\dot{Q}$ ) ratio with a tendency toward lower ratios in spontaneously breathing volunteers.<sup>147</sup> This alteration may contribute to less effective pulmonary gas exchange, but these effects were relatively small compared with alterations in  $\dot{V}/\dot{Q}$  distribution that occur during mechanical ventilation.<sup>148,149</sup> Either pressure-controlled or pressure-supported ventilation with sevoflurane caused similar ventral redistributions of ventilation.<sup>148</sup>

Isoflurane produces no clinically significant effects on pulmonary shunt in healthy patients even at concentrations that cause systemic hypotension.<sup>150</sup> Thoracic surgeries are usually performed in the lateral position with an open chest and dramatically affect the relative distribution of ventilation and perfusion. Under these conditions, a diseased, nondependent lung may affect the pulmonary vascular response to hypoxia, as may surgical manipulation of the lung itself. Most studies in animal models or patients undergoing OLV did not demonstrate clinically significant attenuation of HPV by volatile anesthetics. Differences in shunt fraction, PVR, or oxygenation between isoflurane and sevoflurane anesthesia in patients undergoing OLV for lobectomy for lung cancer do not appear to be significant.<sup>151</sup> Some studies also demonstrated that shunt fraction is similar in patients receiving propofol or either isoflurane<sup>152</sup> or sevoflurane<sup>153,154</sup> during OLV. No significant differences in shunt fraction or arterial  $O_2$  tension were observed during intravenous infusions of ketamine, which does not inhibit HPV, and inhalation of enflurane. In contrast, isoflurane<sup>155,156</sup> and sevoflurane<sup>156</sup> impaired oxygenation and increased shunt fraction more than an intravenous infusion of propofol during OLV. However, the differences in oxygenation observed in these studies were small and clinically insignificant. The relative depth of anesthesia may affect interpretation of the differences in oxygenation between intravenous and volatile anesthetics in these studies. When doses of propofol and sevoflurane were chosen based on a similar depth of anesthesia, assessed by a bispectral index monitor, similar reductions in arterial oxygenation were observed in patients undergoing OLV.<sup>154</sup> Similar changes in shunt fraction and oxygenation were shown to occur with halothane,<sup>157</sup> isoflurane,<sup>151,157,158</sup> desflurane,<sup>158</sup> and sevoflurane in patients undergoing thoracotomy and OLV (Fig. 21.14).<sup>151,156-158</sup>

Convincing evidence suggests that all volatile anesthetics may be safely used in patients undergoing thoracotomy and OLV. The increase in shunt and the decrease in oxygenation caused by halothane or isoflurane<sup>157</sup> were consistent with an approximately 20% inhibition of HPV at 1 MAC. Instead of the expected 50% reduction in pulmonary blood flow in a hypoxic lung in the absence of a volatile anesthetic, blood flow decreases by 40% during hypoxia in the presence of 1 MAC isoflurane. This change in flow corresponds to an increase in pulmonary shunt by approximately 4% of the cardiac output. Carlsson and colleagues<sup>159</sup> applied multiple inert gas elimination techniques to measure the true shunt fraction in humans

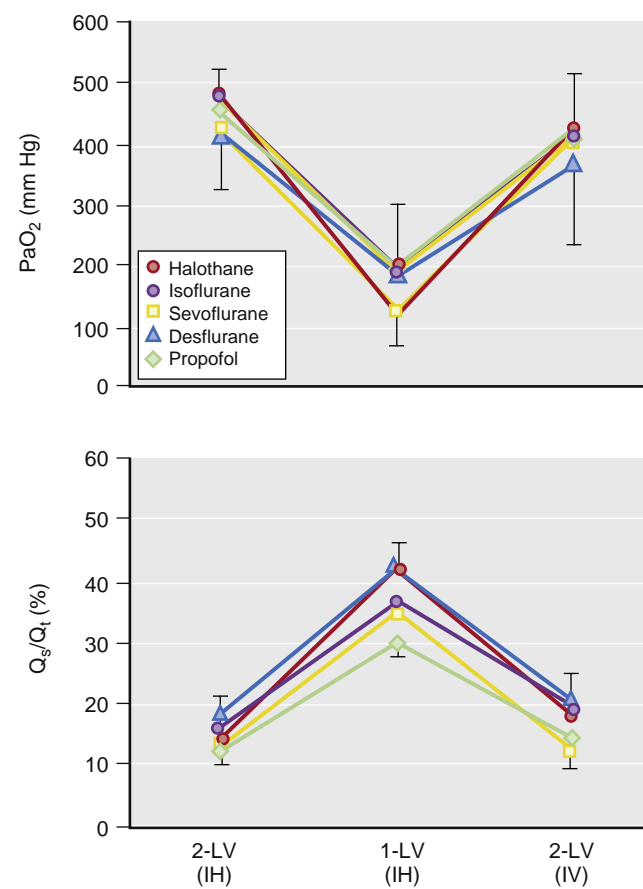


**Fig. 21.14** Partial arterial pressure of oxygen ( $PaO_2$ ) and intrapulmonary shunt fraction ( $Q_s/Q_t$ ) in patients with both lungs ventilated (2-LV) or with one lung ventilated (1-LV). Patients received an inhaled agent (IH) halothane, isoflurane, sevoflurane, or desflurane or the intravenous (IV) anesthetic propofol. Note the minimal effect on  $PaO_2$  and shunt fraction that occurs in changing from a volatile anesthetic to an IV agent. (Data modified from Abe and colleagues,<sup>148,153</sup> Benumof and colleagues,<sup>154</sup> and Pagel and colleagues.<sup>155</sup>)

anesthetized with volatile anesthetics and demonstrated a 2% to 3% increase in shunt fraction corresponding to approximately 20% HPV inhibition at 1.5% isoflurane. In addition, no significant effects on arterial oxygenation occurred with clinically relevant concentrations of isoflurane or enflurane. Indeed, the use of total intravenous anesthesia with propofol and alfentanil did not reduce the occurrence of hypoxemia during OLV, compared with a volatile anesthetic.<sup>152</sup>

Functionally, volatile anesthetics exert only mild, if any, inhibitory effects on HPV and oxygenation.<sup>160,161</sup> The relatively small inhibition of HPV should not significantly influence clinical decision making, especially considering the efficacy of drugs such as the peripheral chemoreceptor agonist, almitrine<sup>162</sup> (which enhances HPV), or inhaled NO (which selectively increases perfusion to adequately ventilated pulmonary regions). In addition, ventilatory strategies (e.g., nondependent lung continuous positive airway pressure, permissive hypercapnia) and fiberoptic bronchoscopy to ensure proper positioning of a double-lumen endotracheal tube help alleviate hypoxemia. The net effect of volatile anesthetics on HPV is multifactorial and depends on the direct effects of these agents not only on pulmonary vasomotor tone, but also by indirect actions that occur during anesthesia and surgery.

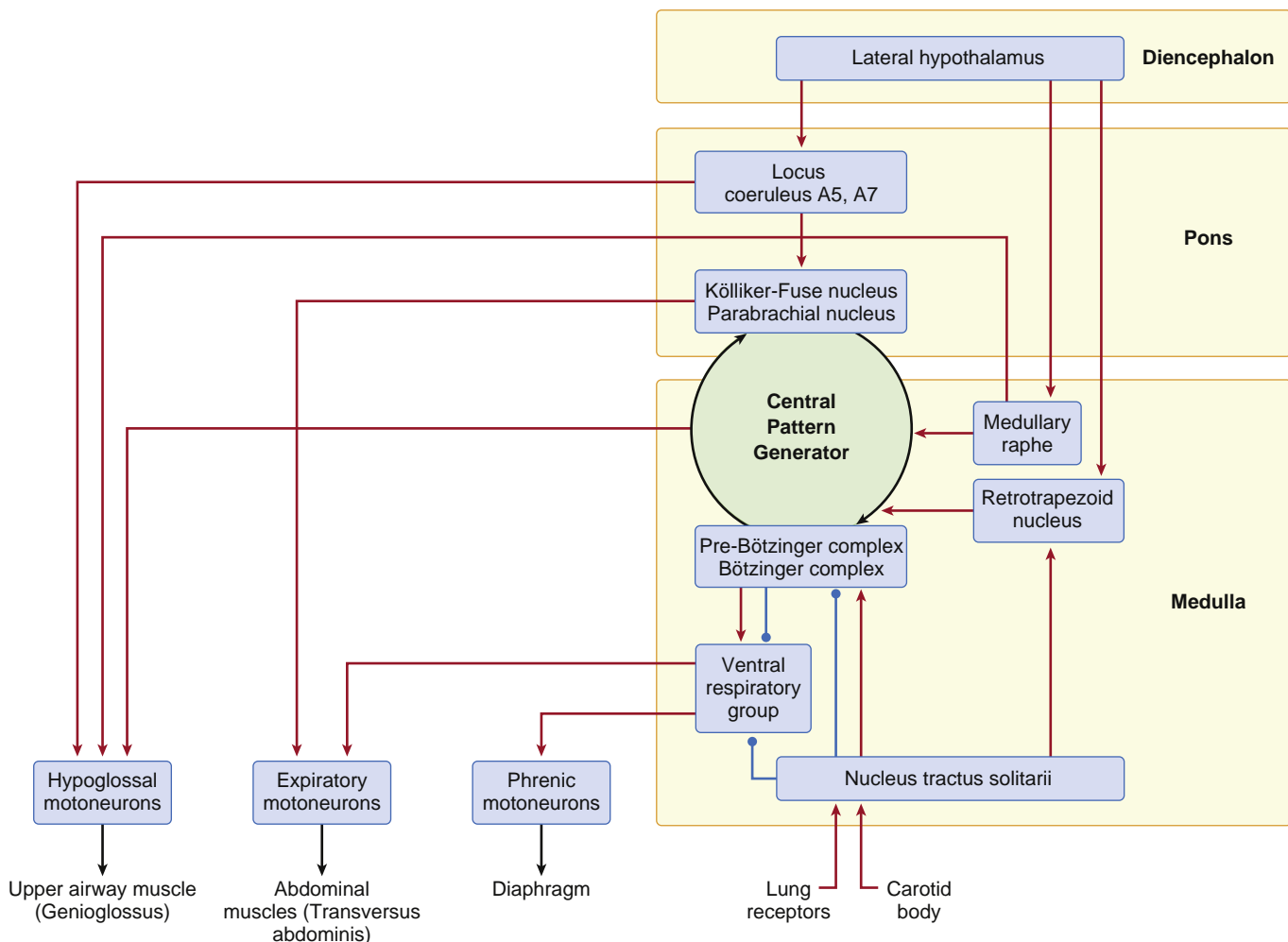


**Fig. 21.15** Anatomic components of the respiratory system and the main nuclei involved in the generation of respiration from chemoreception to motoneuron activation (see text for details). Wakefulness drive is derived from the lateral hypothalamus. The *central pattern generator*, where respiratory drive is converted into a respiratory pattern, is thought to consist of several nuclei in the medulla and pons. Potential sites of central chemoreception are the locus coeruleus, areas A5 and A7, in the pons, and the medullary raphe and retrotrapezoid nucleus in the medulla. Expiratory and inspiratory excitatory drive is relayed to premotor neurons (ventral respiratory group), which project to expiratory motoneurons and inspiratory motoneurons (e.g., phrenic nerve) in the spinal cord. These motor nerves innervate abdominal muscles (expiratory) and diaphragm (inspiratory). Respiratory pattern and chemoreception are influenced by afferents from the lungs and carotid bodies. Excitatory inputs (red arrows); inhibitory inputs (blue buttons).

## CONTROL OF RESPIRATION

### Components of the Respiratory Regulatory System

The regulation of respiratory function is very complex, occurs both on unconscious and conscious levels, and is precisely controlled by neuronal circuits, which are mainly located in the brainstem and include the medulla oblongata, pons, and midbrain (Fig. 21.15).

The neuronal networks in these areas are sufficient to generate involuntary, automatic breathing, which may be superseded by cortical centers for voluntary efforts such as speech, swallowing, laughing, sneezing, and coughing. Respiration *per se* is to ensure adequate gas exchange in order to meet metabolic demand during various levels of activity. Reflex inputs from the upper airways, lungs, and carotid bodies modulate respiration when inadequacy of gas exchange is sensed. Connections to the lateral hypothalamus also convey wakefulness drive to the respiratory center. Physiological status like sleep and pregnancy alter the

respiratory function; so does nonphysiological status such as sedation. This chapter is not intended to discuss respiratory physiology in detail. Rather, its focus is on the major regulatory components of the respiratory system and how they are affected by inhalational anesthetics (Fig. 21.16).

Readers are referred to [Chapters 13 and 41](#) for a detailed discussion of respiratory physiology and monitoring.

In general, respiratory drive is suppressed by all inhalational anesthetics except nitrous oxide.<sup>163,164</sup> Volatile anesthetics decrease glutamatergic excitatory drive to bulbo-spinal respiratory neurons and increase GABA<sub>A</sub>ergic inhibitory mechanisms at the postsynaptic neuronal membrane.<sup>165</sup> In hypoglossal upper airway motor neurons, volatile anesthetics hyperpolarize neuronal membrane resting potential by activating K<sup>+</sup> channels that are linked to serotonin or norepinephrine receptors.<sup>166,167</sup> The magnitude of respiratory depression by volatile anesthetics may also depend on the position of the neuron in the neuronal hierarchy, which extends from the neurons generating excitatory respiratory drive to the respiratory pattern generator

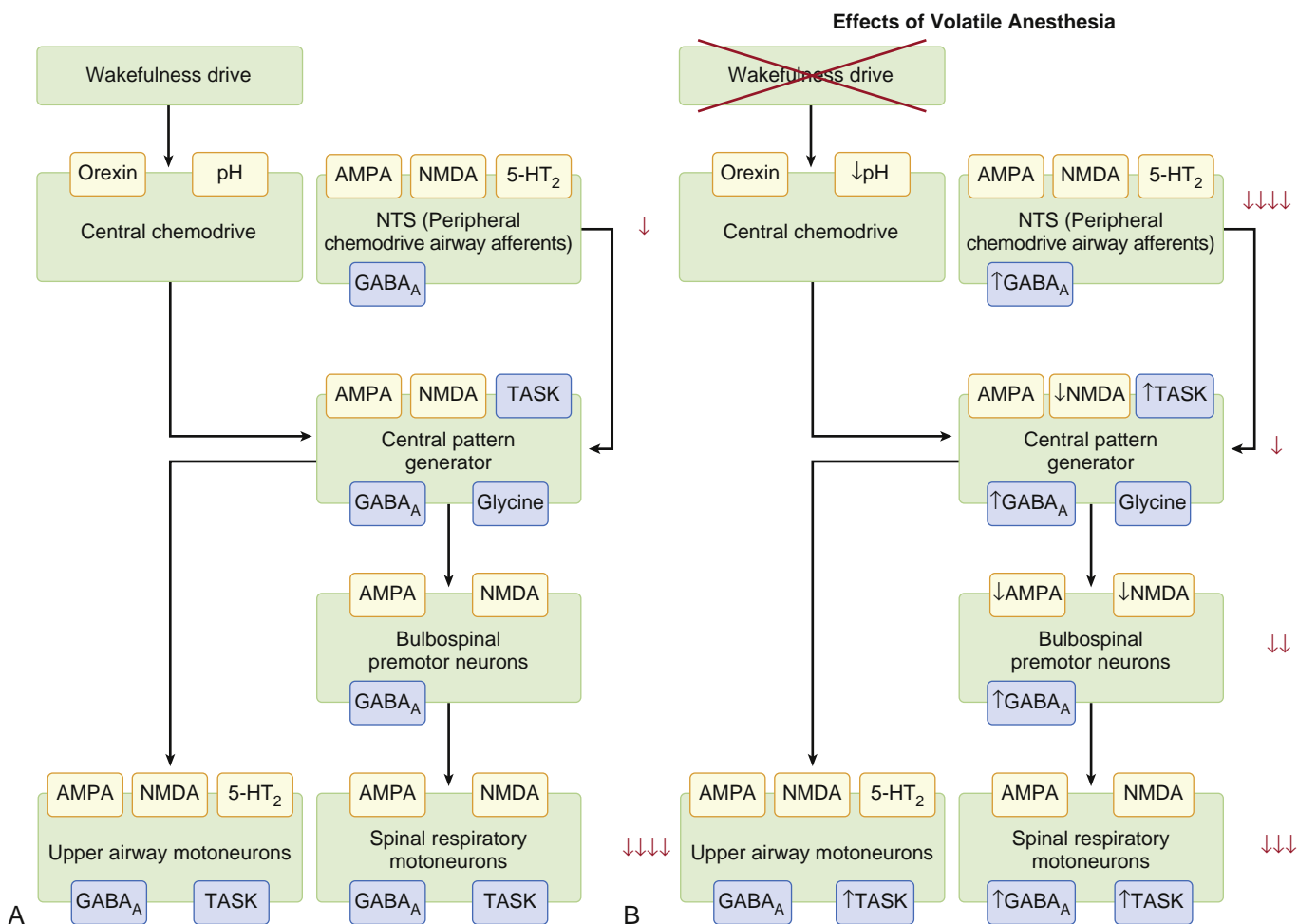


**Fig. 21.16** (A) Ligand-gated receptors and ion channels on respiratory-related neurons. Excitatory receptors and channels are marked in yellow, inhibitory in blue. Opening of pH sensitive channels excites the neuron, whereas the opening of two-pore domain, acid-sensitive potassium ( $K^+$ ) (TASK) channels causes membrane hyperpolarization and inhibition of neuronal discharge. (B) Effects of volatile anesthetics on respiratory-related neurons. Volatile anesthetics eliminate wakefulness drive to the respiratory system (red cross out). Black arrows indicate changes in receptor function (up, increase; down, decrease) that have been published in the literature. Volatile anesthetics reduce the presynaptic release of glutamate and  $\gamma$ -aminobutyric acid A ( $GABA_A$ ) in respiratory premotor neurons. The cumulative anesthetic effects on the respective neuron groups are depicted (red arrows). The relative magnitude of the depressant effect is visualized (number of arrows). In humans, peripheral chemodrive is significantly more depressed than central chemodrive. Upper airway motoneurons are significantly more depressed than inspiratory motoneurons.  $5-HT_2$ , 5-Hydroxytryptamine; AMPA, alpha-amino-3-hydroxy-5-methyl-4-isoxazolepropionate acid; NMDA, *N*-methyl-D-aspartate; NTS, nucleus of the solitary tract.

and down to the phrenic and hypoglossal respiratory output motor neurons (see Fig. 21.16). Consequently, volatile anesthetics, which strongly affect synaptic neurotransmission, have a greater depressant effect on polysynaptic neuronal circuits that include many synapses, compared with those comprised of only few neurons (paucisynaptic). Fortunately, most connections between the single components of the respiratory system seem to be paucisynaptic, which may explain a relative resistance of automatic breathing to the depressant effects of volatile anesthetics.

The depressant effect of inhalational anesthetics on respiratory system may be further demonstrated at the molecular and genetic levels. Heterozygous paired-like homeobox 2b (PHOX2B) gene mutations have been found in the majority of patients diagnosed with late-onset central hypventilation syndrome and may increase sensitivity of those patients to anesthetic-induced depression of breathing.<sup>168</sup> A recent study demonstrated that isoflurane can potentiate aggregation and mislocalization of PHOX2B variants, alter protein folding, and induce endoplasmic reticulum stress,

indicating a mechanism by which these agents may affect respiratory neuronal function after surgery and promote the onset of the neurologic respiratory disease.<sup>169</sup>

Importantly, most data on respiratory regulatory systems are derived from animal models and may not directly translate to humans, as summarized in a review by Forster and Smith.<sup>170</sup> This section will therefore cover important animal study results to help understand the basic respiratory structure and function, as well as present recent clinical studies demonstrating the correlation of those findings to clinical practice.

## CENTRAL CHEMORECEPTION

For many years, the prevailing view was that  $CO_2/H^+$  sensitivity was due exclusively to the central chemoreceptors. Recent studies showed that central chemoreceptors contribute about two thirds of the ventilatory response to  $CO_2/H^+$ , while peripheral chemoreceptors contribute about one third.<sup>170</sup> These excitatory chemodrive mechanisms ensure

automatic breathing under normoxic, normocapnic conditions in healthy individuals.<sup>170</sup> Central chemoreceptors discharge in response to the decrease in extracellular pH or an increase in  $[H^+]$ . In addition, they project to other areas of the respiratory system where they form excitatory synapses. This pathway is well recognized, but its exact location remains to be defined. Animal studies have pointed to multiple chemosensitive sites in the brainstem<sup>171</sup> including the retrotrapezoid nucleus (RTN), medullary raphe, locus coeruleus, nucleus tractus solitarius (NTS), lateral hypothalamus, and caudal ventrolateral medulla. The RTN is a particularly strong candidate as the absence of RTN likely causes severe central apneas in congenital central hypoventilation syndrome. Glial cells in these areas may also theoretically contribute to chemoreception through their effect on extracellular pH or by hypoxia- or  $CO_2$ -induced ATP release potentially altering the function of chemosensitive neurons.<sup>172</sup>

Central chemoreceptors also promote excitatory drive to neurons regulating upper airway patency and arousal from sleep.<sup>171</sup> The genioglossus muscle, considered a typical representative for the muscles maintaining upper airway patency, receives significant tonic and phasic excitatory drive in the conscious state. Genioglossal muscle activity is reduced during sleep, but high levels of inspiratory  $CO_2$  ( $>5\%$ ) are capable of recruiting near-normal levels of phasic activity. This phenomenon does not occur during rapid eye movement (REM) sleep because genioglossal muscle activity is absent, and therefore the upper airway collapses and hypoventilation follows.

Hypercapnia secondary to upper airway obstruction and hypoventilation may recruit the normal phasic activity of genioglossal muscle through central chemoreceptors and function as another mechanism (aside from hypoxia) by which patients with obstructive sleep apnea (OSA) arouse from sleep and reestablish airway patency. Residual subanesthetic concentrations of volatile anesthetics, which may be present for hours in postoperative patients, inhibit both peripheral hypoxic<sup>173</sup> and  $CO_2$  chemosensitivity<sup>174</sup> and may also substantially impair the spontaneous arousal and resolution of upper airway obstruction that would otherwise occur with severe hypoxia or hypercarbia. This is a particularly important issue to recognize for same-day surgery patients, especially with a history of OSA.<sup>175</sup>

## CENTRAL PATTERN GENERATOR

The cyclic breathing pattern is controlled by the central pattern generator (CPG). A recent review by Abdala and colleagues nicely summarizes the progress in the field.<sup>176</sup> Even though several models of the CPG network have been proposed, many of the circuit interactions and their functionalities remain unknown. CPG is believed to be located in nuclei of the pontomedullary network (see Fig. 21.15).<sup>177</sup> In the related nuclei, the network consists of excitatory and inhibitory neurons that control the inspiratory and expiratory phase of breathing. The breathing cycle is complexly regulated, and the type of neurons and the related neurotransmitters have been well illustrated (Fig. 21.17). This neuronal circuit can be pharmacologically modulated by inhaled anesthetics, affecting respiratory rate, upper airway patency, and relative contributions of the chest wall versus the diaphragm to tidal volume and minute alveolar ventilation.

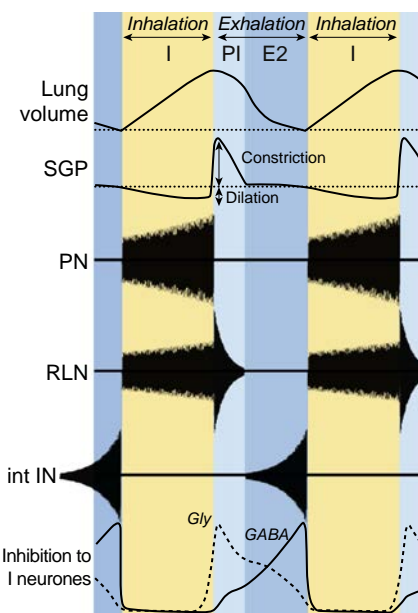


**Fig. 21.17 Schematic diagram of a three-phase respiratory cycle and its neuro-mechanical components.** Top schematic plots and neurograms represent lung volume, subglottal pressure (SGP), phrenic (PN), recurrent laryngeal (RLN), and internal intercostal (int IN) nerve activities during the three phases of a respiratory cycle, i.e., inspiration (I), postinspiration (PI), and late expiration (E2). Note that RLN conveys outputs from both abductor and adductor motoneurones, which fire respectively during inspiration (to dilate the glottis during inhalation) and postinspiration (to narrow the glottis during exhalation). Bottom overlay plots represent hypothetical time courses of glycine- (Gly, dotted line) and GABA-mediated (continuous line) inhibition to inspiratory (I) neurones during the respiratory cycle. These time courses reflect the activity of medullary postinspiratory (PI) inhibitory neurones, thought to be predominantly glycinergic, and GABAergic augmenting expiratory (E-AUG) inhibitory neurones active during E2 phase, both of which inhibit inspiratory neurones during expiration. Phasic inhibition of inspiratory neurones is minimal during inspiration, when active inspiratory neurones inhibit expiratory neurones, but rises abruptly during PI to orchestrate the inspiratory-expiratory phase transition and initiate exhalation. (Redrawn from Abdala AP, Paton JF, Smith JC. Defining inhibitory neurone function in respiratory circuits: opportunities with optogenetics? *J Physiol*. 2015;593[14]:3033–3046. Used with permission.)

## INTEGRATION OF PERIPHERAL INPUTS

Afferent inputs from the periphery reach the brainstem respiratory center and influence respiratory drive. These inputs include the carotid body chemoreceptors, vagal inputs from the lungs and airways, and pulmonary baroreceptor inputs. The carotid body is the major peripheral chemoreceptor. It senses hypoxia or hypercapnia, which in turn increases carotid sinus nerve discharge. This information then reaches the RPG via NTS glutamatergic neurons, which also targets rostral ventrolateral medulla presynaptic neurons thereby raising sympathetic nerve activity (SNA). Chemoreceptors also regulate presynaptic neurons and cardio VPN indirectly via inputs from the RPG.<sup>178</sup> In essential hypertension, OSA, and congestive heart failure, chronically elevated carotid body afferent activity contributes to increasing SNA but breathing remains unchanged or becomes periodic.

The function of the carotid body was discovered nearly 80 years ago, and for a long time it was thought that the carotid body chemoreceptors function independently from central chemoreceptors.<sup>179</sup> However, more recent studies

suggested that the peripheral and central chemoreceptors are not functionally separate but are interdependent. The sensitivity of the medullary chemoreceptors is critically determined by input from the peripheral chemoreceptors and possibly other breathing-related reflex afferents as well.<sup>170</sup> This effect might be mediated through interactions within the NTS and/or through NTS projections to parafacial respiratory group/RTN integrating neurons and/or through projections to neurons of a raphe-pontomedullary respiratory network.

Afferent vagal inputs from the lungs and airways are also relayed through the NTS. Pulmonary baroreceptor inputs project to second-order pump neurons in the NTS, which can provide both excitatory and inhibitory inputs to various parts of the medullary respiratory column. In general, pulmonary baroreceptor inputs promote the phase switch from inspiration to expiration. This vagal expiratory-facilitating reflex (Hering-Breuer reflex) is most prominent in immature mammals but also modulates respiratory phase-timing during resting ventilation in adult humans.<sup>180</sup> Although some of these inputs directly influence the CPG, others are integrated at the level of the bulbospinal or premotor neurons, which project to the motor neurons in the spinal cord.

### RESPIRATORY MOTOR OUTPUT AND UPPER AIRWAY PATENCY

The pontomedullary respiratory network generates the respiratory pattern and then projects to and controls respiratory motor outputs in the brainstem and spinal cord. The phrenic motor neurons are the main inspiratory neurons in the spinal cord. They are located at the levels C<sub>3</sub> to C<sub>5</sub> of the spinal cord and innervate the diaphragm.<sup>177</sup> Phrenic motor neurons are also directly depressed by volatile anesthetics.<sup>181</sup> Expiratory motor neurons are located at approximately T<sub>7</sub>-T<sub>12</sub> of the spinal cord and innervate truncal abdominal muscles that aid with forceful expiration and with expiratory expulsive efforts such as coughing. Expiratory motor neurons receive inputs from expiratory bulbospinal neurons and the pons.<sup>177</sup> The spinal motor neurons are the final neurons in the respiratory neuronal hierarchy. Their activity tends to be reduced by the cumulative effect of anesthetics on all previous steps of chemoreception and neurotransmission.

To ensure effective ventilation, inspiratory muscle activity needs to be closely coordinated with upper airway muscles that maintain airway patency. Central respiratory motor output almost simultaneously engages both the phrenic motor neurons (serving chest wall pump muscles) and hypoglossal motor neurons (serving pharyngeal muscle dilators).<sup>182,183</sup> The hypoglossal motor nerve innervates upper airway muscles, particularly the genioglossal muscle. The strength of excitatory and inhibitory drive to hypoglossal motor neurons strongly depends on the level of consciousness and differs between the REM and non-REM sleep phases.

The onset of the sleeping state results in a reduced tonic activation of upper airway dilator musculature and enhances collapsibility. This effect is especially problematic for patients with OSA whose airway is narrower, longer, and more collapsible than that of those without OSA. Patients with OSA critically rely on compensatory

activation of airway dilator muscles to maintain patency during wakefulness. The reduced lung volumes in obese recumbent patients during sleep also decrease caudal traction on the trachea, promoting pharyngeal collapse.<sup>184,185</sup> In addition, the loss of wakefulness removes an important vigilance component in the ventilatory control system, leaving the regulation of central respiratory motor output largely under chemoreceptor and mechanoreceptor feedback control.

The mechanisms of airway collapse during sleep and anesthesia are closely related. Hypoventilation and/or hypoxia secondary to upper airway collapse during anesthesia/sedation represent a significant challenge for anesthesia care providers, particularly in ambulatory surgery patients. The effect of inhalational anesthetics on pharyngeal airway collapsibility can best be illustrated by visualizing the changes as the depth of sedation increases.

### EFFECTS OF INHALED ANESTHETICS ON RESTING VENTILATION

Volatile anesthetics suppress conscious control of breathing at concentrations of less than 1 MAC and completely abolish conscious breathing drive at higher concentrations. Breathing is then largely controlled by automatic brainstem mechanisms and chemoreflex inputs. All volatile anesthetics also cause a dose-dependent decrease in minute ventilation at concentrations greater than 1 MAC because of a decrease in tidal volume. However, in a pressure chamber, Hornbein and colleagues demonstrated that nitrous oxide does not significantly reduce minute ventilation within 1.5 MAC (well beyond an atmosphere).<sup>186</sup> The respiratory rate typically increases for all inhalational agents tested, except for xenon, which causes a significant reduction in respiratory rate (Fig. 21.18). Indeed, there are several reports indicating that xenon can cause hypopnea or apnea.<sup>187,188</sup>

Most volatile anesthetics cause an increase in respiratory rate by producing a decrease in both inspiratory and expiratory duration, whereas opioids cause a very prominent decrease in respiratory rate that primarily results from a large increase in expiratory duration. However, the observed modest decrease in minute ventilation with volatile anesthetics could underestimate the magnitude of the respiratory depressant effects of these agents. This is due to volatile anesthetic-induced hypoventilation increasing PaCO<sub>2</sub> in a closed central chemoreflex feedback loop. In turn, central chemoreceptors are stimulated, thereby increasing central chemodrive to the respiratory center and increasing minute ventilation.<sup>199-202</sup>

### EFFECTS OF INHALED ANESTHETICS ON CHEMOREFLEXES

Volatile anesthetics impair peripheral chemoreceptor responses to hypoxia and hypercarbia in a dose dependent manner. In the presence of volatile anesthetic concentrations of 1 MAC or higher, breathing in humans is entirely dependent on the automatic control from the pontomedullary respiratory center and afferent excitatory inputs from the central chemoreceptors. These anesthetic concentrations lead to a complete depression of the peripheral chemoreflex loop with further respiratory depression rather than

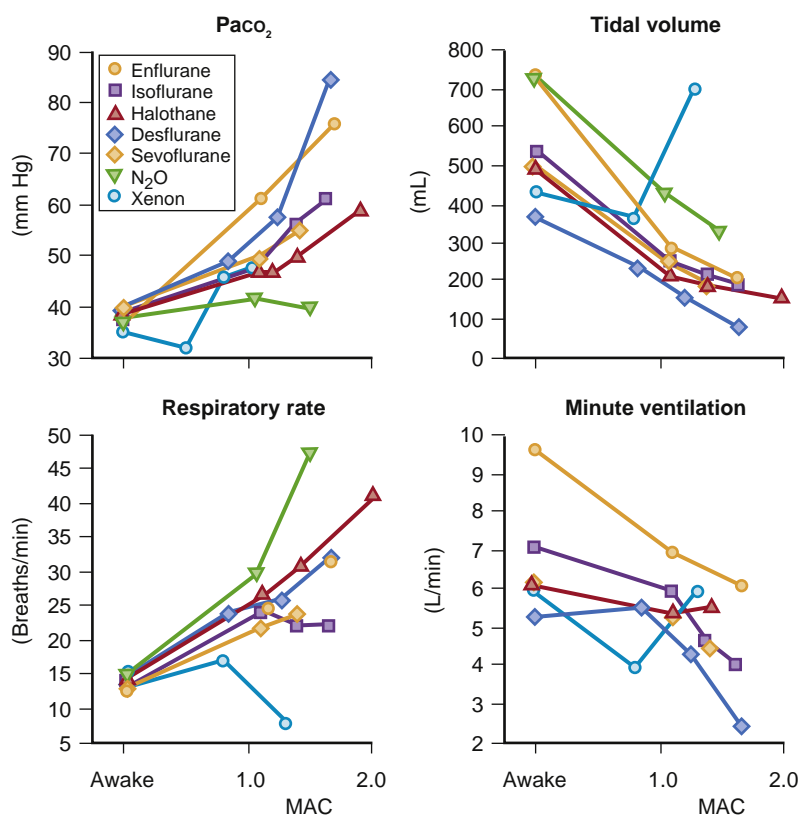


**Fig. 21.18** Comparison of mean changes in resting partial arterial pressure of carbon dioxide (PaCO<sub>2</sub>), tidal volume, respiratory rate, and minute ventilation in patients anesthetized with various inhaled agents. Most agents cause dose-dependent tachypnea, decreases in minute ventilation and tidal volume, and an increase in PaCO<sub>2</sub>. MAC, Minimum alveolar concentration, N<sub>2</sub>O, nitrous oxide.<sup>189-194</sup> Note: data for xenon has been extrapolated from references.<sup>195-198</sup>

stimulation in response to hypoxia.<sup>203</sup> Even very low concentrations of the agent (0.1 MAC of isoflurane and sevoflurane) depress the peripheral chemoreflex loop, without affecting the central chemoreflex loop. Desflurane at the same MAC showed no effect on peripheral and central CO<sub>2</sub> sensitivity.<sup>204</sup> A loss of upper airway muscle tone and function accompanies this process, as does differential depression of neurotransmission at the level of the spinal cord.<sup>205</sup>

The effect of inhaled anesthetics on respiratory drive may not be clinically relevant in the patient undergoing controlled ventilation. However, it does matter in spontaneously breathing patients. Because the suppressive effect of inhaled anesthetics on respiratory drive is synergistic with narcotics and frequently these two drug classes are administered concurrently, the suppression on the hypoxic and hypercarbic drive can increase the risk of postoperative respiratory complications.

### EFFECTS OF INHALED ANESTHETICS ON THE HYPERCAPNIC VENTILATORY RESPONSE

In awake humans, about one third of the CO<sub>2</sub>-mediated respiratory drive is through peripheral chemoreceptors and other two thirds through the central chemoreceptors. The respiratory drive mediated by the peripheral chemoreceptors is augmented by hypoxia.<sup>206</sup> However, the hypoxia-mediated component is abolished by the majority of volatile anesthetics at concentration even under 1 MAC. When the anesthetic concentration increases above 1 MAC, the peripheral

chemoreceptor-mediated portion of the CO<sub>2</sub> responsive respiratory drive are abolished, and only the central chemoreceptor loop remains functional.<sup>173,207-209</sup> Depression of the respiratory drive is often described in a quantitative manner by plotting the CO<sub>2</sub> response curve (an increase in PaCO<sub>2</sub> vs. an increase in minute alveolar ventilation). Volatile anesthetics also cause a rightward shift of the apneic threshold,<sup>210</sup> that is the minimum PaCO<sub>2</sub> required to initiate spontaneous respiration. Thus spontaneous breathing efforts do not occur if mechanical or assisted ventilation efforts drive the PaCO<sub>2</sub> levels below the CO<sub>2</sub> threshold during anesthesia.<sup>211</sup>

Patients under general anesthesia with volatile anesthetics become hypercarbic if they are spontaneously breathing without any ventilatory support. Pressure support ventilation is often used to counteract the suppression of the respiratory drive by the volatile anesthetics. However, it remains to be determined if an increase in pressure support would lead to a proportional increase in minute alveolar ventilation as the intrinsic CO<sub>2</sub> response curve at a given level of sedation is not altered. An increase in minute alveolar ventilation secondary to increased tidal volumes from pressure support may result in a decreased respiratory rate and therefore minute alveolar ventilation may not be increased as much as expected.

### EFFECTS OF VOLATILE ANESTHETIC ON THE HYPOXIC VENTILATORY RESPONSE IN HUMANS

Hypoxic ventilatory response (HVR) is rarely encountered in conscious healthy humans at sea level. However, for

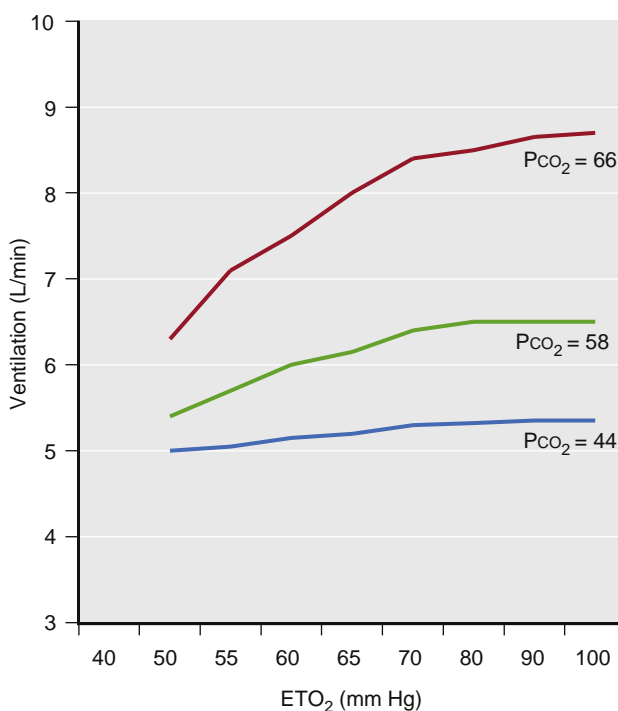


**Fig. 21.19** Effects of halothane anesthesia on the hypoxic ventilatory response in humans at three steady-state levels of partial pressure of carbon dioxide ( $\text{PCO}_2$ ). Halothane anesthesia (1.1 minimum alveolar concentration) completely eliminates the hypoxic ventilatory response and the hypoxic hypercapnic interaction at the peripheral chemoreceptors.  $\text{ETO}_2$ , End-tidal oxygen. (Modified from Knill RL, Gelb AW. Ventilatory responses to hypoxia and hypercapnia during halothane sedation and anesthesia in man. *Anesthesiology*. 1978;49:244. Used with permission.)

special occupations, such as tunnel workers at sea level, or mountain climbers staying at high altitude, hypoxia does occur and therefore the HVR becomes an important mechanism to compensate for low inspired  $\text{O}_2$  concentrations. One example is humans living at high altitude. At the top of Mt. Everest (8848 m), the partial pressure of  $\text{O}_2$  of ambient air is only about 50 mm Hg compared with 159.6 mm Hg at sea level. The corresponding arterial blood  $\text{PaO}_2$  is only 37.6 mm Hg, which is lower than the partial pressure of  $\text{O}_2$  in the mixed venous blood in healthy resting adults living at sea level. The estimated minute ventilation is approximately 166 L/min as a result of severe hypoxic hyperventilation.<sup>212</sup> However, this powerful compensation mechanism is significantly compromised under anesthesia with volatile anesthetics under 1 MAC and completely abolished at 1.1 MAC of halothane (Fig. 21.19). It is important to realize that even a subanesthetic concentration (0.1 MAC) of inhalational anesthetics profoundly diminishes hypoxic respiratory drive without concurrent use of narcotics.<sup>213</sup> The potency of the suppression of HVR has been proposed as the following order: halothane > enflurane > sevoflurane > isoflurane > desflurane.<sup>173</sup>

Certain patient populations are particularly vulnerable to the inhibition of hypoxic respiratory drive at subanesthetic concentrations, including premature infants and patients with OSA.<sup>214,215</sup> The depressant effect on the HVR is due to selective inhibition of the peripheral chemoreflex loop. The carotid body appears to be the most likely target. However, the mechanisms by which subanesthetic concentrations of

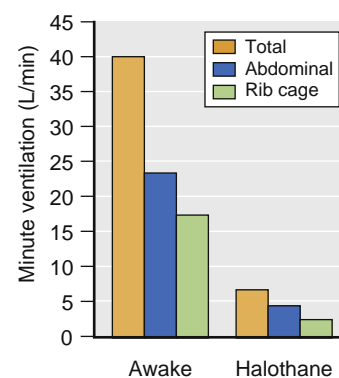


**Fig. 21.20** Effects of halothane anesthesia on rib cage and abdominal ventilation during hypercapnia (calculated ventilation at partial arterial pressure of carbon dioxide [ $\text{PaCO}_2$ ] of 55 mm Hg). Compared with being awake, halothane anesthesia strongly depresses minute ventilation. Halothane depresses the rib cage component to ventilation more than the abdominal component (diaphragmatic). Data are means. (Graph is based on data from Warner DO, Warner MA, Ritman EL. Mechanical significance of respiratory muscle activity in humans during halothane anesthesia. *Anesthesiology*. 1996;84:309.)

volatile anesthetics attenuate hypoxic ventilatory drive are not completely understood. Interestingly, acute pain and central nervous system arousal do not restore impaired HVR during sevoflurane sedation. Thus compromise of the central nervous system arousal state per se does not contribute to the impairment of the acute HVR by sevoflurane.<sup>216</sup> Additionally, audiovisual stimulation does not prevent the blunting of acute HVR by low-dose halothane, but by isoflurane. This finding raises the possibility that volatile anesthetics might differently affect the hypoxic chemoreflex loop.<sup>217</sup>

## EFFECTS OF INHALED ANESTHETICS ON RESPIRATORY MUSCLE ACTIVITY

Humans are bipeds and very different from the quadruped mammals in terms of contribution of various muscle groups, particularly the truncal muscles, to the normal respiratory effort, probably due to differences in posture. Thus the results of respiratory control studies in animals could not be directly extrapolated to humans, whether under normal resting conditions or under anesthesia. At quiet breathing in supine and conscious nonpregnant adult humans, scalene and parasternal inspiratory activity is universally present, but abdominal expiratory activity is absent.<sup>218,219</sup> This means that at quiet breathing, expiration is mostly passive and likely occurs via recoiling of chest wall and lungs. When breathing is stimulated by inhaling  $\text{CO}_2$ , the inspiratory activity is enhanced and expiratory muscles are recruited.

Volatile anesthetics, such as halothane, depress various respiratory muscles differently (Fig. 21.20). The diaphragm, as the main inspiratory muscle, is unique in that regard because it is relatively spared from the respiratory depression by volatile anesthetics, probably because of its low position in the hierarchy of the neurotransmission system. At 1 MAC of halothane, the tidal volume was reduced by 59%, respiratory rate was increased by 146%, and FRC was decreased by  $335 \pm 75$  mL. The decrease in minute ventilation could be because of rib cage/chest wall activity but is not because of a reduction in abdominal breathing,

and the contribution of the diaphragm is also substantially less affected.<sup>220</sup> Abdominal expiratory activity is routinely recruited during halothane anesthesia in male subjects.

The depressive effect of halothane on respiratory muscle is also gender dependent. Of note, pregnancy significantly alters the physiology and contribution of each respiratory muscle groups. The reduction in FRC is from both remaining activity of expiratory transverse abdominal muscles, which reduces thoracic volume, and cephalad motion of diaphragm. Paradoxical rib cage motion develops in some subjects during halothane anesthesia, such that the rib cage continues to expand during the first portion of expiration. Such paradoxical rib cage motion is exaggerated during a CO<sub>2</sub>-stimulated rebreathing.<sup>218,220</sup>

## EFFECTS OF INHALED ANESTHETICS ON THE UPPER AIRWAY

Inspiratory upper airway patency is maintained by the cortical wakefulness drive, fully preserved chemical chemoreceptor sensitivity and chemodrive transmission, and an optimal reflex feedback from upper airway receptors in the conscious state. These upper airway receptors are activated by the negative pressure and airflow<sup>221,222</sup> that are generated by the inspiratory muscles (e.g., diaphragm, respiratory chest wall muscles). During sleep or volatile anesthesia, the cortical wakefulness drive is absent, and the sensitivity of the chemoreceptors and upper airway receptors is decreased. Thus both phasic and tonic inspiratory excitatory drives to the upper airway muscles are decreased or entirely absent. The loss of tone in the upper airway muscles (genioglossus and other pharyngeal muscles) predisposes individuals with anatomic limitations to upper airway obstruction.<sup>223,224</sup> Even in the presence of subanesthetic concentrations of volatile anesthetics (frequently in immediate postoperative period), the cortical wakefulness drive, the drive from peripheral chemoreceptors, and excitatory inputs from upper airway mechanoreceptors are all significantly impaired. This may lead to partial or even complete upper airway obstruction, a situation that can be further complicated by inhibition of hypoxia-mediated arousal reflexes.<sup>203</sup>

## EFFECTS OF INHALED ANESTHETICS ON DEFENSIVE AIRWAY REFLEXES

Humans have very effective protective mechanisms to prevent aspiration by closing glottis and coughing. Volatile anesthetics ( $\geq 1$ -1.3 MAC) progressively abolish defensive airway reflexes. The loss of airway protection against gastroesophageal reflux with consequent aspiration of orogastric content into the trachea can be catastrophic. However, lower concentrations of volatile anesthetics may paradoxically enhance and prolong the duration of protective defensive reflexes. Laryngospasm is the sustained and complete reflex glottic closure in response to foreign material (e.g., oral secretions) contacting the vocal cords, or to a poorly timed noxious stimulus (e.g., pain from incision, venipuncture) during the administration of inadequately low concentrations of a volatile anesthetic. This occurs

during induction before anesthesia reaches adequate depth and during emergence when the agent is washing out but not completely eliminated. A recent study also showed that laryngospasm could still be observed in 18% of children under deep anesthesia with sevoflurane, but higher concentration (4.7% = MAC<sub>ED95</sub> intubation) provided better protection from laryngospasm as compared with lower concentration (2.5% = 1 MAC).<sup>225</sup>

Not all volatile anesthetics are equally prone to elicit unwanted sustained defensive airway reflexes. Desflurane and isoflurane appear to be the most irritating to the airways; neither anesthetic is recommended for an inhaled induction of anesthesia. The maintenance and emergence from desflurane anesthesia caused more severe adverse airway events than did isoflurane anesthesia in spontaneously breathing infants and children with an LMA, especially when the LMA was removed before emergence.<sup>226</sup> Sevoflurane has the most favorable profile and is frequently used for inhalational induction in the pediatric population.

## INHALED ANESTHETICS AND ACUTE LUNG INJURY

### Pathophysiology of Sepsis-Induced Acute Lung Injury

ALI represents the pulmonary manifestation of a global inflammatory process that is commonly associated with gram-negative bacterial sepsis.<sup>227-230</sup> Derangements of pulmonary hemodynamics,<sup>231</sup> fluid filtration, and gas exchange are pathophysiological manifestations.<sup>232</sup> Bacterial endotoxin often triggers ALI.<sup>233</sup> In addition, other humoral and cellular cascades are involved, such as eicosanoids,<sup>234</sup> cytokines, O<sub>2</sub> free radicals, endothelin,<sup>235</sup> NO, as well as the coagulation, the NOTNOT complement,<sup>236</sup> the fibrinolytic, and the kinin/kallikrein systems,<sup>237</sup> as well as degradation fragments of NOT extracellular matrix.<sup>238</sup>

It is now well established that NO is involved in the pathogenesis of sepsis and sepsis-induced ALI. In hyperdynamic sepsis, increased iNOS-dependent formation of NO and, subsequently, cGMP is associated with myocardial depression, reduced contractile responses to vasoconstrictor agents, and circulatory shock.<sup>239</sup> In addition, NO may mediate cytotoxic effects following its reaction with the superoxide anion to yield the strong oxidant anion peroxynitrite and eventually its breakdown cytotoxic product OH<sup>•</sup>.<sup>240</sup> Large amounts of NO may also activate enzymes in the cyclooxygenase pathway and modify gene expression.<sup>241</sup> Interaction of NO with many molecular targets represents a pathway for its breakdown and inactivation. The most important is the reaction of NO with molecular O<sub>2</sub> to form nitrite, which in the presence of hemoproteins (i.e., hemoglobin) is oxidized further to nitrate.<sup>242</sup>

Moreover, NO may attenuate HPV, thereby contributing to derangement of gas exchange.<sup>243</sup> The latter changes may cause tissue hypoxia and microvascular damage that may result in multiple organ failure and death. However, in less extreme conditions, generation of minute amounts of NO by eNOS and/or iNOS might be protective. Vasodilatation may enhance tissue perfusion. NO inhibition of platelet adhesion and aggregation may produce antithrombotic effects. NO scavenging of superoxide anions and other free radicals

and inhibition of leukocyte-endothelial cell adhesion may prevent crucial steps in the inflammatory reactions. Finally, stimulation of cGMP production may preserve the integrity of the microvascular barrier.<sup>244,245</sup>

### EFFECTS OF INHALED ANESTHETICS ON EXPERIMENTAL SEPSIS-INDUCED ACUTE LUNG INJURY

There is a substantial debate surrounding the choice of anesthetic regimens for patients with ALI that require surgery. Animal studies suggest an important antiinflammatory role of volatile anesthetics in ALI. Pretreatment with sevoflurane significantly reduced the inflammatory response and attenuated LPS-induced chemotaxis of neutrophils from alveolar type II cells.<sup>246</sup> Compared with thiopental anesthesia, pigs anesthetized with sevoflurane exhibited decreased expression of TNF $\alpha$  and IL-1 $\beta$  in lung tissue.<sup>247</sup> Volatile anesthetics exert other antiinflammatory effects including reduction of proinflammatory cytokine production in alveolar type II cells, reduction of neutrophil migration into the lung interstitium and alveolar space, and decreased protein leakage and pulmonary edema.<sup>248-250</sup> In a rat model, LPS-induced ALI was markedly attenuated by sevoflurane compared with propofol anesthesia. Rats receiving sevoflurane demonstrated improved gas exchange, reduced amounts of albumin and total cell count in bronchoalveolar lavage fluid, and lower cytokine levels in bronchoalveolar lavage fluid and RNA levels in lung tissue compared with rats receiving propofol. Sevoflurane, but not propofol, also decreased the amount of pulmonary edema most likely through a reduction in edema formation rather than water reabsorption.<sup>249</sup> When administered after the onset of oleic acid-induced ALI in dogs, sevoflurane reduced the elevated PA pressure and PVR, attenuated pulmonary edema as evidenced by reduced extravascular lung water index, and decreased TNF $\alpha$  production and diffuse alveolar damage score compared with propofol. However, despite of these effects, sevoflurane worsened systemic oxygenation possibly via inhibition of HPV.<sup>251</sup> In a rat model of cecal ligation and puncture (CLP)-induced sepsis, both sevoflurane and isoflurane attenuated inflammatory response, lipid peroxidation, oxidative stress, and improved survival. Furthermore, sevoflurane was more effective in modulating sepsis-induced inflammatory response.<sup>252</sup> Induction of heme oxygenase-1 and suppression of iNOS expression provide cytoprotection in lung and vascular injury. In a rat model of ALI induced by CLP, the isoflurane posttreatment reduced pulmonary microvascular permeability, as well as lung injury as assessed by histological and immunohistochemical examinations. Furthermore, isoflurane decreased iNOS and increased heme oxygenase-1 expression in lung tissue. These findings suggest that the protective role of isoflurane postconditioning against CLP-induced ALI may be associated with its role in upregulating heme oxygenase-1.<sup>253</sup>

### INHALED ANESTHETICS AND VENTILATOR-INDUCED LUNG INJURY

Mechanical ventilation is a life-saving clinical treatment, but it can also produce pulmonary inflammatory changes and injury known as ventilator-induced lung injury (VILI). Cyclic stretching of the lung during mechanical ventilation

releases proinflammatory cytokines such as IL-1 and MIP-2 leading to pulmonary neutrophil accumulation; enhances activity of phospholipase A<sub>2</sub>, which degrades surfactant; and results in pulmonary edema, hyaline membrane formation, and cellular infiltration.<sup>254</sup> Volatile anesthetics have been shown to attenuate lung injury due to mechanical ventilation. In mice, mechanical ventilation led to induction of lung injury, reactive O<sub>2</sub> species production, proinflammatory cytokine release, and neutrophil influx. Sevoflurane post-treatment reduced histological signs of VILI, as well as prevented increased production of reactive O<sub>2</sub> species, release of IL-1 $\beta$  and MIP-1 $\beta$ , and neutrophil transmigration.<sup>255</sup> Similarly, isoflurane reduced VILI in mice, as indicated by reduced inflammation, transmigration of neutrophils, and cytokine levels. Phosphorylation of Akt protein was significantly increased during mechanical ventilation with isoflurane. Inhibition of phosphoinositide 3-kinase/Akt signaling before mechanical ventilation completely reversed the lung-protective effects of isoflurane. These findings suggest that isoflurane-mediated pulmonary protection is mediated via phosphoinositide 3-kinase/Akt signaling.<sup>256</sup> Moreover, in a murine two-hit model of LPS-induced inflammation followed by VILI, isoflurane exposure before initiation of mechanical ventilation ameliorated VILI by improving both lung mechanics and vascular leakage. In addition, isoflurane prevented a decrease of a key tight junction protein (zona occludens 1) in lung tissue and lung epithelial cells.<sup>257</sup> In another study in murine VILI, animals anesthetized with isoflurane and sevoflurane showed thinner alveolar septa, lower VILI scores, lower polymorph neutrophil counts, lower IL-1 $\beta$  concentrations, less reactive O<sub>2</sub> species production, and higher glutathione contents compared to ketamine-anesthetized mice. Unexpectedly, desflurane-ventilated mice showed signs of lung injury similar to mice receiving ketamine anesthesia. Desflurane also failed to inhibit inflammatory responses and reactive O<sub>2</sub> species production in lung tissue.<sup>258</sup>

### INHALED ANESTHETICS AND LUNG ISCHEMIA-REPERFUSION

Lung ischemia-reperfusion (IR) injury is a hallmark of many lung diseases, and it also occurs during surgical procedures such as lung transplantation. The re-establishment of blood flow and O<sub>2</sub> delivery into the previously ischemic lung exacerbates the ischemic injury and leads to increased microvascular permeability and PVR as well as activation of the immune response. These events trigger ALI with subsequent edema formation that can result in systemic hypoxemia and multiorgan failure. Reactive O<sub>2</sub> and nitrogen species have been suggested as crucial mediators of such responses during IR in the lung.<sup>259</sup> Isoflurane attenuated increases in PVR and the filtration coefficient and the wet-to-dry ratio in isolated rabbit lungs subjected to IR.<sup>260</sup> Isoflurane also protected against warm IR injury in an isolated, perfused rat lung model when it was administered after the onset of ischemia.<sup>261</sup> Moreover, reductions in inflammatory responses and oxidative stress were observed during sevoflurane compared with propofol anesthesia in a porcine model of IR injury.<sup>262</sup> In a rat lung transplantation model, preconditioning and postconditioning using sevoflurane significantly improved the oxygenation of lung grafts and decreased pulmonary edema. Sevoflurane treatment also reduced levels of

IL-1 $\beta$ , IL-6, and TNF $\alpha$ . In addition, sevoflurane significantly inhibited cell apoptosis by a decrease in cytochrome C release into cytosol and caspase-3 cleavage.<sup>263</sup> In contrast, pretreatment with desflurane exacerbated IR injury in isolated rabbit lungs perfused with saline by increasing pulmonary microvascular permeability and NO production.<sup>264</sup> Furthermore, postconditioning with xenon during prolonged ex vivo lung perfusion did not improve graft function in a porcine warm ischemic lung injury model.<sup>265</sup>

## CLINICAL EVIDENCE

Clinical evidence supports potential beneficial effects of volatile anesthetics in ALI. For example, short-term positive pressure ventilation with high tidal volumes did not affect cytokine production in the lungs of healthy patients anesthetized with isoflurane.<sup>266</sup> Several studies investigated the effects of volatile anesthetics in patients undergoing thoracic surgery with OLV.<sup>267-269</sup> OLV is associated with hypoxia-reoxygenation injury in the deflated and subsequently reventilated lung. OLV increased the release of proinflammatory mediators in both the dependent and the nondependent lung.<sup>268</sup> Sevoflurane suppressed local alveolar inflammatory responses and cytokine release compared with propofol. Furthermore, the antiinflammatory effects of sevoflurane were greater in the dependent compared with the nondependent lung.<sup>268,269</sup> Patients receiving sevoflurane also had an improved postoperative course as indicated by a shorter ICU stay and fewer adverse events including pneumonia, pleural effusion, and bronchopleural fistula compared with those anesthetized with propofol.<sup>267</sup> In addition, a recent meta-analysis in cardiac surgical patients demonstrated that volatile as opposed to intravenous anesthesia is associated with a significant reduction in pulmonary complications and overall mortality.<sup>270</sup> However, in a randomized multicenter controlled trial in patients scheduled for surgery with OLV, the incidence of major complications during hospitalization and within 6 months from surgery was similar in propofol and desflurane groups.<sup>271</sup> This finding seems to be in agreement with an earlier study demonstrating that in healthy surgical

patients desflurane increased lipid peroxidation as measured in BALF, indicating injury to the pulmonary alveolar membranes. Sevoflurane caused less pronounced effects, suggesting that it may exert a protective effect compared with desflurane.<sup>272</sup> Proinflammatory response and elevated levels of TNF $\alpha$ , IL-1 $\beta$ , and IL-6 in healthy patients undergoing tympanoplasty were also more evident following desflurane anesthesia compared with sevoflurane.<sup>273</sup>

In a recent parallel, open-label, single-center randomized controlled trial, adult patients with moderate-to-severe ARDS were randomized to receive either intravenous midazolam or inhaled sevoflurane for 48 hours. On day 2,  $\text{PaO}_2/\text{FiO}_2$  ratio was significantly higher in the sevoflurane group than in the midazolam group. There was also a significant reduction in cytokines and the soluble form of the receptor for advanced glycation end-product levels in the sevoflurane group, compared with the midazolam group. No serious adverse events were observed with sevoflurane. This study suggests therapeutic utility of inhaled sevoflurane in patients with ARDS.<sup>274</sup> Moreover, the use of inhaled anesthetics in the ICU is conceptually appealing as they offer a safe, effective, and easily titratable method of sedation. A recent retrospective analysis of patients receiving inhaled sedation in the ICU suggests an association between its use and reductions in one-year and in-hospital mortality, perhaps related to a significant increase in ventilator-free days compared to sedation with intravenous agents.<sup>275</sup> Prospective randomized clinical trials are needed to further elucidate the therapeutic potential of inhaled anesthetics in intubated patients with ALI/ARDS and ICU patients requiring long term sedation.

## Nonvolatile Inhaled Agents

The pharmacokinetics of all inhalational anesthetics follow the same principle. At initial uptake, the dynamic change of the ratio of the fraction of a gas in alveoli (FA) to its fraction in the inspiratory gas (FI) (FA/FI) is dependent on initial FI, solubility of the anesthetic, minute alveolar ventilation, and cardiac output. **Fig. 21.21**

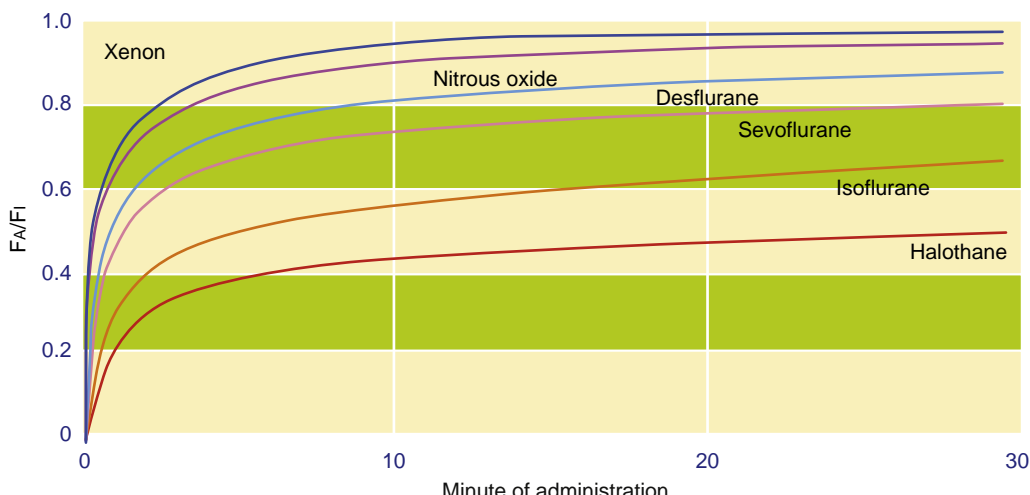


**Fig. 21.21 Pharmacokinetics of the inhalational anesthetics.** The rise in alveolar (FA) anesthetic concentration towards inspired (FI) is most rapid with the least soluble anesthetic, N<sub>2</sub>O, and slowest with the most soluble, methoxyflurane. All data from human studies (Data from Yashuda N, Lockhart SH, Eger EI II, et al. Kinetics of desflurane, isoflurane and halothane in humans. *Anesthesiology* 74:489-498, 1991; & *Anesth Analg* 72:316-24, 1991; Data for Xenon only recently available).

demonstrates the dynamic changes in FA/FI of inhalational anesthetics during the phase of uptake. Because xenon has the lowest solubility among the all inhalational anesthetics, it reaches equilibrium quickly, and even faster than nitrous oxide. The speed of washout of anesthetics also follows the same principle but in the reverse direction. Among the four factors affecting washout (solubility, fresh gas flow rate, minute alveolar ventilation, and cardiac output), fresh gas flow is the only one the provider can fully control besides partially controlling minute alveolar ventilation. Adequate fresh gas flow plays an important role in preventing rebreathing expired gas and affects the rate of its elimination. Fresh gas flow has to be higher than the peak inspiratory flow rate for the adult breathing circuit. If a tidal volume is 500 mL, respiratory rate is 10, and I:E ratio is 1:2, the inspiratory phase is 4 seconds. The mean inspiratory flow rate is 500 mL/4 seconds, 125 mL/s, or 7500 mL/min. Therefore maximal O<sub>2</sub> flow rate of 10 to 15 L/min for any given modern ventilator should be large enough to prevent rebreathing expired gas. For circuits used in pediatric patients, the minimal fresh gas flow rate for preventing rebreathing is dependent on the type of the circuit. In the following section, two commonly used nonvolatile gases, xenon and nitrous oxide, are discussed with focus on their clinically related aspects.

## NITROUS OXIDE

Advantages of nitrous oxide (N<sub>2</sub>O) are well established including the ability to quickly reach its target MAC value and quick washout. N<sub>2</sub>O does not significantly interfere with respiratory drive and has no negative impact on bronchial mucosa or bronchial smooth muscle activity in healthy individuals. N<sub>2</sub>O enhances catecholamine release and does not reduce systemic vascular resistance or cardiac output, maintaining hemodynamic stability. Because its MAC value is 104%, N<sub>2</sub>O cannot be used as a sole anesthetic at 1 atmosphere pressure to achieve adequate sedation. However, because it is odorless, it is often used as an adjuvant at the beginning of inhalational induction, especially in pediatric patients, prior to administration of volatile anesthetics. It is also commonly used for analgesia and sedation for dental procedures.<sup>276</sup> Its use for labor pain has faded but it is still used for labor analgesia in some centers.<sup>277</sup>

### Sedative and Analgesic Effects

Nitrous oxide has both sedative and analgesic effects. Because MAC is determined as the threshold of an individual's response to the painful stimulation of skin incision, and N<sub>2</sub>O is analgesic, it is difficult to dissect its sedative from analgesic effects. Therefore the sedative potency of N<sub>2</sub>O at equal MAC values is different from other inhalational anesthetics which do not possess analgesic effects. The MAC of N<sub>2</sub>O and other inhalational anesthetics are additive relative to a subjects' movement in response to nociceptive stimulation, but not necessarily when it comes to the level of sedation. For most volatile anesthetics, MAC awake is approximately 0.3 MAC value.<sup>278</sup> However, the MAC awake of N<sub>2</sub>O is 0.61 MAC (63.3%).<sup>278</sup> Even at 50% of N<sub>2</sub>O or 0.48 MAC, the majority of adults may be conscious. Clinicians often use N<sub>2</sub>O at the end anesthesia in order to facilitate washout of a

volatile anesthetic. Even though the sum of the MAC values of the volatile anesthetic and that of N<sub>2</sub>O is above the MAC awake value of the volatile anesthetic alone, this does not guarantee the unconsciousness of the patient. Awareness may occur even though it may not be associated with post-operative recall.<sup>279</sup>

In humans, the analgesic effect of 66% to 70% of N<sub>2</sub>O is equal to that of an intravenous infusion of remifentanil at 0.085 to 0.17 mg/kg/min, or a whole-blood concentration of 2 ng/mL.<sup>280,281</sup> Analgesic potency of N<sub>2</sub>O can be attenuated by sevoflurane (Fig. 21.22).<sup>282</sup> The detailed pathway of its analgesic action remains to be determined. However, animals tolerant to N<sub>2</sub>O are cross-tolerant to morphine,<sup>283</sup> and the analgesic effect of N<sub>2</sub>O can be reversed by naloxone.<sup>284</sup> This means that at least in part, the analgesic action of N<sub>2</sub>O occurs via the mu opioid receptor. Small animals develop tolerance quickly (6-24 hours) following continuous administration of N<sub>2</sub>O.<sup>284</sup> Humans can also develop acute tolerance to N<sub>2</sub>O in only 40 minutes.<sup>285</sup> In clinical practice, N<sub>2</sub>O is commonly administered for several hours. However, it is to be determined whether its sedative and/or analgesic effects remain during prolonged administration.

### Gas Volume Expansion

Nitrous oxide has greater diffusibility across tissues than nitrogen. Therefore N<sub>2</sub>O would diffuse into any closed air-containing space, more specifically any nitrogen-containing space, more quickly than nitrogen diffuses out, resulting in gas volume expansion. One of the major concerns related to this gas expansion effect is bowel dilatation.<sup>286</sup> However, this observation is based on surgical procedures lasting 3 hours. The increase in pressure and volume in a closed space due to accumulation of N<sub>2</sub>O is dependent of the duration of exposure and pressure

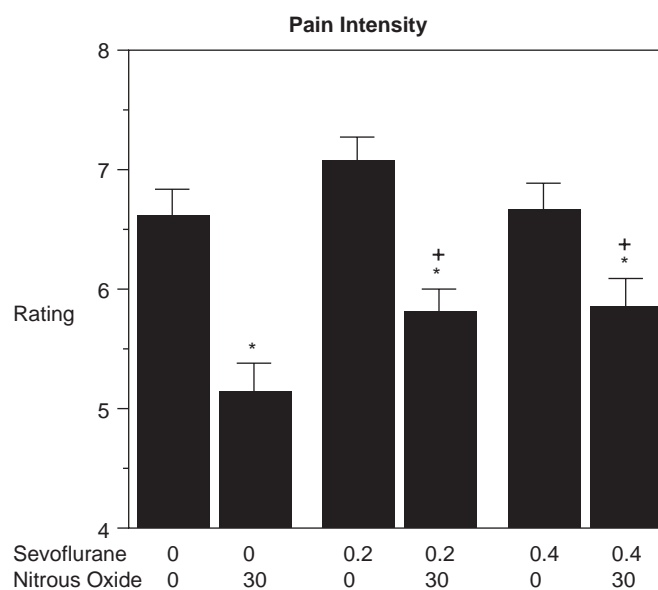


**Fig. 21.22 Effects of sevoflurane and nitrous oxide on ratings of pain intensity to cold.** Each bar is the mean across all subjects. Brackets represent SEM. \*Significant decrease from placebo (0% sevoflurane/0% nitrous oxide) ratings. +Significant increase from the 0% sevoflurane/30% nitrous oxide ratings. (Redrawn from Janiszewski DJ, Galinkin JL, Klock PA, et al. The effects of subanesthetic concentrations of sevoflurane and nitrous oxide, alone and in combination, on analgesia, mood, and psychomotor performance in healthy volunteers. *Anesth Analg*. 1998;88(5):1149-1154. With permission.)

### Right Ventricular Ejection Fraction

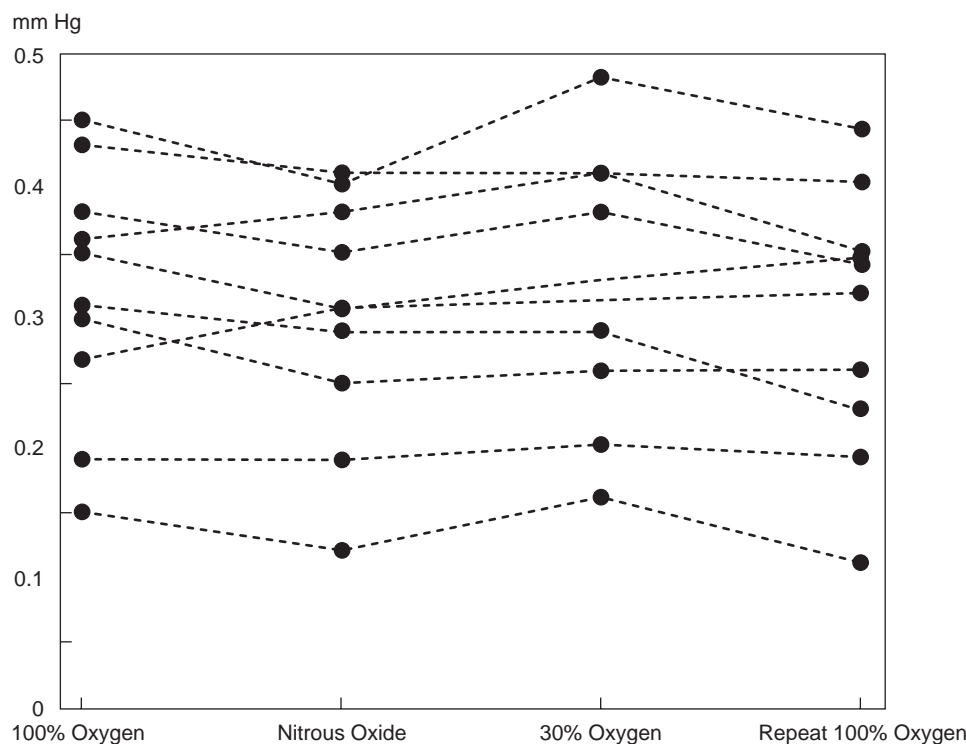


**Fig. 21.23** Individual patient responses in mean pulmonary arterial pressure (mm Hg) to nitrous oxide administration. (Redrawn from Konstadt SN, Reich DL, Thys DM. Nitrous oxide does not exacerbate pulmonary hypertension or ventricular dysfunction in patients with mitral valvular disease. *Can J Anaesth*. 1990;37(6):613-617. With permission.)

gradient of  $\text{N}_2\text{O}$ . Briefly using  $\text{N}_2\text{O}$  for periods of 15 to 20 minutes during emergence enhances washout of volatile anesthetics and may not lead to clinically relevant bowel dilation.

#### Nausea And Vomiting

Postoperative nausea and vomiting (PONV) is a common complication of  $\text{N}_2\text{O}$ .<sup>287</sup> However, a recent meta-analysis demonstrated that  $\text{N}_2\text{O}$ -related PONV is clinically insignificant following a less than 1 hour exposure.<sup>288</sup> The authors suggested that a minor risk of PONV should not preclude  $\text{N}_2\text{O}$  use for a limited time period, such as for minor or ambulatory surgeries. Even though others questioned the methodology of the meta-analysis,<sup>289,290</sup> the trend consistently suggests that the incidence of PONV is associated primarily with the *duration* of  $\text{N}_2\text{O}$  exposure. Therefore clinicians can take advantage of the beneficial properties of  $\text{N}_2\text{O}$ , especially at the end of an anesthetic, to facilitate the washout of volatile agents and shorten the time of emergence.

#### Pulmonary Hypertension

Several studies were conducted to test whether  $\text{N}_2\text{O}$  worsens pulmonary hypertension with no consistent conclusions due to variation of the experimental protocols. In an earlier study, Konstadt and colleagues demonstrated no significant changes in PA pressure and cardiac output in patients with pulmonary hypertension when 70%  $\text{N}_2\text{O}$  versus 70% nitrogen was used (Fig. 21.23).<sup>291</sup> The authors concluded that  $\text{N}_2\text{O}$  does not have adverse effects on the pulmonary circulation or right ventricular function, and may be used with

appropriate monitoring in patients with pulmonary hypertension. This conclusion should be interpreted with caution in patients with elevated PVR, particularly in the presence of right ventricular dysfunction and/or right coronary artery disease.<sup>292</sup> More recently, the ENIGMA II study, a large randomized clinical trial, demonstrated no difference in the risk of death or cardiovascular complications with  $\text{N}_2\text{O}$ .<sup>293</sup>

#### Potential Neurotoxicity of Nitrous Oxide

Prolonged use of  $\text{N}_2\text{O}$  can cause nitrous oxide-induced blockade of N-methyl-D-aspartate (NMDA) receptors and can manifest as swelling of neuronal organelles including mitochondria and endoplasmic reticulum,<sup>294</sup> presenting as neurotoxicity<sup>295</sup> with an acute neuropathy postoperatively.<sup>296</sup> Nitrous oxide also increases plasma homocysteine levels<sup>297</sup> caused by oxidation of methionine synthase.<sup>298</sup> As homocysteine can be easily measured in blood, it can be used as a biomarker of  $\text{N}_2\text{O}$ -induced modulation of methionine synthase activity. After an 8-hour exposure to  $\text{N}_2\text{O}$ , an eight-fold increase in blood homocysteine levels was detected.<sup>299</sup> Increased homocysteine may be prevented by continuous infusion of vitamin  $\text{B}_{12}$ , which is an enzyme cofactor of methionine synthase.<sup>300</sup>

#### XENON

Xenon has been suggested as an ideal inhalational anesthetic. It is stable, nonbiotransformable, nontoxic, nonflammable, nonirritant, and has a low blood-gas partition coefficient. Because of its specific molecular properties, xenon ( $\text{Xe}^{129}$ ) can be hyperpolarized, with ventilation

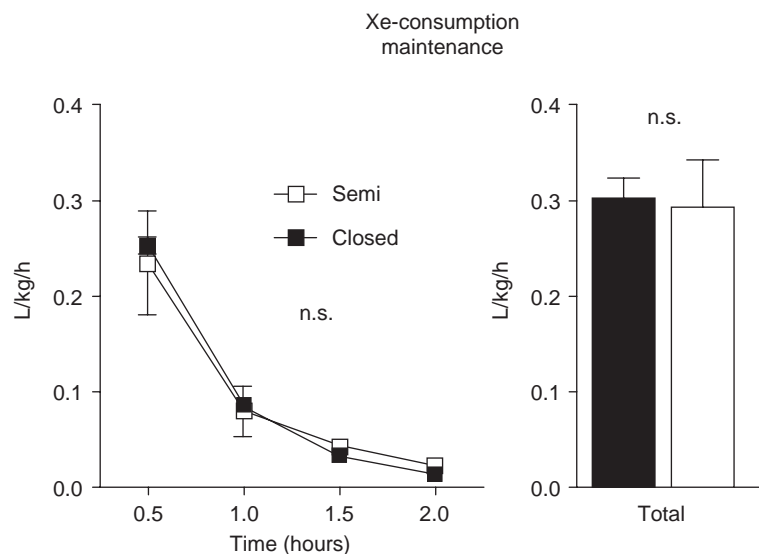


**Fig. 21.24** Xenon consumption during the maintenance phase in a semi-closed and closed circuit, shown for 30 minute intervals and in total for 2 hours. n.s., not significant. (Redrawn from Roehl AB, Goetzenich A, Rossaint R, et al. A practical rule for optimal flows for xenon anaesthesia in a semi-closed anaesthesia circuit. *Eur J Anaesthesiol*. 2010;27(7), 660–665. With permission.)

distribution and gas uptake yielding a highly selective tool for 3D MRI evaluation of lung disease.<sup>301</sup> Therefore xenon is used more frequently as an agent for imaging rather than as an inhalational anesthetic. However, its sedative effect is unique and mainly conferred by the inhibition of NMDA receptors in the central nervous system. In 1969, Cullen and colleagues determined the MAC of xenon to be 71% in O<sub>2</sub>.<sup>302</sup> Using more modern measurements, Nakata and colleagues determined the MAC to be 63.1%.<sup>303</sup> A recent meta-analysis concluded that xenon anesthesia provides more stable intraoperative blood pressure, lower heart rate, and faster emergence from anesthesia than volatile agents and propofol, but xenon is associated with a higher risk of PONV (Fig. 21.24).<sup>304</sup>

### Speed of Emergence and Postoperative Cognitive Dysfunction with Xenon

Compared with volatile anesthetics and propofol, anesthetic emergence is faster with xenon. It shortens time to extubation by approximately 4 minutes.<sup>304</sup> However, the shortening of emergence is not associated with the reduction in length of PACU or hospital stays. There is some evidence suggesting that, compared with other general anesthetic agents, xenon is associated with better neurological outcomes.<sup>305</sup> Therefore it might reduce the occurrence of postoperative cognitive dysfunction. A recent study did show that compared with sevoflurane, xenon was associated with faster emergence and with better early postoperative cognitive recovery.<sup>306</sup> However, such a benefit did not extend beyond 2 to 3 days post operation.<sup>307</sup> Xenon did not show benefits in postoperative cognitive dysfunction in elderly patients compared with desflurane<sup>308</sup> or propofol.<sup>309</sup> Therefore its neuro-protective potential remains debatable for patients undergoing general anesthesia.

### Intraoperative Hemodynamics and Postoperative Outcome

Multiple studies have demonstrated that xenon produces a more stable intraoperative hemodynamic response.

Xenon is a sympathetic stimulant and better maintains systolic, diastolic, and mean arterial blood pressures and reduces heart rate.<sup>310</sup> Such a favorable hemodynamic profile is very unique and beneficial in contrast to most volatile anesthetics that reduce systemic vascular resistance and perfusion pressure and increase heart rate. Hofland and colleagues recently demonstrated that compared with total intravenous anesthesia or anesthesia with sevoflurane, xenon reduces postoperative cardiac troponin I release and was noninferior to sevoflurane in low-risk, on-pump coronary artery bypass graft surgery patients.<sup>311</sup> However, the benefit of xenon as a cellular protectant observed *in vitro*<sup>312</sup> has not yet been demonstrated in human studies.

### Use of Xenon in Critical Care

Sedation in the ICU usually lasts much longer than it does in anesthesia. Xenon could potentially be an ideal agent for sedation in the critical care setting, provided that its neuroprotective effect demonstrated in preclinical studies will be confirmed in humans.<sup>313</sup> However, there is currently a lack of clinical trials to determine the outcome of sedation with xenon compared to conventional sedation regimens in the ICU. A recent study by Bedi and colleagues<sup>314</sup> demonstrated the safety and feasibility of its use in critical care. Compared with a conventional propofol sedation regimen, similar sedation can be achieved at xenon concentrations of  $28 \pm 9.0\%$  (range 9%–62%).<sup>315</sup>

### Postoperative Nausea and Vomiting

Xenon is a potent antagonist at the 5-HT3 receptor,<sup>316</sup> and could theoretically exert intrinsic antiemetic properties. However, a previous study demonstrated that xenon causes an increase in risk of PONV by 72% (34.4% vs. 19.9%) when compared with volatile and propofol anesthesia.<sup>304</sup> In contrast, Schaefer and colleagues recently assessed the risk of nausea and vomiting among several anesthetic regimens and concluded that xenon causes nausea and vomiting no more frequently than other regimens.<sup>317</sup>

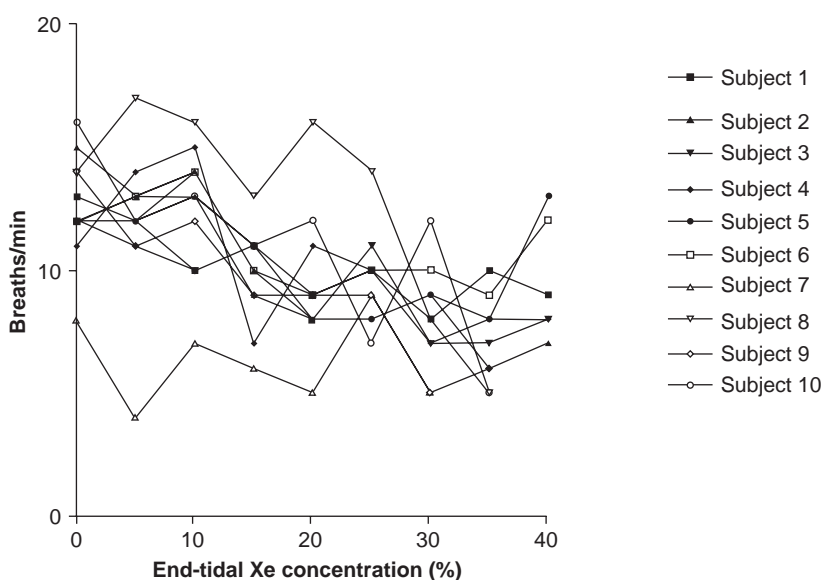


**Fig. 21.25** The respiratory rate (breath/min) for individual subjects at increasing end-tidal concentration of xenon in oxygen. (Redrawn from Bedi A, McCarroll C, Murray JM, et al. The effects of subanaesthetic concentrations of xenon in volunteers. *Anaesthesia*. 2002;57(3):233–241. With permission.)

### Airway Resistance

Xenon has a high density and viscosity. Therefore when using xenon, airway resistance is greater compared to other inhalational anesthetics at equivalent MAC values. The increase in airway resistance with 70% xenon mixed with 30% O<sub>2</sub> compared to 70% nitrogen mixed with 30% O<sub>2</sub> was minimal in healthy lungs in a pig model. However, the airway resistance was further increased in a bronchoconstriction model of asthma. Increased airway resistance is an intrinsic property of xenon and probably not a result of bronchoconstriction. The increase in airway resistance does not negatively affect oxygenation<sup>318</sup> and is not associated with decreased airway diameter.<sup>319</sup> Similar results were also reached in a dog model.<sup>320</sup> A human study with 33% xenon and 67% O<sub>2</sub> showed a significant increase in airway pressure but no alteration in oxygenation was reported.<sup>321</sup>

### Apnea

Xenon is the only inhalational anesthetic that causes a decrease in respiratory rate (Fig. 21.25).<sup>187</sup> There are a few case reports describing prolonged apnea occurring in spontaneously breathing patients, even with subanesthetic concentrations of xenon.<sup>188</sup>

### COMPARISON OF NITROUS OXIDE AND XENON

Both N<sub>2</sub>O and xenon are nonvolatile inhaled anesthetics. Their pharmacodynamics are similar, although the solubility of N<sub>2</sub>O is higher than that of xenon. The site of action of xenon<sup>322,323</sup> and N<sub>2</sub>O<sup>324,325</sup> are believed to be the same: the NMDA receptor. However, imaging studies show that xenon and N<sub>2</sub>O do not work on the same regions of the brain.<sup>326,327</sup> In addition, their sedative<sup>328</sup> and analgesic<sup>329,330</sup> properties, and their side effects<sup>331,332</sup> are not the same. Recently, concern has been raised for air pollution associated with the use of

**TABLE 21.2** Comparison of Xenon and Nitrous Oxide

	Nitrous oxide	Xenon
Pharmacodynamics	Comparable	Comparable
Sedation mechanism	NMDA	NMDA
Analgesic effect	Yes	Yes
Gas expansion	Yes	No
Nausea and vomiting	Yes	Yes
Increase in airway resistance	No	Yes
Increase in pulmonary vasculature resistance	Maybe	No
Diffusion hypoxia	Yes	No
MAC value	104%	63.1%-71%
MAC awake	63.3%	32.6%
Use as a sole anesthetic at ambient pressure at sea level	No	Yes
Respiratory rate	No effect	Decrease
Maintain hemodynamic stability	Yes	Yes
Acute tolerance	Yes	Unknown
Cost-efficiency	Favorable	Not favorable at present

MAC, Minimum alveolar concentration; NMDA, N-methyl-D-aspartate.

N<sub>2</sub>O, and whether it should be routinely used in anesthesia. Since N<sub>2</sub>O has not been shown to be associated with an increased rate of wound infections and its cost-effectiveness is favorable, there is no evidence to support abandoning N<sub>2</sub>O for routine inhalational anesthetic use. On the other hand, since the superiority of xenon over the volatile anesthetics and N<sub>2</sub>O remains to be determined and its cost is high, routine use of xenon as anesthetic is not recommended (Table 21.2).<sup>333-335</sup>

## Summary

Even though the popularity of total intravenous anesthesia has been growing over the last two decades, inhalational anesthetics remain the most commonly used agents for general anesthesia. At least in part, this is due to our current thorough understanding of the pharmacology of these agents and their cost-efficiency. Measurement of the expiratory gas concentrations is readily available in any modern anesthesia machine and therefore the depth of sedation is much easier to determine and monitor, compared with intravenous anesthesia. Thus inhalational anesthesia will remain in the mainstream of anesthesia practice for the foreseeable future. Careful selection of a particular agent based on the mechanism of its action can improve quality of patient care. Such care will continue to be based on an individual's needs, with consideration of the pharmacokinetics and interactions of these agents with the respiratory system. Further research into the clinical utility of the inhalational agents is essential for advancing the goals of precision medicine in anesthesia.

## Acknowledgment

This chapter is a consolidation of two chapters in the eighth edition, **Chapter 27** Inhaled Anesthetics: Pulmonary Pharmacology and **Chapter 28** Inhaled Anesthetics: Cardiovascular Pharmacology. The editors and publisher would like to thank the following authors: Neil E. Farber, Eckehard A.E. Stuth, Astrid G. Stucke, and Paul S. Pagel for their contributions to the prior edition of this work. It has served as the foundation for the current chapter.

 Complete references available online at [expertconsult.com](http://expertconsult.com).

## References

1. Kumeta Y, et al. *Masui*. 1995;44:396.
2. Pizov R, et al. *Anesthesiology*. 1995;82:1111.
3. Forrest JB, et al. *Anesthesiology*. 1992;76:3.
4. Cheney FW, et al. *Anesthesiology*. 1991;75:932.
5. Auroy Y, et al. *Anesthesia*. 2009;64:366.
6. Caulfield MP, Birdsall NJ. *Pharmacol Rev*. 1998;50(2):279.
7. Belmonte KE. *Proc Am Thorac Soc*. 2005;2(4):297. discussion 311.
8. Zhang WC, et al. *J Biol Chem*. 2010;285:5522.
9. Prakash YS, et al. *Am J Physiol Cell Physiol*. 1998;274:C1653.
10. Bogard AS, et al. *J Pharmacol Exp Ther*. 2011;337:209.
11. Ito S, et al. *Am J Resp Cell Mol Biol*. 2008;38:407.
12. Rho EH, et al. *J Appl Physiol*. 2002;92:257.
13. Panula P, et al. *Pharmacol Rev*. 2015;67(3):601.
14. Tamaoki J, et al. *Mediators Inflamm*. 1994;3:125.
15. Katoh T, Ikeda KCJA. *Can J Anaesth*. 1994;41:1214.
16. Yamakage M, et al. *Eur J Anaesthesiol*. 2008;25(1):67.
17. Emala CW, et al. *Chest*. 2002;121:722.
18. Park KW, et al. *Anesth Analg*. 2000;90:778.
19. Fehr JJ, et al. *Crit Care Med*. 2000;28:1884.
20. Brown RH, et al. *Anesthesiology*. 1993;78:1097.
21. D'Angelo E, et al. *Anesthesiology*. 2001;94:604.
22. Mazzeo AJ, et al. *Anesth Analg*. 1994;78:948.
23. Park KW, et al. *Anesthesiology*. 1997;86:1078.
24. Habre W, et al. *Anesthesiology*. 2001;94:348.
25. Yamakage M, et al. *Anesthesiology*. 2001;94:683.
26. Cheng EY, et al. *Anesth Analg*. 1996;83:162.
27. Dikmen Y, et al. *Anesthesia*. 2003;58:745.
28. Nyktari VG, et al. *Anesthesiology*. 2006;104:1202.
29. Nyktari V, et al. *Br J Anaesth*. 2011;107(3):454.
30. Goff MJ, et al. *Anesthesiology*. 2000;93:404.
31. Hashimoto Y, et al. *J Cardiothorac Vasc Anesth*. 1996;10:213.
32. Myers CF, et al. *Can J Anaesth*. 2011;58:1007.
33. Lele E, et al. *Acta Anaesthesiol Scand*. 2006;50:1145.
34. Lele E, et al. *Anesth Analg*. 2013;116(6):1257.
35. Satoh J, Yamakage M. *J Anesth*. 2009;23:620.
36. Satoh JI, et al. *Br J Anaesth*. 2009;102:704.
37. Rooke GA, et al. *Anesthesiology*. 1997;86:1294.
38. Correa FCF, et al. *J Appl Physiol*. 2001;91:803.
39. Burburan SM, et al. *Anesth Analg*. 2007;104:631.
40. Ruiz P, Chartrand D. *Can J Anaesth*. 2003;50:67.
41. Arakawa H, et al. *J Asthma*. 2002;39:77.
42. Johnston RG, et al. *Chest*. 1990;97(3):698–701.
43. Koninckx M, et al. *Paediatr Respir Rev*. 2013;14(2):78.
44. Morimoto N, et al. *Anesth Analg*. 1994;78:328.
45. Tobias JD, Hirshman CA. *Anesthesiology*. 1990;72:105.
46. Wu RSC, et al. *Anesth Analg*. 1996;83:238.
47. Yamamoto K, et al. *Anesthesiology*. 1993;78:1102.
48. Yamakage M, et al. *Anesthesiology*. 2000;93:179.
49. Iwasaki S, et al. *Anesthesiology*. 2006;105:753.
50. Volta CA, et al. *Anesth Analg*. 2005;100:348.
51. Crawford MW, et al. *Anesthesiology*. 2006;105:1147.
52. von Ungern-Sternberg BS, et al. *Anesthesiology*. 2008;108:216.
53. Kai T, et al. *Anesthesiology*. 1998;89:1543.
54. Yu J, Ogawa K, et al. *Anesthesiology*. 2003;99:646.
55. Lynch C, et al. *Anesthesiology*. 2000;92(3):865.
56. Janssen LJ. *Am J Physiol Cell Physiol*. 1997;272:C1757.
57. Chen X, et al. *Anesthesiology*. 2002;96:458.
58. Yamakage M, et al. *Anesth Analg*. 2002;94:84.
59. Pabelick CM, et al. *Anesthesiology*. 2001;95:207.
60. Hanazaki M, et al. *Anesthesiology*. 2001;94:129.
61. Ay B, et al. *Am J Physiol Lung Cell Mol Physiol*. 2006;290(2):L278.
62. Jude JA, et al. *Proc Am Thorac Soc*. 2008;5(1):15.
63. Wettschureck N, Offermanns S, et al. *J Mol Med (Berl)*. 2002;80(10):629.
64. Iizuka K, et al. *Eur J Pharmacol*. 2000;406(2):273.
65. Sakihara C, et al. *Anesthesiology*. 2004;101:120.
66. Nakayama T, et al. *Anesthesiology*. 2006;105:313.
67. Duracher C, et al. *Anesth Analg*. 2005;101:136.
68. Gallos G, et al. *Anesthesiology*. 2009;110:748.
69. Gallos G, et al. *Am J Physiol Lung Cell Moll Physiol*. 2011;302:L248.
70. Park KW, et al. *Anesth Analg*. 1998;86:646.
71. Moudgil GC. *Can J Anaesth*. 1997;44:R77.
72. Warner DO, et al. *Anesthesiology*. 1990;72:1057.
73. Wiklund CU, et al. *Br J Anaesth*. 1999;83:422.
74. Brown RH, et al. *Anesthesiology*. 1993;78:295.
75. Akhtar S, Brull SJ. *Pulm Pharmacol Ther*. 1998;11:227.
76. Barberi NF, et al. *Curr Biol*. 2009;19:R526.
77. Czarnecki PG, Shah JV. *Trends Cell Biol*. 2012;22:201.
78. Wu J, et al. *Chest*. 2009;136:561.
79. Ferkol TW, Leigh MW. *J Pediatr*. 2012;160:366.
80. Christopher AB, et al. *Front Pediatr*. 2014;2:111.
81. Lindberg S, et al. *Acta Otolaryngol*. 1997;117:728.
82. Lund VJ. *Allergy Asthma Proc*. 1996;17:179.
83. Keller C, Brimacombe J. *Anesth Analg*. 1998;86:1280.
84. Raphael JH, Butt MW. *Br J Anaesth*. 1997;79:473.
85. Iida H, et al. *Can J Anaesth*. 2006;53:242.
86. Raphael JH, et al. *Br J Anaesth*. 1996;76:116.
87. Matsuura S, et al. *Anesth Analg*. 2006;102:1703.
88. Gamsu G, et al. *Am Rev Respir Dis*. 1976;114:673.
89. Lichtiger M, et al. *Anesthesiology*. 1975;42:753.
90. Konrad F, et al. *Anaesthesia*. 1997;46:403.
91. Konrad F, et al. *Chest*. 1994;105:237.
92. Konrad FX, et al. *J Clin Anesth*. 1993;5:375.
93. Rivero DH, et al. *Chest*. 2001;119:1510.
94. Mollie S, et al. *Anesthesiology*. 1994;81:668.
95. Yang T, et al. *Drug Metabol Drug Interact*. 2001;18:243.
96. Patel AB, et al. *Anesth Analg*. 2002;94:943.
97. Li Y, et al. *Drug Metabol Drug Interact*. 2004;20:175.
98. Rezaiguai-Delclaux S, et al. *Anesthesiology*. 1998;88:751.
99. Paugam-Burtz C, et al. *Anesthesiology*. 2000;93:805.
100. Malacrida L, et al. *Pulm Pharmacol Ther*. 2014;28(2):122.
101. Bilgi M, et al. *Eur J Anaesthesiol*. 2011;28(4):279.
102. Sweeney M, et al. *J Appl Physiol*. 1998;85:2040.
103. Myers JL, et al. *Ann Thorac Surg*. 1996;62:1677.
104. Moncada S. *Pharmacol Rev*. 1991;43(2):109.
105. Bredt DS, et al. *Neuron*. 1991;7(4):615.
106. Lamas S, et al. *Proc Natl Acad Sci U S A*. 1992;89(14):6348.

107. Moncada S, Palmer RM. *Semin Perinatol*. 1991;15(1):16.
108. Ichinose F. *Circulation*. 2004;109(25):3106.
109. Lian TY. *Drug Des Devel Ther*. 2017;11:1195.
110. Galvin I, et al. *Br J Anaesth*. 2007;98:420.
111. Arai TJ, et al. *J Appl Physiol*. 2009;106:1057.
112. Adding LC, et al. *Acta Anaesthesiol Scand*. 1999;167:167.
113. Yamamoto Y, et al. *J Appl Physiol*. 2001;91:1121.
114. Robertson TP, et al. *Cardiovasc Res*. 2001;50:145.
115. Morio Y, McMurry IF. *J Appl Physiol*. 2002;92:527.
116. Evans AM, et al. *Current Opinions Anesthesiology*. 2011;24:13.
117. Firth AL, et al. *Am J Physiol Lung Cell Mol Physiol*. 2008;295:L61.
118. Nagendran J, et al. *Current Opinions Anesthesiology*. 2006;19:34.
119. Wang L, et al. *J Clin Invest*. 2012;122(11):4218.
120. Goldenberg NM. *Anesthesiology*. 2015;122(6):1338–1348.
121. Lumb AB, Slinger P. *Anesthesiology*. 2015;122(4):932.
122. Akata T. *Anesthesiology*. 2007;106:365.
123. Gambone LM, et al. *Am J Physiol Heart Circ Physiol*. 1997;272:H290.
124. Seki S, et al. *Anesthesiology*. 1997;86:923.
125. Nakayama M, et al. *Anesthesiology*. 1998;88:1023.
126. Lennon PF, Murray PA. *Anesthesiology*. 1995;82:723.
127. Sato K, et al. *Anesthesiology*. 2002;97:478.
128. Liu R, et al. *Can J Anaesth*. 2003;50:301.
129. Olszewski A. *Adv Exp Med Biol*. 2010;661:459.
130. Su JY, Vo AC. *Anesthesiology*. 2002;97:207.
131. Zhong L, Su JY. *Anesthesiology*. 2002;96:148.
132. Loer SA, et al. *Anesthesiology*. 1995;83(3):552.
133. Lennon PF, Murray PA. *Anesthesiology*. 1996;84:404.
134. Johns RA. *Anesthesiology*. 1993;79:1381.
135. Marshall C, Marshall BE. *Anesthesiology*. 1993;79:A1238.
136. Marshall C, Marshall BE. *Anesthesiology*. 1990;73:441.
137. Jing M, et al. *Life Sci*. 1995;56(1):19.
138. Gambone LM, et al. *Anesthesiology*. 1997;86:936.
139. Liu R, et al. *Anesthesiology*. 2001;95:939.
140. Eisenkraft JB. *Br J Anaesth*. 1990;65:63.
141. Lesitsky MA, et al. *Anesthesiology*. 1998;89:1501.
142. Schwarzkopf K, et al. *Anesth Analg*. 2005;100:335.
143. Schwarzkopf K, et al. *J Cardiothorac Vasc Anesth*. 2003;17:73.
144. Karzai W, et al. *Anesth Analg*. 1999;89:215.
145. Schwarzkopf K, et al. *Anesth Analg*. 2001;93:1434.
146. Kleinsasser A, et al. *Anesthesiology*. 2001;95:1422.
147. Nyren S, et al. *Anesthesiology*. 2010;113:1370.
148. Radke OC, et al. *Anesthesiology*. 2012;116:1186.
149. Bindsev L, et al. *Acta Anaesthesiol Scand*. 1981;25:360.
150. Nishiwaki K, et al. *Am J Physiol Heart Circ Physiol*. 1992;262:H1331.
151. Abe K, et al. *Anesth Analg*. 1998;86:266.
152. Reid CW, et al. *J Cardiothorac Vasc Anesth*. 1996;10:860.
153. Beck DH, et al. *Br J Anaesth*. 2001;86:38.
154. Pruszkowski O, et al. *Br J Anaesth*. 2007;98:539.
155. Kellow NH, et al. *Br J Anaesth*. 1995;75:578.
156. Abe K, et al. *Anesth Analg*. 1998;87:1164.
157. Benumof JL, et al. *Anesthesiology*. 1987;67:910.
158. Pagel P, et al. *Anesth Analg*. 1998;87:800.
159. Carlsson AJ, et al. *Anesthesiology*. 1987;66:312.
160. Ng A, Swanepoel J. *Br J Anaesth*. 2011;106:761.
161. Karzai W, Schwarzkopf K. *Anesthesiology*. 2009;110:1402.
162. Dalibon N, et al. *Anesth Analg*. 2004;98:590.
163. Teppema LJ, Baby S. *Respir Physiol Neurobiol*. 2011;177:80.
164. Stuth EAE, et al. Central Effects of General Anesthesia. In: Denham S, Ward ADLJ, eds. *Pharmacology and Pathophysiology of the Control of Breathing*. Boca Raton, FL: Taylor and Francis Group; 2005:571.
165. Stuth EA, et al. *Respir Physiol Neurobiol*. 2008;164:151.
166. Sirois JE, et al. *J Neurosci*. 2000;20:16347.
167. Sirois JE, et al. *J Physiol*. 2002;541:717.
168. Trochet D, et al. *Am J Respir Crit Care Med*. 2008;177:906–911.
169. Coghlan M, Richards E. *ER Trafficking*. 2018;8(1):5275.
170. Forster HV, Smith CA. *J Appl Physiol*. 2010;108:989.
171. Nattie E, et al. *J Appl Physiol*. 2011;110:1.
172. Erlichman JS, et al. *Respir Physiol Neurobiol*. 2010;173:305.
173. Pandit JJ. *Anaesthesia*. 2002;57:632.
174. Pandit JJ. *Anaesthesia*. 2005;60:461.
175. Baugh R, et al. *Otolaryngol Head Neck Surg*. 2013;148(5):867.
176. Abdala AP, et al. *J Physiol*. 2015;593(14):3033.
177. Rybak IA, et al. *J Neurophysiol*. 2008;100:1770.
178. Smith CA, et al. *Respir Physiol Neurobiol*. 2010;173:288.
179. von Euler US LG, Zotterman Y. *Scand Arch Physiol*. 1939;83:132.
180. BuSha BF, et al. *J Appl Physiol*. 2002;93:903.
181. Lazarenko RM, et al. *J Neurosci*. 2010;30:7691.
182. Haxhiu MA, et al. *Respir Physiol*. 1987;70(2):183–193.
183. Horner RL. *Respir Physiol Neurobiol*. 2008;164:179.
184. Begle RL, et al. *Am Rev Respir Dis*. 1990;141(4 Pt 1):854.
185. Taga Y, et al. *J Appl Physiol* (1985). 2007;103(4):1379.
186. Hornbein TF, et al. *Anesth Analg*. 1982;61(7):553.
187. Bedi A, et al. *Anaesthesia*. 2002;57(3):233.
188. Cormack JR, Gott J, Kondogiannis S, et al. *A Case Rep*. 2017;8(4):90.
189. Fourcade HE, et al. *Anesthesiology*. 1971;35(1):26.
190. Calverley RK, et al. *Anesth Analg*. 1978;57(6):610.
191. Lockhart SH, et al. *Anesthesiology*. 1991;74(3):484.
192. Doi M, Ikeda K, et al. *J Anesth*. 1987;1(2):137.
193. Hickey RF, Severinghaus JW. Regulation of breathing: drug effects. In: Hornbein TF, ed. *Regulation of Breathing - Pt. 2*. New York, NY: Marcel Dekker; 1981:1251–1312.
194. Eger EI. *Anesthesiology*. 1981;55(5):559.
195. Fujii Y, et al. *Int Anesthesiol Clin*. 2001;39(2):95.
196. Winkler SS, et al. *J Comput Assist Tomogr*. 1987;11(3):496.
197. Winkler STP, et al. Xenon effects on CNS control of respiratory rate and tidal volume—the danger of apnea. In: Hartmann AHS, ed. *Cerebral Blood Flow and Metabolism Measurement*. Berlin: Springer-Verlag; 1985:356–360.
198. Holl K, et al. *Acta Neurochir (Wien)*. 1987;87(3-4):129.
199. Ballantyne D, Scheid P. *Adv Exp Med Biol*. 2001;499:17.
200. Ballantyne D, Scheid P. *Respir Physiol*. 2001;129:5.
201. Branco LG, et al. *J Appl Physiol*. 2009;106:1467.
202. Heeringa J, et al. *Respir Physiol*. 1979;37:365.
203. Knill RL, Gelb AW. *Anesthesiology*. 1978;49:244.
204. van den Elsen M. *Br J Anaesth*. 1998;80(2):174.
205. Kammer T, et al. *Anesthesiology*. 2002;97:1416.
206. Barnard P, et al. *J Appl Physiol*. 1987;63:685.
207. Dahan A, Teppema L. *Br J Anaesth*. 1999;83:199.
208. Sarton E, et al. *Anesthesiology*. 1999;90:1288.
209. van den Elsen MJLJ, et al. *Anesthesiology*. 1994;81:860.
210. Hickey RF, et al. *Anesthesiology*. 1971;35:32.
211. Nakayama H, et al. *Am J Respir Crit Care Med*. 2002;165:1251.
212. West JB. *Respiration physiology*. 1983;52(3):265.
213. Dahan A, et al. *Anesthesiology*. 1994;80:727.
214. Chung F, Liao P. *Anesthesiology*. 2014;120(2):287.
215. Chung F, et al. *Anesthesiology*. 2014;120(2):299–311.
216. Sarton E, et al. *Anesthesiology*. 1996;85:295.
217. Pandit JJ, et al. *Anesthesiology*. 2004;101(6):1409.
218. Warner DO. *Anesthesiology*. 1996;84(2):309.
219. Warner DO, et al. *Anesthesiology*. 1995;82:6.
220. Warner DO, Warner MA. *Anesthesiology*. 1995;82:20.
221. Gauda EB, et al. *J Appl Physiol*. 1994;76:2656.
222. Wheatley JR, et al. *J Appl Physiol*. 1991;70:2242.
223. Schwartz AR, et al. *Am J Respir Crit Care Med*. 1998;157(4 Pt 1):1051.
224. Kuna ST, et al. *Med Clin North Am*. 1985;69(6):1221.
225. Erb TO, et al. *Paediatric Anaesthesia*. 2017;27(3):282.
226. Lerman J, et al. *Paediatric Anaesth*. 2010;20:495.
227. Ulevitch RJ. *Adv Immunol*. 1993;53:267.
228. Chow JC, et al. *J Biol Chem*. 1999;274(16):10689.
229. Marini JJ, Evans TW. *Intensive Care Med*. 1998;24(8):878.
230. Meyrick B, et al. *Prog Clin Biol Res*. 1989;308:91.
231. Brigham KL. *Am Rev Respir Dis*. 1987;136(3):785.
232. Bulger EM, Maier RV. *Crit Care Med*. 2000;28(suppl 4):N27.
233. Ermert L, et al. *Am J Physiol Lung Cell Mol Physiol*. 2000;278(4):L744.
234. Quinn JV, Slotman GJ. *Crit Care Med*. 1999;27(11):2485.
235. Langleben D, et al. *Am Rev Respir Dis*. 1993;148(6 Pt 1):1646.
236. Suffredini AF, et al. *Am Rev Respir Dis*. 1992;145(6):1398.
237. O'Grady NP, et al. *Am J Respir Crit Care Med*. 2001;163(7):1591.
238. Bachofen M, Weibel ER. *Clin Chest Med*. 1982;3(1):35.
239. Kumar A, et al. *Am J Physiol*. 1999;276(1 Pt 2):R265.
240. McQuaid KE, Keenan AK. *Exp Physiol*. 1997;82(2):369.
241. Salvemini D. *Cell Mol Life Sci*. 1997;53(7):576.
242. Ignar LJ, et al. *Proc Natl Acad Sci U S A*. 1993;90(17):8103.
243. Weissmann N, et al. *Am J Physiol Lung Cell Mol Physiol*. 2000;279(4):L683.
244. Singh S, Evans TW. *Eur Respir J*. 1997;10(3):699.
245. Westendorp RG, et al. *J Vasc Res*. 1994;31(1):42.
246. Suter D, et al. *Anesth Analg*. 2007;104(3):638.
247. Takala RS, et al. *Acta Anaesthesiol Scand*. 2006;50(2):163.

248. Giraud O, et al. *Anesthesiology*. 2003;98(1):74.
249. Voigtsberger S, et al. *Anesthesiology*. 2009;111(6):1238.
250. Schlapfer M, et al. *Clin Exp Immunol*. 2012;168(1):125.
251. Du G, et al. *Anesth Analg*. 2017;124(5):1555.
252. Bedirli N, et al. *J Surg Res*. 2012;178(1):e17.
253. Dong X, et al. *Exp Lung Res*. 2013;39(7):295.
254. Beitle JR, et al. *Clin Chest Med*. 2016;37(4):633.
255. Wagner J, et al. *PLoS One*. 2018;13(2):e0192896.
256. Faller S, et al. *Anesth Analg*. 2012;114(4):747.
257. Englert JA, et al. *Anesthesiology*. 2015;123(2):377.
258. Strosing KM, et al. *Anesth Analg*. 2016;123(1):143.
259. Pak O, et al. *Adv Exp Med Biol*. 2017;967:195.
260. Liu R, et al. *Anesth Analg*. 1999;89(3):561.
261. Fujinaga T, et al. *Transplantation*. 2006;82:1168.
262. Casanova J, et al. *Anesth Analg*. 2011;113:742.
263. Ohsumi A, et al. *Ann Thorac Surg*. 2017;103(5):1578.
264. Oshima Y, et al. *Springerplus*. 2016;5(1):2031.
265. Martens A, et al. *J Surg Res*. 2016;201(1):44.
266. Wrigge H, et al. *Anesthesiology*. 2000;93:1413.
267. De Conno E, et al. *Anesthesiology*. 2009;110:1316.
268. Schilling T, et al. *Anesthesiology*. 2011;115:65.
269. Sugasawa Y, et al. *J Anesth*. 2012;26:62.
270. Uhlig C, et al. *Anesthesiology*. 2016;124(6):1230.
271. Beck-Schimmer B, et al. *Anesthesiology*. 2016;125(2):313.
272. Koksal GM, et al. *Eur J Anaesthesiol*. 2004;21(3):217.
273. Koksal GM, et al. *Acta Anaesthesiol Scand*. 2005;49(6):835.
274. Jabaudon M, et al. *Am J Respir Crit Care Med*. 2017;195(6):792.
275. Bellgardt M, et al. *Eur J Anaesthesiol*. 2016;33(1):6.
276. Wilson KE. *Dent Update*. 2013;40(10):822, 826.
277. Likis FE, et al. *Anesth Analg*. 2014;118(1):153.
278. Goto T. *Anesthesiology*. 2000;93(5):1188.
279. Mashour GA, Avidan MS. *Br J Anaesth*. 2015;115(suppl 1):i20.
280. Mathews DM, et al. *Anesth Analg*. 2008;106(1).
281. Lee LH, et al. *Anesthesiology*. 2005;102(2):398.
282. Janiszewski DJ, et al. *Anesth Analg*. 1999;88(5):1149.
283. Berkowitz BA, et al. *Anesthesiology*. 1979;51(4):309.
284. Berkowitz BA, et al. *J Pharmacol Exp Ther*. 1977;203(3):539.
285. Ramsay DS, et al. *Pain*. 2005;114(1-2):19.
286. Akca O, et al. *Acta Anaesthesiol Scand*. 2004;48(7):894.
287. Fernandez-Guisasola J, et al. *Anesthesia*. 2010;65(4):379-387.
288. Peyton PJ, Peyton PJ. *Anesthesiology*. 2014;120(5):1137.
289. Pace NL. *Anesthesiology*. 2014;121(6):1356.
290. Zhou L, Chen C, Yu H. *Anesthesiology*. 2014;121(6):1356.
291. Konstadt SN, et al. *Can J Anaesth*. 1990;37(6):613.
292. Schulte-Sasse U, et al. *Anesthesiology*. 1982;57(1):9.
293. Beattie WS, et al. *Anesth Analg*. 2018.
294. Jevtic-Todorovic V, et al. *Br J Anaesth*. 2013;111(2):143.
295. Savage S, Ma D. *Brain Sci*. 2014;4(1):73.
296. Morris N, et al. *Muscle Nerve*. 2015;51(4):614.
297. Myles PS, et al. *Anesthesiology*. 2008;109(4):657.
298. Drummond JT, Matthews RG. *Biochemistry*. 1994;33(12):3742.
299. Nagele P, et al. *Anesth Analg*. 2011;113(4):843.
300. Kiasari AZ, et al. *Oman Med J*. 2014;29(3):194.
301. Mugler JP, et al. *Proc Natl Acad Sci U S A*. 2010;107(50):21707.
302. Cullen SC. *Anesthesiology*. 1969;31(4):305.
303. Nakata Y, et al. *Anesthesiology*. 2001;94(4):611.
304. Law LS. *Anesth Analg*. 2016;122(3):678.
305. Law LS, et al. *Can J Anaesth*. 2018;65(9):1041.
306. Bronco A, et al. *Eur J Anaesthesiol*. 2010;27(10):912.
307. Cremer J, et al. *Med Gas Res*. 2011;1(1):9.
308. Coburn M, et al. *Br J Anaesth*. 2007;98(6):756.
309. Hocker J, et al. *Anesthesiology*. 2009;110(5):1068.
310. Neukirchen M, et al. *Br J Anaesth*. 2012;109(6):887.
311. Hofland J, et al. *Anesthesiology*. 2017;127(6):918.
312. Petzelt C, et al. *BMC Neurosci*. 2004;5:55.
313. Sacchetti ML. *Stroke*. 2008;39(6):1659.
314. Bedi A, et al. *Crit Care Med*. 2003;31(10):2470.
315. Roehl AB, et al. *Eur J Anaesthesiol*. 2010;27(7):660.
316. Suzuki T, et al. *Anesthesiology*. 2002;96(3):699.
317. Schaefer MS, et al. *Br J Anaesth*. 2015;115(1):61.
318. Calzia E, et al. *Anesthesiology*. 1999;90(3):829.
319. Baumert JH, et al. *Br J Anaesth*. 2002;88(4):540.
320. Zhang P. *Can J Anaesth*. 1995;42(6):547.
321. Rueckoldt H, et al. *Acta Anaesthesiol Scand*. 1999;43(10):1060.
322. Dickinson R, et al. *Anesthesiology*. 2007;107(5):756.
323. Kratzler S, et al. *Anesthesiology*. 2012;116(3):673.
324. Nagele P, et al. *Proc Natl Acad Sci U S A*. 2004;101(23):8791.
325. Richardson KJ, et al. *J Pharmacol Exp Ther*. 2015;352(1):156.
326. Hagen T, et al. *J Comput Assist Tomogr*. 1999;23(2):257.
327. Reinstrup P, et al. *Anesthesiology*. 1994;81(2):396.
328. Yagi M, et al. *Br J Anaesth*. 1995;74(6):670.
329. Petersen-Felix S, et al. *Br J Anaesth*. 1998;81(5):742.
330. Utsumi J, et al. *Anesth Analg*. 1997;84(6):1372.
331. Yonas H. *J Comput Assist Tomogr*. 1981;5(4):591.
332. Kamp HD. *Klin Anasthesiol Intensivther*. 1993;42:17.
333. de Vasconcellos K, Sneyd JR. *Br J Anaesth*. 2013;111(6):877.
334. Imberger G, et al. *Br J Anaesth*. 2014;112(3):410.
335. Myles PS, et al. *Lancet*. 2014;384(9952):1446.

## References

1. Kumeta Y, Hattori A, Mimura M, Kishikawa K, Namiki A. [A survey of perioperative bronchospasm in 105 patients with reactive airway disease]. *Masui*. 1995;44(3):396–401.
2. Pizov R, Brown RH, Weiss YS, et al. Wheezing during induction of general anesthesia in patients with and without asthma. A randomized, blinded trial. *Anesthesiology*. 1995;82(5):1111–1116.
3. Forrest JB, Rehder K, Cahalan MK, Goldsmith CH. Multicenter study of general anesthesia. III. Predictors of severe perioperative adverse outcomes. *Anesthesiology*. 1992;76(1):3–15.
4. Cheney FW, Posner KL, Caplan RA. Adverse respiratory events infrequently leading to malpractice suits. A closed claims analysis. *Anesthesiology*. 1991;75(6):932–939.
5. Auroy Y, Benhamou D, Pequignot F, Bovet M, Jouglard E, Lienhart A. Mortality related to anaesthesia in France: analysis of deaths related to airway complications. *Anaesthesia*. 2009;64(4):366–370.
6. Caulfield MP, Birdsall NJ. International Union of Pharmacology. XVII. Classification of muscarinic acetylcholine receptors. *Pharmacol Rev*. 1998;50(2):279–290.
7. Belmonte KE. Cholinergic pathways in the lungs and anticholinergic therapy for chronic obstructive pulmonary disease. *Proc Am Thorac Soc*. 2005;2(4):297–304. discussion 311–292.
8. Zhang WC, Peng YJ, Zhang GS, et al. Myosin light chain kinase is necessary for tonic airway smooth muscle contraction. *J Biol Chem*. 2010;285(8):5522–5531.
9. Prakash YS, Kannan MS, Walseth TF, Sieck GC. Role of cyclic ADP-ribose in the regulation of  $[Ca^{2+}]_i$  in porcine tracheal smooth muscle. *Am J Physiol*. 1998;274(6 Pt 1):C1653–1660.
10. Bogard AS, Xu C, Ostrom RS. Human bronchial smooth muscle cells express adenylyl cyclase isoforms 2, 4, and 6 in distinct membrane microdomains. *J Pharmacol Exp Ther*. 2011;337(1):209–217.
11. Ito S, Kume H, Naruse K, et al. A novel  $Ca^{2+}$  influx pathway activated by mechanical stretch in human airway smooth muscle cells. *Am J Respir Cell Mol Biol*. 2008;38(4):407–413.
12. Rho EH, Perkins WJ, Lorenz RR, Warner DO, Jones KA. Differential effects of soluble and particulate guanylyl cyclase on  $Ca^{2+}$  sensitivity in airway smooth muscle. *J Appl Physiol* (1985). 2002;92(1):257–263.
13. Panula P, Chazot PL, Cowart M, et al. International Union of Basic and Clinical Pharmacology. XCVIII. Histamine receptors. *Pharmacol Rev*. 2015;67(3):601–655.
14. Tamaoki J, Chiyotani A, Tagaya E, Isono K, Konno K. Histamine N-methyltransferase modulates human bronchial smooth muscle contraction. *Mediators Inflamm*. 1994;3(2):125–129.
15. Katoh T, Ikeda K. A comparison of sevoflurane with halothane, enflurane, and isoflurane on bronchoconstriction caused by histamine. *Can J Anaesth*. 1994;41(12):1214–1219.
16. Deleted in proofs
17. Emala CW, McQuitty CK, Eleff SM, et al. Asthma, allergy, and airway hyperresponsiveness are not linked to the beta(2)-adrenoceptor gene. *Chest*. 2002;121(3):722–731.
18. Park KW, Sato K, Dai HB, Comunale ME, Sellke FW. Epithelium-dependent bronchodilatory activity is preserved in pig bronchioles after normothermic cardiopulmonary bypass. *Anesth Analg*. 2000;90(4):778–783.
19. Fehr JJ, Hirshman CA, Emala CW. Cellular signaling by the potent bronchoconstrictor endothelin-1 in airway smooth muscle. *Crit Care Med*. 2000;28(6):1884–1888.
20. Brown RH, Zerhouni EA, Hirshman CA. Comparison of low concentrations of halothane and isoflurane as bronchodilators. *Anesthesiology*. 1993;78(6):1097–1101.
21. D'Angelo E, Calderini IS, Tavola M. The effects of  $CO_2$  on respiratory mechanics in anesthetized paralyzed humans. *Anesthesiology*. 2001;94(4):604–610.
22. Mazzeo AJ, Cheng EY, Bosnjak ZJ, Coon RL, Kampine JP. Differential effects of desflurane and halothane on peripheral airway smooth muscle. *Br J Anaesth*. 1996;76(6):841–846.
23. Park KW, Dai HB, Lowenstein E, Kocher ON, Sellke FW. Isoflurane- and halothane-mediated dilation of distal bronchi in the rat depends on the epithelium. *Anesthesiology*. 1997;86(5):1078–1087; discussion 1023A–1024A.
24. Habre W, Petak F, Sly PD, Hantos Z, Morel DR. Protective effects of volatile agents against methacholine-induced bronchoconstriction in rats. *Anesthesiology*. 2001;94(2):348–353.
25. Yamakage M, Chen X, Tsujiguchi N, Kamada Y, Namiki A. Differential inhibitory effects of volatile anesthetics on T- and L-type voltage-dependent  $Ca^{2+}$  channels in porcine tracheal and bronchial smooth muscles. *Anesthesiology*. 2001;94(4):683–693.
26. Cheng EY, Mazzeo AJ, Bosnjak ZJ, Coon RL, Kampine JP. Direct relaxant effects of intravenous anesthetics on airway smooth muscle. *Anesth Analg*. 1996;83(1):162–168.
27. Dikmen Y, Eminoglu E, Salihoglu Z, Demiroluk S. Pulmonary mechanics during isoflurane, sevoflurane and desflurane anaesthesia. *Anaesthesia*. 2003;58(8):745–748.
28. Nyktari VG, Papaioannou AA, Prinianakis G, Mamidakis EG, Georgopoulos D, Askitopoulou H. Effect of the physical properties of isoflurane, sevoflurane, and desflurane on pulmonary resistance in a laboratory lung model. *Anesthesiology*. 2006;104(6):1202–1207.
29. Nyktari V, Papaioannou A, Volakakis N, Lappa A, Margaritsanaki P, Askitopoulou H. Respiratory resistance during anaesthesia with isoflurane, sevoflurane, and desflurane: a randomized clinical trial. *Br J Anaesth*. 2011;107(3):454–461.
30. Goff MJ, Arain SR, Ficke DJ, Uhrich TD, Ebert TJ. Absence of bronchodilation during desflurane anaesthesia: a comparison to sevoflurane and thiopental. *Anesthesiology*. 2000;93(2):404–408.
31. Hashimoto Y, Hirota K, Ohtomo N, Ishihara H, Matsuki A. In vivo direct measurement of the bronchodilating effect of sevoflurane using a superfine fiberoptic bronchoscope: comparison with enflurane and halothane. *J Cardiothorac Vasc Anesth*. 1996;10(2):213–216.
32. Myers CF, Fontao F, Janosi TZ, Boda K, Petak F, Habre W. Sevoflurane and desflurane protect cholinergic-induced bronchoconstriction of hyperreactive airways in rabbits. *Can J Anaesth*. 2011;58(11):1007–1015.
33. Lele E, Petak F, Fontao F, Morel DR, Habre W. Protective effects of volatile agents against acetylcholine-induced bronchoconstriction in isolated perfused rat lungs. *Acta Anaesthesiol Scand*. 2006;50(9):1145–1151.
34. Lele E, Petak F, Carnesecchi S, Virag K, Argiroffo CB, Habre W. The protective effects of volatile anesthetics against the bronchoconstriction induced by an allergic reaction in sensitized rabbit pups. *Anesth Analg*. 2013;116(6):1257–1264.
35. Satoh J, Yamakage M. Desflurane induces airway contraction mainly by activating transient receptor potential A1 of sensory C-fibers. *J Anesth*. 2009;23(4):620–623.
36. Satoh JI, Yamakage M, Kobayashi T, Tohse N, Watanabe H, Namiki A. Desflurane but not sevoflurane can increase lung resistance via tachykinin pathways. *Br J Anaesth*. 2009;102(5):704–713.
37. Rooke GA, Choi JH, Bishop MJ. The effect of isoflurane, halothane, sevoflurane, and thiopental/nitrous oxide on respiratory system resistance after tracheal intubation. *Anesthesiology*. 1997;86(6):1294–1299.
38. Correa FC, Ciminielli PB, Falcao H, et al. Respiratory mechanics and lung histology in normal rats anesthetized with sevoflurane. *J Appl Physiol* (1985). 2001;91(2):803–810.
39. Burburian SM, Xisto DG, Ferreira HC, et al. Lung mechanics and histology during sevoflurane anesthesia in a model of chronic allergic asthma. *Anesth Analg*. 2007;104(3):631–637.
40. Ruiz P, Chartrand D. The effect of isoflurane 0.6% on respiratory mechanics in anesthetized-paralyzed humans is not increased at concentrations of 0.9% and 1.2%. *Can J Anaesth*. 2003;50(1):67–70.
41. Arakawa H, Takizawa T, Tokuyama K, Mochizuki H, Morikawa A. Efficacy of inhaled anticholinergics and anesthesia in treatment of a patient in status asthmaticus. *J Asthma*. 2002;39(1):77–80.
42. Deleted in proofs
43. Deleted in proofs
44. Morimoto N, Yamamoto K, Jones KA, Warner DO. Halothane and pertussis toxin-sensitive G proteins in airway smooth muscle. *Anesth Analg*. 1994;78(2):328–334.
45. Tobias JD, Hirshman CA. Attenuation of histamine-induced airway constriction by albuterol during halothane anesthesia. *Anesthesiology*. 1990;72(1):105–110.
46. Wu RS, Wu KC, Wong TK, et al. Isoflurane anesthesia does not add to the bronchodilating effect of a beta 2-adrenergic agonist after tracheal intubation. *Anesth Analg*. 1996;83(2):238–241.
47. Yamamoto K, Morimoto N, Warner DO, Rehder K, Jones KA. Factors influencing the direct actions of volatile anesthetics on airway smooth muscle. *Anesthesiology*. 1993;78(6):1102–1111.
48. Yamakage M, Tsujiguchi N, Hattori J, Kamada Y, Namiki A. Low-temperature modification of the inhibitory effects of volatile anesthetics on airway smooth muscle contraction in dogs. *Anesthesiology*. 2000;93(1):179–188.

49. Iwasaki S, Yamakage M, Satoh J, Namiki A. Different inhibitory effects of sevoflurane on hyperreactive airway smooth muscle contractility in ovalbumin-sensitized and chronic cigarette-smoking guinea pig models. *Anesthesiology*. 2006;105(4):753–763.
50. Volta CA, Alvisi V, Petroni S, et al. The effect of volatile anesthetics on respiratory system resistance in patients with chronic obstructive pulmonary disease. *Anesth Analg*. 2005;100(2):348–353.
51. Crawford MW, Arrica M, Macgowan CK, Yoo SJ. Extent and localization of changes in upper airway caliber with varying concentrations of sevoflurane in children. *Anesthesiology*. 2006;105(6):1147–1152; discussion 1145A.
52. von Ungern-Sternberg BS, Saudan S, Petak F, Hantos Z, Habre W. Desflurane but not sevoflurane impairs airway and respiratory tissue mechanics in children with susceptible airways. *Anesthesiology*. 2008;108(2):216–224.
53. Kai T, Jones KA, Warner DO. Halothane attenuates calcium sensitization in airway smooth muscle by inhibiting G-proteins. *Anesthesiology*. 1998;89(6):1543–1552.
54. Yu J, Ogawa K, Tokinaga Y, Hatano Y. Sevoflurane inhibits guanosine 5'-[gamma-thio]triphosphate-stimulated, Rho/Rho-kinase-mediated contraction of isolated rat aortic smooth muscle. *Anesthesiology*. 2003;99(3):646–651.
55. Lynch C, Baum J, Tenbrinck R. Xenon anesthesia. *Anesthesiology*. 2000;92(3):865–868.
56. Janssen LJ. T-type and L-type Ca<sup>2+</sup> currents in canine bronchial smooth muscle: characterization and physiological roles. *Am J Physiol*. 1997;272(6 Pt 1):C1757–1765.
57. Chen X, Yamakage M, Namiki A. Inhibitory effects of volatile anesthetics on K<sup>+</sup> and Cl<sup>-</sup> channel currents in porcine tracheal and bronchial smooth muscle. *Anesthesiology*. 2002;96(2):458–466.
58. Yamakage M, Chen X, Kimura A, Iwasaki S, Namiki A. The repolarizing effects of volatile anesthetics on porcine tracheal and bronchial smooth muscle cells. *Anesth Analg*. 2002;94(1):84–88; table of contents.
59. Pabelick CM, Prakash YS, Kannan MS, Warner DO, Sieck GC. Effects of halothane on sarcoplasmic reticulum calcium release channels in porcine airway smooth muscle cells. *Anesthesiology*. 2001;95(1):207–215.
60. Hanazaki M, Jones KA, Perkins WJ, Warner DO. Halothane increases smooth muscle protein phosphatase in airway smooth muscle. *Anesthesiology*. 2001;94(1):129–136.
61. Ay B, Iyanobe A, Sieck GC, Prakash YS, Pabelick CM. Cyclic nucleotide regulation of store-operated Ca<sup>2+</sup> influx in airway smooth muscle. *Am J Physiol Lung Cell Mol Physiol*. 2006;290(2):L278–283.
62. Jude JA, Wylam ME, Walseth TF, Kannan MS. Calcium signaling in airway smooth muscle. *Proc Am Thorac Soc*. 2008;5(1):15–22.
63. Wettschureck N, Offermanns S. Rho/Rho-kinase mediated signaling in physiology and pathophysiology. *J Mol Med (Berl)*. 2002;80(10):629–638.
64. Iizuka K, Shimizu Y, Tsukagoshi H, et al. Evaluation of Y-27632, a rho-kinase inhibitor, as a bronchodilator in guinea pigs. *Eur J Pharmacol*. 2000;406(2):273–279.
65. Sakihara C, Perkins WJ, Warner DO, Jones KA. Anesthetics inhibit acetylcholine-promoted guanine nucleotide exchange of heterotrimeric G proteins of airway smooth muscle. *Anesthesiology*. 2004;101(1):120–126.
66. Nakayama T, Penharter AR, Penharter SG, et al. Differential effects of volatile anesthetics on M3 muscarinic receptor coupling to the Galphaq heterotrimeric G protein. *Anesthesiology*. 2006;105(2):313–324.
67. Duracher C, Blanc FX, Gueugniaud PY, et al. The effects of isoflurane on airway smooth muscle crossbridge kinetics in Fisher and Lewis rats. *Anesth Analg*. 2005;101(1):136–142; table of contents.
68. Gallos G, Gleason NR, Virag L, et al. Endogenous gamma-aminobutyric acid modulates tonic guinea pig airway tone and propofol-induced airway smooth muscle relaxation. *Anesthesiology*. 2009;110(4):748–758.
69. Gallos G, Yim P, Chang S, et al. Targeting the restricted alpha-subunit repertoire of airway smooth muscle GABA<sub>A</sub> receptors augments airway smooth muscle relaxation. *Am J Physiol Lung Cell Mol Physiol*. 2012;302(2):L248–256.
70. Park KW, Dai HB, Lowenstein E, Sellke FW. Epithelial dependence of the bronchodilatory effect of sevoflurane and desflurane in rat distal bronchi. *Anesth Analg*. 1998;86(3):646–651.
71. Moudgil GC. The patient with reactive airways disease. *Can J Anaesth*. 1997;44(5 Pt 2):R77–89.
72. Warner DO, Vettermann J, Brichant JF, Rehder K. Direct and neurally mediated effects of halothane on pulmonary resistance in vivo. *Anesthesiology*. 1990;72(6):1057–1063.
73. Wiklund CU, Lim S, Lindsten U, Lindahl SG. Relaxation by sevoflurane, desflurane and halothane in the isolated guinea-pig trachea via inhibition of cholinergic neurotransmission. *Br J Anaesth*. 1999;83(3):422–429.
74. Brown RH, Mitzner W, Zerhouni E, Hirshman CA. Direct in vivo visualization of bronchodilation induced by inhalational anesthesia using high-resolution computed tomography. *Anesthesiology*. 1993;78(2):295–300.
75. Akhtar S, Brull SJ. Effect of isoflurane on endothelin-1 mediated airway smooth muscle contraction. *Pulm Pharmacol Ther*. 1998;11(2–3):227–230.
76. Berbari NF, O'Connor AK, Haycraft CJ, Yoder BK. The primary cilium as a complex signaling center. *Curr Biol*. 2009;19(13):R526–535.
77. Czarnecki PG, Shah JV. The ciliary transition zone: from morphology and molecules to medicine. *Trends Cell Biol*. 2012;22(4):201–210.
78. Wu J, Du H, Wang X, Mei C, Sieck GC, Qian Q. Characterization of primary cilia in human airway smooth muscle cells. *Chest*. 2009;136(2):561–570.
79. Ferkol TW, Leigh MW. Ciliopathies: the central role of cilia in a spectrum of pediatric disorders. *J Pediatr*. 2012;160(3):366–371.
80. Christopher AB, Ochoa S, Krushansky E, et al. The effects of temperature and anesthetic agents on ciliary function in murine respiratory epithelia. *Front Pediatr*. 2014;2:111.
81. Lindberg S, Cervin A, Runer T. Low levels of nasal nitric oxide (NO) correlate to impaired mucociliary function in the upper airways. *Acta Otolaryngol*. 1997;117(5):728–734.
82. Lund VJ. Nasal physiology: neurochemical receptors, nasal cycle, and ciliary action. *Allergy Asthma Proc*. 1996;17(4):179–184.
83. Keller C, Brimacombe J. Bronchial mucus transport velocity in paralyzed anesthetized patients: a comparison of the laryngeal mask airway and cuffed tracheal tube. *Anesth Analg*. 1998;86(6):1280–1282.
84. Raphael JH, Butt MW. Comparison of isoflurane with propofol on respiratory cilia. *Br J Anaesth*. 1997;79(4):473–475.
85. Iida H, Matsuura S, Shirakami G, Tanimoto K, Fukuda K. Differential effects of intravenous anesthetics on ciliary motility in cultured rat tracheal epithelial cells. *Can J Anaesth*. 2006;53(3):242–249.
86. Raphael JH, Strupish J, Selwyn DA, Hann HC, Langton JA. Recovery of respiratory ciliary function after depression by inhalation anesthetic agents: an in vitro study using nasal turbinate explants. *Br J Anaesth*. 1996;76(6):854–859.
87. Matsuura S, Shirakami G, Iida H, Tanimoto K, Fukuda K. The effect of sevoflurane on ciliary motility in rat cultured tracheal epithelial cells: a comparison with isoflurane and halothane. *Anesth Analg*. 2006;102(6):1703–1708.
88. Gamsu G, Singer MM, Vincent HH, Berry S, Nadel JA. Postoperative impairment of mucous transport in the lung. *Am Rev Respir Dis*. 1976;114(4):673–679.
89. Lichtiger M, Landa JF, Hirsch JA. Velocity of tracheal mucus in anesthetized women undergoing gynecologic surgery. *Anesthesiology*. 1975;42(6):753–756.
90. Konrad F, Marx T, Schraag M, Kilian J. [Combination anesthesia and bronchial transport velocity. Effects of anesthesia with isoflurane, fentanyl, vecuronium and oxygen-nitrous oxide breathing on bronchial mucus transport]. *Anaesthetist*. 1997;46(5):403–407.
91. Konrad F, Schreiber T, Brecht-Kraus D, Georgieff M. Mucociliary transport in ICU patients. *Chest*. 1994;105(1):237–241.
92. Konrad FX, Schreiber T, Brecht-Kraus D, Georgieff M. Bronchial mucus transport in chronic smokers and nonsmokers during general anesthesia. *J Clin Anesth*. 1993;5(5):375–380.
93. Rivero DH, Lorenzi-Filho G, Pazetti R, Jatene FB, Saldiva PH. Effects of bronchial transection and reanastomosis on mucociliary system. *Chest*. 2001;119(5):1510–1515.
94. Molliex S, Crestani B, Dureuil B, et al. Effects of halothane on surfactant biosynthesis by rat alveolar type II cells in primary culture. *Anesthesiology*. 1994;81(3):668–676.
95. Yang T, Li Y, Liu Q, Tao J, Wu W, Huang H. Isoflurane aggravates the decrease of phosphatidylcholine synthesis in alveolar type II cells induced by hydrogen peroxide. *Drug Metabol Drug Interact*. 2001;18(3–4):243–249.
96. Patel AB, Sokolowski J, Davidson BA, Knight PR, Holm BA. Halothane potentiation of hydrogen peroxide-induced inhibition of surfactant synthesis: the role of type II cell energy status. *Anesth Analg*. 2002;94(4):943–947; table of contents.

97. Li Y, Yang T, Liu Q, Tao J, Wu W, Huang H. Effect of isoflurane on proliferation and  $\text{Na}^+,\text{K}^+$ -ATPase activity of alveolar type II cells injured by hydrogen peroxide. *Drug Metabol Drug Interact*. 2004;20(3):175–183.
98. Rezaiqia-Delclaux S, Jayr C, Luo DF, Saidi NE, Meignan M, Duvaldestin P. Halothane and isoflurane decrease alveolar epithelial fluid clearance in rats. *Anesthesiology*. 1998;88(3):751–760.
99. Paugam-Burtz C, Molliex S, Lardeux B, et al. Differential effects of halothane and thiopental on surfactant protein C messenger RNA in vivo and in vitro in rats. *Anesthesiology*. 2000;93(3):805–810.
100. Malacrida L, Reta G, Piriz H, et al. Sevoflurane anesthesia deteriorates pulmonary surfactant promoting alveolar collapse in male Sprague-Dawley rats. *Pulm Pharmacol Ther*. 2014;28(2):122–129.
101. Bilgi M, Goksu S, Mizrak A, et al. Comparison of the effects of low-flow and high-flow inhalational anaesthesia with nitrous oxide and desflurane on mucociliary activity and pulmonary function tests. *Eur J Anaesthesiol*. 2011;28(4):279–283.
102. Sweeney M, Beddy D, Honner V, Sinnott B, O'Regan RG, McLoughlin P. Effects of changes in pH and  $\text{CO}_2$  on pulmonary arterial wall tension are not endothelium dependent. *J Appl Physiol* (1985). 1998;85(6):2040–2046.
103. Myers JL, Wizorek JJ, Myers AK, et al. Pulmonary arterial endothelial dysfunction potentiates hypercapnic vasoconstriction and alters the response to inhaled nitric oxide. *Ann Thorac Surg*. 1996;62(6):1677–1684.
104. Moncada S, Palmer RM, Higgs EA. Nitric oxide: physiology, pathophysiology, and pharmacology. *Pharmacol Rev*. 1991;43(2):109–142.
105. Bredt DS, Glatt CE, Hwang PM, Fotuhi M, Dawson TM, Snyder SH. Nitric oxide synthase protein and mRNA are discretely localized in neuronal populations of the mammalian CNS together with NADPH diaphorase. *Neuron*. 1991;7(4):615–624.
106. Lamas S, Marsden PA, Li GK, Tempst P, Michel T. Endothelial nitric oxide synthase: molecular cloning and characterization of a distinct constitutive enzyme isoform. *Proc Natl Acad Sci U S A*. 1992;89(14):6348–6352.
107. Moncada S, Palmer RM. Biosynthesis and actions of nitric oxide. *Semin Perinatol*. 1991;15(1):16–19.
108. Ichinose F, Roberts JD, Zapol WM. Inhaled nitric oxide: a selective pulmonary vasodilator: current uses and therapeutic potential. *Circulation*. 2004;109(25):3106–3111.
109. Lian TY, Jiang X, Jing ZC. Riociguat: a soluble guanylate cyclase stimulator for the treatment of pulmonary hypertension. *Drug Des Devel Ther*. 2017;11:1195–1207.
110. Galvin I, Drummond GB, Nirmalan M. Distribution of blood flow and ventilation in the lung: gravity is not the only factor. *Br J Anaesth*. 2007;98(4):420–428.
111. Arai TJ, Henderson AC, Dubowitz DJ, et al. Hypoxic pulmonary vasoconstriction does not contribute to pulmonary blood flow heterogeneity in normoxia in normal supine humans. *J Appl Physiol* (1985). 2009;106(4):1057–1064.
112. Adding LC, Agvald P, Persson MG, Gustafsson LE. Regulation of pulmonary nitric oxide by carbon dioxide is intrinsic to the lung. *Acta Physiol Scand*. 1999;167(2):167–174.
113. Yamamoto Y, Nakano H, Ide H, et al. Role of airway nitric oxide on the regulation of pulmonary circulation by carbon dioxide. *J Appl Physiol* (1985). 2001;91(3):1121–1130.
114. Robertson TP, Ward JP, Aaronson PI. Hypoxia induces the release of a pulmonary-selective,  $\text{Ca}(2+)$ -sensitizing, vasoconstrictor from the perfused rat lung. *Cardiovasc Res*. 2001;50(1):145–150.
115. Morio Y, McMurtry IF.  $\text{Ca}(2+)$  release from ryanodine-sensitive store contributes to mechanism of hypoxic vasoconstriction in rat lungs. *J Appl Physiol* (1985). 2002;92(2):527–534.
116. Evans AM, Hardie DG, Peers C, Mahmoud A. Hypoxic pulmonary vasoconstriction: mechanisms of oxygen-sensing. *Curr Opin Anesthesiol*. 2011;24(1):13–20.
117. Firth AL, Yuill KH, Smirnov SV. Mitochondria-dependent regulation of  $\text{K}^+$  currents in rat pulmonary artery smooth muscle cells. *Am J Physiol Lung Cell Mol Physiol*. 2008;295(1):L61–70.
118. Nagendran J, Stewart K, Hoskinson M, Archer SL. An anesthesiologist's guide to hypoxic pulmonary vasoconstriction: implications for managing single-lung anesthesia and atelectasis. *Curr Opin Anesthesiol*. 2006;19(1):34–43.
119. Wang L, Yin J, Nickles HT, et al. Hypoxic pulmonary vasoconstriction requires connexin 40-mediated endothelial signal conduction. *J Clin Invest*. 2012;122(11):4218–4230.
120. Goldenberg NM, Wang L, Ranke H, Liedtke W, Tabuchi A, Kuebler WM. TRPV4 is required for hypoxic pulmonary vasoconstriction. *Anesthesiology*. 2015;122(6):1338–1348.
121. Lumb AB, Slinger P. Hypoxic pulmonary vasoconstriction: physiology and anesthetic implications. *Anesthesiology*. 2015;122(4):932–946.
122. Akata T. General anesthetics and vascular smooth muscle: direct actions of general anesthetics on cellular mechanisms regulating vascular tone. *Anesthesiology*. 2007;106(2):365–391.
123. Gambone LM, Fujiwara Y, Murray PA. Endothelium-dependent pulmonary vasodilation is selectively attenuated during isoflurane anesthesia. *Am J Physiol*. 1997;272(1 Pt 2):H290–298.
124. Seki S, Sato K, Nakayama M, Murray PA. Halothane and enflurane attenuate pulmonary vasodilation mediated by adenosine triphosphate-sensitive potassium channels compared to the conscious state. *Anesthesiology*. 1997;86(4):923–935.
125. Nakayama M, Kondo U, Murray PA. Pulmonary vasodilator response to adenosine triphosphate-sensitive potassium channel activation is attenuated during desflurane but preserved during sevoflurane anesthesia compared with the conscious state. *Anesthesiology*. 1998;88(4):1023–1035.
126. Lennon PF, Murray PA. Isoflurane and the pulmonary vascular pressure-flow relation at baseline and during sympathetic alpha- and beta-adrenoreceptor activation in chronically instrumented dogs. *Anesthesiology*. 1995;82(3):723–733.
127. Sato K, Seki S, Murray PA. Effects of halothane and enflurane anesthesia on sympathetic beta-adrenoreceptor-mediated pulmonary vasodilation in chronically instrumented dogs. *Anesthesiology*. 2002;97(2):478–487.
128. Liu R, Ishibe Y, Okazaki N, Ueda M, Hirosewa J. Volatile anesthetics regulate pulmonary vascular tension through different potassium channel subtypes in isolated rabbit lungs. *Can J Anaesth*. 2003;50(3):301–304.
129. Olschewski A. Targeting TASK-1 channels as a therapeutic approach. *Adv Exp Med Biol*. 2010;661:459–473.
130. Su JY, Vo AC.  $\text{Ca}(2+)$ -calmodulin-dependent protein kinase II plays a major role in halothane-induced dose-dependent relaxation in the skinned pulmonary artery. *Anesthesiology*. 2002;97(1):207–214.
131. Zhong L, Su JY. Isoflurane activates PKC and  $\text{Ca}(2+)$ -calmodulin-dependent protein kinase II via MAP kinase signaling in cultured vascular smooth muscle cells. *Anesthesiology*. 2002;96(1):148–154.
132. Loer SA, Scheeren TW, Tarnow J. Desflurane inhibits hypoxic pulmonary vasoconstriction in isolated rabbit lungs. *Anesthesiology*. 1995;83(3):552–556.
133. Lennon PF, Murray PA. Attenuated hypoxic pulmonary vasoconstriction during isoflurane anesthesia is abolished by cyclooxygenase inhibition in chronically instrumented dogs. *Anesthesiology*. 1996;84(2):404–414.
134. Johns RA. Endothelium, anesthetics, and vascular control. *Anesthesiology*. 1993;79(6):1381–1391.
135. Marshall CM, BE. Inhalational anesthetics directly inhibit hypoxic pulmonary vasoconstriction. *Anesthesiology*. 1993;79:A1238.
136. Marshall C, Marshall BE. Endothelium-derived relaxing factor is not responsible for inhibition of hypoxic pulmonary vasoconstriction by inhalational anesthetics. *Anesthesiology*. 1990;73(3):441–448.
137. Jing M, Hart JL, Masaki E, Van Dyke RA, Bina S, Muldoon SM. Vascular effects of halothane and isoflurane: cGMP dependent and independent actions. *Life Sci*. 1995;56(1):19–29.
138. Gambone LM, Murray PA, Flavahan NA. Isoflurane anesthesia attenuates endothelium-dependent pulmonary vasorelaxation by inhibiting the synergistic interaction between nitric oxide and prostacyclin. *Anesthesiology*. 1997;86(4):936–944.
139. Liu R, Ueda M, Okazaki N, Ishibe Y. Role of potassium channels in isoflurane- and sevoflurane-induced attenuation of hypoxic pulmonary vasoconstriction in isolated perfused rabbit lungs. *Anesthesiology*. 2001;95(4):939–946.
140. Eisenkraft JB. Effects of anaesthetics on the pulmonary circulation. *Br J Anaesth*. 1990;65(1):63–78.
141. Lesitsky MA, Davis S, Murray PA. Preservation of hypoxic pulmonary vasoconstriction during sevoflurane and desflurane anesthesia compared to the conscious state in chronically instrumented dogs. *Anesthesiology*. 1998;89(6):1501–1508.
142. Schwarzkopf K, Schreiber T, Gaser E, et al. The effects of xenon or nitrous oxide supplementation on systemic oxygenation and pulmonary perfusion during one-lung ventilation in pigs. *Anesth Analg*. 2005;100(2):335–339.

143. Schwarzkopf K, Schreiber T, Preussler NP, et al. Lung perfusion, shunt fraction, and oxygenation during one-lung ventilation in pigs: the effects of desflurane, isoflurane, and propofol. *J Cardiothorac Vasc Anesth*. 2003;17(1):73–75.
144. Karzai W, Haberstroh J, Priebe HJ. The effects of increasing concentrations of desflurane on systemic oxygenation during one-lung ventilation in pigs. *Anesth Analg*. 1999;89(1):215–217.
145. Schwarzkopf K, Schreiber T, Bauer R, et al. The effects of increasing concentrations of isoflurane and desflurane on pulmonary perfusion and systemic oxygenation during one-lung ventilation in pigs. *Anesth Analg*. 2001;93(6):1434–1438; table of contents.
146. Kleinsasser A, Lindner KH, Hoermann C, Schaefer A, Keller C, Loeckinger A. Isoflurane and sevoflurane anesthesia in pigs with a preexisting gas exchange defect. *Anesthesiology*. 2001;95(6):1422–1426.
147. Nyren S, Radell P, Mure M, et al. Inhalation anesthesia increases V/Q regional heterogeneity during spontaneous breathing in healthy subjects. *Anesthesiology*. 2010;113(6):1370–1375.
148. Radke OC, Schneide T, Heller AR, Koch T. Spontaneous breathing during general anesthesia prevents the ventral redistribution of ventilation as detected by electrical impedance tomography: a randomized trial. *Anesthesiology*. 2012;116(6):1227–1234.
149. Bindslev L, Hedenstierna G, Santesson J, Gottlieb I, Carvalhas A. Ventilation-perfusion distribution during inhalation anaesthesia. Effects of spontaneous breathing, mechanical ventilation and positive end-expiratory pressure. *Acta Anaesthesiol Scand*. 1981;25(4):360–371.
150. Nishiaki K, Nyhan DP, Rock P, et al. N omega-nitro-L-arginine and pulmonary vascular pressure-flow relationship in conscious dogs. *Am J Physiol*. 1992;262(5 Pt 2):H1331–1337.
151. Abe K, Mashimo T, Yoshiya I. Arterial oxygenation and shunt fraction during one-lung ventilation: a comparison of isoflurane and sevoflurane. *Anesth Analg*. 1998;86(6):1266–1270.
152. Reid CW, Slinger PD, Lenis S. A comparison of the effects of propofol-alfentanil versus isoflurane anesthesia on arterial oxygenation during one-lung ventilation. *J Cardiothorac Vasc Anesth*. 1996;10(7):860–863.
153. Beck DH, Doepfner UR, Sinemus C, Bloch A, Schenk MR, Kox WJ. Effects of sevoflurane and propofol on pulmonary shunt fraction during one-lung ventilation for thoracic surgery. *Br J Anaesth*. 2001;86(1):38–43.
154. Pruszkowski O, Dalibon N, Moutafis M, et al. Effects of propofol vs sevoflurane on arterial oxygenation during one-lung ventilation. *Br J Anaesth*. 2007;98(4):539–544.
155. Kellow NH, Scott AD, White SA, Feneck RO. Comparison of the effects of propofol and isoflurane anaesthesia on right ventricular function and shunt fraction during thoracic surgery. *Br J Anaesth*. 1995;75(5):578–582.
156. Abe K, Shimizu T, Takashina M, Shiozaki H, Yoshiya I. The effects of propofol, isoflurane, and sevoflurane on oxygenation and shunt fraction during one-lung ventilation. *Anesth Analg*. 1998;87(5):1164–1169.
157. Benumof JL, Augustine SD, Gibbons JA. Halothane and isoflurane only slightly impair arterial oxygenation during one-lung ventilation in patients undergoing thoracotomy. *Anesthesiology*. 1987;67(6):910–915.
158. Pagel PS, Fu JL, Damask MC, et al. Desflurane and isoflurane produce similar alterations in systemic and pulmonary hemodynamics and arterial oxygenation in patients undergoing one-lung ventilation during thoracotomy. *Anesth Analg*. 1998;87(4):800–807.
159. Carlsson AJ, Bindslev L, Hedenstierna G. Hypoxia-induced pulmonary vasoconstriction in the human lung. The effect of isoflurane anesthesia. *Anesthesiology*. 1987;66(3):312–316.
160. Ng A, Swanepoel J. Hypoxaemia associated with one-lung anaesthesia: new discoveries in ventilation and perfusion. *Br J Anaesth*. 2011;106(6):761–763.
161. Karzai W, Schwarzkopf K. Hypoxemia during one-lung ventilation: prediction, prevention, and treatment. *Anesthesiology*. 2009;110(6):1402–1411.
162. Dalibon N, Moutafis M, Liu N, Law-Koune JD, Monsel S, Fischler M. Treatment of hypoxemia during one-lung ventilation using intravenous almitrine. *Anesth Analg*. 2004;98(3):590–594; table of contents.
163. Teppema LJ, Baby S. Anesthetics and control of breathing. *Respir Physiol Neurobiol*. 2011;177(2):80–92.
164. Stuth EAEZE, Stucke AG. Effects of general anesthesia. In: Denham SWAL, ed. *Pharmacology and Pathophysiology of the Control of Breathing*. Boca Raton, FL: Taylor and Francis Group; 2005:571.
165. Stuth EA, Stucke AG, Brandes IF, Zuperku EJ. Anesthetic effects on synaptic transmission and gain control in respiratory control. *Respir Physiol Neurobiol*. 2008;164(1-2):151–159.
166. Sirois JE, Lei Q, Talley EM, Lynch C, Bayliss DA. The TASK-1 two-pore domain K<sup>+</sup> channel is a molecular substrate for neuronal effects of inhalation anesthetics. *J Neurosci*. 2000;20(17):6347–6354.
167. Sirois JE, Lynch C, Bayliss DA. Convergent and reciprocal modulation of a leak K<sup>+</sup> current and I(h) by an inhalational anaesthetic and neurotransmitters in rat brainstem motoneurones. *J Physiol*. 2002;541(Pt 3):717–729.
168. Trochet D, de Pontual L, Straus C, et al. PHOX2B germline and somatic mutations in late-onset central hypoventilation syndrome. *Am J Respir Crit Care Med*. 2008;177(8):906–911.
169. Coglan M, Richards E. Inhalational anesthetics induce neuronal protein aggregation and affect. *ER Trafficking*. 2018;8(1):5275.
170. Forster HV, Smith CA. Contributions of central and peripheral chemoreceptors to the ventilatory response to CO<sub>2</sub>/H<sup>+</sup>. *J Appl Physiol* (1985). 2010;108(4):989–994.
171. Nattie E, Julius H, Comroe. distinguished lecture: central chemoreception: then ... and now. *J Appl Physiol* (1985). 2011;110(1):1–8.
172. Erlichman JS, Leiter JC, Gourine AV. ATP, glia and central respiratory control. *Respir Physiol Neurobiol*. 2010;173(3):305–311.
173. Pandit JJ. The variable effect of low-dose volatile anaesthetics on the acute ventilatory response to hypoxia in humans: a quantitative review. *Anesthesia*. 2002;57(7):632–643.
174. Pandit JJ. Effect of low dose inhaled anaesthetic agents on the ventilatory response to carbon dioxide in humans: a quantitative review. *Anesthesia*. 2005;60(5):461–469.
175. Baugh R, Burke B, Fink B, Garcia R, Kominsky A, Yaremchuk K. Safety of outpatient surgery for obstructive sleep apnea. *Otolaryngol Head Neck Surg*. 2013;148(5):867–872.
176. Abdala AP, Paton JF, Smith JC. Defining inhibitory neurone function in respiratory circuits: opportunities with optogenetics? *J Physiol*. 2015;593(14):3033–3046.
177. Rybak IA, O'Connor R, Ross A, et al. Reconfiguration of the pontomedullary respiratory network: a computational modeling study with coordinated in vivo experiments. *J Neurophysiol*. 2008;100(4):1770–1799.
178. Smith CA, Forster HV, Blain GM, Dempsey JA. An interdependent model of central/peripheral chemoreception: evidence and implications for ventilatory control. *Respir Physiol Neurobiol*. 2010;173(3):288–297.
179. von Euler US LG, Zotterman Y. The excitation mechanism of the chemoreceptors of the carotid body. *Scand Arch Physiol*. 1939;83:132–152.
180. BuSha BF, Stella MH, Manning HL, Leiter JC. Termination of inspiration by phase-dependent respiratory vagal feedback in awake normal humans. *J Appl Physiol* (1985). 2002;93(3):903–910.
181. Lazarenko RM, Willcox SC, Shu S, et al. Motoneuronal TASK channels contribute to immobilizing effects of inhalational general anesthetics. *J Neurosci*. 2010;30(22):7691–7704.
182. Haxhiu MA, van Lunteren E, Mitra J, Cherniack NS. Comparison of the response of diaphragm and upper airway dilating muscle activity in sleeping cats. *Respiration physiology*. 1987;70(2):183–193.
183. Horner RL, Liu X, Gill H, Nolan P, Liu H, Sood S. Effects of sleep-wake state on the genioglossus vs. diaphragm muscle response to CO<sub>2</sub> in rats. *J Appl Physiol* (1985). 2002;92(2):878–887.
184. Bogle RL, Badr S, Skatrud JB, Dempsey JA. Effect of lung inflation on pulmonary resistance during NREM sleep. *Am Rev Respir Dis*. 1990;141(4 Pt 1):854–860.
185. Tagaito Y, Isono S, Remmers JE, Tanaka A, Nishino T. Lung volume and collapsibility of the passive pharynx in patients with sleep-disordered breathing. *J Appl Physiol* (1985). 2007;103(4):1379–1385.
186. Hornbein TF, Eger EI, Winter PM, Smith G, Wetstone D, Smith KH. The minimum alveolar concentration of nitrous oxide in man. *Anesth Analg*. 1982;61(7):553–556.
187. Bedi A, McCarroll C, Murray JM, Stevenson MA, Fee JP. The effects of subanaesthetic concentrations of xenon in volunteers. *Anesthesia*. 2002;57(3):233–241.
188. Cormack JR, Gott J, Kondogiannis S. Profound hypopnea with xenon anesthesia in a free diver. *A Case Rep*. 2017;8(4):90.
189. Fourcade HE, Stevens WC, Larson CP, et al. The ventilatory effects of Forane, a new inhaled anesthetic. *Anesthesiology*. 1971;35(1):26–31.

190. Calverley RK, Smith NT, Jones CW, Prys-Roberts C, Eger EI. Ventilatory and cardiovascular effects of enflurane anesthesia during spontaneous ventilation in man. *Anesth Analg*. 1978;57(6):610–618.
191. Lockhart SH, Rampil IJ, Yasuda N, Eger EI, Weiskopf RB. Depression of ventilation by desflurane in humans. *Anesthesiology*. 1991;74(3):484–488.
192. Doi M, Ikeda K. Postanesthetic respiratory depression in humans: a comparison of sevoflurane, isoflurane and halothane. *J Anesth*. 1987;1(2):137–142.
193. Hickey RF, Severinghaus JW. Regulation of breathing: drug effects. In: Hornbein TF, ed. *Regulation of Breathing - Pt. 2*. New York, NY: Marcel Dekker; 1981:1251–1312.
194. Eger EI. Isoflurane: a review. *Anesthesiology*. 1981;55(5):559–576.
195. Fujii Y. Respiratory effects of xenon. *Int Anesthesiol Clin*. 2001;39(2):95–103.
196. Winkler SS, Nielsen A, Mesina J. Respiratory depression in goats by stable xenon: implications for CT studies. *J Comput Assist Tomogr*. 1987;11(3):496–498.
197. Winkler STP, Holden J, et al. Xenon effects on CNS control of respiratory rate and tidal volume—the danger of apnea. In: Hartmann AHS, ed. *Cerebral Blood Flow and Metabolism Measurement*. Berlin: Springer-Verlag; 1985:356–360.
198. Holl K, Nemati N, Kohmura E, Gaab MR, Samii M. Stable-xenon-CT: effects of xenon inhalation on EEG and cardio-respiratory parameters in the human. *Acta Neurochir (Wien)*. 1987;87(3-4):129–133.
199. Ballantyne D, Scheid P. Central respiratory chemosensitivity: cellular and network mechanisms. *Adv Exp Med Biol*. 2001;499:17–26.
200. Ballantyne D, Scheid P. Central chemosensitivity of respiration: a brief overview. *Respiration physiology*. 2001;129(1-2):5–12.
201. Branco LG, Moreira TS, Guyenet PG, et al. Commentaries on viewpoint: central chemoreception is a complex system function that involves multiple brain stem sites. *J Appl Physiol* (1985). 2009;106(4):1467–1470.
202. Heeringa J, Berkenbosch A, de Goede J, Olievier CN. Relative contribution of central and peripheral chemoreceptors to the ventilatory response to CO<sub>2</sub> during hyperoxia. *Respiration Physiology*. 1979;37(3):365–379.
203. Knill RL, Gelb AW. Ventilatory responses to hypoxia and hypercapnia during halothane sedation and anesthesia in man. *Anesthesiology*. 1978;49(4):244–251.
204. Deleted in proofs
205. Kammer T, Rehberg B, Menne D, Wartenberg HC, Wenningmann I, Urban BW. Propofol and sevoflurane in subanesthetic concentrations act preferentially on the spinal cord: evidence from multimodal electrophysiological assessment. *Anesthesiology*. 2002;97(6):1416–1425.
206. Barnard P, Andronikou S, Pokorski M, Smatresk N, Mokashi A, Lahiri S. Time-dependent effect of hypoxia on carotid body chemosensory function. *J Appl Physiol* (1985). 1987;63(2):685–691.
207. Dahan A, Teppema L. Influence of low-dose anaesthetic agents on ventilatory control: where do we stand? *Br J Anaesth*. 1999;83(2):199–201.
208. Sarton E, van der Wal M, Nieuwenhuijse D, Teppema L, Robotham JL, Dahan A. Sevoflurane-induced reduction of hypoxic drive is sex-independent. *Anesthesiology*. 1999;90(5):1288–1293.
209. van den Elsen MJ, Dahan A, Berkenbosch A, DeGoede J, van Kleef JW, Olievier IC. Does subanesthetic isoflurane affect the ventilatory response to acute isocapnic hypoxia in healthy volunteers?. *Anesthesiology*. 1994;81(4):860–867; discussion 826A.
210. Hickey RF, Fourcade HE, Eger EI, et al. The effects of ether, halothane, and Forane on apneic thresholds in man. *Anesthesiology*. 1971;35(1):32–37.
211. Nakayama H, Smith CA, Rodman JR, Skatrud JB, Dempsey JA. Effect of ventilatory drive on carbon dioxide sensitivity below eupnea during sleep. *Am J Respir Crit Care Med*. 2002;165(9):1251–1260.
212. West JB. Climbing Mt. Everest without oxygen: an analysis of maximal exercise during extreme hypoxia. *Respir Physiol*. 1983;52(3):265–279.
213. Dahan A, van den Elsen MJ, Berkenbosch A, et al. Effects of subanesthetic halothane on the ventilatory responses to hypercapnia and acute hypoxia in healthy volunteers. *Anesthesiology*. 1994;80(4):727–738.
214. Chung F, Liao P, Yegneswaran B, Shapiro CM, Kang W. Postoperative changes in sleep-disordered breathing and sleep architecture in patients with obstructive sleep apnea. *Anesthesiology*. 2014;120(2):287–298.
215. Chung F, Liao P, Elsaied H, Shapiro CM, Kang W. Factors associated with postoperative exacerbation of sleep-disordered breathing. *Anesthesiology*. 2014;120(2):299–311.
216. Sarton E, Dahan A, Teppema L, et al. Acute pain and central nervous system arousal do not restore impaired hypoxic ventilatory response during sevoflurane sedation. *Anesthesiology*. 1996;85(2):295–303.
217. Pandit JJ, Moreau B, Donoghue S, Robbins PA. Effect of pain and audiovisual stimulation on the depression of acute hypoxic ventilatory response by low-dose halothane in humans. *Anesthesiology*. 2004;101(6):1409–1416.
218. Warner DO, Warner MA, Ritman EL. Mechanical significance of respiratory muscle activity in humans during halothane anesthesia. *Anesthesiology*. 1996;84(2):309–321.
219. Warner DO, Warner MA, Ritman EL. Human chest wall function while awake and during halothane anesthesia. I. Quiet breathing. *Anesthesiology*. 1995;82(1):6–19.
220. Warner DO, Warner MA. Human chest wall function while awake and during halothane anesthesia. II. Carbon dioxide rebreathing. *Anesthesiology*. 1995;82(1):20–31.
221. Gauda EB, Carroll TP, Schwartz AR, Smith PL, Fitzgerald RS. Mechano- and chemoreceptor modulation of respiratory muscles in response to upper airway negative pressure. *J Appl Physiol* (1985). 1994;76(6):2656–2662.
222. Wheatley JR, Kelly WT, Tully A, Engel LA. Pressure-diameter relationships of the upper airway in awake supine subjects. *J Appl Physiol* (1985). 1991;70(5):2242–2251.
223. Schwartz AR, O'Donnell CP, Baron J, et al. The hypotonic upper airway in obstructive sleep apnea: role of structures and neuromuscular activity. *Am J Respir Crit Care Med*. 1998;157(4 Pt 1):1051–1057.
224. Kuna ST, Remmers JE. Neural and anatomic factors related to upper airway occlusion during sleep. *Med Clin North Am*. 1985;69(6):1221–1242.
225. Erb TO, von Ungern-Sternberg BS, Moll J, Frei FJ. Impact of high concentrations of sevoflurane on laryngeal reflex responses. *Paediatr Anaesth*. 2017;27(3):282–289.
226. Lerman J, Hammer GB, Verghese S, et al. Airway responses to desflurane during maintenance of anesthesia and recovery in children with laryngeal mask airways. *Paediatr Anaesth*. 2010;20(6):495–505.
227. Ulevitch RJ. Recognition of bacterial endotoxins by receptor-dependent mechanisms. *Adv Immunol*. 1993;53:267–289.
228. Chow JC, Young DW, Golenbock DT, Christ WJ, Gusovsky F. Toll-like receptor-4 mediates lipopolysaccharide-induced signal transduction. *J Biol Chem*. 1999;274(16):10689–10692.
229. Marini JJ, Evans TW. Round table conference: acute lung injury, 15th–17th March 1997 Brussels, Belgium. *Intensive Care Med*. 1998;24(8):878–883.
230. Meyrick B, Johnson JE, Brigham KL. Endotoxin-induced pulmonary endothelial injury. *Prog Clin Biol Res*. 1989;308:91–99.
231. Brigham KL. Conference summary: lipid mediators in the pulmonary circulation. *Am Rev Respir Dis*. 1987;136(3):785–788.
232. Bulger EM, Maier RV. Lipid mediators in the pathophysiology of critical illness. *Crit Care Med*. 2000;28(suppl 4):N27–36.
233. Ermert L, Ermert M, Duncker HR, Grimminger F, Seeger W. In situ localization and regulation of thromboxane A(2) synthase in normal and LPS-primed lungs. *Am J Physiol Lung Cell Mol Physiol*. 2000;278(4):L744–753.
234. Quinn JV, Slotman GJ. Platelet-activating factor and arachidonic acid metabolites mediate tumor necrosis factor and eicosanoid kinetics and cardiopulmonary dysfunction during bacteremic shock. *Crit Care Med*. 1999;27(11):2485–2494.
235. Langleben D, DeMarchie M, Laporta D, Spanier AH, Schlesinger RD, Stewart DJ. Endothelin-1 in acute lung injury and the adult respiratory distress syndrome. *Am Rev Respir Dis*. 1993;148(6 Pt 1):1646–1650.
236. Suffredini AF, Shelhamer JH, Neumann RD, Brenner M, Baltaro RJ, Parrillo JE. Pulmonary and oxygen transport effects of intravenously administered endotoxin in normal humans. *Am Rev Respir Dis*. 1992;145(6):1398–1403.
237. O'Grady NP, Preas HL, Pugin J, et al. Local inflammatory responses following bronchial endotoxin instillation in humans. *Am J Respir Crit Care Med*. 2001;163(7):1591–1598.
238. Bachofen M, Weibel ER. Structural alterations of lung parenchyma in the adult respiratory distress syndrome. *Clin Chest Med*. 1982;3(1):35–56.

239. Kumar A, Brar R, Wang P, et al. Role of nitric oxide and cGMP in human septic serum-induced depression of cardiac myocyte contractility. *Am J Physiol*. 1999;276(1 Pt 2):R265–276.
240. McQuaid KE, Keenan AK. Endothelial barrier dysfunction and oxidative stress: roles for nitric oxide? *Exp Physiol*. 1997;82(2):369–376.
241. Salvemini D. Regulation of cyclooxygenase enzymes by nitric oxide. *Cell Mol Life Sci*. 1997;53(7):576–582.
242. Ignarro LJ, Fukuto JM, Griscavage JM, Rogers NE, Byrns RE. Oxidation of nitric oxide in aqueous solution to nitrite but not nitrate: comparison with enzymatically formed nitric oxide from L-arginine. *Proc Natl Acad Sci U S A*. 1993;90(17):8103–8107.
243. Weissmann N, Tadic A, Hanze J, et al. Hypoxic vasoconstriction in intact lungs: a role for NADPH oxidase-derived H<sub>2</sub>O<sub>2</sub>? *Am J Physiol Lung Cell Mol Physiol*. 2000;279(4):L683–690.
244. Singh S, Evans TW. Nitric oxide, the biological mediator of the decade: fact or fiction? *Eur Respir J*. 1997;10(3):699–707.
245. Westendorp RG, Draijer R, Meinders AE, van Hinsbergh VW. Cyclic-GMP-mediated decrease in permeability of human umbilical and pulmonary artery endothelial cell monolayers. *J Vasc Res*. 1994;31(1):42–51.
246. Suter D, Spahn DR, Blumenthal S, et al. The immunomodulatory effect of sevoflurane in endotoxin-injured alveolar epithelial cells. *Anesth Analg*. 2007;104(3):638–645.
247. Takala RS, Soukka H, Salo MS, Kirvela O, Kaapa P, Aantaa R. Gene expression of pulmonary cytokines after sevoflurane or thiopentone anaesthesia in pigs. *Acta Anaesthesiol Scand*. 2006;50(2):163–167.
248. Giraud O, Molliex S, Rolland C, et al. Halogenated anesthetics reduce interleukin-1beta-induced cytokine secretion by rat alveolar type II cells in primary culture. *Anesthesiology*. 2003;98(1):74–81.
249. Voigtberger S, Lachmann RA, Leutert AC, et al. Sevoflurane ameliorates gas exchange and attenuates lung damage in experimental lipopolysaccharide-induced lung injury. *Anesthesiology*. 2009;111(6):1238–1248.
250. Schlapfer M, Leutert AC, Voigtberger S, Lachmann RA, Booy C, Beck-Schimmer B. Sevoflurane reduces severity of acute lung injury possibly by impairing formation of alveolar oedema. *Clin Exp Immunol*. 2012;168(1):125–134.
251. Du G, Wang S, Li Z, Liu J. Sevoflurane posttreatment attenuates lung injury induced by oleic acid in dogs. *Anesth Analg*. 2017;124(5):1555–1563.
252. Bedirli N, Demirtas CY, Akkaya T, et al. Volatile anesthetic preconditioning attenuated sepsis induced lung inflammation. *J Surg Res*. 2012;178(1):e17–e23.
253. Dong X, Hu R, Sun Y, Li Q, Jiang H. Isoflurane post-treatment improves pulmonary vascular permeability via upregulation of heme oxygenase-1. *Exp Lung Res*. 2013;39(7):295–303.
254. Beitler JR, Malhotra A, Thompson BT. Ventilator-induced lung injury. *Clin Chest Med*. 2016;37(4):633–646.
255. Wagner J, Strosing KM, Spassov SG, et al. Sevoflurane posttreatment prevents oxidative and inflammatory injury in ventilator-induced lung injury. *PLoS One*. 2018;13(2):e0192896.
256. Faller S, Strosing KM, Ryter SW, et al. The volatile anesthetic isoflurane prevents ventilator-induced lung injury via phosphoinositide 3-kinase/Akt signalling in mice. *Anesth Analg*. 2012;114(4):747–756.
257. Englert JA, Macias AA, Amador-Munoz D, et al. Isoflurane ameliorates acute lung injury by preserving epithelial tight junction integrity. *Anesthesiology*. 2015;123(2):377–388.
258. Strosing KM, Faller S, Gyllenram V, et al. Inhaled anesthetics exert different protective properties in a mouse model of ventilator-induced lung injury. *Anesth Analg*. 2016;123(1):143–151.
259. PakO, Sydkov A, Kosanovic D, et al. Lung ischaemia-reperfusion injury: the role of reactive oxygen species. *Adv Exp Med Biol*. 2017;967:195–225.
260. Liu R, Ishibe Y, Ueda M, Hang Y. Isoflurane administration before ischemia and during reperfusion attenuates ischemia/reperfusion-induced injury of isolated rabbit lungs. *Anesth Analg*. 1999;89(3):561–565.
261. Fujinaga T, Nakamura T, Fukuse T, et al. Isoflurane inhalation after circulatory arrest protects against warm ischemia reperfusion injury of the lungs. *Transplantation*. 2006;82(9):1168–1174.
262. Casanova J, Garutti I, Simon C, et al. The effects of anesthetic preconditioning with sevoflurane in an experimental lung autotransplant model in pigs. *Anesth Analg*. 2011;113(4):742–748.
263. Ohsumi A, Marseu K, Slinger P, et al. Sevoflurane attenuates ischemia-reperfusion injury in a rat lung transplantation model. *Ann Thorac Surg*. 2017;103(5):1578–1586.
264. Oshima Y, Sakamoto S, Yamasaki K, et al. Desflurane inhalation before ischemia increases ischemia-reperfusion-induced vascular leakage in isolated rabbit lungs. *Springerplus*. 2016;5(1):2031.
265. Martens A, Montoli M, Faggi G, et al. Argon and xenon ventilation during prolonged ex vivo lung perfusion. *J Surg Res*. 2016;201(1):44–52.
266. Wrigge H, Zinslerling J, Stuber F, et al. Effects of mechanical ventilation on release of cytokines into systemic circulation in patients with normal pulmonary function. *Anesthesiology*. 2000;93(6):1413–1417.
267. De Conno E, Steurer MP, Wittlinger M, et al. Anesthetic-induced improvement of the inflammatory response to one-lung ventilation. *Anesthesiology*. 2009;110(6):1316–1326.
268. Schilling T, Kozian A, Senturk M, et al. Effects of volatile and intravenous anesthesia on the alveolar and systemic inflammatory response in thoracic surgical patients. *Anesthesiology*. 2011;115(1):65–74.
269. Sugasawa Y, Yamaguchi K, Kumakura S, et al. Effects of sevoflurane and propofol on pulmonary inflammatory responses during lung resection. *J Anesth*. 2012;26(1):62–69.
270. Uhlig C, Bluth T, Schwarz K, et al. Effects of volatile anesthetics on mortality and postoperative pulmonary and other complications in patients undergoing surgery: a systematic review and meta-analysis. *Anesthesiology*. 2016;124(6):1230–1245.
271. Beck-Schimmer B, Bonyini JM, Braun J, et al. Which anesthesia regimen is best to reduce morbidity and mortality in lung surgery?: a multicenter randomized controlled trial. *Anesthesiology*. 2016;125(2):313–321.
272. Koksal GM, Sayilgan C, Aydin S, Uzun H, Oz H. The effects of sevoflurane and desflurane on lipid peroxidation during laparoscopic cholecystectomy. *Eur J Anaesthesiol*. 2004;21(3):217–220.
273. Koksal GM, Sayilgan C, Gungor G, et al. Effects of sevoflurane and desflurane on cytokine response during tympanoplasty surgery. *Acta Anaesthesiol Scand*. 2005;49(6):835–839.
274. Jabaudon M, Boucher P, Imhoff E, et al. Sevoflurane for sedation in acute respiratory distress syndrome. a randomized controlled pilot study. *Am J Respir Crit Care Med*. 2017;195(6):792–800.
275. Bellgardt M, Bomberg H, Herzog-Nescery J, et al. Survival after long-term isoflurane sedation as opposed to intravenous sedation in critically ill surgical patients: retrospective analysis. *Eur J Anaesthesiol*. 2016;33(1):6–13.
276. Wilson KE. Overview of paediatric dental sedation: 2. Nitrous oxide/oxygen inhalation sedation. *Dent Update*. 2013;40(10):822–824. 826–829.
277. Likis FE, Andrews JC, Collins MR, et al. Nitrous oxide for the management of labor pain: a systematic review. *Anesth Analg*. 2014;118(1):153–167.
278. Goto T, Nakata Y, Ishiguro Y, Niimi Y, Suwa K, Morita S. Minimum alveolar concentration-awake of xenon alone and in combination with isoflurane or sevoflurane. *Anesthesiology*. 2000;93(5):1188–1193.
279. Mashour GA, Avidan MS. Intraoperative awareness: controversies and non-controversies. *Br J Anaesth*. 2015;115(suppl 1):i20–i26.
280. Mathews DM, Gaba V, Zaku B, Neuman GG. Can remifentanil replace nitrous oxide during anesthesia for ambulatory orthopedic surgery with desflurane and fentanyl? *Anesth Analg*. 2008;106(1):101–108; table of contents.
281. Lee LH, Irwin MG, Lui SK. Intraoperative remifentanil infusion does not increase postoperative opioid consumption compared with 70% nitrous oxide. *Anesthesiology*. 2005;102(2):398–402.
282. Janiszewski DJ, Galinkin JL, Klock PA, Coalson DW, Pardo H, Zaczynski JP. The effects of subanesthetic concentrations of sevoflurane and nitrous oxide, alone and in combination, on analgesia, mood, and psychomotor performance in healthy volunteers. *Anesth Analg*. 1999;88(5):1149–1154.
283. Berkowitz BA, Finck AD, Hynes MD, Ngai SH. Tolerance to nitrous oxide analgesia in rats and mice. *Anesthesiology*. 1979;51(4):309–312.
284. Berkowitz BA, Finck AD, Ngai SH. Nitrous oxide analgesia: reversal by naloxone and development of tolerance. *J Pharmacol Exp Ther*. 1977;203(3):539–547.
285. Ramsay DS, Leroux BG, Rothen M, Prall CW, Fiset LO, Woods SC. Nitrous oxide analgesia in humans: acute and chronic tolerance. *Pain*. 2005;114(1-2):19–28.
286. Akca O, Lenhardt R, Fleischmann E, et al. Nitrous oxide increases the incidence of bowel distension in patients undergoing elective colon resection. *Acta Anaesthesiol Scand*. 2004;48(7):894–898.

287. Fernandez-Guisasola J, Gomez-Arnau JI, Cabrera Y, del Valle SG. Association between nitrous oxide and the incidence of postoperative nausea and vomiting in adults: a systematic review and meta-analysis. *Anaesthesia*. 2010;65(4):379–387.
288. Peyton PJ, Wu CY. Nitrous oxide-related postoperative nausea and vomiting depends on duration of exposure. *Anesthesiology*. 2014;120(5):1137–1145.
289. Pace NL. Questioning a relationship between nitrous oxide duration of exposure and postoperative nausea and vomiting. *Anesthesiology*. 2014;121(6):1356–1358.
290. Zhou L, Chen C, Yu H. Nitrous oxide-related postoperative nausea and vomiting depends on duration of exposure: more questions than answers. *Anesthesiology*. 2014;121(6):1356.
291. Konstadt SN, Reich DL, Thys DM. Nitrous oxide does not exacerbate pulmonary hypertension or ventricular dysfunction in patients with mitral valvular disease. *Can J Anaesth*. 1990;37(6):613–617.
292. Schulte-Sasse U, Hess W, Tarnow J. Pulmonary vascular responses to nitrous oxide in patients with normal and high pulmonary vascular resistance. *Anesthesiology*. 1982;57(1):9–13.
293. Beattie WS, Wijeyesundara DN, Chan MTV, et al. Implication of major adverse postoperative events and myocardial injury on disability and survival: a planned subanalysis of the ENIGMA-II trial. *Anesth Analg*. 2018.
294. Jevtic-Todorovic V, Absalom AR, Blomgren K, et al. Anaesthetic neurotoxicity and neuroplasticity: an expert group report and statement based on the BJA Salzburg Seminar. *Br J Anaesth*. 2013;111(2):143–151.
295. Savage S, Ma D. The neurotoxicity of nitrous oxide: the facts and “putative” mechanisms. *Brain Sci*. 2014;4(1):73–90.
296. Morris N, Lynch K, Greenberg SA. Severe motor neuropathy or neuropathy due to nitrous oxide toxicity after correction of vitamin B12 deficiency. *Muscle Nerve*. 2015;51(4):614–616.
297. Myles PS, Chan MT, Kaye DM, et al. Effect of nitrous oxide anaesthesia on plasma homocysteine and endothelial function. *Anesthesiology*. 2008;109(4):657–663.
298. Drummond JT, Matthews RG. Nitrous oxide inactivation of cobalamin-dependent methionine synthase from *Escherichia coli*: characterization of the damage to the enzyme and prosthetic group. *Biochemistry*. 1994;33(12):3742–3750.
299. Nagele P, Tallchief D, Blood J, Sharma A, Kharasch ED. Nitrous oxide anaesthesia and plasma homocysteine in adolescents. *Anesth Analg*. 2011;113(4):843–848.
300. Kiasari AZ, Firouzian A, Baradari AG, Nia HS, Kiasari SH. The effect of Vitamin B12 infusion on prevention of nitrous oxide-induced homocysteine increase: a double-blind randomized controlled trial. *Orn Med J*. 2014;29(3):194–197.
301. Mugler JP, Altes TA, Ruset IC, et al. Simultaneous magnetic resonance imaging of ventilation distribution and gas uptake in the human lung using hyperpolarized xenon-129. *Proc Natl Acad Sci U S A*. 2010;107(50):21707–21712.
302. Cullen SC, Eger EI, Cullen BF, Gregory P. Observations on the anesthetic effect of the combination of xenon and halothane. *Anesthesiology*. 1969;31(4):305–309.
303. Nakata Y, Goto T, Ishiguro Y, et al. Minimum alveolar concentration (MAC) of xenon with sevoflurane in humans. *Anesthesiology*. 2001;94(4):611–614.
304. Law LS, Lo EA, Gan TJ. Xenon anaesthesia: a systematic review and meta-analysis of randomized controlled trials. *Anesth Analg*. 2016;122(3):678–697.
305. Law LS, Lo EA, Chan CC, Gan TJ. Neurologic and cognitive outcomes associated with the clinical use of xenon: a systematic review and meta-analysis of randomized-controlled trials. *Can J Anaesth*. 2018.
306. Bronco A, Ingelmo PM, Aprigliano M, et al. Xenon anaesthesia produces better early postoperative cognitive recovery than sevoflurane anaesthesia. *Eur J Anaesthesiol*. 2010;27(10):912–916.
307. Cremer J, Stoppe C, Fahlenkamp AV, et al. Early cognitive function, recovery and well-being after sevoflurane and xenon anaesthesia in the elderly: a double-blinded randomized controlled trial. *Med Gas Res*. 2011;1(1):9.
308. Coburn M, Baumert JH, Roertgen D, et al. Emergence and early cognitive function in the elderly after xenon or desflurane anaesthesia: a double-blinded randomized controlled trial. *Br J Anaesth*. 2007;98(6):756–762.
309. Hocker J, Stapeifeldt C, Leiendoer J, et al. Postoperative neurocognitive dysfunction in elderly patients after xenon versus propofol anaesthesia for major noncardiac surgery: a double-blinded randomized controlled pilot study. *Anesthesiology*. 2009;110(5):1068–1076.
310. Neukirchen M, Hipp J, Schaefer MS, et al. Cardiovascular stability and unchanged muscle sympathetic activity during xenon anaesthesia: role of norepinephrine uptake inhibition. *Br J Anaesth*. 2012;109(6):887–896.
311. Hofland J, Ouattara A, Fellahi JL, et al. Effect of xenon anaesthesia compared to sevoflurane and total intravenous anaesthesia for coronary artery bypass graft surgery on postoperative cardiac troponin release: an international, multicenter, phase 3, single-blinded, randomized noninferiority trial. *Anesthesiology*. 2017;127(6):918–933.
312. Petzelt C, Blom P, Schmehl W, Muller J, Kox WJ. Xenon prevents cellular damage in differentiated PC-12 cells exposed to hypoxia. *BMC Neurosci*. 2004;5:55.
313. Sacchetti ML. Is it time to definitely abandon neuroprotection in acute ischemic stroke? *Stroke*. 2008;39(6):1659–1660.
314. Bedi A, Murray JM, Dingley J, Stevenson MA, Fee JP. Use of xenon as a sedative for patients receiving critical care. *Crit Care Med*. 2003;31(10):2470–2477.
315. Roehl AB, Goetzenich A, Rossaint R, Zoremba N, Hein M. A practical rule for optimal flows for xenon anaesthesia in a semi-closed anaesthesia circuit. *Eur J Anaesthesiol*. 2010;27(7):660–665.
316. Suzuki T, Koyama H, Sugimoto M, Uchida I, Mashimo T. The diverse actions of volatile and gaseous anaesthetics on human-cloned 5-hydroxytryptamine3 receptors expressed in *Xenopus* oocytes. *Anesthesiology*. 2002;96(3):699–704.
317. Schaefer MS, Apfel CC, Sachs HJ, et al. Predictors for postoperative nausea and vomiting after xenon-based anaesthesia. *Br J Anaesth*. 2015;115(1):61–67.
318. Calzia E, Stahl W, Handschuh T, et al. Continuous arterial P(O<sub>2</sub>) and P(CO<sub>2</sub>) measurements in swine during nitrous oxide and xenon elimination: prevention of diffusion hypoxia. *Anesthesiology*. 1999;90(3):829–834.
319. Baumert JH, Reyle-Hahn M, Hecker K, Tenbrinck R, Kuhlen R, Rossaint R. Increased airway resistance during xenon anaesthesia in pigs is attributed to physical properties of the gas. *Br J Anaesth*. 2002;88(4):540–545.
320. Zhang P, Ohara A, Mashimo T, Imanaka H, Uchiyama A, Yoshiya I. Pulmonary resistance in dogs: a comparison of xenon with nitrous oxide. *Can J Anaesth*. 1995;42(6):547–553.
321. Rueckoldt H, Vangerow B, Marx G, et al. Xenon inhalation increases airway pressure in ventilated patients. *Acta Anaesthesiol Scand*. 1999;43(10):1060–1064.
322. Dickinson R, Peterson BK, Banks P, et al. Competitive inhibition at the glycine site of the N-methyl-D-aspartate receptor by the anaesthetics xenon and isoflurane: evidence from molecular modeling and electrophysiology. *Anesthesiology*. 2007;107(5):756–767.
323. Kratzer S, Mattusch C, Kochs E, Eder M, Haseneder R, Rammes G. Xenon attenuates hippocampal long-term potentiation by diminishing synaptic and extrasynaptic N-methyl-D-aspartate receptor currents. *Anesthesiology*. 2012;116(3):673–682.
324. Nagele P, Metz LB, Crowder CM. Nitrous oxide (N<sub>2</sub>O) requires the N-methyl-D-aspartate receptor for its action in *Caenorhabditis elegans*. *Proc Natl Acad Sci U S A*. 2004;101(23):8791–8796.
325. Richardson KJ, Shelton KL. N-methyl-D-aspartate receptor channel blocker-like discriminative stimulus effects of nitrous oxide gas. *J Pharmacol Exp Ther*. 2015;352(1):156–165.
326. Hagen T, Bartylla K, Piepras U. Correlation of regional cerebral blood flow measured by stable xenon CT and perfusion MRI. *J Comput Assist Tomogr*. 1999;23(2):257–264.
327. Reinstrup P, Ryding E, Algotsen L, Berntman L, Uski T. Effects of nitrous oxide on human regional cerebral blood flow and isolated pial arteries. *Anesthesiology*. 1994;81(2):396–402.
328. Yagi M, Mashimo T, Kawaguchi T, Yoshiya I. Analgesic and hypnotic effects of subanaesthetic concentrations of xenon in human volunteers: comparison with nitrous oxide. *Br J Anaesth*. 1995;74(6):670–673.
329. Petersen-Felix S, Luginbuhl M, Schnider TW, Curatolo M, Arendt-Nielsen L, Zbinden AM. Comparison of the analgesic potency of xenon and nitrous oxide in humans evaluated by experimental pain. *Br J Anaesth*. 1998;81(5):742–747.
330. Utsumi J, Adachi T, Miyazaki Y, et al. The effect of xenon on spinal dorsal horn neurons: a comparison with nitrous oxide. *Anesth Analg*. 1997;84(6):1372–1376.

331. Yonas H, Grundy B, Gur D, Shabason L, Wolfson SK, Cook EE. Side effects of xenon inhalation. *J Comput Assist Tomogr*. 1981;5(4): 591–592.
332. Kamp HD. [Side effects and risks in the use of nitrous oxide in the course of general anesthesia]. *Klin Anästhesiol Intensivther*. 1993;42: 17–24.
333. de Vasconcellos K, Sneyd JR. Nitrous oxide: are we still in equipoise? A qualitative review of current controversies. *Br J Anaesth*. 2013;111(6):877–885.
334. Imberger G, Orr A, Thorlund K, Wetterslev J, Myles P, Moller AM. Does anaesthesia with nitrous oxide affect mortality or cardiovascular morbidity? A systematic review with meta-analysis and trial sequential analysis. *Br J Anaesth*. 2014;112(3):410–426.
335. Myles PS, Leslie K, Chan MT, et al. The safety of addition of nitrous oxide to general anaesthesia in at-risk patients having major non-cardiac surgery (ENIGMA-II): a randomised, single-blind trial. *Lancet*. 2014;384(9952):1446–1454.

MICHAEL P. BOKOCH and STEPHEN D. WESTON

## KEY POINTS

- The modern anesthesia workstation has evolved into a complex device with a number of safety features. However, if there is any possibility that the workstation or the breathing circuit is a potential cause of difficulty with ventilation or oxygenation, ventilating the patient using an oxygen cylinder and a manual ventilation bag is an appropriate decision. *When in doubt, ventilate and oxygenate the patient first via another method—troubleshoot later.*
- The most important part of the preanesthesia workstation checkout procedure is to verify the presence of a self-inflating resuscitation bag and that an alternative oxygen source (E-cylinder) is available.
- The Diameter Index Safety System (DISS) is designed to prevent the misconnection of hospital gas supply lines to the anesthesia workstation. The Pin Index Safety System (PISS) is designed to prevent incorrect gas cylinder connections in the anesthesia workstation. Quick coupling systems may be utilized to connect to the central gas supply. No system is immune to misconnection.
- In the event of hospital pipeline crossover or contamination, two actions must be taken: the backup oxygen cylinder valve must be opened, and the wall supply sources must be disconnected. Otherwise, the suspect hospital pipeline gas will continue to flow to the patient.
- The oxygen flush valve provides a high flow of 100% oxygen directly to the patient's breathing circuit, allowing the anesthesia provider to overcome circuit leaks or to rapidly increase inspired oxygen concentration. Improper use can be associated with barotrauma or patient awareness.
- When using nitrous oxide, there is a risk of delivering a hypoxic mixture to the patient. "Fail-safe" valves and nitrous oxide/oxygen proportioning systems help minimize this risk, but they are not truly fail-safe. Delivery of a hypoxic mixture to the fresh gas outlet can result from (1) the wrong supply gas, (2) a defective or broken safety device, (3) leaks downstream from these safety devices, (4) administration of a fourth inert gas (e.g., helium), and (5) dilution of the inspired oxygen concentration by high concentrations of inhaled anesthetic agents (e.g., desflurane).
- The low-pressure section (LPS) of the gas supply system includes the flow control valves, flow-meters or flow sensors, and the anesthetic vaporizers. This section of the anesthesia workstation is most vulnerable to leaks, which can cause delivery of a hypoxic gas mixture or an inadequate concentration of anesthetic agent to the patient. The workstation must be checked for leaks before delivery of an anesthetic.
- The oxygen analyzer is the only protection against a hypoxic mixture within the low-pressure section of the pneumatic system.
- Anesthesia workstations with a one-way check valve in the LPS require a manual negative-pressure leak test. On machines without a check valve in this location, manual positive-pressure testing or automated testing is used to test the LPS for leaks.
- On machines with manually controlled anesthetic vaporizers, internal vaporizer leaks can be detected only when the vaporizer is turned on. This is true even during automated machine self-tests. Machines with electronically controlled vaporizers (e.g., the GE/Datex-Ohmeda Aladin cassette vaporizer, Maquet FLOW-i anesthesia workstation vaporizer) can check the installed vaporizer during self-test.
- Variable bypass vaporizers route a portion of the fresh gas flow into a vaporizing chamber to create the desired anesthetic concentration. Injection-type vaporizers utilize microprocessor control to inject small amounts of anesthetic liquid into an evaporating chamber.
- Desflurane's low boiling point and high vapor pressure make it unsuitable for a variable bypass vaporizer. Misfilling a variable bypass vaporizer with desflurane could theoretically cause delivery of a hypoxic mixture and a massive overdose of inhaled desflurane.
- The major advantage of the *circle breathing system* is the capability to rebreathe exhaled gas, including volatile anesthetic. The major disadvantage is its complex design with multiple connections.
- Before an anesthetic agent is administered, the circle system must be checked both to rule out *leaks* and to verify *flow*. To test for leaks, a static test is performed: the circle system is pressurized and the airway pressure gauge is observed not to fall. An automated test may perform this

function on many modern machines. To rule out obstruction or faulty valves, a dynamic test is performed, ventilating a test lung (usually a breathing bag) using the anesthesia workstation's ventilator, and observing for appropriate "lung" motion.

- Increasing the fresh gas flow rate into the circle breathing system causes less rebreathing of volatile anesthetic gas and more waste gas. To avoid rebreathing of carbon dioxide, a carbon dioxide absorbent is essential to the circle system's function.
- Inhaled anesthetic agents can interact with carbon dioxide absorbents and produce potentially harmful degradation products. Sevoflurane can form compound A, especially at low fresh gas flows. Several volatile anesthetics, though especially desflurane, can lead to release of carbon monoxide when exposed to desiccated absorbents. Carbon dioxide absorbents without strong bases such as potassium hydroxide or sodium hydroxide decrease this risk.
- The Mapleson breathing circuits are simple, lightweight breathing systems that support both spontaneous and manual ventilation. The particular circuit design has implications on the required fresh gas flow to avoid rebreathing of exhaled gases. None are economical for volatile anesthetic use, as they do not support carbon dioxide absorbent use.
- Anesthesia ventilators differ from intensive care unit ventilators in that they must support the rebreathing of exhaled gases. Types of anesthesia ventilators include bellows, piston, volume reflector, and turbine. Each design has its own benefits and limitations. Contemporary anesthesia ventilators support a wide variety of ventilation modes similar to intensive care unit ventilators.
- For bellows-type anesthesia ventilators, ascending bellows (bellows that ascend during the expiratory phase) are safer than descending bellows (bellows that descend during the expiratory phase) because disconnections are readily manifested by failure of ascending bellows to refill.
- Piston ventilators can potentially draw room air into the breathing circuit if a leak is present. The Maquet FLOW-i volume reflector compensates for leaks with 100% oxygen. Both are susceptible to lower than expected levels of inhaled anesthetic.
- On older anesthesia machines, the portion of fresh gas flow that occurs during inspiration is added to the tidal volume. Therefore increased fresh gas flow leads to increased tidal volume and increased airway pressure during positive-pressure ventilation. Newer-generation anesthesia workstations either *decouple* the fresh gas flow from the inspired tidal volume, or *compensate* for the fresh gas flow in calculating the amount of gas to deliver as tidal volume. Anesthesia providers should know whether their machines compensate for changes in fresh gas flow.
- The anesthesia gas scavenging system protects the operating room from waste anesthesia gases. Active systems, which apply vacuum suction to the scavenge system, are most common in contemporary operating rooms. Obstruction of, or inadequate vacuum to, the scavenging system transfer tubing can result in increased breathing circuit pressure or discharge of waste anesthesia gases to the operating room, depending on design.
- The American Society of Anesthesiologists *Recommendations for Pre-Anesthesia Checkout Procedures* (2008) serves as an excellent template for the creation of machine-specific checkout procedures. However, it is not a one-size-fits-all checklist.

Although the modern anesthesia workstation bears little resemblance to the ether-soaked rags of the mid-1800s, it is at its heart a device for delivering inhaled anesthesia. Early inhaled anesthetics provided no certainty regarding the delivered concentration of anesthetic, relied on spontaneous breathing of room air, possessed little more than the vigilance of the anesthesia provider for safety systems, and exposed the operating room to the anesthetic vapor. The evolution of the anesthesia workstation has provided increasingly sophisticated solutions to each of these problems. Today, anesthesia workstations are designed to do all of the following:

- Deliver volatile anesthetic gas at precise concentrations.
- Individually meter oxygen and two or more other breathing gases, and continuously enrich the inhaled gas with anesthetic vapor.
- Allow the patient to be ventilated manually ("bag" ventilation) with adjustable breathing circuit pressure.

- Ventilate the patient mechanically, with sophisticated ventilator modes comparable to the intensive care unit (ICU).
- Allow rebreathing of the exhaled anesthetic gases after removing carbon dioxide.
- Eliminate ("scavenge") excess gas from the patient's breathing circuit and remove this gas from the room.
- Continuously measure and display the inspired oxygen concentration, as well as ventilatory parameters such as respiratory rate and tidal volume.
- Prevent hypoxic gas mixtures caused by operator error or gas supply failure.
- Provide a breathing circuit manual oxygen flush feature.
- Possess a backup supply of oxygen.
- Display gas pipeline and backup tank supply pressures.
- Provide an integrated platform for displaying anesthetic, hemodynamic, and respiratory parameters, and for collecting this data into an electronic medical record.

The sheer number of tasks and solutions for which the anesthesia workstation is designed explains its complexity. Newcomers to the specialty often find the anesthesia machine to be both mysterious and intimidating, even though they sometimes have had experience with other ventilation equipment, such as ICU ventilators. Understanding the anesthetic workstation is important because the workstation is one of the most essential pieces of equipment used by anesthesia care providers. Nevertheless, it is worth emphasizing that if there is any doubt about the correct functioning of an anesthesia workstation, and there is difficulty with ventilation or oxygenation, then ventilating the patient with an alternative source of oxygen such as an E-cylinder is of top priority. Troubleshooting the anesthesia machine can commence once the patient is safe.

While some of the design and engineering innovations in anesthesia workstations make the anesthesia provider's job easier or more efficient, many of the innovations aim to enhance patients' safety. Closed claims analysis of adverse anesthetic outcomes related to anesthetic gas delivery equipment shows that such claims now account for only approximately 1% of the claims in the American Society of Anesthesiologists (ASA) closed claims database.<sup>1</sup> Further, the severity of the events leading to the claims has tended to decrease compared with closed claims analysis of earlier decades, with more reports of awareness under anesthesia, and fewer reports of death or permanent brain injury.<sup>1,2</sup>

To prevent mishaps, anesthesia providers must be aware of the operational characteristics and functional anatomy of their anesthesia workstations. Many workstations and their components share very similar characteristics, but the variation among them is growing. Similarly, the operational and pre-use checkout procedures are becoming more divergent, thus mandating device-specific familiarity. Unfortunately, a lack of knowledge pertaining to the anesthesia workstation and a lack of understanding and application of a proper pre-use check are common.<sup>3-7</sup> Contemporary machines have automated pre-use checkout procedures, but performance adherence is uneven.<sup>6</sup> More importantly, machines can pass automated checkouts despite the presence of unsafe conditions.<sup>8,9</sup> Safe use requires a solid generic understanding of any anesthesia workstation, as well as machine-specific knowledge of features and checkout procedures.

Providing a detailed description of each gas system, subsystem component, and patient breathing circuit is not practical within the scope of a single chapter. However, because anesthesia workstations must adhere to basic standards, a generic approach to all machines will be presented. Although several subsystems are described in detail in this chapter, anesthesia providers must acquire a functional understanding of their own workstations and ensure that their local pre-use checkout procedures are suitable for their machines. This chapter will review guidelines for anesthesia workstations; functional anatomy including gas supply, vaporizers, breathing circuits, ventilators, and scavenging; and the anesthesia machine pre-use checkout.

## Standards and Guidelines for Anesthesia Workstations

Standards for medical devices and anesthesia workstations provide guidelines for manufacturers regarding device minimum performance, design characteristics, and safety requirements. For the anesthesia workstation, many of these requirements are outlined in the standards of the International Organization for Standardization (ISO). The ISO is a developer of international voluntary consensus standards based on global expert opinion, including industry and academia, as well as governments, consumer organizations, and other nongovernmental organizations.<sup>10</sup> The current standards are defined within the *Particular Requirements for Basic Safety and Essential Performance of an Anesthetic Workstation*, ISO 80601-2-13, of 2011.<sup>11</sup> The ISO standards also reference a large number of other components such as: electrical standards, device construction and performance, and even software standards. The relevant standards promulgated by the ASTM International (formerly known as the American Society for Testing and Materials), were withdrawn in 2014 because they had not been updated. Additional key standards for machine subsystems arise from the Compressed Gas Association and the Institute of Electrical and Electronics Engineers.

The ISO standards for the anesthetic workstation—or “anesthesia workstation,” or “anesthesia machine,” all used interchangeably in this chapter—include standards for numerous aspects of the design and construction of the workstation, including the anesthetic gas delivery system and anesthetic breathing system, as well as for monitoring equipment, alarm systems, and protection devices. The focus of this chapter is on design and functional aspects of the anesthesia workstation relevant to the delivery of inhaled anesthesia.

The ASA publishes several guidelines pertaining to the anesthesia workstation.<sup>11a</sup> The *Recommendations for Pre-Anesthesia Checkout*, which was updated last in 2008, serves as a general guideline for individual departments and practitioners to design checkout procedures specific to their anesthetic delivery systems.<sup>11b</sup> The *ASA Guidelines for Determining Anesthesia Machine Obsolescence* helps assist anesthesia providers and other healthcare personnel, administrators, and regulatory bodies to determine when an anesthesia machine is obsolete by applying both absolute and relative criteria.<sup>11c</sup> Finally, the ASA publishes *Standards for Basic Anesthetic Monitoring*, which outlines minimal monitoring standards pertaining to oxygenation, ventilation, circulation, body temperature, and the requirements for the presence of anesthesia personnel.<sup>11d</sup> Standards and recommendations pertaining to the anesthesia workstation are published by several other international anesthesiology societies.<sup>11e,11f</sup>

## Functional Anatomy of the Anesthesia Workstation

### GAS SUPPLY SYSTEM

Modern anesthesia machines are often largely electronically controlled, such that the clinician's relationship with

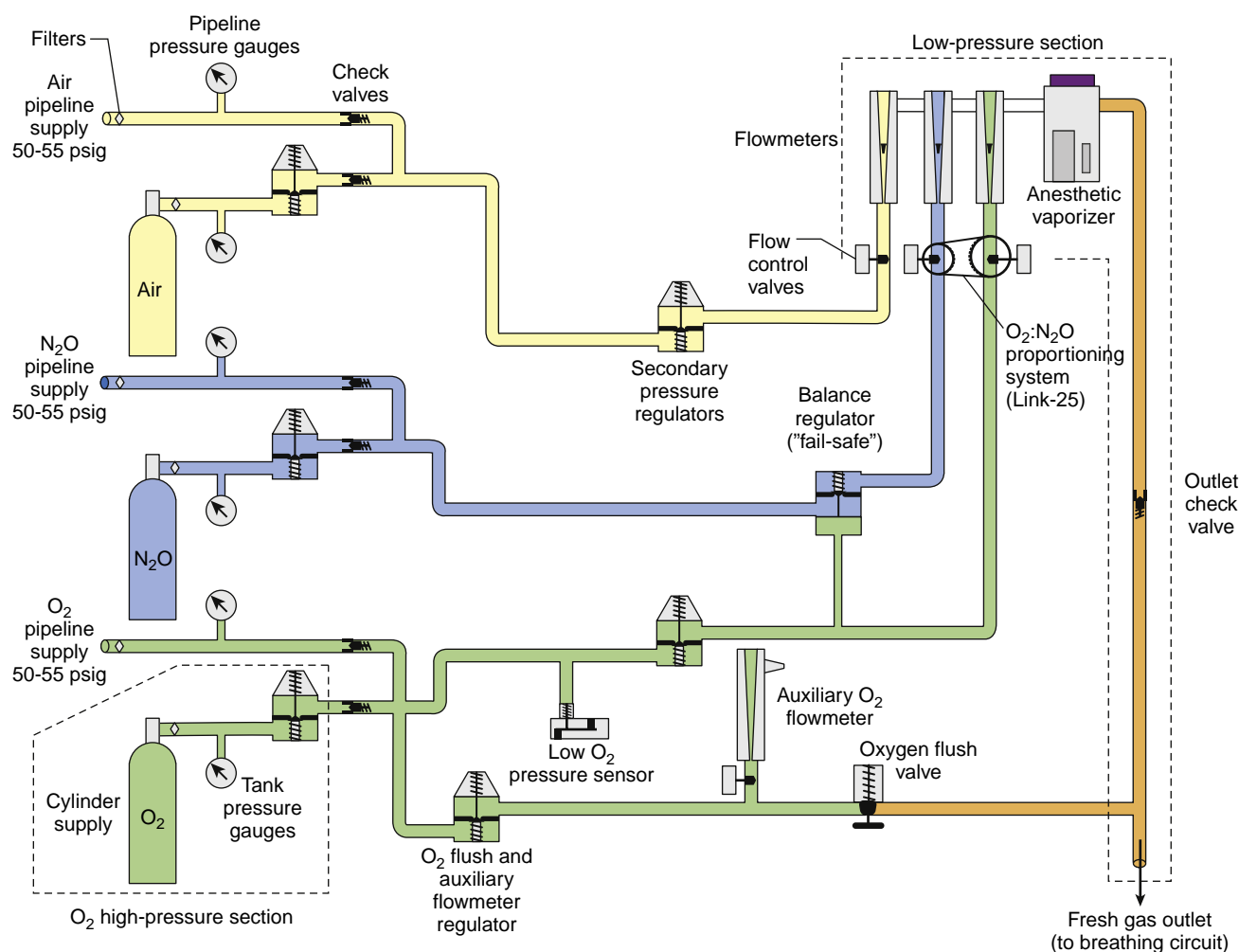


**Fig. 22.1 The GE Healthcare Aespire anesthesia workstation gas supply system.** The high-pressure system extends from the gas cylinders to the high-pressure regulators (dashed lines around O<sub>2</sub> high-pressure section only). The intermediate-pressure section extends from the high-pressure regulators to the flow control valves and also includes the tubing and components originating from the pipeline inlets. The low-pressure section (dashed lines) extends from the flow control valves to the breathing circuit. See text for additional details. (From Datex-Ohmeda. S/5 Aespire Anesthesia Machine: Technical Reference Manual. Madison, WI: Datex-Ohmeda; 2004.)

the pneumatic system is no longer mediated by a flowmeter, but rather by a touchscreen. However, the interior of the anesthesia machine remains a pneumatic system. It is where breathing gases are delivered from their supply sources, measured, mixed, passed through an anesthetic vaporizer, and delivered to the patient's breathing circuit. The details of this gas supply system may differ between the various manufacturers' anesthesia workstations, but their overall schematic is similar. Fig. 22.1 presents the gas supply system of a more traditional anesthesia machine, without electronic controls. Fig. 22.2 demonstrates a typical contemporary workstation with electronic controls.

The gas supply system consists of the following elements: oxygen, air, and nitrous oxide may enter the anesthesia machine from either the hospital gas pipeline system, or from E-cylinders mounted on the back of the anesthesia machine. The gases flow through pressure regulators to reach flow control valves before reaching flowmeters, anesthetic vaporizers, and the patient's breathing circuit via the fresh gas outlet. There are a number of safety mechanisms in place along this route to avoid delivering

a hypoxic gas mixture at the fresh gas outlet. In addition, the system is designed to be able to rapidly fill the patient's breathing circuit with 100% oxygen (oxygen flush valve), and to provide 100% oxygen from a flowmeter; both of these features are active even when the machine is off or without power.

The gas supply system can be divided into three sections: high-pressure, intermediate-pressure, and low-pressure. The only high-pressure elements in the anesthesia machine are the auxiliary gas tanks (E-cylinders) on the back of the anesthesia machine. The pressure in these tanks (approximately 2000 pounds per square inch gauge [psig] for air and oxygen, 745 psig for nitrous oxide) is immediately stepped down to an intermediate pressure. The hospital's gas pipelines are themselves of intermediate pressure (50–55 psig), so the intermediate pressure section starts from the pipelines or from the stepped-down input from the E-cylinders, and extends up to the flowmeter control valves. The low-pressure section begins at the flowmeter control valves, includes the flowmeters and anesthetic vaporizer, and ends at the fresh gas outlet.

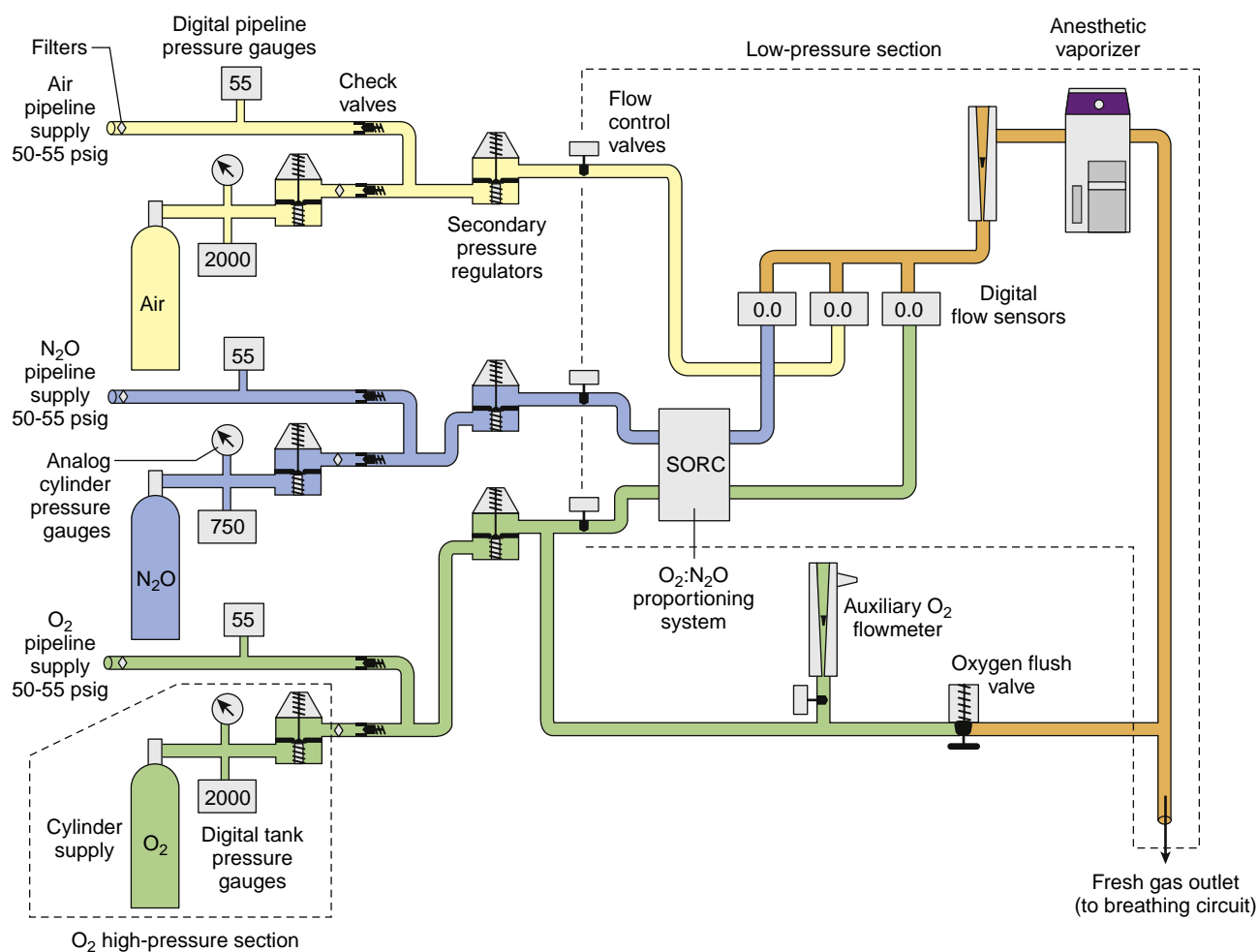


**Fig. 22.2 Dräger Apollo anesthesia workstation gas supply system.** The high-pressure system extends from the gas cylinders to the high-pressure regulators (dashed lines around O<sub>2</sub> high-pressure section only). The intermediate-pressure section extends from the high-pressure regulators to the flow control valves and also includes the tubing and components originating from the pipeline inlets. The low-pressure section (dashed lines) extends from the flow control valves to the breathing circuit. See text for additional details. (From Dräger Medical. *Instructions for Use: Apollo*. Telford, PA: Dräger Medical; 2012.)

### High-Pressure Section

**Auxiliary E-Cylinder Inlet.** During normal operation, the high-pressure section of the anesthesia machine is not active, because the hospital's central gas supply system serves as the primary gas source for the machine. However, it is a requirement to have at least one attachment for an oxygen cylinder to serve as a backup oxygen source in case of failure of the hospital supply. Many machines have up to three and sometimes four E-cylinder attachment points to accommodate oxygen, air, and nitrous oxide. Some machines have attachments for two oxygen tanks, and some rare systems can accommodate carbon dioxide (CO<sub>2</sub>) or helium tanks used for special applications. The cylinders are mounted to the anesthesia machine by the hanger yoke assembly, as seen in Fig. 22.3. The hanger yoke assembly orients and safely supports the cylinder, provides a gas-tight seal, and ensures unidirectional flow of gases into the machine.<sup>12,13</sup> Each yoke assembly must have a label designating which gas it is intended to accept. Each hanger yoke is also equipped with the Pin Index Safety System (PISS), which is a safeguard to reduce the risk of a medical gas error caused by interchanging cylinders. Two metal pins on the

yoke assembly are arranged to project precisely into corresponding holes on the cylinder head–valve assembly of the tank. Each gas or combination of gases has a specific pin arrangement.<sup>14</sup> Although infrequent, failures of the PISS have been reported, and like all safety systems, the PISS should be considered partial protection. Conditions in which failure occurred have included the following: excessive seating (jamming) of the pins back into the hanger yoke; the presence of bent or broken pins; and an excessive use of washers between the cylinder and the yoke that can override pin alignment, yet allow for a gas-tight seal.<sup>15–17</sup> Medical gas cylinder errors can have tragic outcomes, so it is critical to ensure that the proper gas is being connected to the proper inlet by also checking the tank and yoke labels.<sup>18</sup>

Once a gas cylinder valve is opened by the operator, gas flows first through a filter to entrap any particulate matter from the tank inflow. The maximum pressure in full E-cylinders (approximately 750 psig for nitrous oxide, 2200 psig for air, and 2200 psig for oxygen) is much higher than the normal hospital pipeline supply pressure of 50 to 55 psig. A *high-pressure regulator* reduces the variable high pressure to a constant pressure slightly lower than

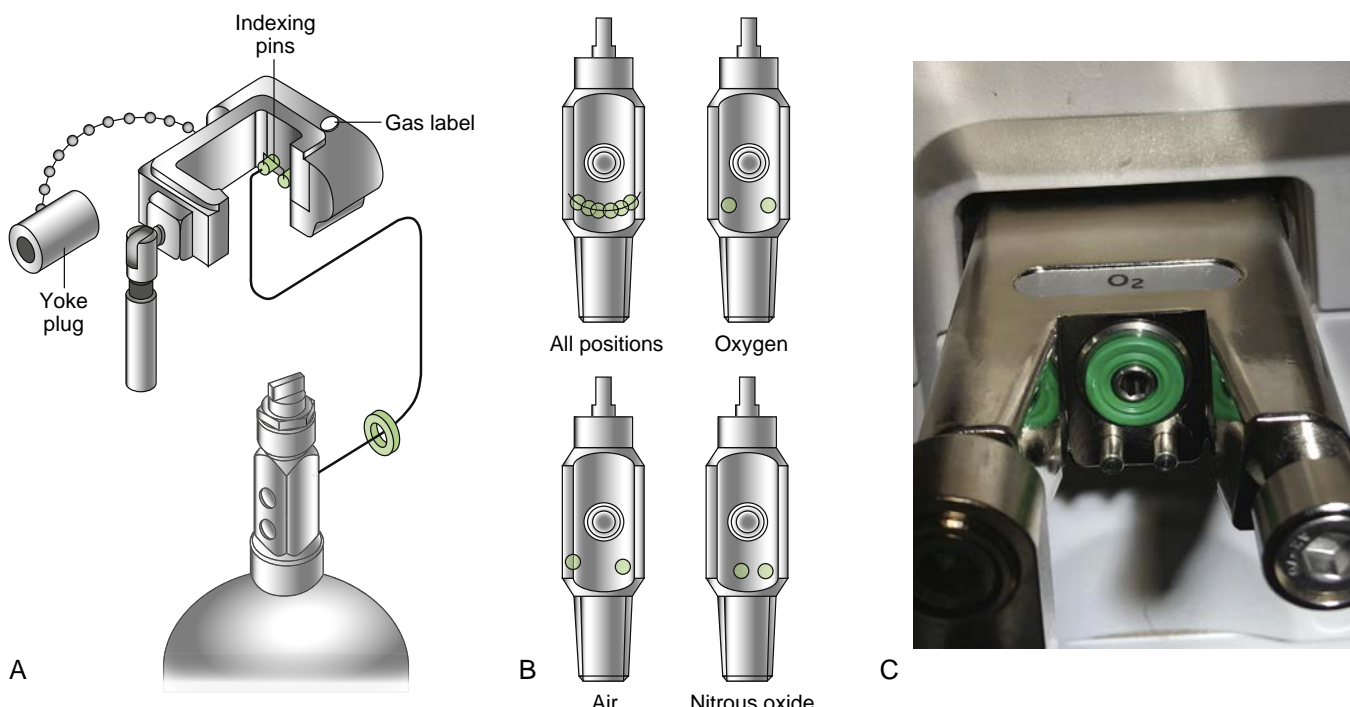


**Fig. 22.3 E-cylinder hanger yoke assembly.** (A) Standard E-cylinder hanger yoke assembly highlighting the gas-specific indexing pins, sealing gas-cket, and yoke plug. The yoke plug should be inserted when a tank is not in place. (B) Pin Index Safety System holes machined into the cylinder head-valve mechanism of the compressed gas cylinders. (C) Oxygen yoke with indexing pins. (A and B, From Yoder M. Gas supply systems. In: *Understanding Modern Anesthesia Systems*. Telford, PA: Dräger Medical; 2009.)

the normal pipeline supply pressure, approximately 40 to 45 psig (depending on the specific anesthesia machine)<sup>13</sup> (see the O<sub>2</sub> high-pressure section in Fig. 22.1). The lower pressure is a safety feature: if both the E-cylinder and the oxygen pipeline are connected and the E-cylinder is open, the anesthesia machine will draw its gas from the pipeline rather than the E-cylinder, thereby preserving the contents of the E-cylinder in case of pipeline failure. Fluctuations in the pipeline pressure below 40 to 45 psig could allow the E-cylinder to be drained, as could silent leaks in the high-pressure system, so E-cylinders should be closed during normal operation. One implication of this design warrants emphasis: in case of known or suspected pipeline contamination or crossover leading to delivery of a hypoxic gas mixture (as might be caused by nitrous oxide in the oxygen pipeline), backup oxygen from the E-cylinder will not flow unless the anesthesia machine is disconnected from the pipeline. Merely turning the backup tank on will not help, if the pipeline pressure remains higher than the high-pressure regulator's output.<sup>13,18a</sup>

After the high-pressure regulator, cylinder gas flows through a one-way valve called the cylinder check valve, which prevents any backflow of machine gas out through an empty yoke or back into a nearly empty cylinder (see Fig. 22.1). If the anesthesia machine allows two oxygen E-cylinders to be mounted on a common manifold, then each mount must have a check valve. On some machines, a single high pressure regulator is downstream from the two check valves; on others, each mount on the manifold has its own high pressure regulator and check valve. In either configuration, transfer of gas from a full tank to an empty tank is prevented, and the system allows for a cylinder to be exchanged while the other cylinder on the manifold continues to supply gas to the anesthesia machine.

As noted on Fig. 22.1, there are a number of pressure gauges in the system. The pressure in each of the gas pipelines and each of the auxiliary E-cylinder manifolds must be displayed on the front of the anesthesia machine. The E-cylinder pressures are accurate only when the tank is open; in the case of a two-tank manifold, the pressure of the open tank with higher pressure will be displayed. In systems with electronic pressure displays, the pipeline and tank pressures are visible only when the machine is on.

Two points about the safe use of the auxiliary E-cylinder system should be noted. First, checking the E-cylinders is *not* part of an automatic machine checkout. The practitioner must manually open each cylinder and check the pressure gauges on the front of the machine. In the case of a two-tank oxygen manifold, the tanks must be serially opened and checked. The oxygen flush valve may be used to vent the pressure from the system after closing the first tank, so the pressure in the second tank can be accurately assessed. Second, it is imperative to keep the auxiliary E-cylinders closed during normal operation using pipeline gases because of the possibility of small leaks in the high-pressure system, or fluctuations in pipeline pressures allowing flow from the cylinder to be activated. An open oxygen cylinder may allow the anesthesiologist to be unaware of catastrophic pipeline failure. When the oxygen cylinder is closed, the immediate result of oxygen pipeline failure is a low oxygen pressure alarm. The auxiliary E-cylinder can then be opened, ensuring continued flow of oxygen to the patient while troubleshooting occurs. If the oxygen tank is *already open* when pipeline failure occurs, there may be only a subtle indication from the anesthesia machine that the oxygen source has

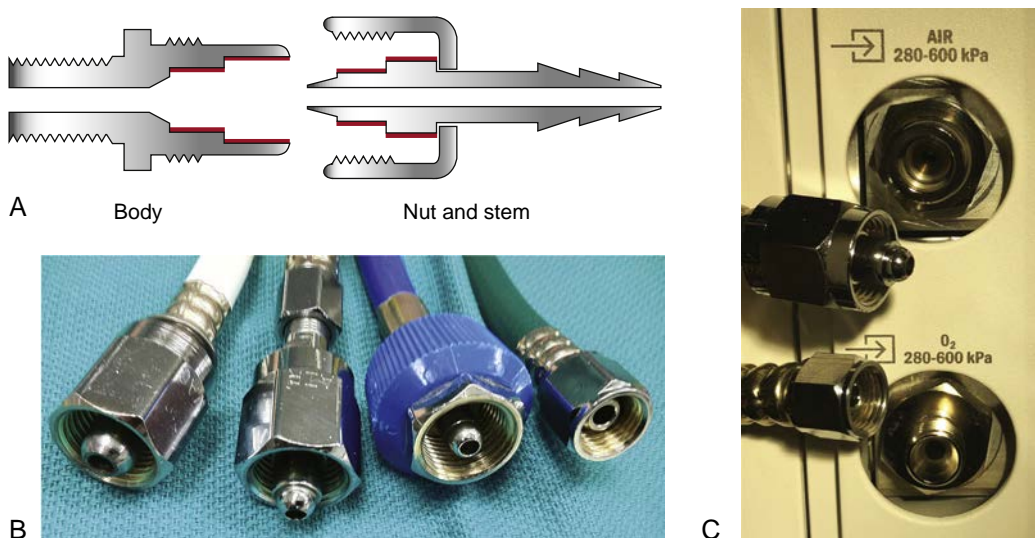


**Fig. 22.4 Diameter Index Safety System.** Diameter Index Safety System (DISS) connectors are used for noninterchangeable, removable medical gas connections at pressures less than 200 psig. They are also used for suction and waste gas connections. Indexing is accomplished through differing diameters of the connection components, resulting in key-like fitting when matched connectors come together. The oxygen connector is additionally distinguished from the other gas connectors by a unique threaded fitting diameter and a unique thread count. (A) DISS connector cross section. (B) Nut and stem connectors for (left to right) vacuum, air, nitrous oxide, and oxygen. (C) DISS connections at the back of an anesthesia workstation. (A, Modified from Yoder M. Gas supply systems. In: *Understanding Modern Anesthesia Systems*. Telford, PA: Dräger Medical; 2009.)

switched from pipeline to auxiliary tank. In this case, the low oxygen pressure alarm only occurs once the auxiliary tank has been depleted, nullifying the utility of the backup system.<sup>12,19</sup>

### Intermediate-Pressure Section

**Gas Pipeline Inlet: Central Gas Supply Source.** Three gases are typically piped into the operating room by the hospital's central gas supply system: oxygen, air, and nitrous oxide. The main supply source of oxygen in a large hospital usually is a large cryogenic bulk oxygen storage system. These are refilled on site from a truck carrying liquid oxygen. Smaller hospitals may use liquid oxygen tanks that can be replaced rather than refilled on site, or even a bank of oxygen H-cylinders connected by a manifold. Oxygen storage systems must have backup supply and alarm systems in place.<sup>14</sup> Most hospitals use compressors to deliver cleaned, dried air to a pressurized reservoir for delivery to the pipeline system. Centrally supplied nitrous oxide arises either from a bank of H-type cylinders, or a bulk liquid storage system similar to that for oxygen.<sup>14</sup>

The gas pipeline terminates in patient care areas of the hospital with one of two types of connector: the Diameter Index Safety System (DISS) connector system, or the quick coupler system. Within each type, the connectors for oxygen, air, and nitrous oxide are mutually incompatible, which helps to minimize the potential for connecting to the wrong gas. DISS connectors (as seen in Fig. 22.4) rely on matching diameters in the male and female connections to properly seat and thread the connection.<sup>14,20</sup> The quick couplers (Fig. 22.5) utilize pins and corresponding slots on the male and female ends, respectively, in order to ensure correct connections. Because these connectors can be plugged together or released with a simple twisting motion, they are especially appealing for equipment that needs to be moved between locations. In addition, in both

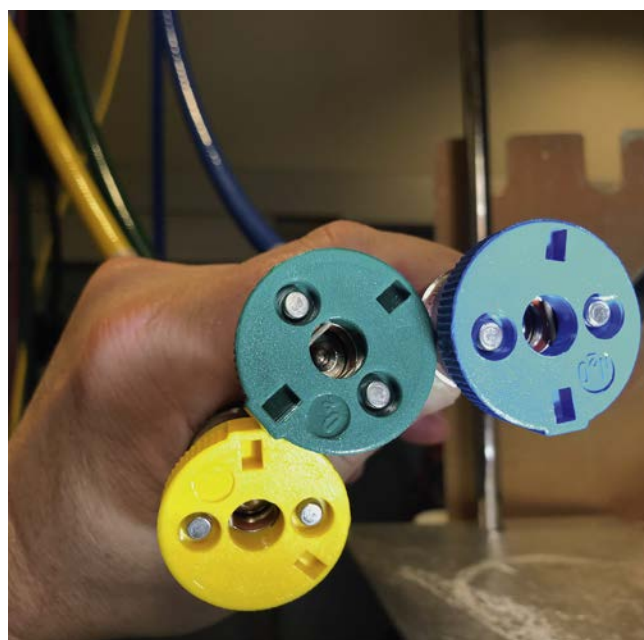


**Fig. 22.5 Quick couplers.** Quick couplers, like Diameter Index Safety System connectors, are used for noninterchangeable, removable medical gas, suction, and waste gas connections. Indexing is accomplished by the configuration of pins on one plate which match to recesses on the other plate (shown). The two plates lock together, allowing an airtight connection. A twist to the housing of the male plate allows the two plates to be disengaged.

systems the wall plates and hoses are color-coded for ease of identification.

The final medical gas pipeline connection to the anesthesia workstation is always through a DISS connector (Fig. 22.4C). Once the gas enters the machine, it encounters a filter followed by a pipeline check valve. This one-way valve prevents reverse flow of gas from the machine

into the medical gas pipeline system or into the atmosphere from an open inlet. Interposed between the DISS inlet and the pipeline check valves is a sample port to measure pipeline oxygen pressure. The pipeline pressure must always be clearly visible on the front of the machine.

**Oxygen Flush Valve.** The oxygen flush valve is probably one of the oldest safety features on the machine and remains a machine standard today.<sup>11,20,21</sup> The oxygen flush valve allows manual delivery of a high flow rate of 100% oxygen directly to the patient's breathing circuit in order to overcome circuit leaks or to rapidly increase the inhaled oxygen concentration. Flow from the oxygen flush valve bypasses the anesthetic vaporizers (see Fig. 22.1). The intermediate-pressure segment of the gas supply system feeds the valve, which remains closed until the operator opens it. The feature is usually available even when the machine is not turned on because the valve is located upstream from the machine's pneumatic power switch. Flow from the oxygen flush valve enters the low-pressure circuit downstream from the vaporizers at a rate between 35 and 75 L/min, depending on the machine and operating pressure.<sup>11,20,21</sup>

Several hazards have been reported with the oxygen flush valve. A defective or damaged valve can stick in the fully open position and result in barotrauma.<sup>22</sup> Oxygen flow from a valve sticking in a partially open position or overzealous oxygen flushing can dilute the inhaled anesthetic agent concentration, potentially resulting in awareness under anesthesia.<sup>23,24,24a</sup> Oxygen flushing during the inspiratory phase of positive-pressure ventilation can produce barotrauma if the anesthesia machine does not incorporate a fresh gas decoupling feature or an appropriately adjusted inspiratory pressure controller. Fresh gas decoupling prevents the fresh gas inflow from either the flowmeters or the oxygen flush valve from increasing the delivered ventilator tidal volume presented to the patient's lungs (see section on fresh gas flow compensation and fresh gas decoupling). With most older anesthesia breathing circuits, excess volume could not be vented during the inspiratory phase of mechanical ventilation because the ventilator relief valve was closed and the breathing circuit adjustable pressure-limiting (APL) valve was either out of circuit or closed.<sup>25</sup>

Although the oxygen flush valve can potentially provide a high-pressure, high-flow oxygen source at the machine's fresh gas outlet suitable for jet ventilation, it has potential limitations. In some machines, the fresh gas outlet is no longer easy to access, and not all machines are capable of generating pressures at the outlet that are sufficient to deliver jet ventilation.<sup>26,27</sup> An alternate source of high-flow oxygen should be sought if jet ventilation is needed and cannot be supported by the machine's oxygen flush function.

**Pneumatic Safety Systems.** One of the primary safety goals of contemporary anesthesia machines is to guard against the potential of delivering an excessive concentration of nitrous oxide relative to oxygen (hypoxic mixture). ISO standards require delivery of a nonhypoxic gas mixture to the patient, or generation of an alarm condition.<sup>11</sup> Several safety devices discussed below have been introduced to prevent generating a hypoxic mixture.

**OXYGEN SUPPLY FAILURE ALARM SENSOR.** Within the oxygen circuit of the intermediate-pressure section of the machine

is a sensor that provides an audible and visual warning to the clinician if the oxygen pressure drops below a manufacturer-specified minimum. The alarm is an ISO requirement<sup>11</sup>; under ASTM guidelines, it cannot be silenced until the pressure is restored to the minimum value.<sup>20</sup> The alarm is triggered by a loss of or significant decrease in pipeline pressure, or a nearly empty oxygen tank if the tank was the oxygen source. During normal operation this alarm signal serves as a prompt for the operator to open the oxygen E-cylinder on the machine and troubleshoot the oxygen pipeline source. The minimum threshold pressure for an alarm condition differs among manufacturers and models, because pipeline pressure standards vary significantly throughout the world. The conditions that trigger the alarm should be delineated in the manufacturer's instructions.<sup>11</sup> Numerous types of pneumatic-electrical switches serve as this sensor. Older machines had a purely pneumatic device that gave an audible signal when oxygen pressure dropped (the "Ritchie whistle").<sup>27a</sup> Current machines integrate the output from electronic pressure transducers to create an alarm if pressures drop below predetermined minimums.<sup>21</sup>

**OXYGEN SUPPLY FAILURE PROTECTION DEVICES.** In addition to generating an alarm condition, oxygen failure influences the flow of other gases within the gas supply system. Sometimes called "fail-safe valves," the oxygen supply failure protection devices are safeguards intended to link the flow of other gases in the gas supply system to the pressure of oxygen. They are an ISO standard.<sup>11</sup> In response to low oxygen pressure within the intermediate-pressure section of the anesthesia machine, the oxygen supply failure protection device either shuts off (binary valve), or reduces (proportional valve) the flow of other gases such as nitrous oxide or air. Unfortunately, the term *fail-safe* as it pertains to these valves is a misnomer and has led to the misconception that they can independently prevent the administration of a hypoxic mixture. If a gas other than oxygen pressurizes the oxygen circuit as a result of hospital pipeline contamination or crossover, the fail-safe valves will remain open. In such a case, only the inspired oxygen concentration monitor and clinical acumen would protect the patient.

**Auxiliary Oxygen Flowmeter.** Although auxiliary oxygen flowmeters are not mandatory, they are commonly encountered. During normal operation, the auxiliary flowmeter is a convenience feature that allows the use of low-flow oxygen for devices independent of the patient's breathing circuit. Similar to the oxygen flush feature, oxygen flow from the flowmeter is usually accessible even when the machine is not turned on, because the flowmeter is typically fed before the pneumatic power switch in the intermediate-pressure section. As long as oxygen is available from the pipeline inlet or from an attached E-cylinder, the auxiliary oxygen flowmeter can serve as a source of oxygen delivery for use with a manually powered resuscitation bag in the case of a system power failure. The auxiliary oxygen flowmeter may also potentially serve as gas source for a manual jet ventilator; however, not all machines can generate sufficient working pressure.<sup>26,28</sup> Some auxiliary oxygen flowmeters have a DISS connector that would be a better source for manual jet ventilation.<sup>13</sup>

The operator should be aware that the source of oxygen for the auxiliary flowmeter is the same as for the other

oxygen flow control valves. This is an important consideration in cases of suspected hospital oxygen pipeline contamination or crossover. If the pipeline oxygen supply line is connected to the machine and the pressure is sufficient, the gas source will be the pipeline even if the auxiliary oxygen tank valve is opened. In a simulation experiment, a nitrous oxide–oxygen pipeline crossover situation was created whereby the inspired oxygen concentration became alarmingly low, and the “patient” became hypoxic after turning the nitrous oxide flow off. Researchers noted that many study participants tried to make inappropriate use of the auxiliary oxygen flowmeter and oxygen E-cylinders on the machine as an external source of oxygen without disconnecting the pipeline source.<sup>29</sup> The participant’s suboptimal management was attributed to a lack of knowledge of the anesthesia machine and its gas supply.

**Second-Stage Pressure Regulators.** Some machines have second-stage regulators located downstream from the gas supply sources in the intermediate-pressure circuit. These regulators supply constant pressure to the flow control valves and the proportioning system regardless of potential fluctuations in hospital pipeline pressures. They are adjusted to lower pressure levels than the pipeline supply, usually between 14 and 35 psig, depending on the workstation.<sup>30,31,31a</sup>

### Low-Pressure Section

The purpose of the high- and intermediate-pressure sections of the anesthesia machine is to deliver a reliable source of breathing gases at a stable and known working pressure to the low-pressure section of the gas supply system. The low-pressure section of the gas supply system begins at the flow control valves and ends at the fresh gas outlet (see Figs. 22.1 and 22.2). The breathing circuit, including the circle system, breathing bag, and ventilator, will be treated separately. Key components include the flow control valves, the flowmeters or flow sensors, the vaporizer manifold, and the anesthetic vaporizers. The low-pressure section is the most vulnerable section to leaks within the gas supply system.

**Flow Control Assemblies.** The flow control valves on the anesthesia workstation allow the operator to select a *total fresh gas flow* of known composition that enters the low-pressure section of the anesthesia workstation. These valves separate the intermediate-pressure section from the low-pressure section. After leaving the flowmeters, the mixture of gases travels through a common manifold and may be directed through an anesthetic vaporizer if selected. The total fresh gas flow and the anesthetic vapor then travel toward the fresh gas outlet (see Figs. 22.1 and 22.2).<sup>12,19</sup>

**ELECTRONIC FLOW SENSORS.** Newer anesthesia workstations are increasingly equipped with electronic flow sensors instead of flow tubes. These systems may employ conventional control knobs or an entirely electronic interface to control gas flow. Flows can be displayed numerically or sometimes graphically in the form of a virtual, digitalized flowmeter. Numerous types of flow sensor technologies can be applied, such as hot-wire anemometers, a differential pressure transducer method, or mass flow sensors. An example of an electronic mass flow sensor is seen in Fig. 22.6. The illustrated device relies on the principle of specific heat to measure gas

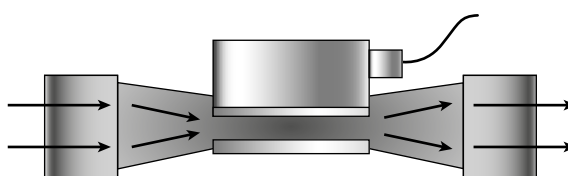


**Fig. 22.6 Electronic mass flow sensor.** Gas flows past a heated chamber of known volume. The amount of heat (electrical energy) that is required to maintain a set chamber temperature is proportional to the specific heat of the gas and its rate of flow through the chamber. Because the specific heat of the gas is relevant to the calculation, each gas must have its own mass flow sensor. Flow is accurately extrapolated from the energy required to keep the chamber at a constant temperature. (Modified from Yoder M. Gas supply systems. In: *Understanding Modern Anesthesia Systems*. Telford, PA: Dräger Medical; 2009.)

flow.<sup>30</sup> As gas flows through a heated chamber of known volume, a specific amount of electricity is required to maintain the chamber temperature. The amount of energy required to maintain the temperature is proportional to the flow and specific heat of the gas. Regardless of the mechanism of flow measurement, these systems depend on electrical power to provide a display of gas flow. When electrical power is totally interrupted, some backup mechanical means usually exists to control (mechanical flow control) and display (flow tube) oxygen gas flow.

**MECHANICAL FLOWMETER ASSEMBLIES.** Mechanical flow control and flow display still remain common, even on some newer workstations, either as primary or backup systems.<sup>31a,31b</sup>

**FLOW CONTROL VALVES.** The flow control valve assembly consists of a flow control knob, a tapered needle valve, a valve seat, and a pair of valve stops (Fig. 22.7).<sup>12</sup> The inlet pressure to the assembly is determined by the pressure characteristics of the machine’s intermediate-pressure segment. The location of the needle valve in the valve seat changes to establish different orifices when the flow control valve is adjusted. Gas flow increases when the flow control valve is turned counterclockwise, and it decreases when the valve is turned clockwise. Because their use is frequent and the consequences of damage are significant, the controls must be constructed so extremes of rotation will not cause disassembly or disengagement.

Contemporary flow control valve assemblies have numerous safety features. The oxygen flow control knob is physically distinguishable from the other gas knobs. It is distinctively fluted, may project beyond the control knobs of the other gases, and is larger in diameter than the flow control knobs of other gases.<sup>11</sup> All knobs are color coded for the appropriate gas, and the chemical formula or name of the gas must be permanently marked on each knob. Flow control knobs are recessed or protected with a shield or barrier to minimize inadvertent change from a preset position. If a single gas has two flow tubes, the tubes are arranged in series and are controlled by a single flow control valve.<sup>20</sup>

**FLOW TUBES.** With a traditional flowmeter assembly, the flow control valve regulates the amount of flow that enters a tapered, transparent flow tube known as a *variable orifice flowmeter* or *Thorpe tube*. These glass tubes are narrowest at the bottom and widen at the top. A mobile indicator float inside the calibrated flow tube indicates the amount of flow passing through the associated flow control valve. The quantity of flow is indicated on a scale specific to the

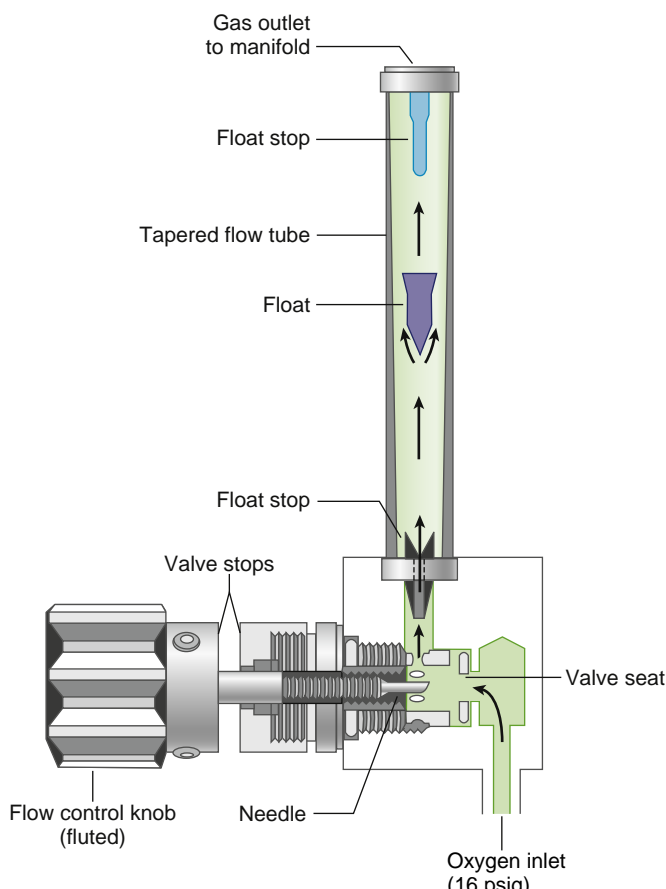


**Fig. 22.7 Oxygen flowmeter assembly.** The oxygen flowmeter assembly is composed of the flow control valve assembly and the flowmeter subassembly. (From Bowie E, Huffman LM. *The Anesthesia Machine: Essentials for Understanding*. Madison, WI: Ohmeda, BOC Group; 1985.)

flow tube.<sup>12,19</sup> Opening the flow control valve allows gas to travel through the space between the float and the flow tube. This space is known as the *annular space*, and it varies in size depending on the position in the tube (Fig. 22.8). The indicator float hovers freely in an equilibrium position in the tube where the upward force resulting from gas flow equals the downward gravity force on the float at a given flow rate. The float moves to a new equilibrium position in the tube when flow is changed. These flowmeters are commonly referred to as *constant-pressure* flowmeters because the decrease in pressure across the float remains constant for all positions in the tube.<sup>12,32,33</sup>

Flow through the annular space can be laminar or turbulent, depending on the gas flow rate (Fig. 22.9). The characteristics of a gas that influence its flow rate through a given constriction are viscosity (laminar flow) and density (turbulent flow). Because the annular space behaves as a tube at low flow rates, laminar flow is present, and viscosity determines the gas flow rate. At high flow rates, the annular space behaves like an orifice. Turbulent gas flow is present and gas density predominantly influences the flow. Because the viscosity and density of the gas affect flow through annular space around the float, the calibrated flow tubes are gas specific. The tube, the float, and the scale are inseparable. Although temperature and barometric pressure can influence gas density and viscosity,

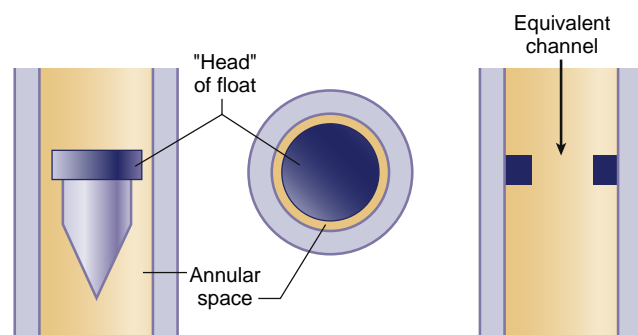


**Fig. 22.8 The annular space.** The clearance between the head of the float and the flow tube is known as the annular space. It can be considered equivalent to a circular channel of the same cross-sectional area. (Redrawn from Macintosh R, Mushin WW, Epstein HG, eds. *Physics for the Anaesthetist*. 3rd ed. Oxford: Blackwell Scientific; 1963.)

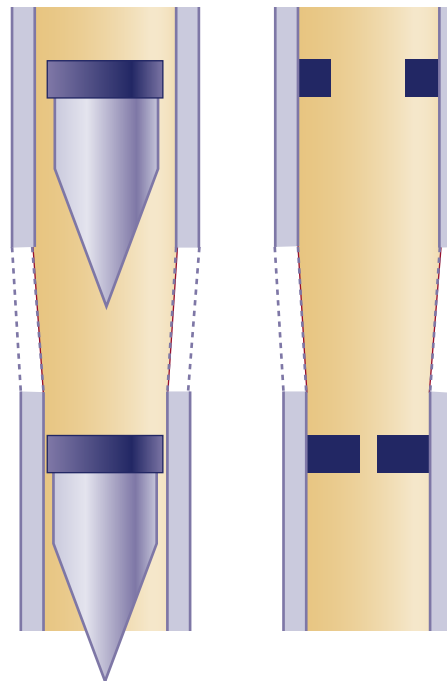


**Fig. 22.9 Flow tube constriction.** The lower pair of illustrations represents the lower portion of a flow tube. The clearance between the head of the float and the flow tube is narrow. The equivalent channel is tubular because its diameter is less than its length. Viscosity is dominant in determining the gas flow rate through this tubular constriction. The upper pair of illustrations represents the upper portion of a flow tube. The equivalent channel is orificial because its length is less than its diameter. Density is dominant in determining the gas flow rate through this orificial constriction. (Redrawn from Macintosh R, Mushin WW, Epstein HG, eds. *Physics for the Anaesthetist*. 3rd ed. Oxford: Blackwell Scientific; 1963.)

under normal clinical circumstances, flow tube accuracy is not significantly affected by mild changes in temperature or pressure.

The float or bobbin within the flow tube is usually constructed so that it rotates to indicate that gas is flowing and that the indicator is not stuck in the tube. A stop at the top of the flowmeter tube prevents the float from occluding the outlet. Two flowmeter tubes are sometimes placed in series, with a fine flow tube displaying low flows and a coarse flow tube indicating higher flows.

**Problems With Flowmeters.** Flow measurement error can occur even when flowmeters are assembled properly. Dirt or static electricity can cause a float to stick and misrepresent actual flow. Sticking of the indicator float is more common in the low-flow ranges because the annular space is smaller. A damaged float can cause inaccurate readings because the precise relationship between the float and the flow tube is altered. Backpressure from the breathing circuit can cause a float to drop so that it reads less than the actual flow. Finally, if flowmeters are not aligned properly in the vertical position (plumb), readings can be inaccurate because tilting distorts the annular space.<sup>12,34,35</sup>

The flow tube has historically been a very fragile component of the anesthesia workstation. Subtle cracks and chips may be overlooked and can cause errors in delivered flow.<sup>34</sup> Leaks can also occur at the O-ring junctions between the glass flow tubes and the metal manifold. Flow tube leaks are a potential hazard because the flowmeters are located downstream from all hypoxemia safety devices, except the breathing circuit oxygen analyzer.<sup>33,36,37</sup> Fig. 22.10 shows an example where an unused air flow tube develops a large leak. When the nitrous oxide flowmeter is in the downstream position (Fig. 22.10A and B), a hypoxic mixture can occur because a substantial portion of the oxygen flow passes through the leak in the air flow tube, and mainly nitrous oxide is directed to the common gas outlet. Safer configurations are shown in Fig. 22.10C and D, in which the oxygen flowmeter is located in the downstream position. A portion of the nitrous oxide flow escapes through the leak, and the remainder goes toward the common gas outlet. A hypoxic mixture is less likely because all the oxygen flow is advanced by the nitrous oxide (this principle is known as the Eger flow sequence). It has been an industry standard that oxygen be delivered downstream of all other gases,<sup>20</sup> although current ISO standards require only that oxygen be at either end of a bank of flowmeters.<sup>11</sup> It is important to remember that in the case of a leak in the oxygen flow tube, a hypoxic mixture may result even when oxygen is located in the downstream position.<sup>34</sup>

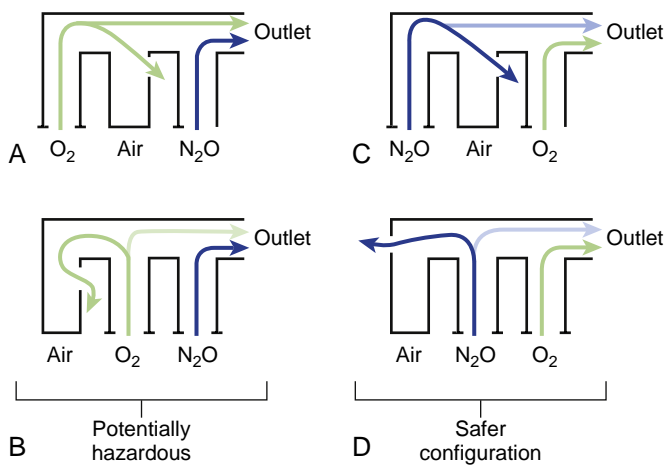


**Fig. 22.10 The flowmeter sequence is a potential cause of hypoxia.**

In the event of a flowmeter leak, a potentially dangerous arrangement exists when nitrous oxide is located in the downstream position (A and B). A safer configuration exists when oxygen is located in the downstream position (C and D). See text for details. (Modified from Eger EI II, Hylton RR, Irwin RH, et al. Anesthetic flowmeter sequence: a cause for hypoxia. *Anesthesiology*. 1963;24:396.)

**PROPORTIONING SYSTEMS.** Anesthesia workstations are equipped with an oxygen failure protection device in the intermediate-pressure section that, in response to reduced oxygen pressure, either proportionally reduces or completely inhibits nitrous oxide. However, this system does not prevent the user from selecting a hypoxic gas mixture for delivery to the fresh gas outlet. On anesthesia workstations with electronically controlled gas flow, the machine is programmed to prevent the user from selecting a hypoxic gas mixture for delivery to the fresh gas outlet. For mechanically controlled flowmeters, the concern is that a user could mistakenly select oxygen and nitrous oxide flows that would result in a hypoxic mixture. According to the ISO, an alarm condition is insufficient and the machine must have a system to prevent delivery of a hypoxic mixture.<sup>11</sup> This is accomplished by a pneumatic-mechanical interface between the oxygen and nitrous oxide flows or by mechanically linking the oxygen and nitrous oxide flow control valves. This way, no matter how high the operator attempts to turn up the nitrous oxide, or how low the operator tries to turn down the oxygen flow, when nitrous oxide is running, the machine will automatically adjust the ratio of these flows so that a hypoxic gas mixture cannot be delivered. The specific devices used to accomplish this control vary among manufacturers. Two examples are briefly discussed here.

The North American Dräger sensitive oxygen ratio controller system (SORC) is a pneumatic-mechanical, oxygen-nitrous oxide interlock system designed to maintain a ratio of no less than 2.5% oxygen to 75% nitrous oxide flow into the breathing circuit by limiting the nitrous oxide flow when necessary.<sup>21</sup> The SORC, located after the flow control valves, consists of an oxygen chamber with a diaphragm, a nitrous oxide chamber with a diaphragm, and a nitrous oxide proportioning valve (Fig. 22.11). All are interconnected by a mobile horizontal shaft. As oxygen flows out of the SORC, it encounters a resistor that creates backpressure in the oxygen chamber, which causes the diaphragm to move to the right, thereby opening the nitrous oxide proportioning valve. As the oxygen flow is increased, so too is the backpressure and the rightward motion of the shaft. If the nitrous oxide flow is now turned on, it will also flow into the SORC, through the proportioning valve, and past its resistor to create backpressure that will press on the diaphragm in its respective chamber. The counterbalance between the two gas flows (backpressures) determines the positioning of the nitrous oxide proportioning valve.<sup>21</sup> If the oxygen is turned down too low (<1/3 of the nitrous oxide flow), the shaft will move to the left and thus limit the nitrous oxide flow. If the operator tries to turn up the nitrous oxide too high relative to the oxygen flow, the SORC will limit the nitrous oxide flow because of the nitrous oxide backpressure and leftward movement of the valve. If the oxygen flow is decreased to less than 200 mL/min, the proportioning valve will close completely.<sup>38</sup>

A mechanical proportioning system that remains in use today on many anesthesia machines is the GE/Datex-Ohmeda Link-25 system. The system provides mechanical integration of the nitrous oxide and oxygen flow control valves to maintain a minimum oxygen concentration with a maximum nitrous oxide:oxygen flow ratio of 3:1. Independent adjustment of either valve is allowed as long as the minimum

threshold is met. The Link-25 automatically increases oxygen flow when the nitrous oxide flow is increased above the 3:1 ratio. It also will lower nitrous oxide flow if oxygen flow is decreased below that ratio. **Fig. 22.12** shows the Link-25 system. A 15-tooth sprocket is attached to the nitrous oxide flow control valve, a 29-tooth sprocket is attached to the oxygen flow control valve and a chain physically links the sprockets. When the nitrous oxide flow control valve is turned through two revolutions, the oxygen flow control valve will revolve once because of the 2:1 gear ratio. The final 3:1 flow ratio

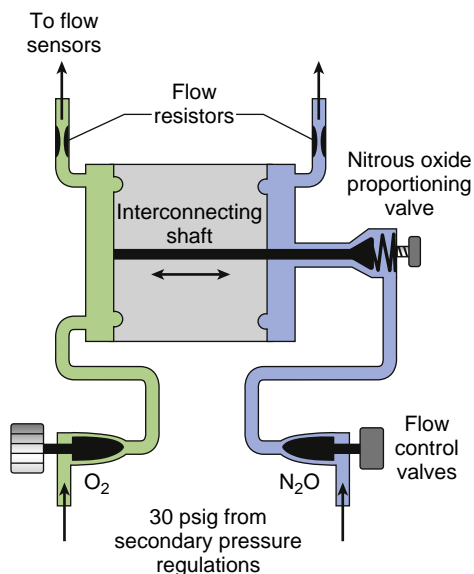


**Fig. 22.11 North American Dräger sensitive oxygen ratio controller system (SORC) (Dräger Medical, Telford, PA).** The SORC is a pneumatic-mechanical interlock system designed to maintain a ratio of no less than 25% oxygen/75% nitrous oxide regardless of operator input. Differential oxygen and nitrous oxide flows and the resultant chamber backpressures determine the position of the nitrous oxide proportioning valve. The SORC requires a minimum oxygen flow of 200 mL/min for the nitrous oxide proportioning valve to open. See text for details. (Modified from Yoder M. Gas supply systems. In: *Understanding Modern Anesthesia Systems*. Telford, PA: Dräger Medical; 2009.)

results because the flow control valve needle for nitrous oxide has a faster taper than does the oxygen valve needle. The Link-25 system uses a stop tab on each valve stem to allow for independent adjustment of oxygen or nitrous oxide as long as the mixture is at least 25% oxygen; attempting to turn the valve controller past that point will engage the chain and effect a change in the other gas. In addition, the system is designed so that nitrous oxide cannot flow unless the oxygen flow is at least 200 mL/min.<sup>3a</sup>

Although both proportioning systems are designed to prevent delivery of a hypoxic gas mixture to the common gas outlet, their effect on the output may be different. If the operator turns down oxygen flow below 25% oxygen, both the Link-25 and SORC systems will respond by decreasing the flow of nitrous oxide. If the operator subsequently increases the set oxygen flow, the nitrous oxide flow will remain at the new, lower value with the Link-25 system, because the mechanical linkage will have physically changed the nitrous oxide control valve setting. With the SORC system, on the other hand, the nitrous oxide flow will return to the higher, previously set value when adequate oxygen flow is restored. If the operator increases nitrous oxide flow beyond the set safe range, the Link-25 system will increase the oxygen flow by changing the setting on the oxygen control valve. The SORC system will instead prevent the increase in nitrous oxide flow from occurring. If the operator subsequently reduces the nitrous oxide flow setting, the oxygen flow will remain at the new, higher level with the Link-25, and will remain unchanged with the SORC.

**PROPORTIONING SYSTEM MALFUNCTION.** Proportioning systems are not immune from failure, and workstations equipped with proportioning systems can still deliver a hypoxic mixture under certain conditions. Many case reports have described proportioning system malfunction.<sup>39-43</sup> Other situations that may defeat the purpose of the proportioning system require operator vigilance. Both mechanical and pneumatic proportioning systems can be defeated if a gas other than oxygen is present in the oxygen pipeline. Proportioning systems such as the Link-25 function at the level of the flow control valves. A leak downstream from these devices, such as a broken



7

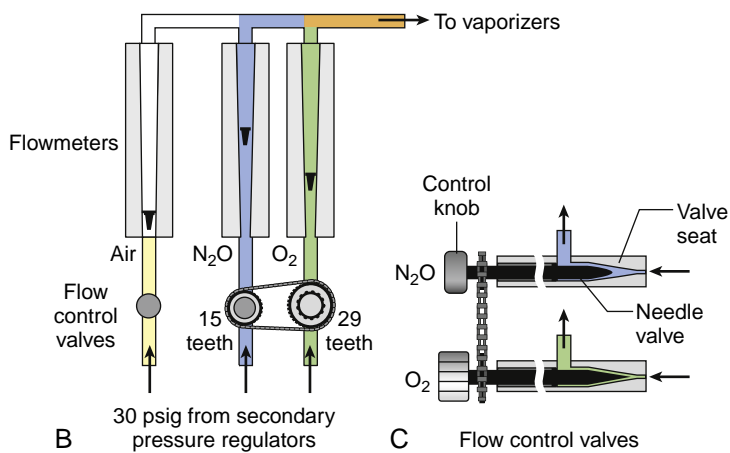


**Fig. 22.12 GE/Datex-Ohmeda Link-25 nitrous oxide: oxygen proportioning system.** The system prevents the operator from selecting more than a 75% nitrous oxide–25% oxygen (3:1) mixture by two separate but interdependent means. (A) Link-25 proportioning system on a GE Healthcare Aestiva anesthesia workstation with front panel removed. (B) Mechanical linkage of the control valves maintains no more than a 2:1 ratio. (C) A faster taper of the nitrous oxide valve needle allows more gas flow through the valve per turn relative to flow through the oxygen valve per turn, thus resulting in the maximal 3:1 ratio. A stable and equal pressure supply to the valves is provided by the secondary pressure regulator for oxygen and a balance regulator for nitrous oxide. See text for additional details. (Datex-Ohmeda: Aestiva anesthesia machine: technical reference manual. Madison, WI: Datex-Ohmeda 2006.)

oxygen flow tube, could result in delivery of a hypoxic mixture to the common gas outlet. In this situation, oxygen escapes through the leak, and the predominant gas delivered is nitrous oxide. Finally, volatile inhaled anesthetic agents are added to the mixed gases downstream from both the flowmeters and the proportioning system. Concentrations of less potent inhaled anesthetic agents such as desflurane may account for a larger percentage of the total fresh gas composition than is the case with more potent agents. Because significant percentages of these inhaled anesthetic agents may be added downstream of the proportioning system, the resulting gas-vapor mixture may contain an inspired oxygen concentration less than 21% despite a functional proportioning system. The additional complexity of the circle system (discussed below) means that the oxygen concentration of the fresh gas flow delivered to the breathing circuit may be very different from the patient's actual fraction of inspired oxygen ( $\text{FiO}_2$ ). In each case, the presence of a functioning oxygen analyzer in the patient's breathing circuit is the last protection against a hypoxic gas mixture.

### Vaporizer Mount and Interlock System

**VAPORIZER MOUNTING SYSTEMS.** Removable modern vaporizer mounts allow for rapid replacement or exchange of anesthetic vaporizers. This allows for ease of maintenance, fewer required vaporizer positions on the workstation, and the ability to remove the vaporizer if malignant hyperthermia is suspected.<sup>44</sup> Detachable mounting systems can lead to problems such as low-pressure systems leaks or fresh gas flow obstruction as a result connection-related failures.<sup>44-49</sup> After adding or changing a vaporizer on the anesthesia machine, the operator should make sure it is seated properly and cannot be dislodged once locked. The operator should then perform a vaporizer leak test, if required by the manufacturer.

**VAPORIZER INTERLOCK DEVICES.** All anesthesia workstations must prevent fresh gas from flowing through more than one vaporizer at time.<sup>11</sup> The design of vaporizer interlock devices varies significantly. Operators should be aware that these devices are not immune from failure, and anesthetic overdose can be a potential consequence.<sup>50-53</sup>

**Outlet Check Valve.** Many older Datex-Ohmeda anesthesia machines and a few contemporary workstations (e.g., GE/Datex-Ohmeda Aestiva and Aespire) have a one-way check valve located between the vaporizer and the common gas outlet in the mixed-gas pipeline (see Fig. 22.1). The purpose of this valve is to prevent backflow into the vaporizer during positive-pressure ventilation, thereby minimizing the effects of intermittent fluctuations in downstream pressure on the concentration of inhaled anesthetics (see the discussion of intermittent backpressure in the section on anesthetic vaporizers). The presence or absence of this check valve historically influenced which *manual* leak test of the low-pressure system was indicated because it precluded positive-pressure tests to detect for leaks upstream of the valve (see the section on checking your anesthesia workstation).

## ANESTHETIC VAPORIZERS

In 1846, William T. G. Morton performed the first public demonstration of ether anesthesia using an ingenious, yet simple inhaler (Fig. 22.13).<sup>54-56</sup> Although the device was effective in delivering anesthetic vapor, Morton's



**Fig. 22.13** Morton's ether inhaler: A replica of the inhaler used by William T. G. Morton during his public demonstration of ether anesthesia in October of 1846 at Massachusetts General Hospital in Boston. (Courtesy the Wood Library–Museum of Anesthesiology, Park Ridge, IL.)

ether inhaler had no means of regulating output concentration or compensating for temperature changes caused by vaporization of the liquid anesthetic and the ambient environment. These two issues were central to the subsequent development and evolution of modern anesthetic vaporizers. Modern variable bypass-type vaporizers are temperature compensated and can maintain desired outputs accurately over a wide range of input gas flow rates. In 1993, with the introduction of desflurane to the clinical setting, an even more sophisticated vaporizer was introduced to handle the unique physical properties of this agent. Vaporizers blending both old technology and computer control have emerged as "cassette" vaporizer systems. An injection-type vaporizer has also been reintroduced. This vaporizer injects precise amounts of liquid anesthetic agent into the fresh gas stream. Before discussing these systems in detail, a brief review of physical/chemical principles is necessary to understand the operation, construction, and design of contemporary anesthetic vaporizers.

### Physics

**The Ideal Gas Law.** When sealed in a container, gas molecules collide with the walls and exert a force or pressure. This pressure is directly proportional to the number of molecules or moles ( $n$ ) of gas present within the container and to the temperature ( $T$ ) in degrees kelvin, and inversely proportional to the volume ( $V$ ) that confines the gas. (One mole of a substance is equal to  $6.022 \times 10^{23}$  [Avogadro's number] molecules of that substance.) The ideal gas law is:

$$PV = nRT$$

R (the universal gas constant) =  $8.314 \text{ L kPa/mol}^{\circ}\text{K}$   
or  $62.364 \text{ L mm Hg/mol}^{\circ}\text{K}$

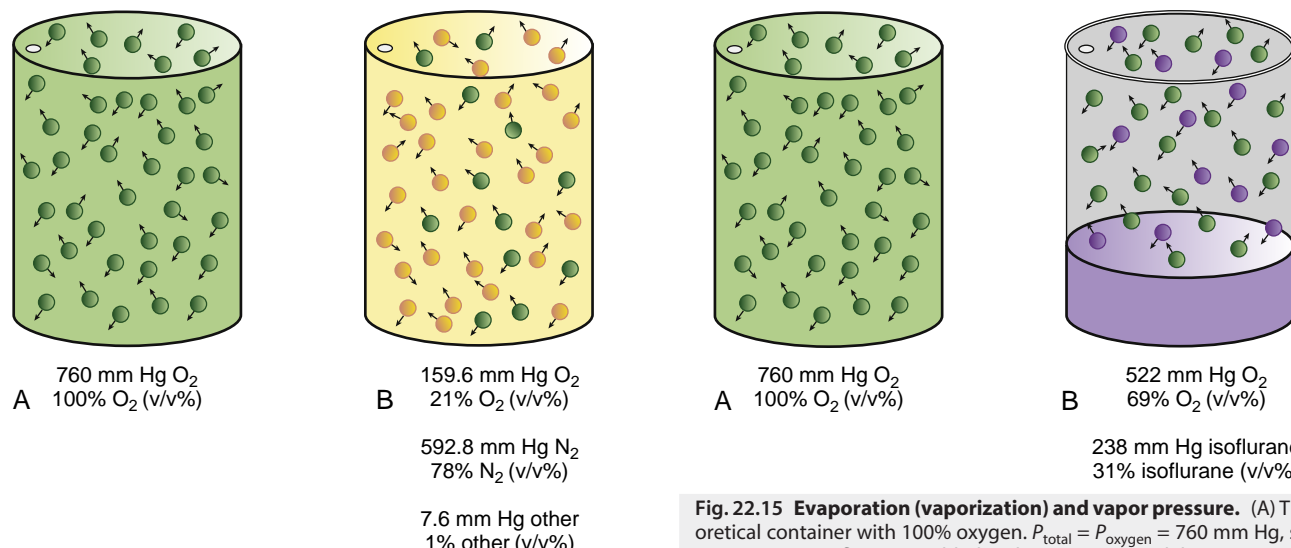


**Fig. 22.14 Partial pressures.** (A) Theoretical container filled with 100% oxygen at 1 atm pressure (760 mm Hg). The oxygen molecules account for the entirety of the pressure.  $P_{\text{total}} = P_{\text{oxygen}} = 760 \text{ mm Hg}$ , see Fig. 22.14. (B) Isoflurane is added to the container, and the temperature is maintained at 20°C (68°F). Evaporation commences, and isoflurane molecules begin to displace oxygen molecules out of the container. When the rate of vaporization is equal to the rate of condensation, the gas above the liquid is said to be "saturated" with isoflurane. The partial pressure of the isoflurane at this point is called the saturated vapor pressure (SVP), which at this temperature equals 238 mm Hg.  $P_{\text{total}} = P_{\text{oxygen}} + P_{\text{isoflurane}} = 760 \text{ mm Hg}$ .

The ideal gas law provides an important framework for understanding the behavior of anesthetic gases within vaporizers, anesthesia delivery equipment, and the pulmonary alveolus. Key assumptions of this law are that gas molecules (1) behave as points in space and (2) undergo perfectly elastic collisions without attracting or repelling one another or the walls of the container. These assumptions are valid for dilute anesthetic gases at normal operating conditions.

**Dalton's Law of Partial Pressures.** When a mixture of ideal gases exists in a container, each gas creates its own pressure, which is the same pressure as if the individual gas occupied the container alone. The total pressure may be calculated by simply adding together the pressures of each gas. This is known as Dalton's law of partial pressures, where the individual pressures ( $P_i$ ) exerted by each of the constituent gases are referred to as *partial pressures*:<sup>57,58</sup>

$$P_{\text{total}} = P_1 + P_2 + P_3 + \dots$$

Another useful expression, which can be derived by combining Dalton's law with the ideal gas law, is:

$$P_A = (n_A/n_{\text{total}}) P_{\text{total}} = (v/v\%) P_{\text{total}}$$

which states that the partial pressure of gas A can be calculated by multiplying the total pressure of the mixture by the mole fraction ( $n_A/n_{\text{total}}$ ), or the volume percent ( $v/v\%$ ), of gas A. The volume percent tends to be more useful in day-to-day anesthesia practice (see below).

As a first step to understanding vaporizer function, it is useful to look at an example of Dalton's law of partial pressures. In Fig. 22.14A, pure oxygen fills a theoretical container that is open to the environment through a very

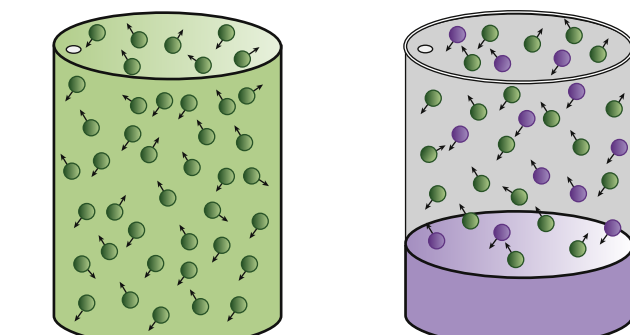


**Fig. 22.15 Evaporation (vaporization) and vapor pressure.** (A) Theoretical container with 100% oxygen.  $P_{\text{total}} = P_{\text{oxygen}} = 760 \text{ mm Hg}$ , see Fig. 22.14. (B) Isoflurane is added to the container, and the temperature is maintained at 20°C (68°F). Evaporation commences, and isoflurane molecules begin to displace oxygen molecules out of the container. When the rate of vaporization is equal to the rate of condensation, the gas above the liquid is said to be "saturated" with isoflurane. The partial pressure of the isoflurane at this point is called the saturated vapor pressure (SVP), which at this temperature equals 238 mm Hg.  $P_{\text{total}} = P_{\text{oxygen}} + P_{\text{isoflurane}} = 760 \text{ mm Hg}$ .

small hole. The pressure in the container is equal to the ambient pressure, which at sea level is 760 mm Hg or 1 atm or 101.325 kPa, and generated entirely by the oxygen molecules. In Fig. 22.14B, the container is filled with air, and the total pressure is generated by the additive partial pressures of oxygen, nitrogen, and trace amounts of rare gases.

**Evaporation and Vapor Pressure.** Volatile liquids, such as inhaled anesthetic agents, are characterized by a high propensity to enter the gas phase, or *vaporize*. When a volatile liquid is exposed to air or other gases, molecules at the liquid surface with sufficient kinetic energy escape and enter the vapor phase. This process is known as *evaporation*, which is purely a surface phenomenon (in contrast to *boiling*, which occurs throughout the liquid). If liquid volatile anesthetic is placed within a contained space, such as a vaporizer, molecules will escape into the vapor phase until the rate of evaporation equals the rate of return to the liquid phase (a process known as *condensation*). When this equilibrium is reached, the gas above the liquid is said to be "saturated" with anesthetic (Fig. 22.15). The anesthetic molecules in the gas phase create a partial pressure known as the *saturated vapor pressure*, or simply *vapor pressure*. Liquids with a greater tendency to evaporate and generate higher vapor pressures are described as "more volatile."

Vapor pressure is a unique physical property of a substance at any given temperature (Fig. 22.16). Vapor pressure is *not* affected by changes in atmospheric pressure.<sup>59</sup> As illustrated in Fig. 22.17 for the isoflurane, evaporation is diminished at colder temperatures because fewer molecules possess sufficient kinetic energy to escape into the vapor phase. Conversely, at warmer temperatures, evaporation is enhanced and vapor pressure increases. Although

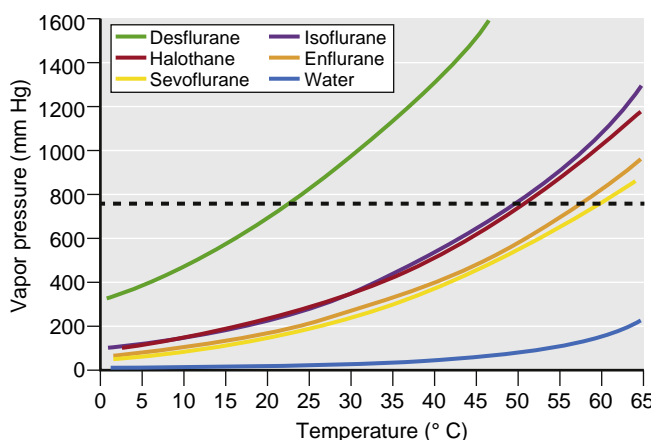


**Fig. 22.16** Vapor pressure-versus-temperature curves for desflurane, isoflurane, halothane, enflurane, sevoflurane, and water. Note that the curve for desflurane differs dramatically from that of the other inhaled anesthetic agents. Also note that all inhaled agents are more volatile than water. Dashed line indicates 1 atm (760 mm Hg) of pressure, which illustrates the boiling point at sea level (normal boiling point). (From inhaled anesthetic package insert equations and Susay SR, Smith MA, Lockwood GG. The saturated vapor pressure of desflurane at various temperatures. *Anesth Analg*. 1996;83:864–866.)

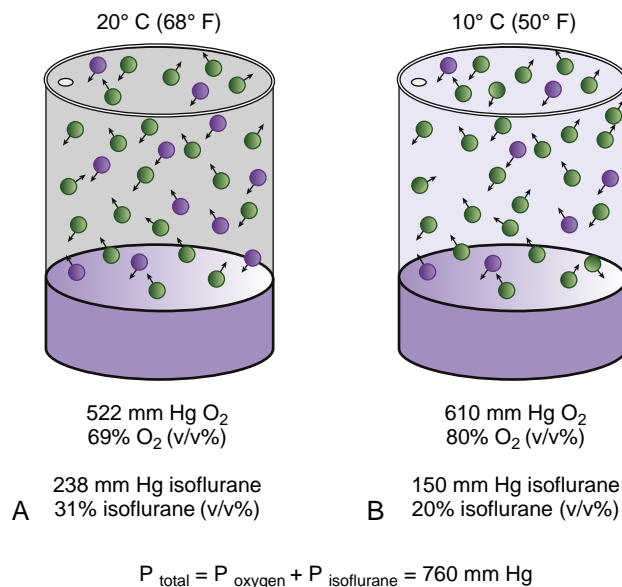


**Fig. 22.17 The impact of temperature on vapor pressure.** (A) Chamber containing oxygen and isoflurane at its saturated vapor pressure (SVP) at 20°C (68°F). At evaporative equilibrium, the SVP of isoflurane in the container represents 31% of the entire gas composition by volume (v/v%). (B) Decreasing the temperature to 10°C (50°F) substantially lowers the isoflurane vapor pressure to 150 mm Hg and causes isoflurane to represent only 20% of the entire gas volume (v/v%). This example assumes that some oxygen can enter the container through a tiny hole to replace the condensed isoflurane molecules.

operating room (ambient) temperature can raise or lower liquid anesthetic vapor pressure, the cooling influence of evaporation (the latent heat of vaporization, *see below*) has a far more pronounced and dynamic effect. The impact of evaporative temperature change on vaporizer and anesthetic inhaler output has been recognized since the mid-1800s, and addressing this phenomenon has been one of the principal factors influencing design of anesthetic vaporizers.

Because vapor pressures are unique to each liquid anesthetic agent, vaporizers must be constructed in an agent-specific manner. If a vaporizer is inadvertently filled with the incorrect liquid anesthetic agent, the vaporizer output will change (see the discussion of misfilling in the section on variable bypass vaporizers).<sup>60,61</sup>

**Expressing Gas Concentrations and Minimum Alveolar Concentration.** When describing a mixture of gases, we can quantify the proportion of an individual gas by either its *partial pressure* (mm Hg), or by the percentage of volume occupied by the gas relative to the sum of all gases present, which is known as *volume percent* or *volume-volume percent* (v/v%):<sup>62</sup>

$$\text{Volume percent (v/v\%)} = (\text{volume of gas } x / \text{total gas volume}) * 100\%$$

The volume that an ideal gas occupies at a given temperature and pressure is related to the number of molecules of gas present, but not the size or identity of the molecules. This statement is known as the *Avogadro Hypothesis*. Using the ideal gas law, it is easy to calculate that at 1 atm (760 mm Hg) of pressure and 20°C (68°F or 293°K), conditions that might be found in a typical operating room, 1 mole of an ideal gas occupies a volume of about 24 L. The same is true for any mixture of ideal gases containing a total of 1 mole of gas molecules. Therefore, because partial pressure is directly proportional to the number of molecules of a gas present in the mixture, we can also use partial pressures to calculate the volume percent of any constituent gas<sup>63</sup>:

$$\begin{aligned} \text{Volume percent (v/v\%)} &= (\text{partial pressure of gas } x / \text{total pressure}) * 100\% \\ &= (P_x / P_{\text{total}}) * 100\% \end{aligned}$$

Using air at sea level ( $P_{\text{total}} = P_{\text{atm}} = 760 \text{ mm Hg}$ ) as an example:

Knowing the partial pressures of the constituent gases of air...

$$P_{\text{atm}} = P_{\text{oxygen}} + P_{\text{nitrogen}} + P_{\text{other}}$$

$$P_{\text{atm}} = 760 \text{ mm Hg} \approx (160 \text{ mm Hg oxygen}) + (592 \text{ mm Hg nitrogen}) + (8 \text{ mm Hg other gases})$$

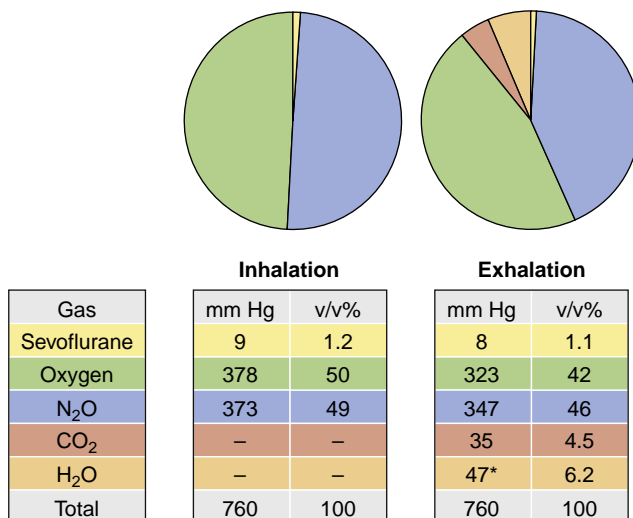
... we can then calculate the volume percent (v/v%) of oxygen...

$$\text{Oxygen (v/v\%)} \sim P_{\text{oxygen}} / P_{\text{atm}} \sim 160 \text{ mm Hg} / 760 \text{ mm Hg} \sim 21\%$$

When anesthesiologists describe inhaled and exhaled anesthetic concentrations, they typically use volume percent. One percent isoflurane is equal to 7.6 mm Hg isoflurane at sea level. The amount of oxygen and nitrous oxide in the breathing gas is also typically described in terms of volume percent. However, CO<sub>2</sub> content (i.e., end-tidal carbon dioxide [ETCO<sub>2</sub>]) is usually displayed as a partial pressure (mm Hg). This was probably adopted because of the relatively close correlation between ETCO<sub>2</sub> and arterial partial pressure of carbon dioxide (Paco<sub>2</sub>), and the latter's common expression as a partial pressure. Fig. 22.18 illustrates a typical composition of the breathing gases during anesthesia in terms of concentration (v/v%) and partial pressures.

The minimum alveolar concentration (MAC) is described in terms of volume percent. MAC is the concentration of anesthetic that prevents movement from surgical stimulus in 50% of individuals.<sup>64</sup> MAC is an age-dependent phenomenon,<sup>65</sup> and it can also be affected by other variables. MAC is a clinically useful value given that vaporizer control knobs are marked and calibrated in terms of anesthetic concentration. However, it is actually the anesthetic partial pressure (mm Hg) value in the brain that is responsible for anesthetic depth. The corresponding partial pressure for each MAC value is known as the minimal alveolar partial pressure (MAPP), as listed in Table 22.1.<sup>66</sup> When discussing anesthetic vaporizers, it is useful to think about their output in terms of partial pressure and how it relates to volume percent and MAC, especially when considering changes in ambient pressure.

**Latent Heat of Vaporization.** When a liquid such as a volatile anesthetic evaporates into the gas phase, energy is



\*Saturated vapor pressure of water at body temperature.

**Fig. 22.18** Common units of measure for breathing circuit gases: typical values for an oxygen-nitrous oxide-sevoflurane anesthetic. Anesthetic agent, oxygen, and nitrous oxide concentrations are typically expressed in volume percent (v/v%). Carbon dioxide is commonly described as a partial pressure (mm Hg).

required to overcome the attractive intermolecular forces between molecules in the liquid phase (a property known as *cohesion*). The needed energy is absorbed from the surroundings in the form of *heat*, and is the reason why the human body is cooled by the evaporation of sweat. The amount of energy absorbed by a specific liquid during evaporation is referred to as the *latent heat of vaporization*. It is more precisely defined as the amount of energy in joules or calories (1 calorie = 4.184 joules) required to change 1 g of liquid into vapor at a constant temperature. In a well-insulated container, the energy for vaporization must come from the liquid itself. In the absence of an outside heat source, the remaining liquid cools as vaporization progresses. This leads to significant reductions in vapor pressure (see Fig. 22.16) and therefore the number of volatile anesthetic molecules in the gas phase (see Fig. 22.17).<sup>44,59,67</sup> If vaporizer design does not mitigate and compensate for evaporative cooling, output will decrease.

**Boiling Point.** The *boiling point* of a liquid is defined as the temperature at which vapor pressure equals atmospheric pressure and the liquid begins to undergo rapid vaporization.<sup>44,67</sup> From the definition above, it is important to note that the boiling point changes depending on atmospheric pressure. Whereas evaporation is a surface phenomenon, boiling is a bulk phenomenon that occurs throughout the interior of the liquid. The boiling point of a liquid is inversely related to volatility. For example, water is not particularly volatile (see Fig. 22.16) and its boiling point of 100°C (212°F) at sea level is much higher than all of the inhaled anesthetic agents. Table 22.1 lists the *normal boiling point* (defined as the boiling point at a pressure of 1 atm) of the common volatile anesthetic agents. While most inhaled anesthetics boil in the range of 48° to 59°C (118°-138°F), desflurane has a normal boiling point close to room temperature (22.8°C or 73°F).

The boiling point of contemporary volatile anesthetic agents is not relevant to vaporizer design under most clinical situations. Desflurane, however, has a high saturated vapor pressure and boils at a temperature commonly encountered in clinical settings. These properties mandate a special vaporizer design to control agent delivery (see section on desflurane vaporizer). Isoflurane and halothane could theoretically boil at high altitudes and very high

**TABLE 22.1** Physical Properties of Inhaled Volatile Anesthetic Agents

Property	Halothane	Isoflurane	Sevoflurane	Desflurane
SVP* @ 20°C (mm Hg)	243	238	157	669
SVC† @ 20°C at 1 atm‡ (v/v%)	32	31	21	88
MAC§ at age 40 year (v/v%)	0.75	1.2	1.9	6.0
MAPP¶ (mm Hg)	5.7	9.1	14.4	45.6
Boiling point @1 atm (°C)	50.2 (122.4°F)	48.5 (119.3°F)	58.6 (137.3°F)	22.8 (73°F)

\*SVP, Saturated vapor pressure. From anesthetic prescribing information.

†SVC, Saturated vapor concentration: the percentage of anesthetic agent relative to ambient pressure within an equilibrated (saturated) container (SVP/ambient pressure).

‡1 atm, 1 atmosphere = ambient pressure at sea level (760 mm Hg).

§MAC, Minimum alveolar concentration: the alveolar concentration that produces immobility in response to a noxious stimulus in 50% of subjects.<sup>64</sup> The denominator is approximately sea level pressure (760 mm Hg).

¶MAPP, Minimum alveolar partial pressure. The alveolar partial pressure that produces immobility in response to a noxious stimulus in 50% of subjects (the numerator in the MAC calculation).<sup>66</sup> Not affected by altitude. Calculated as MAC (fraction) × 760 mm Hg (i.e., for isoflurane = 0.012 × 760 mm Hg).

v/v%, Volume percent.

temperatures. At least one vaporizer manufacturer specifies a maximum safe operating temperature for these anesthetic agents.<sup>68</sup>

**Specific Heat.** The *specific heat* is the amount of energy required to increase the temperature of 1 g of a substance by 1°C.<sup>44,67</sup> Water, for example, has a specific heat of exactly 1 calorie g<sup>-1</sup> deg<sup>-1</sup>. The concept of specific heat is important to the design, operation, and construction of vaporizers in two ways. First, the specific heat of a liquid anesthetic determines how much heat must be supplied to maintain a constant temperature due to the latent heat of vaporization. Second, vaporizers are built from materials with a high specific heat in order to better resist temperature changes associated with evaporative cooling.

**Thermal Conductivity.** Thermal conductivity is a property that describes how well heat flows through a substance. The higher the thermal conductivity, the better a substance conducts heat.<sup>44</sup> Vaporizers are constructed of metals with relatively high thermal conductivity, which helps maintain a uniform internal temperature during evaporation by allowing efficient heat absorption from the environment. By contrast, coffee mugs should be made of materials with a low thermal conductivity to slow heat loss to the environment.

### Modern Vaporizer Types

Vaporizer nomenclature can be somewhat confusing, especially if the historical context of vaporizer, workstation, and breathing circuit evolution is not considered (Table 22.2). Vaporizers are first designated as *in-circuit* or *out-of-circuit*, which describes their relationship to the patient's breathing circuit. Virtually all modern vaporizers are out-of-circuit, and their controlled output is introduced into the breathing circuit through a fresh gas line. In-circuit vaporizers are found mainly within the so-called *draw-over* anesthesia systems, which are of great historical significance in anesthesiology.

The second designation involves the specific types of vaporizers, and these currently include the variable bypass vaporizer (e.g., GE/Datex-Ohmeda Tec 7), the dual-circuit vaporizer (e.g., the classic GE/Datex-Ohmeda Tec 6 desflurane vaporizer), the cassette vaporizer (e.g., GE/Datex-Ohmeda Aladin cassette), the injection vaporizer (e.g., the Maquet vaporizer), and the now historical measured-flow vaporizer (e.g., Copper Kettle). Variable bypass vaporizers can be subcategorized as plenum type, which

are out-of-circuit and have relatively high internal flow resistance (the term "plenum" refers to a chamber where gas flows under positive pressure), or draw-over type, which are in-circuit and have low internal resistance. Most modern variable bypass vaporizers are plenum type and are located out-of-circuit, like those seen in Figs. 22.1 and 22.2. Draw-over type vaporizers are uncommon today, but remain an option for providing anesthesia in resource-poor environments.<sup>68a</sup> Variable bypass vaporizers carry additional designations such as agent-specific, flow-over, temperature-compensated, and pressure-compensated, which are discussed later.

**Variable Bypass Vaporizers.** When volatile anesthetic agents evaporate, their resultant saturated gas concentrations greatly exceed those used clinically, so these concentrations must be diluted to safe ranges (see Table 22.1). *Variable bypass* refers to the method of diluting gas fully saturated with anesthetic agent with a more voluminous flow of gas. A diagram of a variable bypass vaporizer is shown in Fig. 22.19. Basic vaporizer components include a vaporizer inlet port (fresh gas inlet), the concentration control dial, the bypass chamber, the vaporizing chamber, the vaporizer outlet port, and the filling assembly. The maximum safe level of the vaporizer corresponds to the filling port, which is positioned to minimize the chance of overfilling. A concentration control dial determines the ratio of gas that flows through the bypass chamber and the vaporizing chamber, and a temperature-compensating device further adjusts that ratio. Vaporizer concentration control dials are labeled to set vaporizer output in terms of volume percent (v/v%), and the vaporizers are calibrated at sea level.

Fig. 22.20 illustrates volatile anesthetic equilibrium concentrations within a theoretical vaporizing chamber of a variable bypass vaporizer. As can be seen, the saturated vapor concentration of sevoflurane within the chamber (21%) far exceeds the clinical concentration. Fig. 22.20 also depicts the volume of anesthetic vapor that is added to the gas stream as it flows through the chamber. These properties are essential for a quantitative understanding of variable bypass vaporizer function (Box 22.1). Although this example and others in the chapter imply that the gas flowing through the vaporizing chamber becomes fully saturated with anesthetic vapor, this is actually not the case. There is insufficient time to reach evaporative equilibrium due to the constant inflow of fresh gas. As a result, the vaporizing chamber becomes only partially saturated with volatile anesthetic.<sup>69</sup> However, for the purposes of this discussion, it is useful to assume that full saturation occurs.

**TABLE 22.2** Concise Summary of Modern Vaporizer Nomenclature

Type	Subtype(s)	Characteristics
Variable bypass vaporizers	Plenum type	Out-of-circuit, high resistance, gas flow under positive pressure
	Draw-over type	In-circuit, low resistance, gas flow under negative pressure; may be portable
Cassette vaporizer	GE Aladin and Aladin2	Computer-controlled variable bypass vaporizer
Dual-circuit (desflurane) vaporizer	GE Tec 6 and Dräger D-Vapor	Gas-vapor blender, heated & pressurized
Injection vaporizer	Maquet and Dräger DIVA	Direct injection of volatile anesthetic
Anesthetic reflector	AnaConDa, Mirus	Adsorption to and release from a carbon filter

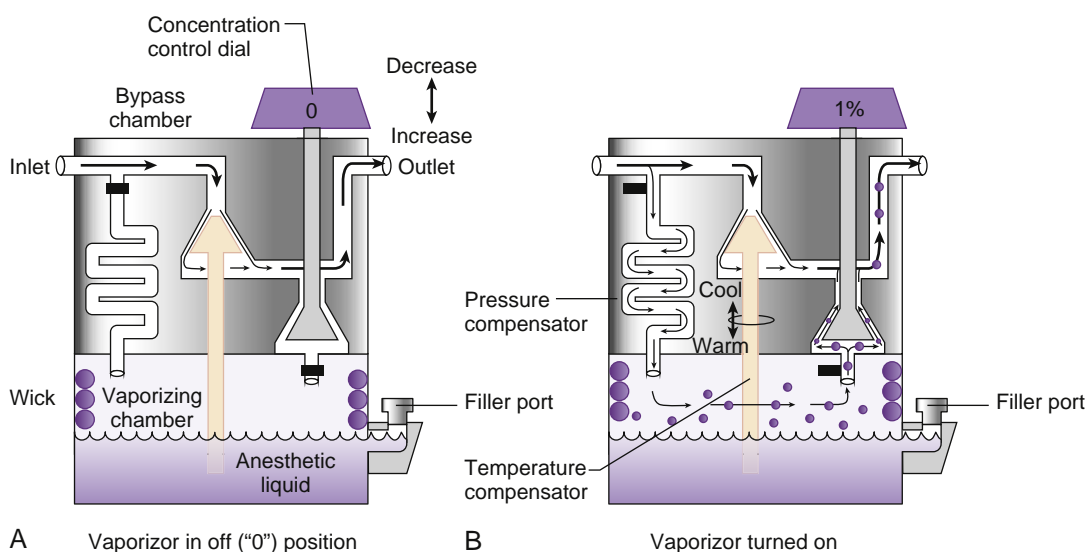


**Fig. 22.19 Variable bypass vaporizer.** (A) Basic components. Vaporizer in the off or "0" position. Fresh gas from the flowmeter assembly enters the vaporizer and then flows through the bypass chamber, around the temperature compensator, and out the vaporizer without passing through the vaporizing chamber. (B) Selecting a vaporizer output (turning the vaporizer "on") diverts an agent-specific ratio of gas through the pressure-compensating labyrinth, into the vaporizing chamber where it becomes saturated with anesthetic vapor, and then past the concentration cone where it reunites with the fresh gas stream. The temperature compensation device further adjusts the ratio of bypass to vaporizing chamber flow, to compensate for changes in anesthetic vapor pressure resulting from temperature changes. As the liquid anesthetic cools by evaporation, more gas is diverted to the vaporizing chamber to compensate for the decrease in vapor pressure. The labyrinth compensates for pressure fluctuations within the vaporizer from the gas supply side and the breathing circuit side to stabilize vaporizer output; it is *not* present to compensate for changes in atmospheric pressure. Please see text for additional details.

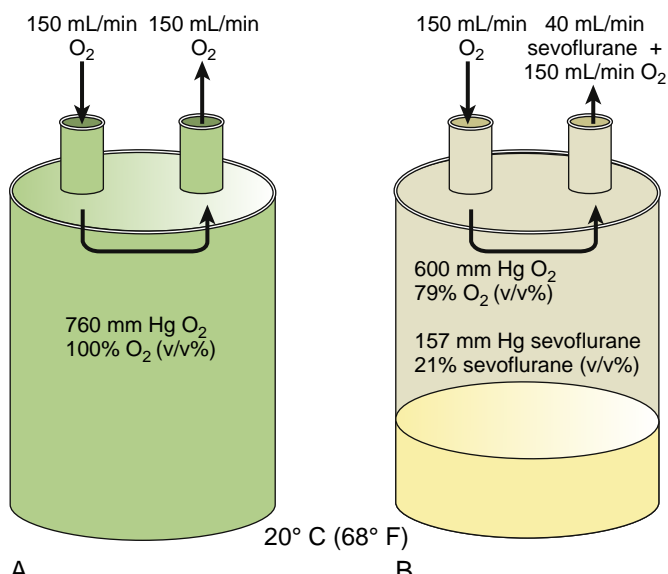


**Fig. 22.20 Theoretical vaporizing chamber demonstrating the volume of anesthetic gas added to the gas flow stream as a result of evaporation:** (A) Pure oxygen flows through the chamber. (B) Liquid sevoflurane is added to the chamber and evaporates to saturated vapor pressure (see Box 22.1 for details).

**Fig. 22.21** illustrates a modern variable bypass vaporizer set to deliver 2% sevoflurane. Note how the majority of fresh gas flows straight through the bypass chamber. The bypass flow and vaporizing chamber output combine to create the desired output concentration. The fresh gas that is diverted to the vaporizing chamber becomes saturated with anesthetic gas by flowing through the wicks and over the liquid agent (hence the designation *flow-over*). The wicks and baffles serve to increase the surface area available for

vaporization and promote mixing of the carrier gas with anesthetic vapor.<sup>69a,69b</sup> The specific ratio of fresh gas flow divided between the bypass chamber and the vaporizing chamber is determined by the concentration control dial setting and the temperature compensation device (see the later discussion of temperature compensation). Because the physical properties and clinical concentrations of each agent are unique, the diverting ratios are specific to each agent and dial setting (hence the designation *agent-specific*). The approximate variable bypass diverting or "splitting ratios" for the common anesthetic agents at 20°C are shown in Table 22.3. Variable bypass vaporizers cannot be used to deliver desflurane, because of this agent's unique physical properties (see section on the desflurane vaporizer).

Virtually all variable bypass vaporizers are equipped with a mechanism that helps maintain constant vaporizer output over a wide range of operating temperatures (hence the designation *temperature-compensated*). This mechanism automatically alters the ratio of gas flowing through the bypass and vaporizing chambers. Temperature compensation is accomplished by an expansion-contraction element, as seen in Fig. 22.19, or a bimetallic strip (Fig. 22.22). At cooler temperatures, the vapor pressure of liquid anesthetic decreases (Fig. 22.16), and it is necessary to reduce the splitting ratio to maintain output. In Fig. 22.19B, as the liquid anesthetic agent cools, the temperature-compensating cone moves upward, restricts bypass flow, and diverts more gas to the vaporizing chamber, thereby maintaining relatively stable vaporizer output. The inverse is also true: warmer temperatures cause the cone to move downward, increasing bypass flow, and diverting less gas to the vaporizing chamber. The most important function of temperature compensation devices is to correct for the effect of evaporative cooling on the liquid anesthetic.

### BOX 22.1 Calculation of the Volume of Gas Added to a Fresh Gas Flow, and Proof of the Splitting Ratio

- Step 1:** Calculate the amount of volatile anesthetic added to the fresh gas stream that makes up a vaporizer chamber output.
- Assume that 150 mL/min of oxygen flows through a vaporizer chamber at 1 atm (760 mm Hg) pressure and 20°C (68°F) (Fig. 22.20A).
  - Liquid sevoflurane is then added to the vaporizer chamber (Fig. 22.20B).
  - Sevoflurane evaporates to its saturated vapor pressure (SVP) of 157 mm Hg, which displaces oxygen from the gas mixture. At this point, sevoflurane has a saturated vapor concentration (SVC) of 157 mm Hg/760 mm Hg ~21% (see Table 22.1).
  - Sevoflurane makes up 21% of the gas flowing out of the vaporizer, and oxygen makes up 79%.
    - To calculate the amount of sevoflurane added to the fresh gas flow through the vaporizer, set up the simple proportion:
      - $(x \text{ mL/min sevoflurane})/21\% = (150 \text{ mL/min oxygen})/79\%$
    - Solve for  $x$ :
      - $x = (150 \text{ mL/min}) * 21\% / 79\% \sim 40 \text{ mL/min sevoflurane}$
  - Therefore 40 mL/min of sevoflurane is added to the vaporizer output, for a total of 190 mL/min (Fig. 22.20B).
- Step 2:** Prove the splitting ratio for a variable bypass vaporizer.
- Building on the example in **Step 1**, consider a sevoflurane vaporizer with 2000 mL/min of fresh gas inflow. Prove that the splitting ratio must be ~12:1 in order to deliver 2% sevoflurane.
- A splitting ratio of 12:1 means that ~150 mL/min of fresh gas is diverted to the vaporizer chamber, and ~1850 mL/min flows through the bypass chamber (see Fig. 22.21).
  - 40 mL/min of sevoflurane is added to the vaporizer output (see **Step 1**).
  - The total vaporizer output is 2040 mL/min.
  - Sevoflurane makes up  $(40 \text{ mL/min})/(2040 \text{ mL/min}) \sim 2\%$  of the total vaporizer output.

Variable bypass vaporizers are also constructed from materials with high specific heat, yielding temperature stability, and high thermal conductivity, which allows rapid transfer of ambient heat. Additionally, the vaporizer wick systems are located in contact with the metal walls to facilitate absorption of environmental heat.

**FACTORS THAT INFLUENCE VARIABLE BYPASS VAPORIZER OUTPUT.** An ideal variable bypass vaporizer would maintain a constant concentration output at a given setting regardless of variables such as the fresh gas flow rate, temperature, intermittent backpressure from the breathing circuit, carrier gas composition, and barometric pressure. ISO standards state that the average output should not deviate from the dial setting by +30% or -20% or more than +7.5% or -5% of the maximum setting.<sup>11</sup> Although modern vaporizers generally have excellent performance characteristics, it is important to understand how these challenges could potentially influence vaporizer output.

**IMPACT OF GAS FLOW RATE.** This factor is notable only at the extremes of flow rates and at higher concentration control dial settings. At low flow rates (<250 mL/min), the output tends to be slightly less than the dial setting due to the relatively high density of volatile anesthetic agents. Insufficient turbulence is generated in the vaporizing chamber to advance the vapor molecules upward. At high flow rates (such as 15 L/min), the output of most variable bypass vaporizers is somewhat less than the dial setting. This discrepancy is due to: cooling during rapid evaporation, incomplete mixing, and failure to saturate the carrier gas in the vaporizing chamber. In addition, the resistance characteristics of the bypass chamber and the vaporizing chamber can vary as flow increases.<sup>68,70</sup>

**IMPACT OF TEMPERATURE CHANGE.** Despite the impact of evaporative cooling and variation in ambient conditions, modern vaporizers maintain fairly constant concentration output over a wide range of common working temperatures. However, the linear change in the temperature-compensating mechanisms does not precisely match the shape of the

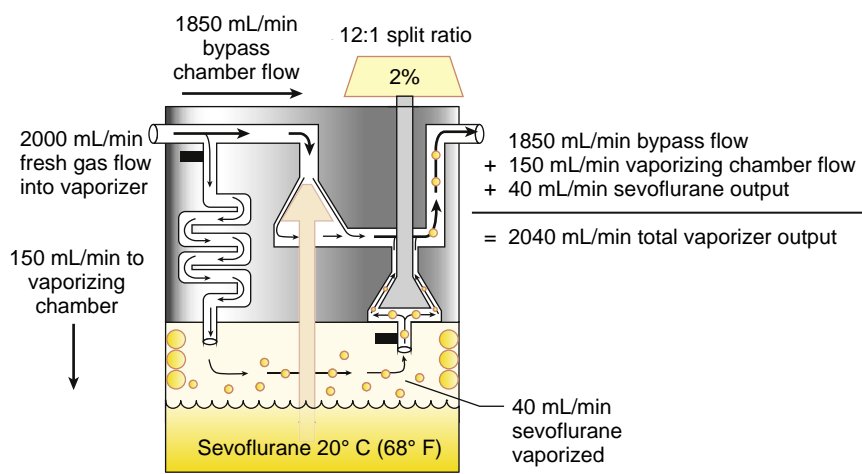


Fig. 22.21 Vaporizer set to deliver 2% sevoflurane at 1 atm (760 mm Hg): 2% sevoflurane requires a splitting ratio of 12:1 (see Table 22.3 and Box 22.1).

**TABLE 22.3** Variable Bypass Vaporizer Splitting Ratios

Concentration Control Dial Setting (v/v%)	BYPASS CHAMBER-TO-VAPORIZING CHAMBER SPLITTING RATIOS AT 20°C (68°F)*		
	Halothane	Isoflurane	Sevoflurane
1	46:1	45:1	25:1
2	23:1	22:1	12:1
3	15:1	14:1	8:1

\*Ratio of fresh gas flowing through the bypass chamber relative to the vaporizing chamber for the listed output concentrations. The temperature compensation device may alter the actual ratio. This applies to variable bypass vaporizers only. Calculated from: % volatile agent output =  $100 \times P_V \times F_V/F_T (P_A - P_V)$  where  $P_A$  = atmospheric pressure,  $P_V$  = vapor pressure at 20°C,  $F_V$  = flow of fresh gas through vaporizing chamber (mL/min), and  $F_T$  = total fresh gas flow (mL/min).

From *Prescribing Information Forane [Isoflurane, USP]*. Deerfield, IL: Baxter Healthcare; 2009.

v/v%, Volume percent.

vapor pressure curves.<sup>19,68</sup> As a result, a slight correlation between vaporizer temperature and delivered concentration remains. This correlation is mainly apparent at higher temperatures and higher concentrations (Fig. 22.23). A dangerous but highly unlikely circumstance could occur if the boiling point of a volatile agent within a variable bypass vaporizer were reached. In this situation, the vaporizer output would be impossible to control by any compensatory mechanism. Although it would be rare to reach ambient temperatures around 50°C at sea level (see Table 22.1), at higher altitudes, where boiling points are lower, this is theoretically more likely. In fact, the Dräger Vapor 2000 user's manual decreases the high-altitude operating specification for the vaporizer from 9880 to 4800 feet if halothane or isoflurane is used at higher ambient temperatures. Manufacturers' published vaporizer operating temperatures range from 10°C to 40°C (50°F-104°F), although the specific ranges vary.<sup>68,70-74</sup>

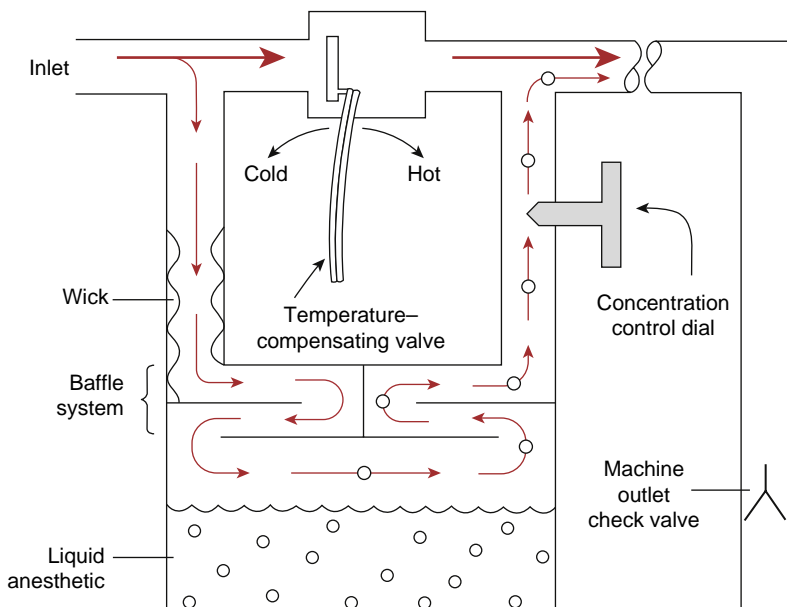


**Fig. 22.22 Temperature compensation with a bimetallic strip.** At cooler temperatures, the strip bends one way and diverts more flow through the vaporizing chamber. At warmer temperatures, the strip bends the opposite way and allows more flow through the bypass chamber. (From Chakravarti S, Basu S. Modern anaesthesia vapourisers. *Ind J Anaesth*. 2013;57[5]:464-471.)

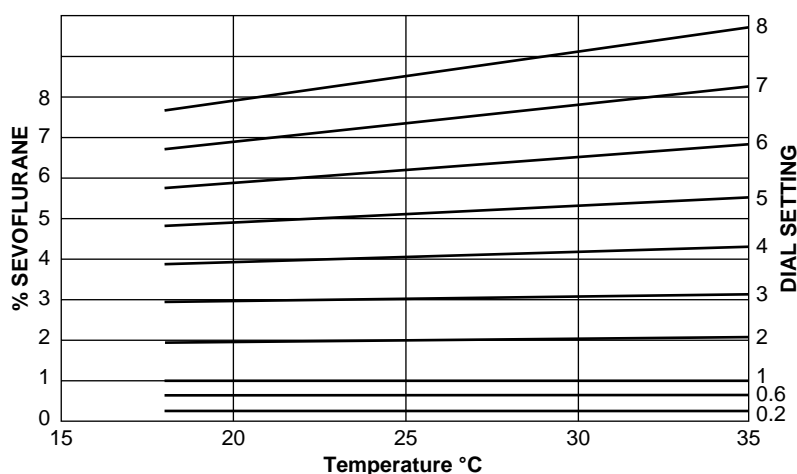


**Fig. 22.23 Effect of ambient temperature on vaporizer output.** See text for explanation. (Redrawn from Datex-Ohmeda. *Tec 7 Vaporizer: User's Reference Manual*. Madison, WI: Datex-Ohmeda; 2002.)

**IMPACT OF INTERMITTENT BACKPRESSURE.** The intermittent backpressure that results from either positive-pressure ventilation or use of the oxygen flush valve may lead to higher than expected vaporizer output. This phenomenon, known as the *pumping effect*, is more pronounced at low flow rates, low dial settings, and low levels of liquid anesthetic in the vaporizing chamber.<sup>44,68,75-77</sup> Additionally, the pumping effect is increased by rapid respiratory rates, high peak inspiratory pressures (PIPs), the use of anesthesia machines without fresh gas decoupling, and rapid drops in pressure during expiration.<sup>44,59,67,68,78,79</sup> Although contemporary variable bypass vaporizers are not highly vulnerable to the pumping effect, the proposed mechanism and preventative design features should be understood. The pumping effect is caused by retrograde transmission of pressure from the patient circuit to the vaporizer during the inspiratory phase of positive-pressure ventilation or use of the oxygen flush function. Gas molecules are compressed in both the bypass and vaporizing chambers. When the backpressure is suddenly released during the expiratory phase, vapor exits the vaporizing chamber both antegrade through the outlet and retrograde through the inlet. This occurs because the output resistance of the bypass chamber is lower than that of the vaporizing chamber, particularly at low dial settings. The enhanced output concentration results from the increment of vapor that travels in the retrograde direction to the bypass chamber.<sup>68,76,77,80</sup>

To decrease the pumping effect, modern vaporizing chambers are smaller than those of early variable bypass vaporizers so that only a small volume of vapor can be discharged retrograde into the bypass chamber.<sup>77</sup> Additionally, some vaporizers have a long spiral tube or labyrinth that serves as the inlet to the vaporizing chamber (see Fig. 22.19).<sup>77</sup> When the pressure in the vaporizing chamber is released, the vapor does not flow back into the bypass chamber because of tube length.<sup>59</sup> This serpentine passage also dampens pressure fluctuations and compensates for fluctuations in gas supply pressure. Other designs may also include an extensive baffle system in the vaporizing chamber. Finally, a one-way check valve can be inserted after the vaporizers and before the breathing circuit inlet to minimize the pumping effect (see the discussion of the gas supply system). This check valve can attenuate but does not eliminate the increase in pressure, because gas still flows from the flowmeters to the vaporizer during the inspiratory phase of positive-pressure ventilation.<sup>44,81</sup> Although intermittent backpressure can result in transient rises in anesthetic concentration at the common gas outlet, the effects are mitigated by dilution within the much larger anesthetic breathing circuit.<sup>82</sup> The goal of all these pressure-compensating mechanisms is to provide an even flow of gas through the vaporizing chamber despite changes in pressure, giving the vaporizers the additional designation *pressure-compensated*.

**IMPACT OF CARRIER GAS COMPOSITION.** Variable bypass vaporizer output can be influenced by fresh gas composition. This phenomenon is the result of differences in the solubility of carrier gases in volatile anesthetic liquids. This effect is most pronounced when nitrous oxide is introduced or removed as a carrier gas.<sup>68,83-90</sup> In the experimental example seen in Fig. 22.24, a change in carrier gas from 100% oxygen to 100% nitrous oxide results in a sudden decrease in halothane output (expressed as volume percent)

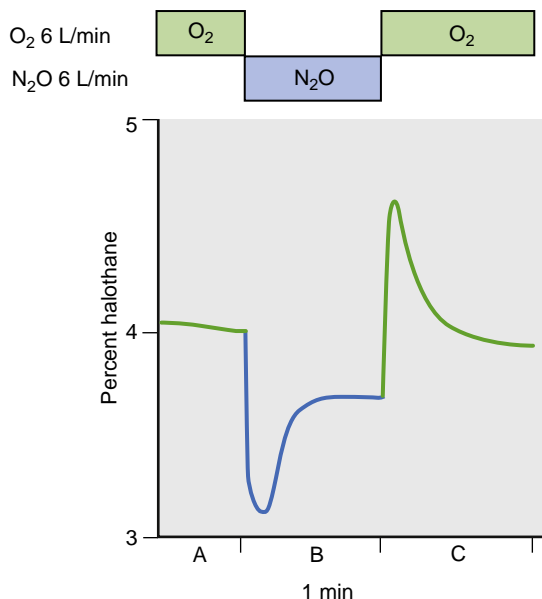


**Fig. 22.24** Halothane output of a North American Dräger Vapor 19.n vaporizer (Dräger Medical, Telford, PA) with different carrier gases. The initial output concentration is approximately 4% halothane when oxygen is the carrier gas at flows of 6 L/min (A). When the carrier gas is quickly switched to 100% nitrous oxide (B), the halothane concentration decreases to 3% within 8 seconds. A new steady-state concentration of approximately 3.5% is then attained within about 1 minute. When O<sub>2</sub> flow is reestablished, halothane output increases abruptly and then settles back to baseline (C). See text for details. (Modified from Gould DB, Lampert BA, MacKrell TN. Effect of nitrous oxide solubility on vaporizer aberrance. *Anesth Analg*. 1982;61:939.)

followed by a slow increase to a new, lower, steady-state (see Fig. 22.24, label B).<sup>88,89</sup> Because nitrous oxide is more soluble than oxygen in the liquid anesthetic within the vaporizer sump, more of the carrier gas dissolves, and the volume output from the vaporizing chamber is transiently reduced.<sup>88</sup> Once the anesthetic liquid becomes saturated with nitrous oxide, the vaporizing chamber output increases and achieves a new steady state.

The explanation for the new steady-state output value is less well understood.<sup>90</sup> Differences in density and viscosity between oxygen and nitrous oxide are likely responsible<sup>90a</sup> because these physical properties affect the relative amount of gas flow through the bypass and vaporizing channels.<sup>86,89,91</sup> Helium, a gas with far lower density than either oxygen or nitrous oxide, has been shown to have variable effect on vaporizer output, depending on the vaporizer model and study design (although the changes tend to be minimal).<sup>92,93</sup>

Although the carrier gas composition can be demonstrated experimentally to affect vaporizer output, deviations are often within specified accuracy ranges. Vaporizer user's manuals usually specify the anticipated response to a change in carrier gas relative to the calibration gas, which may be air or oxygen, depending on the vaporizer model.<sup>68,70,71,94</sup>

**IMPACT OF BAROMETRIC PRESSURE CHANGES.** Understanding the influence of barometric pressure on variable bypass vaporizer output is probably more important for comprehending vaporizer function than for actual clinical reasons. With variable bypass vaporizers, the depth of anesthesia at a given dial setting is relatively independent of atmospheric pressure, and no adjustments need to be made (Table 22.4).<sup>68</sup>

**TABLE 22.4** Comparative Performance of an Isoflurane Variable Bypass Vaporizer and the Tec 6 Desflurane Vaporizer During Changes in Barometric Pressure

Atm	Ambient Pressure (mm Hg)	Isoflurane Variable Bypass Vaporizer With Dial Setting of 0.89% (v/v)			Tec 6 Desflurane Vaporizer With Dial Setting of 6%
		mL Isoflurane Vapor Entrained by 100 mL O <sub>2</sub>	Vaporizer Isoflurane Output (v/v%)	Vaporizer Isoflurane Output (mm Hg)	Vaporizer Desflurane Output (mm Hg)
0.66	500 ( $\approx$ 10,000 ft)	91	1.7	8.8	30
0.74	560 ( $\approx$ 8200 ft)	74	1.5	8	33.6
0.8	608 ( $\approx$ 6000 ft)	64	1.2	7.6	36.5
1.0	760 (sea level)	46	0.89	6.8	45.6
1.5*	1140	26	0.5	5.9	68.4
2*	1520	19	0.36	5.5	91.2
3*	2280	12	0.23	5.2	136

\*ATA or *atmospheres absolute*. ATA = atmospheric pressure + water pressure. Hyperbaric oxygen chamber protocols apply ATA. Many protocols use depths from 2.0 to 2.5 ATA, but some conditions such as gas embolus or carbon monoxide poisoning may require depths to 3.0 ATA.<sup>238</sup> 2 ATA  $\approx$  33 feet of sea water (fsw)  $\approx$  1520 mm Hg *ambient pressure*.

atm, Atmospheres (1 atm = 760 mm Hg); v/v%, volume percent.

Modified from Ehrenwerth J, Eisenkraft J. Anesthesia vaporizers. In: Ehrenwerth J, Eisenkraft J, eds. *Anesthesia Equipment: Principles and Applications*. St. Louis: Mosby; 1993:69-71.

**HIGHER ALTITUDE.** As previously discussed, vapor pressure is independent of barometric pressure. Therefore as altitude increases and barometric pressure declines, the partial pressure of anesthetic agent in the vaporizing chamber remains constant despite decreases in the partial pressures of other constituent breathing gases and the total ambient pressure. This situation results in significantly increased volume percent concentration of anesthetic agent within the vaporizing chamber and at the outlet of the vaporizer (see Table 22.4). However, because anesthetic depth is determined by the *partial pressure* of volatile agent in the brain, the clinical impact is minor (see MAPP in Table 22.1).

Let us consider an example of moving a vaporizer from sea level to higher altitude. With a constant dial setting of 0.89%, at 1 atm, a well-calibrated isoflurane variable bypass vaporizer would deliver 0.89 v/v% isoflurane, and the partial pressure of isoflurane output would be 6.8 mm Hg. Assume that we maintain the same dial setting and lower the atmospheric pressure to 0.66 atm or 502 mm Hg (roughly equivalent to an elevation of 10,000 feet). This results result in an increase in the isoflurane concentration output to 1.75% (a 97% increase), but the partial pressure increases to only 8.8 mm Hg (a 29% increase). A similar change in output partial pressure at sea level, in terms of volume percent, would correspond to an isoflurane concentration increase of only 0.2%. So while the anesthetic concentration (v/v%) changes significantly in this example, it is the partial pressure of volatile agent in the brain that is ultimately responsible for anesthetic depth, and that change is minimal.

As described earlier, MAC values for contemporary inhalational anesthetic agents were determined at sea level. Similarly, anesthetic vaporizers are calibrated at sea level, thus ensuring that vaporizer output (v/v%) matches the dial setting. Using the isoflurane data shown in Table 22.4 as an example, one can see how confusion may arise when thinking of MAC in terms of volume percent and considering barometric change.

The MAPP at altitude is the same as at sea level because it is a partial pressure, whereas the MAC increases because it

is a simple concentration. Table 22.4 shows that the *partial pressure output* of a variable bypass vaporizer changes proportionally less than the volume percent concentration as altitude increases. Because the partial pressure of volatile agent determines anesthetic depth, the operator *does not* need to adjust the dial to a higher setting to compensate for barometric pressure. This holds true for variable bypass vaporizers, but not for the desflurane Tec 6-style vaporizer (see later).

**HYPERBARIC CONDITIONS.** Although anesthesia is sometimes delivered in *hyperbaric conditions*, intravenous anesthesia is easier to deliver in this setting. Under hyperbaric conditions, the partial pressure of volatile anesthetic in the vaporizing chamber remains constant despite an increase in ambient pressure and the partial pressure of the other gases. The net theoretical effects on variable bypass vaporizers are a significant decrease in anesthetic concentration (v/v%) and a mild decrease in partial pressure output. However, the partial pressure of halothane was noted to increase slightly with increasing barometric pressure under experimental conditions.<sup>95</sup> Possible explanations for this finding include the effect of increased atmospheric gas density on the flow of gas through the vaporizer and the increased thermal conductivity of air at higher pressure. The clinical significance of these small changes in partial pressure output under hyperbaric conditions is unclear.

**OTHER SAFETY FEATURES.** Contemporary variable bypass vaporizers incorporate many other safety features. Agent-specific, keyed filling devices help prevent filling with the wrong agent. Overfilling is minimized by locating the filler port at the maximum safe liquid level. Modern vaporizers are firmly secured to a manifold on the anesthesia workstation to prevent tipping. Contemporary interlock systems prevent the administration of more than one inhaled anesthetic agent. However, virtually all safety systems have vulnerabilities, so it remains important to understand these potential hazards.

**MISFILLING.** Misfilling of anesthetic vaporizers with the wrong agent can result in an overdose or underdose of

volatile anesthetic.<sup>96,97</sup> Vaporizer output in these circumstances depends on the erroneous agent's saturated vapor pressure and the splitting ratio of the misfilled vaporizer, since these key parameters must normally be matched to ensure accurate agent delivery (see earlier discussion). Similarly, mixtures of anesthetic agents can also result in harmful dosing.<sup>60</sup> Agent-specific filling devices have reduced, but not eliminated, misfilling. The potential for misfilling exists even in vaporizers equipped with keyed fillers,<sup>98-100</sup> and current standards do not mandate their use.<sup>20</sup> The use of breathing circuit gas analysis may alert the user to misfilling. If a variable bypass vaporizer for isoflurane or sevoflurane is misfilled with desflurane, a substantial overdose could occur because of the high vapor pressure of desflurane (see Fig. 22.16).

**CONTAMINATION.** Although rarely reported, contamination of anesthetic vaporizer contents has occurred. In one instance, organic contaminants (some volatile) in a bottle of isoflurane were detected because of an abnormal acrid odor emanating from the vaporizer.<sup>101</sup> In another report, water accumulation within sevoflurane vaporizers allowed bacteria (*Staphylococcus epidermidis*) to grow and metabolize liquid sevoflurane to volatile and potentially toxic compounds.<sup>101a</sup>

**TIPPING.** Tipping of a variable bypass vaporizer can occur when it is incorrectly removed, transported, or replaced. Excessive tipping can allow the liquid agent to enter the bypass chamber and cause an extremely high output.<sup>102</sup> Although some vaporizers are more sensitive than others, most should not be used after tipping until they have been flushed for a period of time at high flow rates. Manufacturers' instructions differ regarding their post-tipping procedures, so it is best to refer to each specific user manual.<sup>68,70,71,94</sup> A gas analyzer should be used to assess vaporizer output before replacing into clinical use. The Dräger Vapor and D-Vapor series vaporizers have a transport ("T") dial setting that isolates the vaporizer chamber from the bypass chamber to eliminate the possibility of internal overflow during transport.<sup>68</sup>

**OVERFILLING.** Improper filling procedures, combined with failure of the vaporizer sight glass, can cause patient overdose. If overfilled, liquid anesthetic may enter the bypass chamber, and a harmful dose of vapor could be delivered to the common gas outlet.<sup>103</sup> It is a requirement that contemporary vaporizers be designed so that they cannot be overfilled when they are used in a normal operating position.<sup>20</sup> Side-fill variable bypass vaporizers, as opposed to top-fill devices, largely prevent overfilling because the maximum safe level is predetermined by the position of the filler port (see Fig. 22.19). In addition, some vaporizers are equipped with an overflow hole as an additional safeguard.<sup>68</sup> Overfilling can still occur if the vaporizer is tipped or turned on while filling, or air enters at the bottle neck and filler adapter caused by a loose or faulty seal.<sup>103-106</sup>

**LEAKS.** Vaporizers and the vaporizer-machine interface are potential sources of gas leaks that can result in patient awareness during inhaled anesthesia. Loose filler caps, filler plugs, and drain valves are probably the most common sources of leaks. Such a leak may be obvious (e.g., an audible gas leak with spillage of anesthetic agent) or have a more subtle presentation (such as a lower than expected inhaled agent concentration, or the odor of anesthetic gas).<sup>107,108</sup>

Another common source of gas leak occurs at the junction of the vaporizer and the mounting bracket or manifold, where broken mounting assemblies or foreign bodies can compromise the seal between the vaporizer and its point of attachment.<sup>109-112</sup> Gas leaks can also occur within the vaporizer itself as a result of mechanical failure.

**ENVIRONMENTAL CONSIDERATIONS.** Anesthesia delivery has become more common outside the operating rooms, and one challenging location is the magnetic resonance imaging (MRI) suite. The presence of a powerful magnetic field, significant noise pollution, and limited access to the patient during the procedure all complicate care in this setting. The anesthesia provider must appreciate the extremely powerful magnetic fields in these locations and know that only nonferrous (MRI-compatible) equipment can be used. Although some anesthesia vaporizers may appear nonferrous by testing with a horseshoe magnet, they may indeed contain substantial internal ferrous components. Inappropriate use of such devices in an MRI suite may turn them into dangerous missiles if left unsecured.<sup>113</sup>

**Desflurane Vaporizer.** Because of its unique physical characteristics, accurate delivery of desflurane required a different approach to vaporizer design. The Datex-Ohmeda Tec 6 vaporizer was released into clinical use in the early 1990s. The Tec 6 is an electrically heated, pressurized device specifically designed to deliver desflurane (Fig. 22.25).<sup>114,115</sup> Dräger Medical received approval from the U.S. Food and Drug Administration (FDA) for the D-Vapor, its version of the desflurane vaporizer in 2004. The operating principles apply to either system, although the discussion refers to the Tec 6 specifically. The Datex-Ohmeda Aladin cassette vaporizer and the Maquet vaporizers are discussed separately because their operating principles are different.

**UNSUITABILITY OF CONTEMPORARY VARIABLE BYPASS VAPORIZERS FOR CONTROLLED VAPORIZATION OF DESFLURANE.** Desflurane's high volatility and moderate potency (see Table 22.1) preclude its use with contemporary variable bypass vaporizers for three main reasons<sup>114</sup>:

1. *Desflurane's high rate of evaporation would require excessive diluting gas (bypass chamber) flow.* The vapor pressure of desflurane is 669 mm Hg at 20°C (68°F), which is significantly higher than other inhaled anesthetic agents (see Fig. 22.16).<sup>116</sup> At 1 atm and 20°C, 100 mL/min passing through the vaporizing chamber would entrain 735 mL/min of desflurane (as compared with 29, 46, and 47 mL/min of enflurane, isoflurane, and halothane, respectively).<sup>114</sup> To produce a 1% desflurane output, the amount of bypass flow required to dilute the large volume of desflurane-saturated anesthetic vapor would be approximately 73 L/min (in contrast to 5 L/min or less for the other three agents). Prohibitively high bypass chamber flow rates would be required to dilute the vaporizing chamber output to clinical concentrations.
2. *Desflurane's high rate of evaporation would cause substantial anesthetic cooling.* Variable bypass vaporizers require ambient heat to offset evaporative cooling. Although the latent heat of vaporization for desflurane

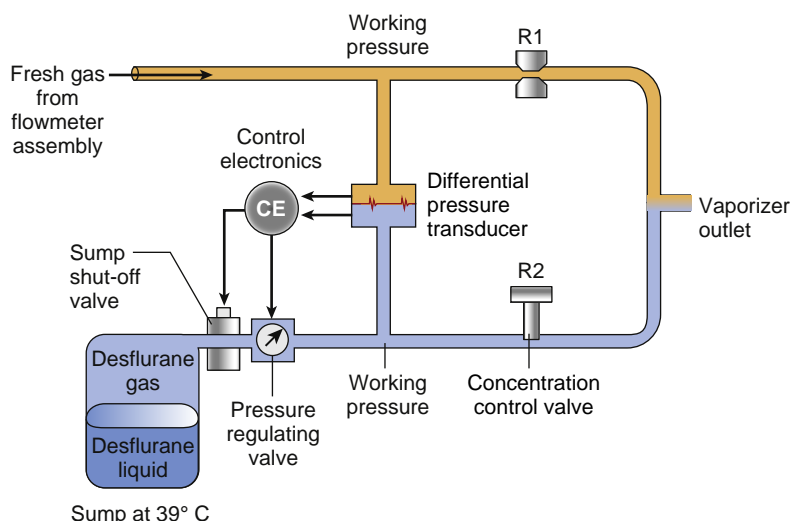


**Fig. 22.25** Simplified schematic of the Tec 6 desflurane vaporizer (Datex-Ohmeda, Madison, WI). See text for details. (From Andrews JJ. *Operating Principles of the Ohmeda Tec 6 Desflurane Vaporizer: A Collection of Twelve Color Illustrations*. Washington, DC: Library of Congress; 1996.)

is approximately equal to that of enflurane, isoflurane, and halothane, its MAC is much higher. The amount of desflurane required to be vaporized over a given period is considerably greater than that of the other inhaled anesthetics. Supplying desflurane in equivalent MAC concentrations would lead to excessive cooling of the vaporizer and reduced output without an external heat source. Because of the broad range of temperatures seen in the clinical setting and desflurane's steep vapor pressure-versus-temperature curve (see Fig. 22.16), desflurane delivery would not be stable in a conventional variable bypass vaporizer.<sup>114</sup>

3. *Desflurane is more likely to boil.* The boiling point of desflurane is 22.8°C (73°F) at 1 atm. This temperature is at the higher end of normal operating room temperatures. If the anesthetic agent were to boil within a variable bypass-type vaporizer, the output would be uncontrollable. The amount of vapor produced would be limited only by heat transfer to the desflurane liquid, which depends upon the specific heat and thermal conductivity of the vaporizer (see discussion above).<sup>114</sup>

**OPERATING PRINCIPLES OF THE TEC 6 AND TEC 6 PLUS.** The Tec 6 desflurane vaporizer was the first clinically available vaporizer to be electrically heated and pressurized, making many aspects of the internal design and operating principles radically different from variable bypass vaporizers. The Tec 6 is probably more accurately described as a dual-gas blender than as a vaporizer. A simplified schematic of the Tec 6 is shown in Fig. 22.25. The vaporizer has two independent gas circuits arranged in parallel. The fresh gas circuit is shown in orange, and the vapor circuit is shown in blue. Fresh gas from the flowmeters enters at the fresh gas inlet, passes through a fixed restrictor (R1), and exits at the vaporizer gas outlet. The vapor circuit originates at the desflurane sump, which is a reservoir of desflurane vapor. It is electrically heated to 39°C, a temperature much higher than desflurane's boiling point. At 39°C, the vapor pressure in the sump is approximately 1300 mm Hg (~2 atm).<sup>117</sup> Just downstream from the sump is the shut-off valve. After the vaporizer warms up, the shut-off valve fully opens when the concentration control valve is turned to the "on" position.

**TABLE 22.5** Fresh Gas Flow Rate Versus Working Pressure in the Tec 6 Desflurane Vaporizer

Fresh Gas Flow Rate (L/min)	Working Pressure at R1 and R2 (mm Hg)
1	7.4
5	37.0
10	74.0

From Andrews JJ, Johnston RV Jr. The new Tec 6 desflurane vaporizer. *Anesth Analg*. 1993;76:1338.

A pressure-regulating valve located downstream from the shut-off valve down regulates the pressure to the pressure of the background gas. The operator controls the output of desflurane by adjusting the concentration control valve (R2), which is a variable restrictor.<sup>114</sup>

The vapor flow through R2 joins the fresh gas flow through R1 at a point downstream from the restrictors. Until this point, the two circuits are physically separated. They are interfaced pneumatically and electronically, however, through differential pressure transducers, a control electronics system, and a pressure-regulating valve. When fresh gas flows past the fixed restrictor R1, a specific backpressure proportional to the flow rate pushes against the diaphragm of the differential pressure transducer. The transducer relays the pressure difference between the fresh gas circuit and the desflurane vapor circuit to the control electronics system. The control system tunes the pressure-regulating valve so that the pressure in the vapor circuit equals the pressure in the fresh gas circuit. This equalized pressure supplying R1 and R2 is the working pressure, which is constant at a fixed fresh gas flow rate. If the operator increases the fresh gas flow rate, more backpressure will be exerted on the diaphragm of the pressure transducer, and the working pressure of the vaporizer will increase.<sup>114</sup> Table 22.5 shows the linear relationship between fresh gas flow rate and working pressure for a typical Tec 6 vaporizer.

The following are two specific examples to demonstrate the operating principles of the Tec 6.<sup>114</sup>

**TABLE 22.6** Dial Setting Versus Flow Through Restrictor R2 at 1 L/min Fresh Gas Flow in the Tec 6 Desflurane Vaporizer

Dial Setting (vol%)	Approximate Vapor Flow Rate Through R2 (mL/min)
1	10
6	64
12	136
18	220

From Andrews JJ, Johnston RV Jr. The new Tec 6 desflurane vaporizer. *Anesth Analg*. 1993;76:1338.

**Example A: Constant fresh gas flow rate of 1 L/min with an increase in the dial setting.** With a fresh gas flow rate of 1 L/min, the pressure supplying R1 and R2 is 7.4 mm Hg. As the operator increases the dial setting, the opening at R2 becomes larger, thereby allowing more vapor to pass through R2. Specific vapor flow values at different dial settings are shown in Table 22.6.

**Example B: Constant dial setting with an increase in fresh gas flow from 1 to 10 L/min.** At a fresh gas flow rate of 1 L/min, the working pressure is 7.4 mm Hg, and at a dial setting of 6%, the vapor flow rate through R2 is 64 mL/min (see Tables 22.5 and 22.6). With a 10-fold increase in the fresh gas flow rate, the working pressure increases to 74 mm Hg. Because R2 is supplied by 10 times more pressure, the vapor flow rate through R2 increases 10-fold to 640 mL/min. Both fresh gas flow and vapor flow increase proportionally, so vaporizer output is constant.

#### FACTORS THAT INFLUENCE TEC 6 DESFLURANE VAPORIZER OUTPUT.

Barometric pressure and carrier gas composition influence the Tec 6 vaporizer output.

**HIGHER ALTITUDE.** Although ambient pressure changes affect the volume percent output of variable bypass vaporizers significantly, the effect on partial pressure output is minimal (and recall that the partial pressure of volatile agent in brain tissue is the main determinant of anesthetic depth). By contrast, the partial pressure output of Tec 6 style desflurane vaporizers is significantly affected by altitude, as can be seen in Table 22.4. One must remember that the Tec 6 device is more accurately described as a dual-gas blender than a vaporizer. Regardless of ambient pressure, the Tec 6 will maintain a constant volume percent output (v/v%), *not a constant partial pressure*. This means that at high altitudes, the partial pressure of desflurane will decrease in proportion to the reduction in atmospheric pressure divided by the calibration pressure (normally 760 mm Hg) per the following formula:

$$\text{Required dial setting (\%)} = \text{Normal dial setting} \times \frac{(760 \text{ mm Hg})}{[\text{Ambient pressure (mm Hg)}]}$$

For example, at an altitude of 2000 m, or 6564 feet, where the ambient pressure is 608 mm Hg, the operator must advance the concentration control dial from 10% to 12.5% to maintain the required anesthetic partial pressure. In hyperbaric settings, the operator must decrease the dial setting to prevent delivery of an overdose. At 2 atm or 1520

mm Hg of pressure, the desflurane output in mm Hg is twice that at sea level (91.2 vs. 45.6 mm Hg).

**CARRIER GAS COMPOSITION.** Vaporizer output most closely matches the dial setting when oxygen is the carrier gas because the Tec 6 vaporizer is calibrated with 100% oxygen. When a carrier gas other than 100% oxygen is used at low flow rates, a clear trend toward reduction in vaporizer output emerges. This reduction correlates with the decrease in viscosity of the carrier gas. Nitrous oxide is less viscous than oxygen, and generates lower backpressure upstream of resistor R1 (see Fig. 22.25). As a result, the working pressure is reduced. At low flow rates with nitrous oxide as the carrier gas, vaporizer output is approximately 20% less than the dial setting.

**SAFETY FEATURES.** Because desflurane's vapor pressure is nearly 1 atm, misfilling a variable bypass vaporizer with desflurane could theoretically result in both overdose and creation of a hypoxic gas mixture. Like most of its contemporaries, the desflurane vaporizer has a unique, anesthetic-specific filling system to minimize this potential hazard. Each desflurane bottle has a "SAF-T-FILL" adapter intended to prevent use with traditional vaporizers. The SAF-T-FILL is essentially a spring-loaded valve that seals the bottle until the bayonet fitment is fully engaged in the filler port of a desflurane vaporizer.<sup>119</sup> This mechanism also helps guard against evaporative loss of agent during storage. The adapter has an O-ring on the tip to minimize spillage during filling.<sup>119a</sup> Thus the SAF-T-FILL system helps prevent both misfilling of variable bypass vaporizers and leakage of desflurane to the atmosphere.<sup>119b</sup>

Major vaporizer faults cause the shut-off valve located just downstream from the desflurane sump (see Fig. 22.25) to close and terminate output. The valve closes, and a no-output alarm is activated, if any of the following conditions occur: (1) the anesthetic level decreases to less than 20 mL, (2) the vaporizer is tilted, (3) a power failure occurs, or (4) the pressure difference between the vapor and fresh gas circuits exceeds a specified tolerance. Although such automated safeguards can enhance patient safety, they may have unintended consequences. For example, a previous generation of Datex-Ohmeda D-Tec Plus vaporizer was reported to be incompatible with a certain model of Dräger anesthesia machine.<sup>120</sup> By design, this workstation interrupted fresh gas flow during the inspiratory phase of volume control ventilation as a means of fresh gas decoupling. These purposeful fresh gas flow interruptions caused an alarm and inappropriate termination of vaporizer output. Although the vaporizer was subsequently modified, this example serves as a reminder that new technology can bring about new problems.

**SUMMARY.** The Tec 6 and Dräger D-Vapor vaporizers are electrically heated, thermostatically controlled, constant-temperature, pressurized, electromechanically coupled dual-circuit, gas vapor blenders. The pressure in the vapor circuit is electronically regulated to equal the pressure in the fresh gas circuit. At a constant fresh gas flow rate, the operator regulates vapor flow with a conventional concentration control dial. When the fresh gas flow rate increases, the working pressure increases proportionally. For a given concentration setting, even when varying the fresh gas flow rate, the vaporizer output is constant because the amount of flow through each circuit remains proportional.<sup>114</sup>

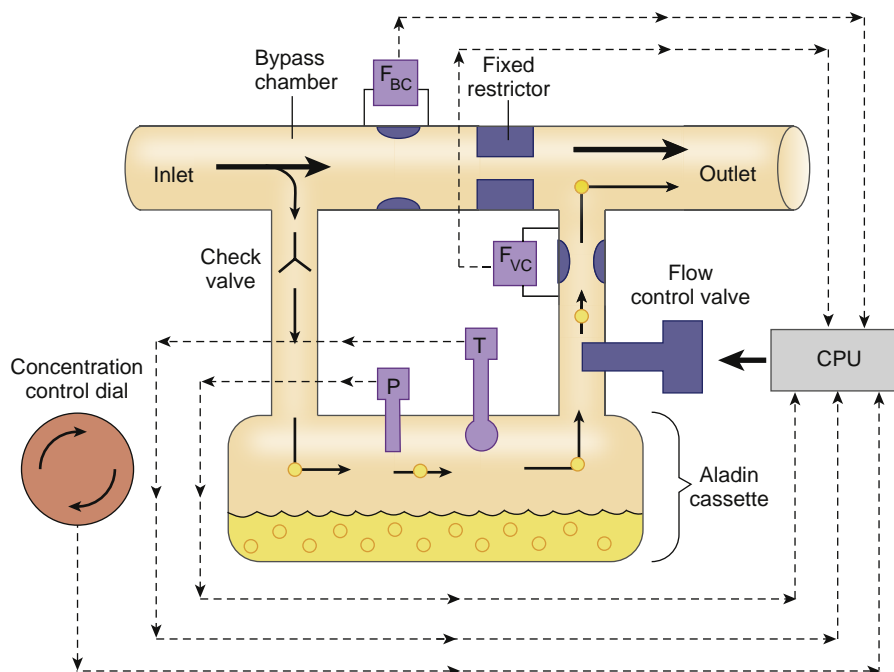


**Fig. 22.26 Simplified schematic of Datex-Ohmeda Aladin cassette vaporizer (Datex-Ohmeda, Madison, WI).** The black arrows inside the vaporizer represent flow from the flowmeters, and the yellow circles represent anesthetic vapor. The heart of the vaporizer is the electronically controlled flow control valve located in the outlet of the vaporizing chamber. *CPU*, Central processing unit;  $F_{BC}$ , flow measurement unit that measures flow through the bypass chamber;  $F_{VC}$ , flow measurement unit that measures flow through the vaporizing chamber;  $P$ , pressure sensor;  $T$ , temperature sensor. Please see text for additional details. (Modified from Andrews JJ. *Operating Principles of the Datex-Ohmeda Aladin Cassette Vaporizer: A Collection of Color Illustrations*. Washington, DC: Library of Congress; 2000.)

**GE/Datex-Ohmeda Aladin and Aladin2 Cassette Vaporizers.** The vaporizer system used in the GE Aisys anesthesia workstations (and some former Datex-Ohmeda models) is unique in that a single electronically controlled vaporizer is designed to deliver several different inhaled anesthetic agents. The vaporizer consists of a permanent internal control unit housed within the workstation and interchangeable cassettes that contain anesthetic liquid and serve as vaporizing chambers. The Aladin cassettes (now superseded by the Aladin2) are filled using agent-specific fillers and color-coded: red (halothane), orange (enflurane), purple (isoflurane), yellow (sevoflurane), and blue (desflurane). They are also magnetically coded to allow the anesthesia workstation to identify which cassette has been inserted.

Operationally, the Aladin cassette vaporizing system is best described, during most circumstances, as a computer-controlled variable bypass vaporizer (Fig. 22.26). It consists of a bypass section and vaporizing chamber, the latter of which is contained within the interchangeable cassette (Fig. 22.27). A fixed restrictor located in the bypass chamber causes gas flow from the inlet to split into two streams. One stream passes through the bypass chamber, and the other is diverted to the vaporizing chamber where it passes through a one-way check valve. This valve prevents retrograde flow of anesthetic vapor into the bypass chamber, and its presence is unique to the Aladin system. The one-way check valve is essential for precise delivery of desflurane (see below). Failure of the check valve to close can result in anesthetic overdose due to retrograde flow into the bypass chamber.

Within the cassette, anesthetic agent vaporizes freely to saturated vapor pressure. A flow control valve, modulated by a central processing unit (CPU), precisely meters the amount of gas flow through the vaporizing chamber, which then rejoins the bypass flow.<sup>44</sup> The CPU receives input from multiple sources: the concentration control dial, pressure and temperature sensors inside the vaporizing chamber, and flow sensors in the bypass and vaporizing chambers. The CPU also receives input from the flowmeters regarding the carrier gas composition, which can affect vaporizer output as described above. Using these data, the CPU precisely regulates fresh gas flow through the vaporizing chamber to obtain the desired vapor concentration output.<sup>121</sup>

As mentioned in the discussion of the Tec 6, controlled vaporization of desflurane presents a unique challenge, particularly when room temperature is higher than the boiling point (22.8°C [73°F]). If the desflurane were to boil, the pressure inside the vaporizing chamber would exceed ambient pressure. When vaporizing chamber pressure exceeds that in the bypass chamber, the one-way check valve closes and prevents carrier gas from entering the cassette. Carrier gas passes straight through the bypass chamber and its flow sensor. Under these conditions, the CPU adjusts the flow control valve to meter in the appropriate flow of pure desflurane vapor needed to achieve the desired final concentration. The vaporizer then begins functioning as an injector, as opposed to resembling a variable bypass unit.

During delivery of inhaled agents at high fresh gas flow rates and/or high dial settings, large quantities of anesthetic liquid are rapidly vaporized. As a result, the temperature of the vaporizer sump decreases due to evaporative

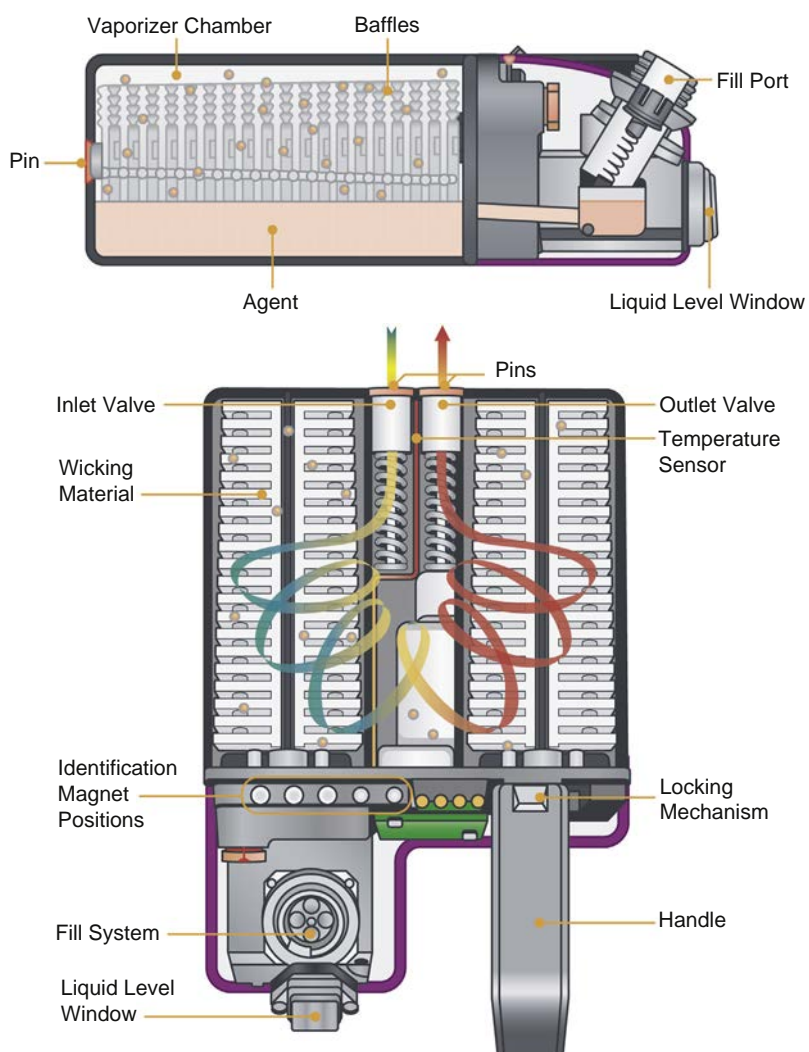


**Fig. 22.27 Gas flow and safety features of the Aladin2 cassette.** Top, side view illustrating filling system and baffles. Bottom, top view showing safety features, wicks, and gas flow during vapor uptake. (From GE HealthCare.)

cooling. To offset this cooling effect, some workstations are equipped with a fan that forces warmed air from a resistor across the cassette to raise its temperature when necessary. The fan is activated during two common clinical situations: (1) desflurane induction and maintenance and (2) sevoflurane induction.

The Aladin vaporizing system incorporates many important safety features. Electronic control of the carrier gas ratio guards against delivery of a hypoxic gas mixture. This ensures that no less than 25% oxygen is delivered at the common gas outlet regardless of carrier gas composition and concentration of anesthetic agent. This feature is unique, since conventional oxygen–nitrous oxide proportioning systems are not affected by the concentration of potent inhaled anesthetic agents. The system is also equipped with a safety relief valve that opens when cassette pressure exceeds 2.5 atm (1899 mm Hg). When the Aladin cassette is removed from the workstation, valves close to prevent loss of fresh gas. Another valve prevents liquid anesthetic from entering the fresh gas line. The system also has an overfilling protection mechanism.<sup>121a</sup> Finally, the

Aladin cassette is immune to tipping and has no restrictions on orientation during handling or storage.<sup>121</sup>

### Injection-Type Vaporizers: Maquet and Dräger Direct Injection of Volatile Anesthetic.

The Maquet vaporizer is an electronically controlled, injection-type vaporizer that is used exclusively with Maquet FLOW-i anesthesia workstations. Because these vaporizers are located upstream from the patient's breathing circuit, they are designated as out-of-circuit vaporizers, similar to the desflurane vaporizers and most variable bypass vaporizers. The Maquet injection vaporizers are agent-specific and available for isoflurane, sevoflurane, and desflurane. Externally, the device has a lid, filling port, electronic level indicator, and alert indicators, but no concentration control dial. Vaporizer output adjustments are accomplished through an electronic interface on the workstation.

The Maquet vaporizer principle of operation is illustrated in Fig. 22.28. Gas from the anesthesia machine enters through the drive gas inlet and pressurizes a reservoir of liquid anesthetic. This pressure provides the force to drive

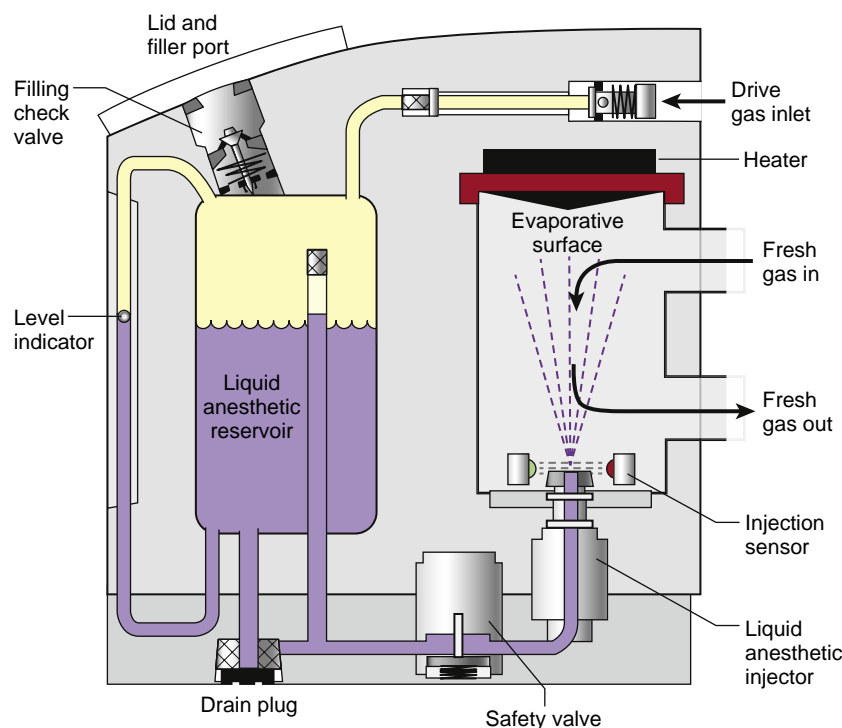


**Fig. 22.28 The Maquet anesthetic vaporizer.** Drive gas from the anesthesia machine is used to pressurize a liquid anesthetic reservoir. Under microprocessor control, liquid agent is injected into a vaporizing chamber. Injection is carefully monitored. A heated surface within the vaporizing chamber facilitates evaporation of the anesthetic agent. Fresh gas flows through the chamber and is enriched with anesthetic gas. A safety valve stops the flow of liquid agent in the case of vaporizer malfunction. (Personal communication, illustration adapted with permission from Maquet Critical Care, Solna, Sweden, January 14, 2013.)

liquid through the injector (and also minimizes evaporation within the reservoir chamber). Liquid anesthetic is injected into a heated vaporizing chamber in pulses that are under microprocessor control. Rapid evaporation occurs. Injection continues in small increments until the desired volume is obtained. The total amount injected in any given interval is based on the desired anesthetic concentration and the fresh gas flow through the vaporizer. A dedicated gas analysis line downstream from the vaporizer monitors the output. An optical sensor in the vaporizer monitors the integrity of the anesthetic injections (personal communication, Maquet Critical Care, January 14, 2013).

Fresh gas from the anesthesia workstation flows through the vaporizing chamber and is enriched with anesthetic agent. Although some of the injected liquid anesthetic evaporates while in flight within the vaporizing chamber, the remainder is deposited on a heated surface that ensures immediate evaporation. Heating of the evaporative surface is carefully regulated to compensate for evaporative cooling (personal communication, Maquet Critical Care, January 14, 2013).

During the daily workstation pre-use check, Maquet vaporizers are automatically tested with respect to functionality and leaks. A safety valve stops the flow of liquid agent in the event of vaporizer malfunction. The vaporizer is not vulnerable to tipping because it has no wicks to saturate, and agent cannot spill into the vaporizing chamber. The vaporizer can be filled during use, although no vaporizer output occurs during filling. An alarm triggers when the liquid anesthetic level is less than 10%, and a higher-priority alarm triggers when it reaches 5%. Limited data is

available on the Maquet vaporizer's performance with different fresh gas flow rates,<sup>121b</sup> but the impact of changing barometric pressure, temperature, and fresh gas composition has not been reported.

Some Dräger anesthesia workstations are also equipped with vaporizers that function by the direct injection of volatile anesthetic (DIVA) principle (Fig. 22.29). Dräger DIVA vaporizers are agent specific. They consist of an interchangeable vaporizing module and a gas supply arrangement that is part of the workstation.<sup>69a,121c</sup> Liquid anesthetic agent is held in a reservoir. The liquid flows by gravity into a dosing chamber, where it is pressurized by gas supply from the workstation. The liquid passes through a dosing valve, and it is sprayed by a fuel injector into a heated vaporizing chamber. The anesthetic agent evaporates rapidly to its vapor pressure and is then conducted into the patient's breathing circuit under microprocessor control. The feedback control unit may be set to target a certain volatile agent concentration as a percentage of either the fresh gas stream or the patient's end-tidal gas.

**Draw-Over Vaporizers in Contemporary Practice.** As described above, most modern anesthesia workstations incorporate plenum-type variable-bypass vaporizers or other sophisticated units that require pressurized flow of carrier gases to drive vaporization and delivery. However, compressed medical gases (oxygen or air) are not available in many resource-constrained environments. Draw-over vaporizers remain a popular option for delivering anesthesia in such settings, including military field operations.<sup>121d</sup> They are characterized by (1) *in-circuit* location, (2)